A balance shift between error-free and error-prone DNA double-strand break repair pathways as a novel mechanism of radiosensitization by nucleoside analogs

Inaugural-Dissertation

zur

Erlangung des Doktorgrades

Dr. rer. nat.

der Fakultät für Biologie

an der

Universität Duisburg-Essen

Standort Essen

vorgelegt von

Simon Magin

aus Trier

Februar, 2014

Die der vorliegenden Arbeit zugrunde liegenden Experimente wurden am Institut für Medizinische Strahlenbiologie an der Universität Duisburg-Essen, Standort Essen, durchgeführt.

1. Gutachter: Prof. Dr. George Iliakis

2. Gutachter: PD Dr. Jürgen Thomale

Vorsitzender des Prüfungsausschusses: Prof. Dr. Hemmo Meyer

Tag der mündlichen Prüfung: 11.06.2014

Contents

List of figures

List of tables

List of abbreviations

5-FU	5-fluorouracil
Ab	Antibody
ADA	Adenosine deaminase

AFIGE	Asymmetric field inversion gel electrophoresis
ATM	Ataxia telangiectasia mutated kinase
ATR	ATM and Rad3 related kinase
ara-A	9-β-D-arabinofuranosyladenosine
Ara-C	cytosine arabinoside; Ara-C
bp	Base pairs
B-NHEJ	Backup Non-homologous end-joining
BrdU	5-bromo-2´-deoxyuridine
CHO	Chinese hamster ovary cell line
CLL	Chronic lymphoid leukemia
CML	Chronic myeloid leukemia
CLSM	Confocal laser scanning microscopy
dCK	Deoxycytidine kinase
DDR	DNA damage response
dHJ	Double Holliday junction
DNA	Deoxyribonucleic acid
DNA-PK	DNA-dependent protein kinase
DNA-PKcs	DNA-dependent protein kinase catalytic subunit
DEQ	Dose equivalent
dFdC	2´2´-difluoro-2´-deoxycytidine; Gemcitabine

DMEM	Dulbecco´s modified Eagle medium
DNA	Deoxyribonucleic acid
DR	Dose response
DSB	Double-strand break/s
dsDNA	Double-stranded DNA
EdU	5-ethynyl-2´-deoxyuridine
FACS	Fluorescence activated cell sorting
FDR	Fraction of DNA released
EGFP	Enhanced green fluorescent protein
Gy	Gray (J/kg)
h	hour
hCNT	Human concentrative nucleoside transporter
hENT	Human equilibrative nucleoside transporter
HU	Hydroxyurea
HRR	Homologous recombination repair
IF	Immunofluorescence
IR	Ionizing radiation
IRIF	Ionizing radiation induced foci
IdU	5-iodo-2´-deoxyuridine
k	Kilo (10^3)

LASER	Light amplification by stimulated emission of radiation
LET	Linear energy transfer
LMA	Low melting agarose
M	Mega (10^6)
MDC1	Mediator of DNA damage checkpoint 1
MEF	Mouse embryonal fibroblasts
MIP	Maximum intensity projection
MMC	Mitomycin C
MRN	Mre11-Rad50-Nbs1 complex
NAHR	Non-allelic homologous recombination
NAs	Nucleoside analogs
NHEJ	Non-homologous end-joining
ORF	Open reading frame
PARP	Poly(ADP-ribose) polymerases
PBS	Phosphate buffered saline
PE	Plating efficiency
PFGE	Pulsed-field gel electrophoresis
PI	Propidium iodide
PIKK	Phosphatidylinositide 3-kinase related kinases
PLD	Potential lethal damage

PMT	Photomultiplier tube
PTM	Post-translational modification
Puro	Puromycin resistance gene
RIPA	Radio-immuno-precipitation buffer
RK	Repair kinetics
RNA	Ribonucleic acid
RNAi	RNA interference
RnR	Ribonucleotide reductase
RPA	Replication protein A
s.d.	Standard deviation
s.e.m.	Standard error of the mean
SER	Sensitizer enhancement ratio
siRNA	Small interfering RNA
SLD	Sub-lethal damage
ssDNA	Single-stranded DNA
SSB	Single-strand breaks

1 Introduction

1.1 The role of chemoradiotherapy in the treatment of cancer

Cancer is the leading cause of death in Western Europe and North America (Ferlay, 2007; Jemal, 2011). Surgery, chemotherapy and radiotherapy (RT) are the three major treatment options for solid cancers. Current estimates state that more than 50% of patients with cancer should receive radiation treatment at least once during their illness (Delaney, 2005) and the U. S. cancer treatment and survivorship statistics 2012 show that RT belongs to the most frequently employed treatments for solid cancers (Siegel, 2012).

Thus, finding ways to improve the efficacy of RT and advancing the understanding of its actions is an important task in oncology. The past 2 decades have seen impressive achievements in delivery and targeting of the radiation dose contributing to this aim (Ahmad, 2012; Thariat, 2013). Despite these advances recurrence after initial eradication of detectable disease remains a major problem (Catton, 2003; Siglin, 2012). Recurrence may be due to radiation resistant sub-populations within the tumor or occult metastases.

An approach that can address both of these issues is the combination of chemotherapy with RT (Seiwert, 2007; Fietkau, 2012). One of the potential benefits of this combination is the gain of systemic action through chemotherapy that can complement the local action of irradiation. Importantly, for a variety of chemotherapeutics a synergistic action with ionizing radiation (IR) has also been observed that results from sensitization of cells to the killing effects of radiation.

Nucleoside analogs (NAs) represent an important family of antimetabolite drugs, several members of which have been demonstrated to possess radiosensitizing potential (Galmarini, 2002; Jordheim, 2013; Lee, 2013). A better understanding of the basic principles of this radiosensitization will help to develop treatments that increase the efficacy of radiotherapy and improve local control. In the present thesis mechanisms of radiosensitization by nucleoside analogs (NAs) are studied at the example of 9-β-D-arabinofuranosyladenosine (ara-A) and compared to the effects of other NAs.

In the following, the roles and effects of nucleoside chemotherapy and radiotherapy as single treatments will be described first to lay the basis for the understanding of their synergistic effects.

1.2 Nucleoside analogs and their role in chemotherapy

1.2.1 Overview and general considerations

NAs represent a class of rationally designed anticancer drugs. They were and are developed based on the knowledge of the chemical structure of nucleic acids and their building blocks. These compounds share high structural similarity with naturally occurring cellular nucleosides. Due to this similarity NAs can interfere with various enzymatic processes and compete with endogenous nucleosides. Prominent among these are processes of the nucleic acid metabolism, namely the synthesis of deoxyribonucleic acid (DNA) and ribonucleic acid (RNA) and nucleoside/nucleotide biosynthesis, where they can be used as fraudulent substrates. Therefore, nucleoside analogs used in anticancer therapy are classified as anti-metabolite drugs. The therapeutic gain of cytotoxic NA treatment derives from the differences in division and replication rates of rapidly proliferating tumor *vs.* normal somatic cells.

In order to unfold their therapeutic potential, NAs have to pass the cell membrane and become activated by mono-, di- and triphosphorylation by intracellular nucleoside and nucleotide kinases (Parker, 2009). Cellular uptake can occur by passive diffusion or by active transport via membrane proteins of the human concentrative and equilibrative nucleoside transporter families (hCNT and hENT respectively). Human cells possess four principal deoxyribonucleoside kinases that can perform the initial monophosphorylation of nucleosides. These are deoxycytidine kinase (dCK), thymidine kinases 1 & 2 and deoxyguanosine kinase (Arner and Eriksson, 1995). Adenosine kinase can be considered as a fifth deoxyribonucleoside kinase, as it was found to phosphorylate deoxyadenosine and several purine analogs (Hershfield, 1982; Cory and Cory, 1994). The nucleoside kinase which is critical for the initial activation of most NAs in cancer therapy is dCK.

Many purine- and pyrimidine analogs have been tested for or are currently in clinical use in cancer therapy. Purine analogs include 6-mercaptopurine (6-MP), 6-thioguanine, cladribine, clofarabine, deoxycoformicin (pentostatin), nelarabine, 9-β-D-arabinofuranosyladenine (ara-A) and 9-β-D-arabinofuranosyl-2-fluoroadenine (fludarabine or F-ara-A). Pyrimidine analogs include 5-fluorouracil (5-FU), capecitabine (a 5-FU prodrug), 5-aza-2-deoxycytidine (decitabine), 1-β-D-arabinofuranosylcytosine (cytarabine or ara-C), and 2´,2´-difluorodeoxycytidine (gemcitabine or dFdC) (Miser, 1992; Galmarini, 2002; Hajdo, 2010). Several other nucleoside analogs like sapacitabine (CNDAC) and troxacitabine are currently in development or being evaluated in clinical trials (Szafraniec, 2004). In their diversity NAs comprise one of the largest classes of cancer therapeutics (Parker, 2009).

NAs often differ from each other or the natural nucleosides they resemble only by small modifications like single substitutions (e.g. a halogenation) or sugar isomery (e.g. arabinoside NAs) (Figure 1). Despite the structural likeness among NAs there is a remarkably high variance in clinical activities between different of these molecules (Ewald, 2008). Ara-C and Fludarabine for example are both extensively used in the treatment of hematological malignancies, but display little action against solid tumors (ara-C against acute lymphoid leukemia [ALL] and acute myeloid leukemia [AML]; fludarabine against chronic lymphoid leukemia [CLL], AML or non-Hodgkin lymphoma [NHL]))(Chun, 1991). Gemcitabine on the other hand has been found to be effective (as a single treatment or together with platinum agents) in the treatment of a number of solid malignancies including non-small cell lung cancer, pancreatic cancer, breast and bladder cancer, while also displaying some activity against hematological malignancies (Jordheim, 2013). 5-FU and its pro-drugs (capecitabine, floxuridine) show activity against a number of solid tumor types, including breast, head and neck and most notably colorectal cancers (Longley, 2003), but find seldom use against hematological malignancies (Pardee, 2012).

This surprisingly high selectivity of structurally similar drugs may on one hand be explained by differences in the uptake, concentration and activation of individual drugs in different cellular compartments, and on the other hand by mechanistic differences of

their actions. The former conditions can arise from differences in the expression of transporters and activating or inactivating enzymes between tissues and lineages. Regarding mechanisms of NA cytotoxicity the interference with cellular replication is a common denominator between most NAs, but further activities also play a role. These include inhibition of RNA synthesis, deregulation of nucleotide pools by inhibition of ribonucleotide reductase (RnR), inhibition of nucleotide biosynthesis, induction of apoptosis, reduction of DNA methylation and induction of DNA damage (Consoli, 1998; McGinn and Lawrence, 2001; Galmarini, 2002; Ewald, 2008; Liu, 2012b).

We wanted to focus our study on the effects of ara-A and ara-C and the fluorinated derivatives fludarabine and gemcitabine (Figure 1). In the following section the cellular metabolism and known modes of action of these NAs are summarized.

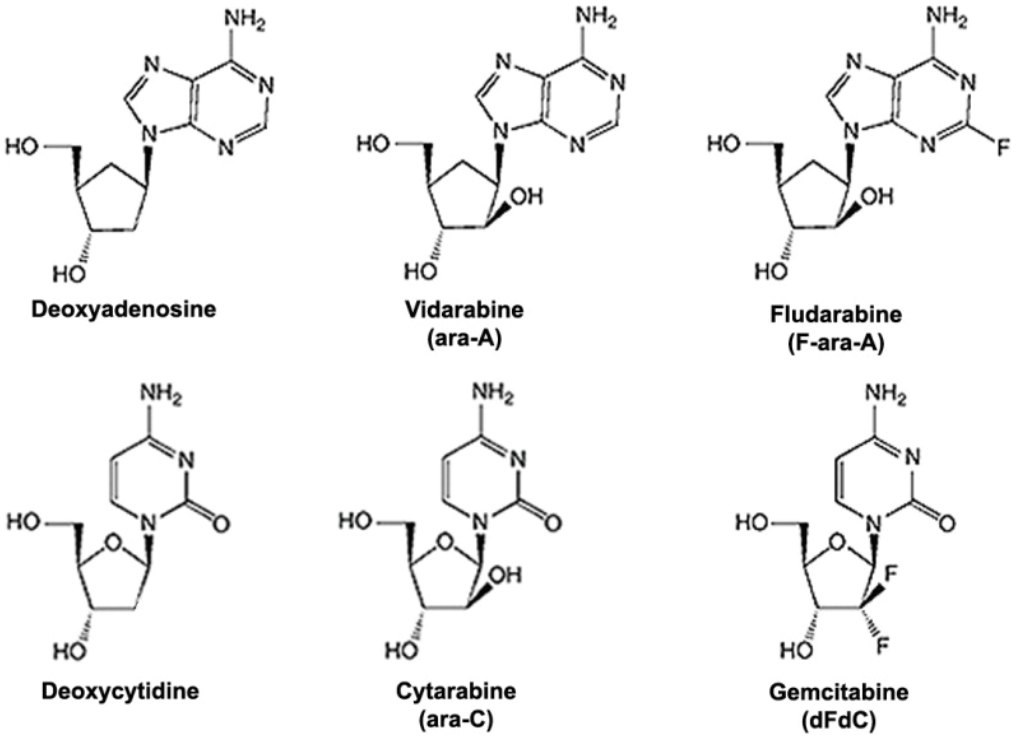

Figure 1 Chemical structures of selected nucleoside analogs. Structures of deoxyadenosine and deoxycytidine and their analogs ara-A, fludarabine, ara-C and gemcitabine.

1.2.2 Cellular metabolism and modes of action of NAs used in this study

1.2.2.1 Ara-A

Ara-A is a functional analog of deoxyadenosine. that is incorporated into DNA, but not RNA (Kufe, 1983). Ara-A differs from deoxyadenosine by having arabinose as sugar moiety instead of deoxyribose. Arabinose is an isomere of ribose in which the 2´ hydroxyl group on the furanosyl ring is in β instead α configuration (Hubeek I, 2006).

Adenosine kinase has been implicated as the activating enzyme that performs the initial phosphorylation of ara-A within the cell, which is uncommon for NAs (Chan and Juranka, 1981; Cass, 1983). However, ara-A has also been reported to be a minor substrate for dCK and deoxyguanosine kinase (Arner and Eriksson, 1995). Ara-A is quickly deaminated by adenosine deaminase (ADA) in cells or plasma resulting in fast deactivation (Lepage, 1975; Tanaka, 1984).

Ara-A effectively inhibits DNA, but not RNA synthesis. In DNA synthesis ara-A is not a definitive chain terminator and most ara-A nucleotides are found in internucleotide linkages at lower concentrations, while the proportion of ara-A at terminal positions appears to increase with rising concentrations (Plunkett, 1974; Muller, 1975; Kufe, 1983; Ohno, 1989). It has been demonstrated, that ara-A inhibits the DNA polymerases α and β (Dicioccio and Srivastava, 1977). It is also a very potent inhibitor of DNA primase, which synthesizes RNA primers during replication and forms a complex with polymerase α (Kuchta and Willhelm, 1991). Additionally, ara-A has been shown to inhibit RnR, whereby it may modify the balance of nucleotide pools in the cells, which is expected to further contribute to inhibition of replication (Moore and Cohen, 1967; Chang and Cheng, 1980).

1.2.2.2 Fludarabine

The development of fludarabine resulted from the search for a deamination resistant derivative of ara-A (Montgomery and Hewson, 1969). Fludarabine is not a substrate for ADA and thus is metabolically more stable (Brockman, 1977). Fludarabine shares a

number of similarities with ara-A regarding its mode of action, but there are also some remarkable differences.

An important difference exists regarding the activation of the two NAs. The initial phosphorylation steps of fludarabine and ara-A seem to be catalyzed by different enzymatic activities as cells deficient for dCK show strongly increased resistance against fludarabine while remaining relatively sensitive to ara-A (Dow, 1980; Cory and Cory, 1994). Thus fludarabine, in contrast to ara-A is mainly activated by dCK.

Like ara-A, fludarabine is incorporated into DNA, but unlike ara-A fludarabine appears to be a veritable chainterminator (Huang, 1990). Also unlike ara-A, fludarabine is incorporated into RNA (Huang and Plunkett, 1991). Similar to ara-A, fludarabine does inhibit the DNA polymerases α and β, as well as DNA primase (White, 1982; Catapano, 1993). Another mechanism that is likely to contribute to the impact of fludarabine on replication is inhibition of Ligase1, which has not been found for ara-A (Yang, 1992). Fludarabine has also been shown to inhibit RnR, but to be at least 10 fold as effective as ara-A in doing so (White, 1982).

1.2.2.3 Ara-C

Ara-C, like ara-A, is an arabinoside NA in which the deoxyribose sugar (deoxyribofuranose) has been replaced by a β-D-furanosylarabinoside ring (Figure 1). It is a structural analog of deoxycytidine. Like other NAs, it needs to be converted to an active metabolite upon cellular uptake.

Transport into the cell is mainly achieved through hENT at plasma concentrations achieved during standard treatment (0.5 -1 µM), but mainly occurs by passive diffusion at the concentrations of around 100 µM that are achieved during high dose ara-C treatment (Early, 1982; Liliemark, 1985; Hubeek I, 2006). The initial step in activation of ara-C is phosphorylation by dCK. Through consecutive phosphorylation by mono- and diphosphate kinases, Ara-CMP is ultimately converted to the active metabolite ara-CTP.

Ara-CTP is incorporated into DNA and causes strong inhibition of DNA synthesis. This inhibition is thought to be elicited by a mechanism of relative chain termination, since

most ara-CMP residues are found in internucleotide linkages (Graham and Whitmore, 1970), although higher concentrations of ara-C seem to increase the proportion of ara-CMP nucleotides in terminal positions (Ohno, 1988). Ara-CTP is a weak competitive inhibitor of DNA polymerase α and to a lesser extent of polymerase β (Matsukage, 1978; Miller and Chinault, 1982). Incorporation of ara-CMP into RNA is barely detectable (Kufe, 1980), but there are reports that show inhibition of RNA synthesis by ara-C (de Vries, 2006), which may take place by an inhibition of RNA polymerase without requiring incorporation (Chuang and Chuang, 1976). Unlike the other NAs used in this study, ara-C is not an inhibitor of RnR (Moore and Cohen, 1967).

1.2.2.4 Gemcitabine

Gemcitabine (2´2´-difluoro-2´-deoxycytidine or dFdC) is a halogenated cytidine analog (Hertel, 1988). It is different from most other halogenated NAs in that the fluorine substitutions are located on the sugar ring instead of the base. Fluorination renders gemcitabine substantially more resistant to deamination than ara-C (Hertel, 1990). Similar to other NAs dFdC has to be converted into active metabolites upon entry into the cell. The first and rate limiting step is phosphorylation performed by dCK. Subsequently gemcitabine is di- and triphosphorylated to dFdCDP and dFdCTP. dFdCTP is incorporated into DNA and to a lesser extent also into RNA by cellular polymerases (Vanhaperen, 1993). dFdCDP is a potent inhibitor of RnR (Heinemann, 1990). The resulting depletion of deoxynucleotide pools contributes to replication inhibition by gemcitabine. It also represents a self-potentiating mechanism of this drug, as reduction of dCTP levels result in increased incorporation of gemcitabine into DNA.

Another self-potentiating mechanism is inhibition of dCMP deaminase by dFdCTP, an enzyme capable of deactivating gemcitabine (Heinemann, 1992). A third self-potentiating mechanism is present at high concentrations of dFdCTP, which lead to inhibition of CTP synthetase. This further contributes to dCTP depletion and the accompanying increase of dFdCTP incorporation. Once a gemcitabine nucleotide is incorporated into DNA only a single further nucleotide is added to the chain, then elongation stops (Huang, 1991). The proofreading function of DNA polymerase ε is

essentially unable to remove the incorporated dFdCMP. This mode of disruption of DNA synthesis has been termed “masked chain-termination” (Plunkett, 1995).

The intracellular half-life of Gemcitabine is exceptionally long compared to most other NAs (Plunkett, 1995). Long half-life, the unusual mode of chain termination and the multiple self-potentiating mechanisms of Gemcitabine may partially explain why it is more effective in solid tumors than many other NAs (Shewach DS, 2006).

1.3 Radiotherapy and the effects of Ionizing radiation

1.3.1 Tumor and normal tissue response to IR

Radiotherapy uses IR to efficiently eradicate tumor cells in a localized, non-invasive way that also allows the treatment of growths that are difficult to resect. A critical parameter limiting the use of radiotherapy is the risk for the occurrence of acute or late side effects like erythema and edema or fibrosis in normal tissue. The incidence and severity of such side effects depends on radiation dose and the radiosensitivity of the irradiated normal tissue. There is a strong correlation between the turnover rate of an irradiated tissue and its radiosensitivity (Begonie, 1906). Fast growing tissues like mucosa are very radiosensitive, while tissues with low mitotic rates like the central nervous system or skeletal muscles are less radiosensitive.

Similarly, rapidly dividing tumor cells also show higher susceptibility towards killing by IR than the surrounding healthy tissue which, depending on the location, usually consists mainly of mitotically inactive, terminally differentiated cells (Hall and Giaccia, 2006). This connection between growth rate and radiosensitivity forms one of the fundamentals of radiotherapy.

Despite this growth rate dependent difference in radiosensitivity, the total doses that are required for curative therapy are so high that they would lead to intolerably high normal tissue damage, if administered as a single dose. This was a major problem in the beginnings of radiotherapy, and side effects were often severe. Reduction of these side effects was and is the main reason to break down the total radiation dose into smaller

portions, so called fractions (Connell and Hellman, 2009). Modern external beam radiotherapy is given almost exclusively as fractionated radiotherapy. Indeed, the risk for side effects can be substantially reduced by fractionation. However, even under these conditions side effects are not completely abolished, and the probability of occurrence strongly depend on the type of tissue in the radiation field (West and Barnett, 2011). Decades of extensive radiobiological research and experiences with fractionation have led to the formulation of some key principles, the so called four Rs of radiotherapy (Withers, 1975), which try to rationalize the advantages gained by fractionation with several distinct, but potentially cooperative mechanisms: repair, redistribution, repopulation and reoxygenation.

Repair refers to the capacity of cells to repair so called sub-lethal damage (SLD) between fractions of radiation, which improves their chance of survival. This “R” is the factor that led to the initial development of fractionated irradiation schemes, since they allow delivery of total doses that would intolerably damage surrounding healthy tissue when given as a single dose. It is usually assumed that normal cells repair SLD better than tumor cells, resulting thus in a net benefit for the patient.

Redistribution of irradiated cells in the cell cycle also occurs between fractions. When tumor tissue is irradiated, cells are hit in all phases of the cell cycle. Cells show strong variations in their radiosensitivity depending on the cell cycle phase they are in. Commonly the radioresistance increases during S-Phase and is lowest for cells in M-Phase (Tamulevicius, 2007). There is evidence that these differences are related to cell cycle dependent regulation of the activity of different DSB repair pathways (Rothkamm, 2003; Tamulevicius, 2007). Upon irradiation cells in sensitive phases of the cycle are killed preferentially. Surviving cells in resistant phases progress through the cell cycle and reach more sensitive phases, where they can be eradicated more efficiently by the subsequent dose fraction.

Besides redistribution of tumor cells, the allowed intervals between fractions may give normal tissues and tumors time to refill their ranks. Inactivation of cells during radiotherapy is often compensated by an increase in the mitotic activity of the tumor.

This repopulation has to be taken into account and potentially counteracted to ensure success of radiation therapy.

While position in the cell cycle is a cell intrinsic determinant of radiosensitivity, a well-known cell extrinsic factor for a cell´s susceptibility to killing is the oxygenation status. Hypoxic regions of tumors are known to be more resistant to radiation than regions that lie close to blood vessels and are therefore well oxygenated. This phenomenon is known as the oxygen effect. A popular explanation for this effect is the Oxygen fixation hypothesis (Ewing, 1998; Bertout, 2008) that postulates that Oxygen di-radicals can act as a fixating agent for DNA lesions induced by IR. After irradiation, cells in better oxygenated regions of the tumor will be killed preferentially. Cells located more distant from blood vessels can now move in into more oxygen rich regions and become oxygenated - or alternatively new blood vessels can form. This development leads to reoxygenation of formerly hypoxic cells enabling more efficient killing of cells during later fractions.

The correlation of mitotic activity and susceptibility to killing, as well as the four “Rs” can help to explain many of the effects of IR in fractionated radiotherapy – both the beneficial action on tumor cells and the partial protection of normal tissue. However, radiosensitivity does not only differ between tissues types, but there is also variability between the same tissues from different patients and between different tumors of the same or similar type (Deacon, 1984; Tucker and Thames, 1989). In cases where growth rate and architecture of tissues or tumors under study are similar, differences in radiosensitivity have to derive from other factors. These individual differences are referred to as intrinsic radiosensitivity (Roberts, 1999; West and Barnett, 2011). Intrinsic cellular radiosensitivity has been shown to be an important factor underlying cell killing by IR and the radioresponse of tumors (Fertil and Malaise, 1981; Deacon, 1984; Steel, 1989; Tucker and Thames, 1989; Gerweck, 2006).

1.3.2 Repair of potentially lethal damage

In the context of radiobiology cell death refers to the mitotic inactivation of treated cells. The sensitivity of cells to killing by IR can be assessed *in vitro* in clonogenic colony

formation assays (Hall and Giaccia, 2006). In these experiments the reproductive potential of cells is assessed at the single cell level. Loss of this potential can be realized via different routes including mitotic catastrophe, senescence, autophagy, apoptosis or necrosis (Balcer-Kubiczek, 2012). The contribution of these mechanisms or pathways to cell killing differs among cells and depends on factors like cell type and radiation dose (Puck and Marcus, 1956; Held, 1997). Apoptosis as an immediate response to radiation (interphase death) for example plays a decisive role only in a small number of cellular systems, e.g. lymphocytes (Ross, 1999). Mitotic catastrophe is considered to be a main route to cell death after IR in most systems, but may not be a genuine pathway of cell death itself. Instead cells running into mitotic catastrophe may eventually die, i.e. cease to proliferate, by any of the other pathways mentioned above (Galluzzi, 2012).

Analysis of cells exposed to increasing doses of IR yield characteristic survival curves (Figure 2). Various treatments or conditions can result in modification of the radiosensitivity of cells in this assay, e.g. the oxygenation status (see above). Post-treatment conditions that can modify the survival of irradiated cells are assumed to exert their effects through either repair or fixation of damage that is only potentially lethal (Phillips and Tolmach, 1966) (Little, 1969; Iliakis, 1988a).

A classic experiment can be performed with cells in the plateau, or stationary phase, of growth. When these cells are irradiated they can be plated as single cells in fresh growth medium either immediately after irradiation (immediate plating) or at increasing periods of time after irradiation (delayed-plating). Plating in fresh, serum supplemented growth medium results in the re-entrance of cells into the cell cycle and their progression through S-Phase, which is also a prerequisite for colony formation. Delayed plating occasionally has a profound impact on the survival of cells. Cells that are plated immediately after irradiation exhibit the lowest survival levels. If plating is delayed for longer times (e.g. 6-24h) the cells display more radioresistance (Figure 2). This phenomenon is ascribed to the repair of potentially lethal damage (PLD). Incubation of cells in their resting state apparently allows the repair of some PLD which is inhibited when cells are stimulated to reenter the cell cycle by immediate plating.

This experimental setup can be used to test a condition or treatment, e.g. incubation with a drug, for its potential to interfere with the repair of PLD by its ability to prevent the increase in survival normally associated with delayed plating. A variety of treatments has been identified that are able to inhibit repair of PLD. Notably, these include NAs like ara-A (Figure 2). When this approach is used, repair of PLD and its inhibition is measured in non-cycling cells. However, PLD repair also occurs in actively cycling cells and is assumed to contribute to the cell cycle dependent fluctuations in radiosensitivity to killing (Iliakis and Nusse, 1983b; Stamato, 1988). Similarly, differences in the intrinsic radiosensitivity of cells can be interpreted as differences in their capability to repair PLD. The precise molecular nature of the lesion/s underlying PLD remains to be fully characterized.

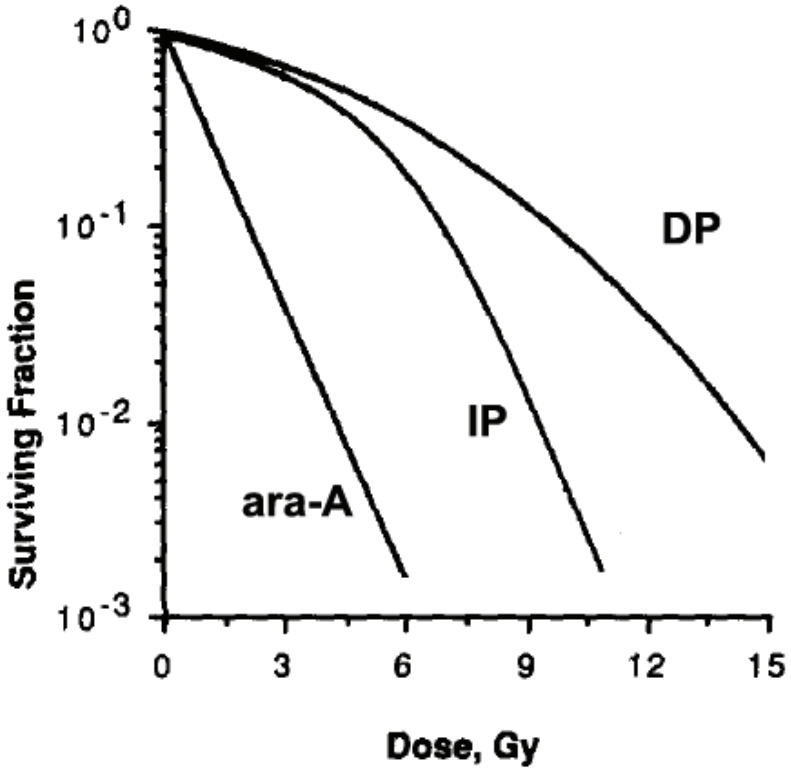

Figure 2 Repair of potentially lethal damage. Survival curves of plateau-phase cells plated either immediately (IP) or after prolonged incubation in the plateau-phase (DP) after irradiation. Also shown is the survival of cells treated with ara-A at concentrations that cause maximum fixation of PLD during incubation in plateau-phase before delayed plating,

In order to understand the repair or fixation of which type of lesion/s may underlie phenomena like the fluctuations of radiosensitivity during the cell cycle, intrinsic cellular radiosensitivity and PLD repair it is necessary to take a look at the physical mechanisms of damage induction by IR and the associated cellular responses on a molecular level.

1.3.3 Basic physics of the interaction of IR with biological matter

Damage to the DNA is the source for the prominent biological effects that can be observed after exposure to IR. These effects include mutation, chromosome aberration, neoplastic transformation, mitotic inactivation and cell death. IR is particularly efficient in inducing lesions that lead to the formation of chromosome aberrations. Excellent correlations have been found for the induction of chromosome aberrations and cell killing as well as the repair of chromosome breaks and PLD repair (Carrano, 1973; Virsik and Harder, 1980; Cornforth and Bedford, 1987).

Ionizing radiation (IR) is highly energetic radiation that is characterized by its potential to expel electrons from atomic shells or chemical bonds. The different types of IR that exist can be categorized into particulate and electromagnetic radiation. Particulate IR includes α (Helium nuclei) and β (electrons) radiation, as well as any other particle that carries sufficient kinetic energy to ionize other atoms (e.g. accelerated neutrons, protons or heavy Ions). X-rays and γ-rays represent the electromagnetic forms of IR. Since all experiments in this work were exclusively carried out with X-rays we will focus mostly on this form of radiation.

X-rays consist of high energy photons that can ionize atoms as a consequence of interactions with orbital electrons. At photon energies that are used in radiation therapy (200 keV to 25 MeV) a process called Compton scattering is the predominant interaction process in soft tissue (Hall and Giaccia, 2006). When this type of interaction takes place, only part of the photon's energy is absorbed by the interacting electron, resulting in expulsion of the electron from its shell. The remaining energy is carried away by a scattered photon. Electrons that have been liberated by interaction with a photon travel through the surrounding medium and can cause further ionizations. Those electrons (as

well as those produced by further interactions) are often referred to as secondary electrons, despite the fact that they represent the product of the primary ionization event. Secondary electrons account for the vast majority of ionizations caused by electromagnetic IR, which is thus considered as indirectly ionizing radiation. Since most of the energy is deposited in a disperse pattern, X-rays are also considered to be a sparsely ionizing radiation. This is in contrast to the pattern of energy deposition of radiation types like alpha particles or neutrons, which produce dense ionization tracks (Figure 3).

A measure for the density of ionizations generated by a particular form of radiation is provided by the physical quantity: linear energy transfer (LET [keV/µM]). Thus, sparsely ionizing radiations are often also referred to as low LET and densely ionizing radiations as high LET radiation. However, secondary electrons induced by X- or γ-rays lose energy during the interactions along their track. With decreasing velocity the interaction probability of such electrons increases. This causes an increase in LET associated with clustering of ionizations especially at the ends of their tracks (Goodhead, 1994).

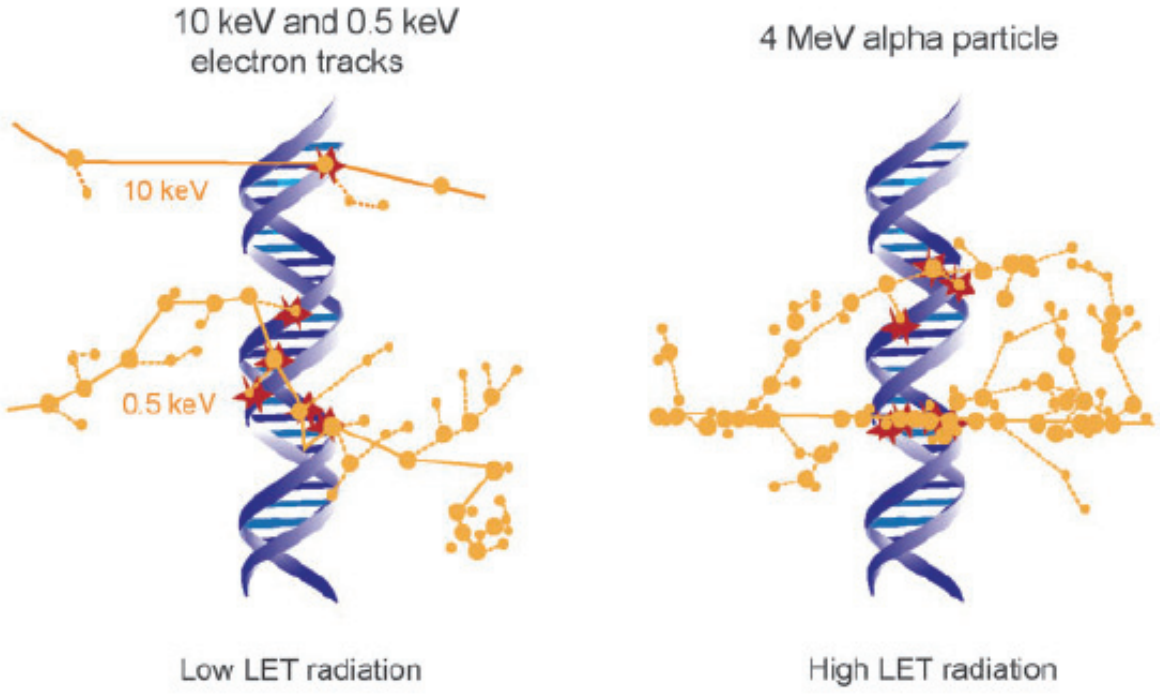

Figure 3 DNA damage induction by low and high LET radiation tracks. Ionization events caused by IR localize along radiation tracks and can induce clustered damage at the DNA. With increasing LET the

probability for DNA damage clustering increases. Large dots represent ionizations and small dots represent excitations along the radiation track. The Monte Carlo simulated tracks are drawn on the same scale as the DNA. (modified from (Schipler and Iliakis, 2013))

1.3.4 Mechanisms of DNA damage induction and types of DNA lesions induced

Ionization of atoms that take part in a molecular bond can result in the formation of free radicals. Radicals are highly reactive, short lived chemical species characterized by an unpaired valence electron. Production of radicals can take place directly in the target molecule (i.e. the DNA), which would be considered as direct effect. However, since a cell is composed of water to approximately 70% (Alberts, 2008) the majority of radicals generated initiate from H_2O (e.g. hydroxyl radicals). Consequently the majority of DNA damage induced by sparsely ionizing radiations is due to the indirect effect exerted by water produced free radicals. Due to the short life time of free radicals the probability of interaction with DNA is only significant when the radical forms in close proximity to the DNA molecule. The spectrum of chemical modifications induced in the DNA by radiation is highly divers and includes oxidative damage to bases and sugars, cross-links between bases or between DNA and proteins and breaks in the sugar phosphate backbone. Breakage of the sugar phosphate backbone on both strands of the double helix within a couple of nucleotides will lead to the formation of a double-strand break (DSB). Accumulation of ionizations in small volumes, as it occurs at the end of secondary electron tracks, increases the likelihood of the induction of multiple damages in short sequence stretches. Such sites of accumulated damage are being referred to as multiply damage sites or clustered DNA damage. Clustering of ionizations increases the probability of induction of two or more single-strand breaks (SSB) in close proximity, thereby increasing the chances for the generation of a DSB. However, DSB are not a uniform class of damage. Instead the term subsumes a variety of chemically different entities, which will be briefly reviewed in the next paragraphs.

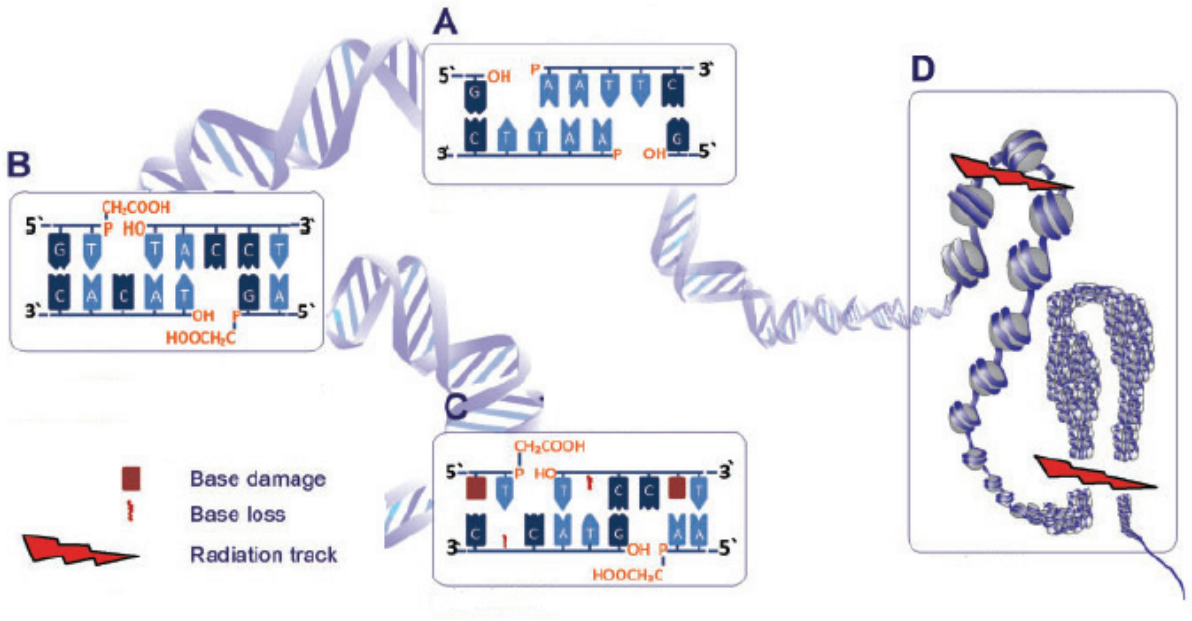

Figure 4 Types of DSB with different levels of complexity A) DSB induced by a RE with a 5`-phosphate and a 3`-OH group. **B)** DSB induced by IR frequently comprise a 3` phosphoglycolate and a 5'-OH. **C)** DSB induced by IR that comprises also other types of lesions like base damages or base loss in close proximity to the DSB. **D)** Clusters of multiple DSBs. Two examples are shown: On the left, a single radiation track induces two DSBs in the linker regions of a nucleosome leading to loss of the nucleosome. On the right, a higher order packaging of nucleosomes is illustrated. Chromatin loops can be severed by a single radiation track if hit appropriately. (modified from (Schipler and Iliakis, 2013))

1.3.5 Different types of DSB and damage complexity

The simplest type of DSB that can be envisaged is the one induced by a restriction endonuclease (Figure 4 A). No further damage is involved and the ends of the DSB are equipped with intact 3´-OH and 5´-phosphate groups that can readily be religated. However, this type of clean break cannot be expected to be found after exposure to IR. Instead, DSB induced by IR usually contain modified ends, e.g. 5´-OH and 3´-phophoglycolate groups, as illustrated in Figure 4 B. In addition, for a proportion of DSB induced by IR further types of damage are to be expected in the vicinity of the break (Figure 4 C). DSB in conjunction with additional DNA lesions are usually referred to as complex DSB. An additional level of complexity can be added by clustering of multiple

DSB, which may lead to loss of nucleosomes or entire chromatin domains (Schipler and Iliakis, 2013). The list of different DSB types presented here is by no means complete and is further complicated by the existence of indirect DSB that can develop from IR-induced non-DSB lesions by enzymatic processing or thermal evolution (Singh, 2009; Singh, 2013). Computational modelling yields distinct ratios for various DSB types as a function of radiation quality. In general, with increasing LET of radiation the complexity of damage induced in the DNA increases (Nikjoo, 1999; Friedland, 2012). Importantly, cellular survival decreases with increasing LET (Figure 5). These observations create a close link between DSB, damage complexity and cell killing.

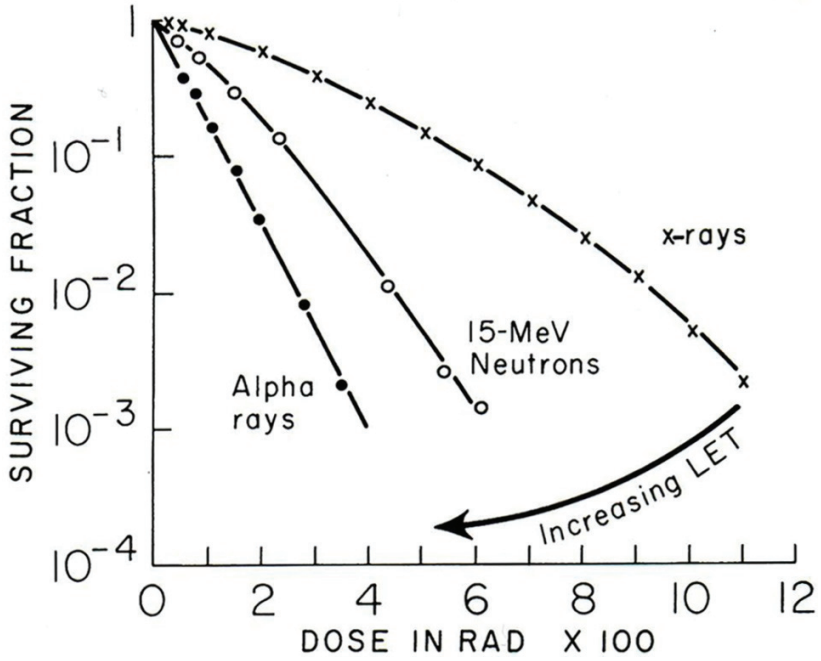

Figure 5 Survival curves for cultured cells of human origin Human cells were exposed to 250 kV X-rays, 15 MeV neutrons and 4 MeV α-particles**.** Survival curves obtained with neutrons and alpha rays have steeper slopes and a smaller initial shoulder than curves generated with x-rays. (modified from (Hall and Giaccia, 2006))

DSB threaten the integrity of chromosomal DNA and undermine the fundamental principle of DNA repair as both strands of the helix are disconnected and no intact strand is available for repair. In contrast, SSB or base damages don´t compromise the continuity of the DNA molecule and the complementary strand of the double helix can serve as repair template. Although conceptually the repair of DSB is particularly difficult,

actually recognition and repair of DSB is in higher eukaryotic cells faster and more efficient than of many other DNA lesions (Eriksson, 2007; Schipler and Iliakis, 2013) (see also Figure 6). Cells have evolved elaborate mechanisms to correct and repair DSB. However, complex DSB consisting of multiple different types of damage pose particularly demanding challenges to the cellular repair machinery. The involvement of several steps of processing and the potential participation of multiple pathways of DNA repair is likely to be associated with a higher risk of accidents. It is now widely believed that the induction of complex DSB is a key aspect of IR, underlying the effective induction of chromosomal aberrations and cell killing (Goodhead, 1994; Schipler and Iliakis, 2013). The chemical nature of a DSB and its complexity may also be factors participating in the determination of repair pathway choice. In the following paragraphs the key events of the cellular response to DSB induction will be described

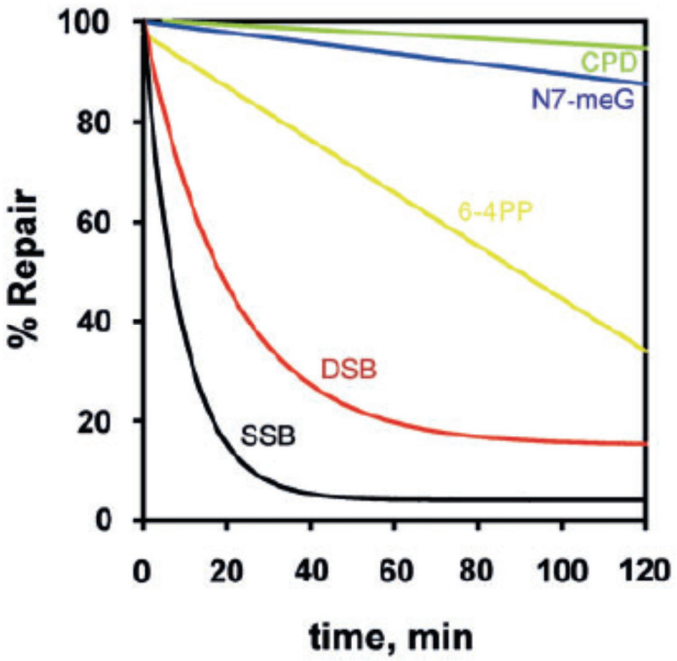

Figure 6 Repair kinetics of different forms of DNA damage Shown is the kinetics of removal of SSBs, DSBs, 6–4 photoproducts (6–4PP), cyclobutane pyrimidine dimers (CPD) from CHO-AA8 cells. Kinetics of N7-meG comes from measurements in human lymphocytes. (from (Schipler and Iliakis, 2013))

1.4 Cellular responses to DSB

1.4.1 DSB detection and signaling- The DNA damage response

Induction of a DSB initiates a cascade of posttranslational protein modifications (PTMs) that signal to the cellular repair and cell cycle control machineries (Grabarz, 2012). The events elicited by this DNA damage response (DDR) include changes in chromatin, in gene expression, the relocation of a large number of proteins, the regulation of DNA repair and the activation of cell cycle checkpoints (Bekker-Jensen and Mailand, 2010). The molecular components of the DDR can be categorized into damage sensors, transducers, mediators and effectors. The recruitment and activation of factors involved in DDR follows a hierarchical order beginning with the recognition of DSB. Candidates for the function of primary damage sensors are the MRE11-RAD50-NBS1 complex (MRN), the KU70/KU80 heterodimer (KU) as well as the Poly(ADP-ribose) polymerases 1 (PARP1) (Wang, 2006b; Polo and Jackson, 2011). All of these proteins and complexes are capable of binding to DSB ends and are among the first proteins that recruited to the breaks (Polo and Jackson, 2011) (Figure 7). The MRN complex can tether DSB ends by binding with its globular domains comprised of the dimerized RAD50 and MRE11 subunits (Lavin, 2007; Williams, 2008). KU is highly abundant in the cell and displays extraordinarily high affinity for dsDNA end. PARP1 becomes directly activated by binding to DNA breaks and start to poly(ADP-ribosylate) substrate proteins (D'Silva, 1999; Kun, 2002). Any of those putative damage sensors is also strongly implicated in other processes related to DNA repair, e.g. DNA end-resection (MRN), non-homologous end-joining (KU) and SSB repair (PARP). Most models in the literature ascribe the role of the major DSB sensor to MRN, although KU and PARP1 arrive earlier at breaks and MRN recruitment is modulated by PARP1 (Haince, 2008; Polo and Jackson, 2011).

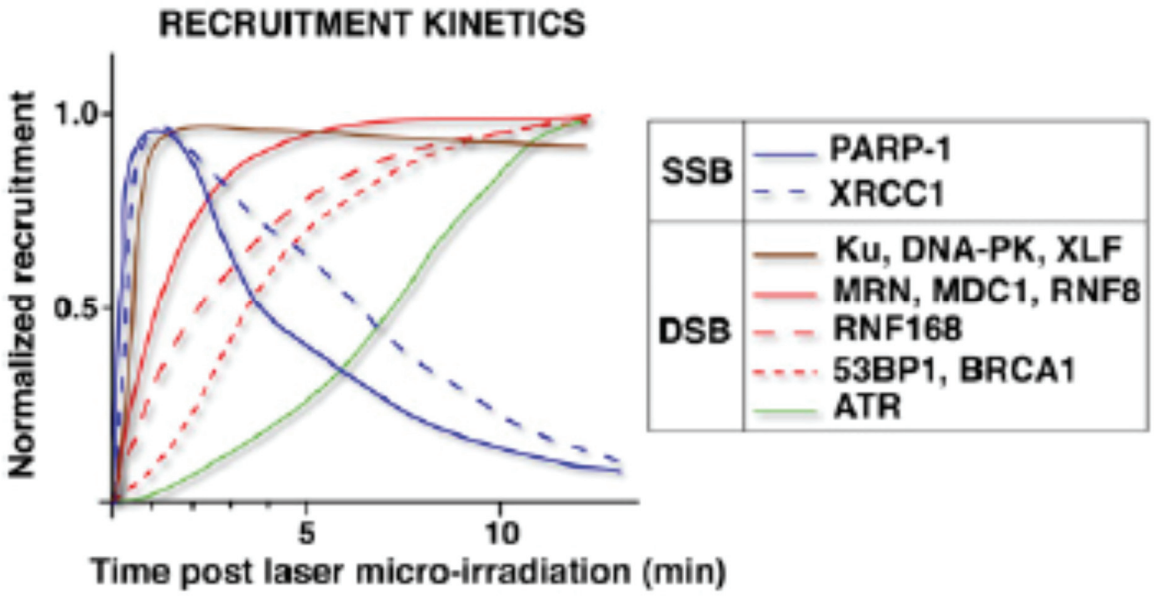

Figure 7 Recruitment kinetics of proteins involved in the DDR Sequential recruitment of DDR factors to SSBs and DSBs generated by laser microirradiation. (from (Polo and Jackson, 2011))

On the next hierarchical level, the role of the signal transducers is taken by three members of the family of phosphatidylinositide 3-kinase related kinases (PIKKs). Among those the ataxia telangiectasia mutated kinase (ATM) has emerged as a master kinase in IR induced DDR signaling. ATM is activated in response to DSB in a MRN dependent manner (Uziel, 2003). In its inactive form ATM persists as a dimer in the cell, which dissociates upon intermolecular autophosphorylation at Serine 1981 (pS1981) in response to DSB (Bakkenist and Kastan, 2003). The DNA-dependent protein kinase catalytic subunit (DNA-PKcs) is another member of the PIKK family that becomes activated in response to DSB. Together with KU it forms the DNA dependent protein kinase (DNA-PK) that plays a central role in the non-homologous end-joining pathway of DSB repair. It is capable of phosphorylating a number of important targets involved in DSB signaling, repair and chromatin structure, but possesses a substantially smaller substrate spectrum than ATM (Stiff, 2004; Tomimatsu, 2009). ATM and Rad3 related kinase (ATR) is a further PIKK involved in the DDR. ATR becomes not directly activated by DSB, but by single-stranded DNA (ssDNA). In conjunction with its partner ATRIP it binds to ssDNA coated with replication protein A (RPA). Thus, ATR activation in

response to DSB requires the resection of 5” strand of the dsDNA at the end of the break. Resection of DSB ends again is tightly regulated and highly depending on the cell cycle phase, as is explained in more detail below (1.4.2.3).

A number of mediator proteins help to maintain and amplify the signaling that is initiated by the transducer kinases. One of the first posttranslational modifications in response to a DSB is phosphorylation of the histone variant H2AX, on Serine 139. This phosphorylation can be mediated by ATM and DNA-PKcs and likely also by ATR (Stiff, 2004; Ward, 2004; Wang, 2005c). In its phosphorylated form the histone variant is termed γH2AX (Rogakou, 1998). γH2AX spreads to both sides of the DSB covering the region around the break up to a length of a few megabases (Nakamura, 2010). It provides a binding platform for the mediator of DNA damage checkpoint protein 1 (MDC1) (Stucki, 2005). MDC1 constitutively interacts with the MRN complex (Spycher, 2008) and can also interact with ATM. Thereby, MDC1 binding to γH2AX leads to accumulation of these factors around DSB and contributes to stabilization and amplification of the damage signal. Phosphorylation of MDC1 by ATM also leads to the recruitment of the E3 Ubiquitin Ligase RNF8, which elicits ubiquitylation of a number of targets, including the histones H2A and H2AX. This in turn leads to the recruitment of RNF168, another E3 Ligase that mediates the polyubiquitylation of H2A (Bohgaki, 2010). Together these ubiquitylations have been implicated in the recruitment of BRCA1 and 53BP1, factors that play important roles in DSB repair pathway choice by regulating the resection of DSB ends (Stewart, 2009; Bunting, 2010; Escribano-Diaz, 2013).

The multiple PTMs and accumulations of proteins at damage sites that are part of the DDR can be visualized by immunofluorescence staining and microscopy. Staining with antibodies against γH2AX, MDC1, ATM-pS1981, 53BP1 and many other proteins involved in the DDR and DSB repair reveals a pattern of focal protein accumulations in the nuclei of cells after exposure to IR. Measurement of induction and decay of these IR induced foci (IRIF) has been used extensively to investigate mechanisms and kinetics of DSB signaling and repair.

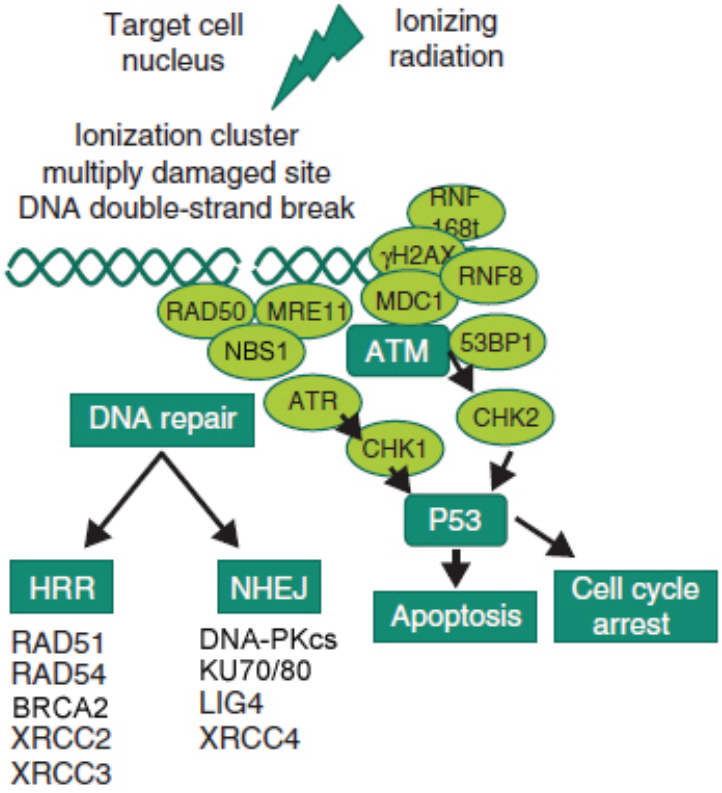

Figure 8 Simplified schematic of the cellular response to DSB Induction of a DSB triggers a complex cascade of events that results in signaling to the cellular DNA repair machinery and cell cycle checkpoint control. (modified from (West and Barnett, 2011))

One of the central functions of DDR is to cause cell cycle arrests that prevent cells with damaged genomes from progressing into subsequent phases. The pathways that elicit these arrests or delays in the progression through the cycle are called checkpoints. The main effectors of cell cycle checkpoints are the checkpoint kinases CHK1 and CHK2. ATM and Chk2, as well as ATR and CHK1 form two signaling modules that primarily coordinate checkpoint activation in response to DNA damage (Reinhardt and Yaffe, 2009). Both pathways converge on members of the CDC25 family of phosphatases. Inactivating phosphorylations placed on CDC25 by CHK1 and CHK2 prevent the removal of inhibitory phosphorylations on CDK/cyclin complexes that are critical for cell cycle progression. In addition, CHK2 phosphorylates p53 in response to DNA damage thereby contributing to the stabilization of this protein and the development of a G1 arrest (Chehab, 2000). Activation of p53 can also trigger the activation of apoptotic

pathways; however apoptosis plays an important role as a response to IR only in some cell systems (see below). The action of CHK1 on the other hand can arrest cells at the G2/M border via phosphorylation of CDC25C. DNA damage checkpoints prevent cells with excessive genetic damage from progressing through the cycle and thereby contributing to genomic stability. By halting cells in the current phase of the cell cycle, checkpoints provide time to the cellular repair machinery to deal with existing DNA lesions. In the following paragraphs the pathways of DSB repair are briefly described.

1.4.2 Mechanisms of DSB Repair in Eukaryotes

1.4.2.1 A short overview of DSB repair pathways

It is important to note that DSB and other DNA damages don´t occur only as a product of exogenous insults like IR, radiomimetic drugs or topoisomerase inhibitors. The genome of a cell is in constant need for maintenance and repair due to attack by byproducts of its own metabolism, thermodynamic degradation of DNA or replication accidents. In addition DSB can be induced in a programmed manner by the cell as part of scheduled processes like the generation of antibody diversity (V(D)J recombination) or meiotic recombination. As a consequence eukaryotic cells have developed highly effective mechanisms for the management of DSB. Classically, the spectrum of DSB repair mechanisms is divided into two main categories: non-homologous end-joining (NHEJ) and homologous recombination repair (HRR). NHEJ operates throughout the cell cycle and rejoins the free ends of DSB with fast kinetics (Mao, 2008). NHEJ frequently introduces sequence alterations at the joints it generates. The chemical nature of DSB induced by IR usually necessitates some processing in order to generate ligatable ends (see Figure 4). In the case of repair by NHEJ loss or gain of bases at the molecular junction is the consequence of this processing. HRR on the other hand uses the intact sequence on a sister chromatid as template to faithfully restore the sequence around the break. The requirement of HRR for the availability of already replicated, homologous sequences restrict this repair pathway to the S- and G2- phases of the cell cycle. Since this type of repair involves search for homology, more extensive processing and synthesis, as well as the resolution of intermediary structures it is considered a slow

process in comparison to NHEJ. More recently other repair pathways, with varying fidelity and requirements for homology, have emerged diversifying the simplistic classification outlined above. Most notably, alternative pathways of NHEJ acting as backup (B-NHEJ) for the classical, DNA-dependent protein kinase (DNA-PK) dependent pathway of NHEJ (D-NHEJ), have been described. Next to different modes of HRR an additional homology directed repair process, single-strand annealing, exists as well, which uses intra-molecular homologies to seal DSB.

Although there is common consent that the majority of breaks are handled by D-NHEJ if this pathway is not compromised, an important contribution of HRR to the repair of DSB and the maintenance of genomic stability is undisputed as well. Importantly, there is a large body of evidence that suggests that HRR is the mechanism that underlies the S-Phase dependent radioresistance that can be observed in proficient cell lines (Iliakis and Nusse, 1983a; Wang, 2003b; Wang, 2004a). How the decision is made for a particular DSB to be repaired by one of the available pathways remains largely unknown, but may involve factors like lesion complexity or radiation dose. The most important DSB repair pathways and sub-pathways are described in more detail below.

1.4.2.2 D-NHEJ

D-NHEJ is considered to be the dominant pathway of DSB repair in mammalian cells, in contrast to yeast, where the dominant repair pathway is HRR (Mansour, 2008; Mao, 2008; Weterings and Chen, 2008). As indicated by its designation, it is dependent on the DNA-PK complex. This consists of the KU70/KU80 heterodimer (KU) and the large DNA-PK catalytic subunit (DNA-PK_{cs}). Unlike most other factors involved in D-NHEJ, DNA-PKcs is not found in yeast and many other lower eukaryotes and is also absent in prokaryotes. This makes it tempting to speculate, that the development of the extremely fast and efficient form of NHEJ that is found in higher eukaryotes today was made possible by this evolutionary new protein. KU is a highly abundant protein in mammalian cells that binds with strong affinity to free DNA ends. Binding of KU to DNA ends results in the recruitment of DNA-PKcs (Mladenov and Iliakis, 2011). This in turn leads to phosphorylation of multiple targets upon formation of the active holoenzyme, including

DNA-PKcs itself (Figure 9). These phosphorylations are an important step for the progression of the NHEJ process, and autophosphorylation of DNA-PKcs is believed to elicit conformational changes that allow for further steps to take place. Various factors like the polymerases μ and λ (Pol μ, Pol λ), the Artemis nuclease, terminal deoxynucleotidyl transferase (TdT) and polynucleotide kinase (PNK) are implicated in processing of DSB ends prior to rejoining by D-NHEJ (Mladenov and Iliakis, 2011). End processing by D-NHEJ usually stays limited as it only serves the cause of creating ligatable ends. Thus the extent of loss or addition of bases at junctions formed by D-NHEJ is usually relatively small (Lieber, 2010). The final ligation step is carried out by DNA Ligase IV (LIG4) aided by its interaction partners XRCC4 and XLF/Cernunnos (Figure 9).

Since D-NHEJ lacks a built-in mechanism to preserve the original sequence around the break site it is usually regarded as an error-prone repair process. Disregarding this error proneness, D-NHEJ is not an adverse process for the cell. On the contrary D-NHEJ is highly important for survival after irradiation and plays a crucial role in maintaining genome integrity and stability (Burma, 2006). Several arguments are conceivable to explain how it could have been advantageous for cells of higher eukaryotes to let an error prone repair pathway evolve to become the dominant mechanism of DSB repair. One might be that for large vertebrate genomes, which are rich in non-coding and repetitive sequences, there is a net-benefit in having an extremely fast pathway of DSB rejoining that quickly removes breaks before other accidents may occur, even if it comes at the cost of an elevated but manageable mutation rate. It is also possible that this beneficial role of D-NHEJ arises from suppression of other, more error prone pathways. Indeed, despite the conceptual capacity of D-NHEJ to rejoin unrelated ends it has been reported that components of the D-NHEJ pathway actively participate in suppressing chromosomal translocations (Simsek and Jasin, 2010).

Other nomenclature like “classical” or “canonical” NHEJ (cNHEJ) have been brought forward to name this repair pathway and discriminate it from alternative B-NHEJ pathways. In this work the term D-NHEJ will be used to refer to this pathway.

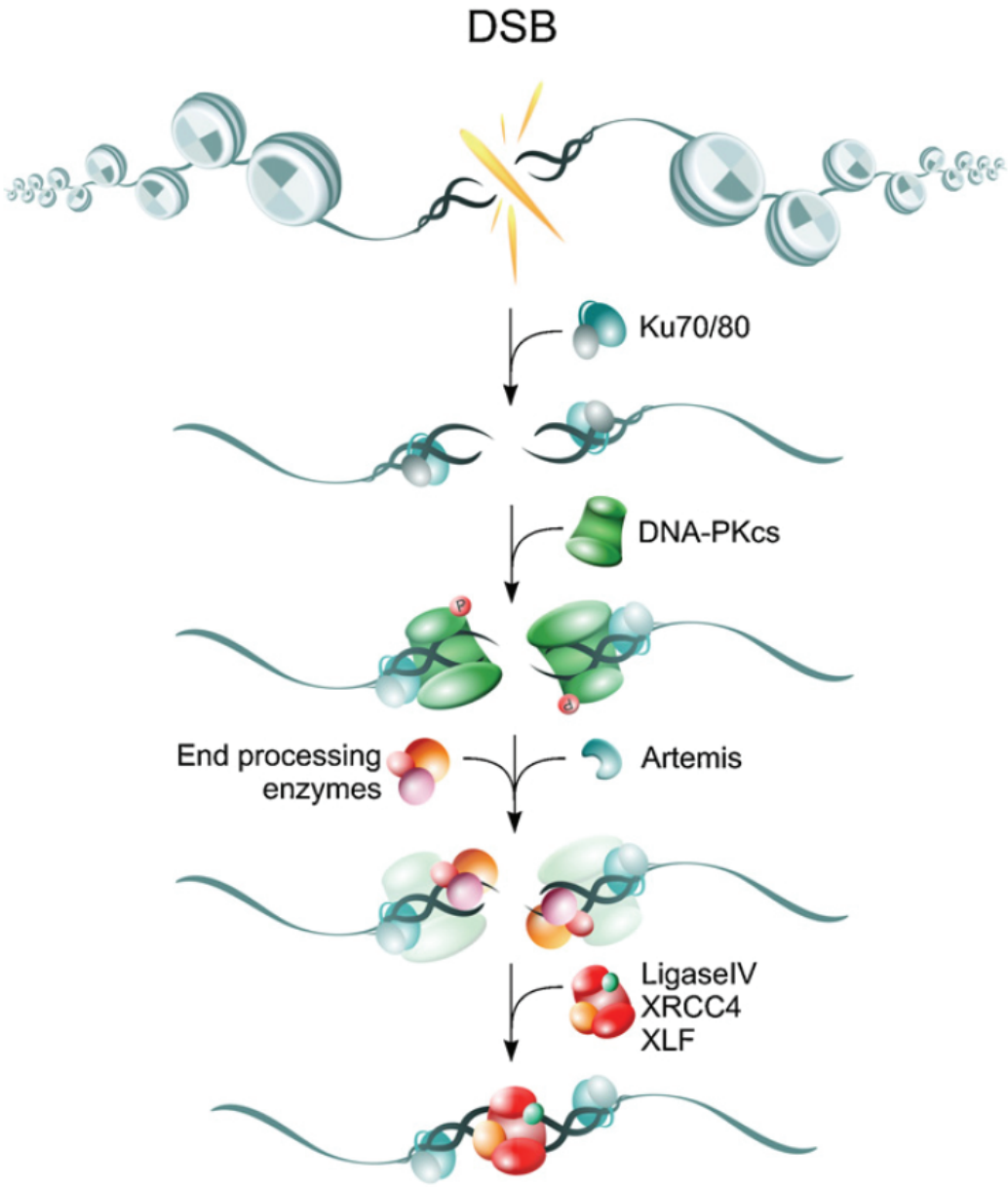

Figure 9 Schematic overview of key factors and steps of D-NHEJ D-NHEJ efficiently restores genomic integrity without ensuring sequence restoration. Association of Ku to DNA ends facilitates the recruitment of DNA-PKcs, a major kinase activated by DNA ends and contributing to the efficiency of this repair pathway. DNA-PKcs promotes end-processing by the Artemis nuclease and subsequent rejoining of broken DNA ends by the LigIV/XRCC4/XLF complex. (from (Mladenov and Iliakis, 2011))

1.4.2.3 HRR

HRR is the other main pathway of DSB repair in mammalian cells (Liang, 1998). In contrast to D-NHEJ, HRR by design faithfully restores the sequence to its original state. To achieve this goal it has to recover this information from an intact template molecule, which in the case of mitotic HRR is the sister chromatid. Intact sister chromatid sequences only start to become available with progression of DNA replication during S-phase. Thus, contrary to D-NHEJ HRR is a highly cell cycle dependent process. This dependence is not only determined by the presence of sister chromatids themselves, but is also tightly regulated through multiple PTMs that prevent crucial steps of HRR to occur outside its appropriate time window (Heyer, 2010; Mladenov, 2013). For HRR to commence an essential step is the creation of a long single-stranded 3´-overhang that can be used to find homology in an annealing based process. This 3´-overhang is created through nucleolytic resection of the 5´-end of the break (Symington and Gautier, 2011). Resection of DNA ends is tightly regulated in a cell cycle phase dependent manner and is restricted to the S and G2 phase (Huertas, 2010). Thereby the regulation of end-resection is likely to be one of the main determinants of the cell cycle specific constrain of HRR mentioned earlier (Ira, 2004). A key mechanism of the control of end resection is the balance between the actions of two proteins antagonizing each other: 53BP1 and BRCA1 (Bunting, 2010).

The opposing roles of these two proteins are impressively illustrated by a phenotype of “synthetic viability” in mice. Mice with a certain BRCA1 mutation display mid-gestational lethality. When these mice are placed in a 53BP1 deficient background this lethality is rescued (Cao, 2009). It has been shown that 53BP1 inhibits end resection, via its effector RIF1, thereby inhibiting HRR (Bunting, 2010; Escribano-Diaz, 2013). BRCA1 on the other hand promotes end resection, thereby favoring HRR over D-NHEJ (Bouwman, 2010; Bunting, 2010). This end resection promoting activity depends on interaction of BRCA1 with CtIP and the MRN complex (Chen, 2008). This interaction in turn is regulated by phosphorylation of CtIP on Serine 327, which is executed by CDKs in the S and G2 phase (Yu and Chen, 2004). Thus, in G1 53BP1 prevents end-resection, prohibiting HRR. However, when cells progress into S and G2 the phosphorylation of CtIP bestows BRCA1 with the power to alleviate the inhibition exerted by 53BP1 and to

stimulate end resection. Although important, the phosphorylation of CtIP is not the only mechanism that supports end-resection in S and G2, but is complemented by a plethora of further cell cycle dependent PTMs of various proteins (Mladenov, 2013). Once a stretch of single-stranded DNA (ssDNA) has formed it will be coated with the hetero-trimeric replication protein A complex (RPA). Coating with RPA prevents further degradation and formation of intramolecular secondary structures (Eggler, 2002). However, for HRR to progress RPA has to be displaced by RAD51, the central recombinase protein in HRR. This process is mediated by the BRCA2 (breast cancer 2, early onset) protein (Yang, 2005; San Filippo, 2008). RAD51 forms a helical nucleoprotein filament with ssDNA that is capable of searching for homologous sequences and invasion of another double-stranded DNA (dsDNA) molecule (Raderschall, 1999; Aly and Ganesan, 2011). Besides core factors like RAD51 and BRCA2 many other factors participate in or facilitate these intricate reactions. These include the members of the RAD52 epistasis group (RAD50, RAD52, RAD54, MRE11), the RAD51 paralogs (RAD51B, C, D and XRCC2 and XRCC3) and CtIP the mammalian Sae2 homolog (San Filippo, 2008; Huertas and Jackson, 2009; Heyer, 2010). Strand invasion leads to formation of a structure called the displacement loop (D-loop). The 3´-end of the invading strand serves to prime DNA synthesis using the homologous sequence as template. Afterwards, depending on several factors, repair by homologous recombination can take several routes:

In the synthesis dependent strand annealing (SDSA) sub-pathway the invading strand is simply disengaged from the donor duplex after DNA synthesis is completed and re-anneals with the complementary strand on the opposing side of the break. Gaps are filled-in by another round of DNA synthesis and the remaining nicks are finally ligated (Figure 10).

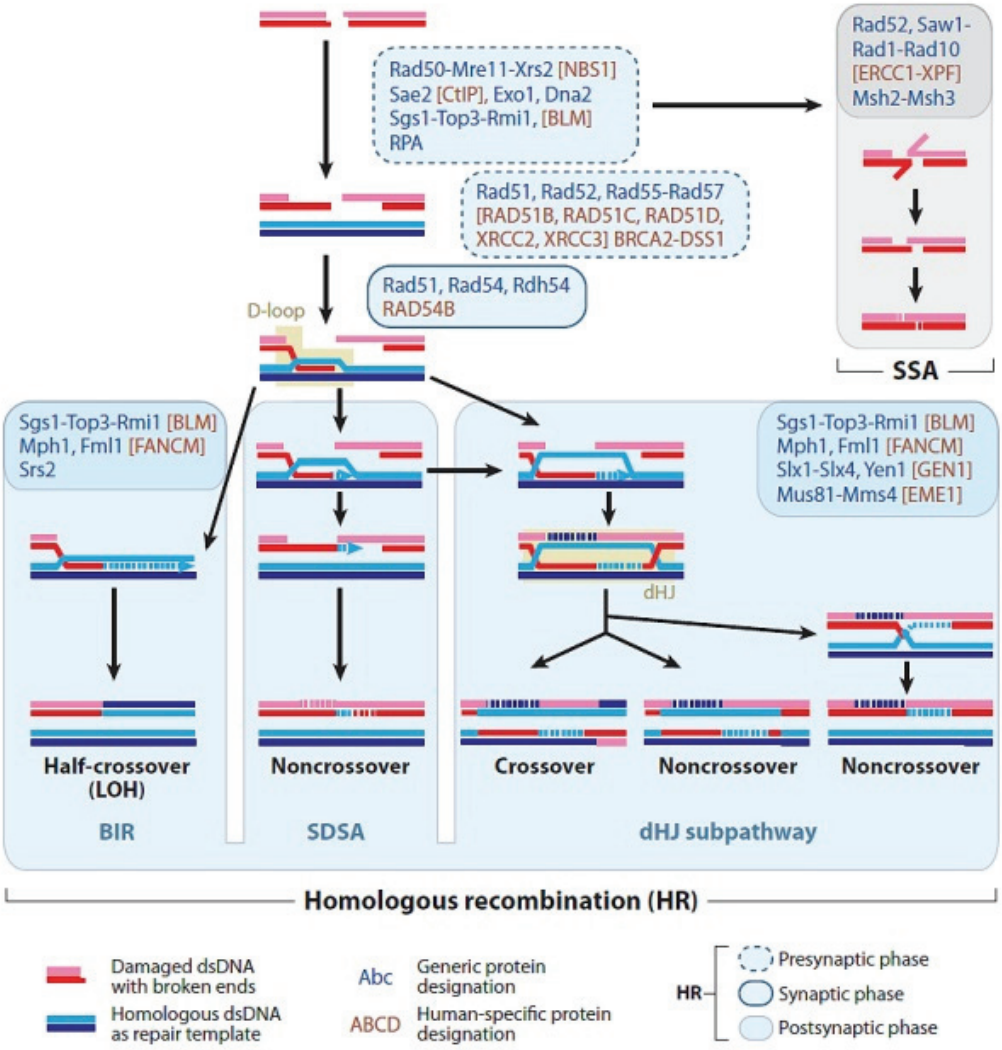

Figure 10 Steps and outcomes of homology directed repair pathways. Protein names refer to the budding yeast *Saccharomyces cerevisiae* (*blue*). Where different in human, names (*brown*) are given in brackets. For proteins without a yeast homolog, brackets for human proteins are omitted. Broken lines indicate new DNA synthesis and stretches of heteroduplex DNA. Abbreviations: BIR, break-induced replication; dHJ, double Holliday junction; LOH, loss of heterozygocity; SDSA, synthesis-dependent strand annealing; SSA, single-strand annealing. (modified from(Heyer, 2010))

In the double Holliday junction sub-pathway the second end of the DSB is captured by the displaced strand and elongated using the latter as a template. After DNA synthesis is

completed on the originally invading strand it is ligated with the 5´-prime end at the opposite side of the break. In this way a complex structure called a double Holliday junction (dHJ) is formed. Nucleolytic incision is required to resolve this structure and several enzymatic activities, like the Bloom's helicase (BLM) and the Mus81/Eme1 have been implicated in this process. Resolution of a dHJ can be achieved in several ways and can yield crossover or non-crossover products (Figure 10). DNA synthesis as it occurs during SDSA or dHJ HRR is limited to a few hundred bases, in contrast to BIR where much longer sequences are synthesized *de novo*.

Recently, in a collaborative effort of our laboratory with the group of Thanos Halazonetis, it could be demonstrated that the BIR pathway is important for genomic stability under conditions of DNA replication stress (Costantino, 2014). In yeast BIR has been characterized as the pathway that repairs one-ended DSB arising when replication forks collapse. This frequently occurs in cells that suffer from replication stress, as it is prevalent in cancer as well. A one-ended DSB cannot be repaired by a joining mechanism. Instead in BIR the break end is used to prime new long range DNA synthesis up to the end of the chromosome after strand invasion (Malkova, 2001; Davis and Symington, 2004; Malkova, 2005)(Figure 10). In this way sequences of 100 kB or more can be synthesized in yeast. BIR requires most essential replication factors as well as the non-essential Polδ subunit Pol32/POLD3 (Wang, 2004c; Lydeard, 2007; Lydeard, 2010). Still, DNA synthesis during BIR does not seem to include assembly of a conventional replication fork. Instead, DNA is replicated in a conservative manner, by a migrating bubble mechanism accompanied by continuous lagging strand synthesis (Donnianni and Symington, 2013; Saini, 2013). In yeast this mechanism has been associated with extensive loss of heterozygosity (LOH), formation of non-reciprocal translocations, inversions and tandem duplications (Smith, 2007; Payen, 2008; Ruiz, 2009; Mizuno, 2013). We could show that in a human model of replication stress these rearrangements are induced and that their frequency is reduced after silencing of the essential BIR factor POLD3 (Costantino, 2014).

It is intriguing that HRR, while being the principal pathway in bacteria and lower eukaryotes and also the only truly faithful DSB repair process available, seems to have been pushed to the background by the emergence of D-NHEJ in higher eukaryotes. A

possible rationalization for this observation would be that HRR is not such an error-free process as it may appear at first glance. While it is true that HRR is the only process that can reliably accomplish the faithful restoration of sequence at complex DSB, there is also potential danger associated with this process. The human genome contains a high amount of shorter and longer repetitive sequences. These include so-called segmental duplications or low copy repeats, which can serve as targets for non-allelic homologous recombination (NAHR). The presence of such sequences may have made it favorable to exert a tighter control about homology directed repair. Indeed several syndromes exist that arise due to NAHR during meiosis (Liu, 2012a). NAHR is believed to be restricted to gametogenesis in mammals. However, this may be a consequence of the cell cycle specific regulation of HRR. If HRR was unleashed in G1/G0 cells, it would have to resort to the use of either the homologous chromosome or dispersed sequence duplications as recombination substrates. The first would result in LOH, the latter in NAHR (Carr and Lambert, 2013).

HRR has gained a lot of attention as a target for radiosensitization recently (Mladenov, 2013). A number of compounds that interact more or less directly with the DNA repair machinery or checkpoint and cell cycle control mechanisms (Asaad, 2000; Bohm, 2006; Morgan, 2010; Takagi, 2010; Meike, 2011; Prevo, 2012), as well as multiple treatments with less obvious connections to this repair pathway have been shown to elicit radiosensitization by inhibition of HRR (Chinnaiyan, 2005; Noguchi, 2006; Adimoolam, 2007; Murakawa, 2007; Li, 2008; Choudhury, 2009).

1.4.2.4 B-NHEJ

To date the description of back-up mechanisms of NHEJ remains incomplete, although an increasing number of proteins is emerging that may play roles in non-homologous DSB repair processes in the absence of D-NHEJ. Other nomenclature than B-NHEJ has been proposed to describe these processes, including alternative end-joining (A-EJ), alternative non-homologous end-joining (A-NHEJ) or microhomology mediated end-joining (MMEJ). B-NHEJ has been initially described based on the observation that mutant cell lines deficient in components of the main D-NHEJ machinery - although

severely impaired in the fast rejoining of DSB - are still capable of repairing DSB and eventually rejoin almost all breaks after prolonged repair times (Nevaldine, 1997; Kabotyanski, 1998; Wang, 2001b; Wang, 2003a; Iliakis, 2004). Defects in HRR did not influence residual repair suggesting that another mechanism of NHEJ, acting as a back-up for D-NHEJ, was at work (Wang, 2001a).

Later studies showed the participation of alternative pathways of NHEJ in physiological processes, like the generation of antibody diversity through V(D)J recombination (Verkaik, 2002; Corneo, 2007), or in class switch recombination (Soulas-Sprauel, 2007; Yan, 2007), when the classical DNA-PKcs dependent NHEJ was inactivated.

There is evidence that B-NHEJ has an increased preference for the usage of short sequence homologies (so called microhomologies) for the formation of joints (Roth and Wilson, 1986; Bogue, 1997; Kabotyanski, 1998), but it is not absolutely dependent on them (McVey and Lee, 2008; Fattah, 2010; Mansour, 2010). Typically, homologies <5bp sometimes <10bp are defined as microhomologies. It has been reported that microhomology mediated B-NHEJ events benefit from resection of DNA ends (Xie, 2009; Bothmer, 2010; Lee-Theilen, 2011; Symington and Gautier, 2011). This is not surprising considering that resection would be a prerequisite for detection and annealing of homologous sequences. Nevertheless, many B-NHEJ mediated junctions harbor large deletions without showing microhomology signature, even when microhomology would have been available. This suggests that end-resection plays a more general role in B-NHEJ than to purposefully reveal microhomologies. The presence and usage of microhomologies however could facilitate ligation of ends by holding them together.

It is possible that two or more B-NHEJ sub-pathways exist, microhomology dependent and independent ones, which fulfill end-joining tasks in the absence of other functional repair. Disregarding possible dependency on microhomology, repair by B-NHEJ has a characteristic tendency to cause large scale chromosomal alterations. Translocations and extensive deletions are found frequently when repair is carried out by B-NHEJ (Soulas-Sprauel, 2007; Yan, 2007; Robert, 2009; Boboila, 2010; Simsek and Jasin, 2010). Thus, B-NHEJ now is considered to be a major contributor to chromosome aberration formation and genomic instability (Mladenov and Iliakis, 2011; Symington and

Gautier, 2011; Mladenov, 2013). This places B-NHEJ not only in the center of cell killing during radiotherapy but also at the heart of carcinogenesis (Greaves and Wiemels, 2003; Edwards, 2008).

B-NHEJ can potentially act throughout the cell cycle, but does display remarkable variations in its efficiency depending on the position in the cycle. In G2 for example B-NHEJ is enhanced (Wu, 2008a; Wu, 2008b). This might be explainable with increased end-resection activities during G2 that facilitate B-NHEJ. In growth inhibited plateau phase or serum starved cells on the other hand B-NHEJ is strongly reduced (Windhofer, 2007; Singh, 2011). Although B-NHEJ is observable best on a D-NHEJ deficient background acting as a backup for this pathway, its association with end resection makes it easy to imagine that it also takes advantage of abortive HRR events (Symington and Gautier, 2011; Dueva and Iliakis, 2013).

B-NHEJ can be best observed when the major beneficial repair processes are impaired globally genetically or by chemical inhibition. Nevertheless it is likely that B-NHEJ can also occur in repair proficient background locally at sites of repair accidents, possibly also accounting for a majority of chromosomal translocations found in repair proficient cells. Candidates for proteins involved in B-NHEJ include LIG3 (Wang, 2005b; Simsek, 2011), LIG1 (Boboila, 2012), Histone 1 (Rosidi, 2008), PARP1 (Wang, 2006b; Robert, 2009; Wray, 2013), MRE11 (Xie, 2009) and CtIP (Zhang and Jasin, 2011).

1.4.2.5 SSA

Single-strand annealing (SSA) is another homology directed cellular DSB repair process besides HRR (Figure 10). In contrast to HRR, SSA does not favor homologous sequences on other DNA molecules, but preferentially on the same molecule where the DSB occurred (Ivanov, 1996; Symington, 2002). Similar to HRR it requires extensive resection to reveal those homologies, but unlike HRR the long 3´-ssDNA is not used for initiation of repair synthesis (Fishman-Lobell, 1992; Sugawara and Haber, 1992). Instead two homologous stretches of sequence are annealed, tails/flaps are removed and gaps are filled in (Symington, 2002). This inevitably leads to the loss of the intervening sequences, which may be hundreds of base pairs long. Thus SSA is a highly mutagenic process with the propensity to cause large deletions. Worse still, due to the

presence of vast numbers of dispersed repetitive elements like LINES and SINES in mammalian genomes SSA can also cause translocations (Elliott, 2005; Weinstock, 2006). SSA is strongly suppressed by HRR and if core components of this faithful homology directed repair pathway, like RAD51 or BRCA2, are inactivated the frequency of SSA event multiplies 4-8 fold (Tutt, 2001; Stark, 2004; Mansour, 2008; Manthey and Bailis, 2010). Similar to HRR, SSA shows strong cell cycle dependence, possibly due to the cell cycle regulated efficiency of end resection activities (Frankenberg-Schwager, 2009; Trovesi, 2011). Important proteins implicated in SSA in mammalian cells are RAD52, the ERCC4/XPF-ERCC1 endonuclease and RPA (Symington, 2002; Stark, 2004; Al-Minawi, 2008) .

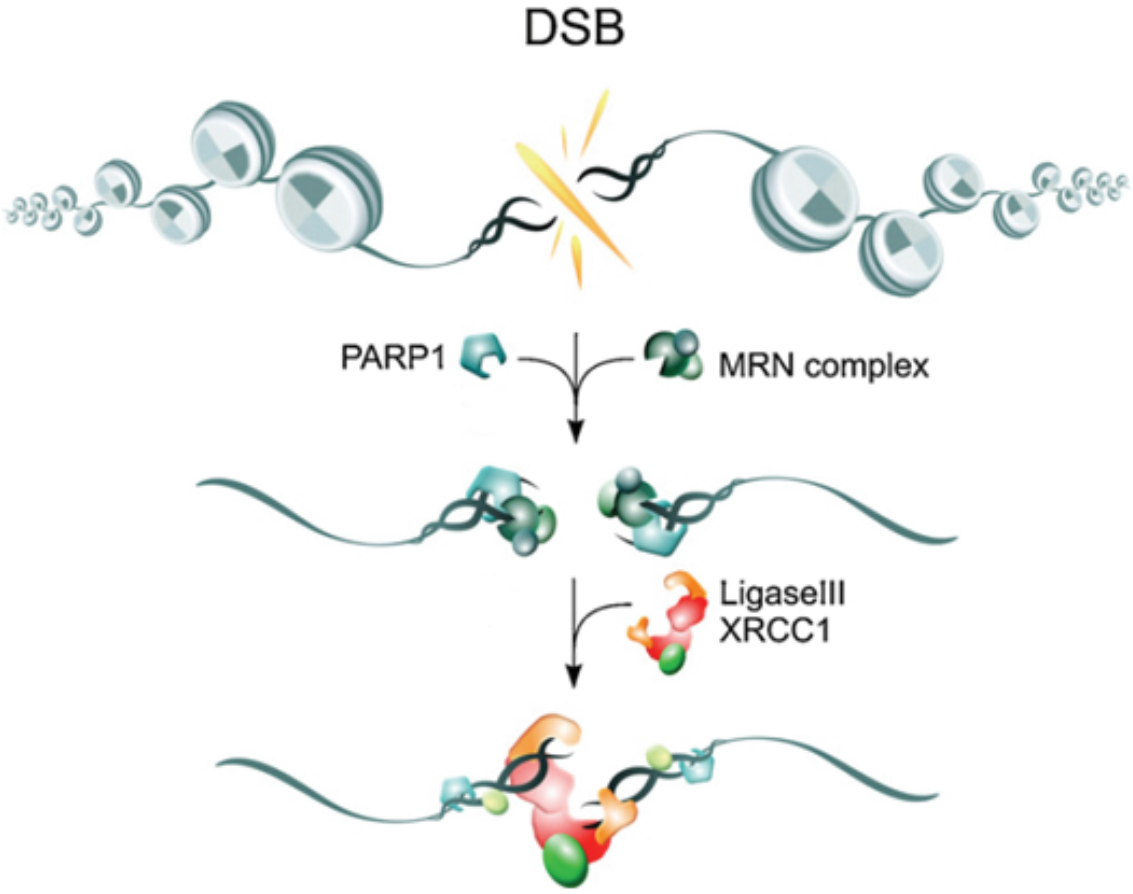

Figure 11 Schematic overview of key factors and steps of B-NHEJ. The enzymatic activities implicated in B-NHEJ are shown together with their possible contributions in the process. (modified from (Mladenov and Iliakis, 2011))

1.5 The role of DSB in cell killing and cancer induction by IR

1.5.1 The DSB as cancerogenic lesion

Only the breakage and rejoining of double-stranded DNA can eventually account for the gross chromosomal abnormalities that can be induced by ionizing radiation and which are also a common hallmark of cancer. There are certain chromosomal translocations that are known to be potent inducers of carcinogenesis, e.g. the t(9;22) translocation – also known as Philadelphia chromosome - that is found in >95% of patients with chronic myeloid leukemia (CML)(Greaves and Wiemels, 2003; Nambiar and Raghavan, 2011). This highlights the important role of DSB, not only for the killing of cells, but also for carcinogenesis. Still, although IR is a mutagenic agent that induces DSB, base damages and other lesions that can drive cancer development, it is the potentially lethal consequences of the DSB that make IR a valuable tool in cancer therapy.

1.5.2 The DSB as lethal lesion

Complex DSB as a product of IR are potent inducers of cell death. Although base damages and SSB are induced at a much higher frequency by IR than DSB, their contribution to the cytotoxicity of IR is far less than that of DSB (Iliakis, 1991; Foray, 1997a; Nikjoo, 1999). It has been shown that a single unrepaired DSB can be sufficient to kill an eukaryotic cell (Frankenberg, 1981). The importance of DSB in cell killing is also highlighted by the pronounced radiosensitivity of cells with defects in DSB processing that is found in several human syndromes or mutant cell lines (Jeggo and Kemp, 1983; Joubert, 2008; Mladenov, 2013). However, there is not a clear general correlation between DSB induction and rejoining (as measured by physical methods) and cell killing respectively survival. While cell lines that show defects in the rejoining of DSB are radiosensitive, not all radiosensitive cell lines have clear defects in the rate with which they rejoin DSB. A better correlation exists with the induction of chromosomal aberrations. So how can the particularly detrimental effects of the DSB be explained? DSB can result in the loss of vital genetic material in subsequent cell divisions if they remain un-rejoined, while rejoining of the wrong DNA ends can result in chromosomal

aberrations like translocations and chromosome or chromatid fusions that may cause cell death or lead to carcinogenesis (Bryant, 1988; Obe, 1992; Ferguson and Alt, 2001). Therefore the DSB can with high certainty be assumed to be the lesion underlying the formation of chromosomal aberrations and - via this route - cell killing (Bender, 1974; Natarajan, 1980; Radford, 1985; Iliakis, 2004).

1.6 Evidence connecting DSB repair to cellular radiosensitivity and PLD

It is known that the main genetic determinants of cellular sensitivity to IR are genes whose products are involved in the detection and repair of DSB, or those that participate in the signaling and control of cell cycle progression in response to DNA damage (checkpoints) (Jeggo and Lavin, 2009b). These genes include *ATM* (Foray, 1997b), *ATR* (Wang, 2004b), *CHK1* (Wang, 2005a), *BRCA1&2* (Foray, 1999), *LIG4* (Plowman, 1990; Badie, 1995), *MRE11* (Matsumoto, 2011), *NBS1* (Carney, 1998), *RAD50* (Waltes, 2009), *RAD51* (Liu, 2011), *RNF168* (Stewart, 2007; Stewart, 2009), *XRCC2&3* (Cui, 1999), Artemis (Moshous, 2001), *DNA-PKcs* (Hendrickson, 1991) and *KU* (Tzung and Rünger, 1998) (reviewed in (Jeggo and Lavin, 2009a; Foray, 2012)). The presence of core components of both major DSB repair pathways in this list indicates that HRR, as well as NHEJ play important roles in conferring radioresistance to the cell. Thus, both pathways present as potentially promising targets for cell radiosensitization (Yoshihisa Matsumoto, 2013).

DSB are also the best candidate for the lesion constituting PLD due to their cytotoxic effects. Pathways of DSB repair can be envisioned to account for repair, as well as for fixation of PLD. The former occurring when the correct ends of DSB are rejoined with high fidelity, the latter when repair of DSB either entirely fails, or when misrejoining occurs that results in the formation of lethal chromosomal aberrations. These considerations are reinforced by observations that implicate NHEJ and HRR in PLD repair and the cell cycle dependent fluctuations in the sensitivity to IR.

XR-1 cells for example are deficient in XRCC4, a component of D-NHEJ. These cells are extremely sensitive to IR in G1, but only moderately sensitive in S/G2. Furthermore, they don´t appear to repair PLD in G1/G0, but show substantial repair of PLD in S/G2 that operates with a halftime of approximately 5h (Stamato, 1988). In the parental cell line on the other hand, much of the PLD repair occurs in G1 and repair halftimes are about 1h (Stamato, 1988). The cell cycle dependence and kinetics of PLD repair in the mutant and parental cell line here reflect exactly what would to be expected, if DSB constituted PLD and repair was carried out by NHEJ and HRR. In the mutant only the slow HRR pathway, which is restricted to S/G2, would be available for repair. In the parental cell line the fast NHEJ pathway, which dominates repair throughout the cell cycle would be capable of repairing most of the PLD.

Further evidence is provided by the hamster cell line irs-1, which is deficient for the RAD51 paralog XRCC2. In irs-1, the S-phase dependent increase in radiosensitivity usually observed in hamster-cells is abolished (Cheong, 1994). Similarly treatment with caffeine, which exerts an inhibitory effect on HRR, flattens the fluctuations of radiosensitivity throughout the cycle in cells that are proficient for this pathway (Beetham and Tolmach, 1984; Asaad, 2000). This list could be considerably extended with various other examples of mutant cell lines and treatments demonstrating the dependence of radiosensitivity during the cell cycle and PLD repair on the repair of DSB (Sonoda, 2006; Tamulevicius, 2007).

Taken together, a large body of evidence suggests that individual differences in cell-intrinsic sensitivity to IR, the fluctuations in radiosensitivity during the cell cycle and the repair of PLD depend largely on the ability of a cell to detect and repair DSB (Roberts, 1999; Joubert, 2008; West and Barnett, 2011). Thus, pathways of DSB repair present promising targets for the modulation of cellular radiosensitivity to killing for the optimization of radiotherapy (Yoshihisa Matsumoto, 2013).

1.7 Synergistic interactions between IR and nucleoside analogs

A number of NAs have been reported to show synergistic action with IR *in vitro* (Dewey and Humphrey, 1965; Iliakis, 1989a; Iliakis, 1989b; Gregoire, 1994; Shewach, 1994; Buchholz, 1995; Meike, 2011). Some of these drugs have been evaluated as radiosensitizers in clinical trials (Goffman, 1991; Miser, 1992; Bartelink, 1997; Aguilar-Ponce, 2004; Nitsche, 2008) and others already belong to the standard of care as concurrent treatments for some diseases (Vallerga, 2004; Gurka, 2013; Lee, 2013). Despite their great clinical promise the mechanisms of radiosensitization by many NAs remain poorly understood. In the following the NAs used in this study are described with respect to their potential radiosensitizing activities.

Early studies could show that ara-A is a particularly effective inhibitor of PLD repair (Iliakis, 1980; Iliakis and Bryant, 1983; Iliakis and Ngo, 1985; Chavaudra, 1989; Iliakis, 1989b; Little, 1989). In comparative studies with other inhibitors of replication and DNA synthesis ara-A consistently showed the strongest inhibitory effect on the repair of PLD (Iliakis and Bryant, 1983; Iliakis, 1989b). In the studies cited above plateau phase cultures were used for the generation of the results. Reports about radiosensitization by ara-A in actively cycling populations are scarcer (Iliakis and Nusse, 1983b; Chavaudra, 1989; Mustafi, 1994). Ara-A has also repeatedly been reported to inhibit the repair of chromosomal breaks (Bryant, 1983; Mozdarani and Bryant, 1987; Iliakis, 1988b; MacLeod and Bryant, 1992; Okayasu and Iliakis, 1993; Bryant, 2004). Intriguingly, the number of exchange type aberrations was observed to increase at the same time in some studies (Bryant, 1983; Mozdarani and Bryant, 1987). Taken together, this suggests that ara-A interferes with pathways of DSB repair that are involved in the repair of PLD and chromosomal breaks.

Radiosensitization by fludarabine has been demonstrated in numerous in vitro studies (Gregoire, 1994; Laurent, 1998; Nitsche, 2008) and also been tested in first clinical studies (Gregoire, 2002; Nitsche, 2012). Radiosensitization by fludarabine was found not to coincide with inhibition of DSB repair measured by pulsed field gel electrophoresis (PFGE) (Gregoire, 1998).

Ara-C is generally not recognized as a radiosensitizer and there are no clinical studies assessing such a potential. However, there are some reports that show a comparatively weak inhibition of PLD repair by ara-C (Iliakis and Bryant, 1983; Nakatsugawa, 1984; Iliakis, 1989b).

The in vivo radiosensitizing potential of Gemcitabine has been tested extensively in preclinical studies (Shewach, 1994; Lawrence, 1996; Latz, 1998; Rosier, 1999; Pauwels, 2003) and confirmed in numerous clinical trials (Eisbruch, 2001; Aguilar-Ponce, 2004; Evans, 2008). Concurrent chemo radiation with gemcitabine is currently considered as standard treatment for locally advanced pancreatic cancers in North America (Gurka, 2013). Like for fludarabine, radiosensitization by gemcitabine was found not to coincide with inhibition of DSB repair measured by (PFGE) (Gregoire, 1998).

Previous reports and preliminary data generated in the beginning of this study suggested that radiosensitization elicited by ara-A exceeds the effects of fludarabine, ara-C and gemcitabine. Thus, we chose to use ara-A as a model compound in most of our experiments to study NA mediated radiosensitization and to investigate the mechanisms that underlie its superior sensitization characteristics.

2 Aims and scope of this work

Improving the treatment of cancer belongs to the most important and most challenging tasks of modern medicine. The diversity of malignant entities and the variety of possible steps that can lead to carcinogenic transformation make solid cancers a highly heterogeneous group of diseases. The combination of different treatment modalities is one of the most promising current approaches to achieve improvements in cancer treatment for a broad range of patients. Radiotherapy is one of the most efficient means to eradicate cancer cells. However, some cancers are relatively radioresistant and even when tumors can be treated successfully, surviving cells are often responsible for relapses. Combining IR with drugs that sensitize targeted cancer cells to killing can significantly improve the outcome of radiotherapy.

NAs represent a large group of anticancer drugs, several members of which have been shown to possess radiosensitizing potential. Aim of the present study was to elucidate the mechanisms of radiosensitization by NAs using as a model compound ara-A, due to its superior radiosensitizing properties.

The DSB is the most detrimental IR-induced lesion, whose misrepair underlies cell killing and likely also ara-A radiosensitization. Therefore, we studied in detail the effects of ara-A on the main pathways of DSB repair: HRR, NHEJ and B-NHEJ, placing particular emphasis on cell cycle specific effects. To this end, we employed advanced methods of microscopy, flow cytometry and various cell biological and biophysical techniques. This approach led to the generation of a wealth of data that allowed the development of a mechanistic model of ara-A radiosensitization. This model invokes the selective inhibition of the error-free DSB repair pathway HRR and the parallel activation of the error-prone DSB repair pathway B-NHEJ by ara-A. This information also formed the basis for a comparative analysis of the mode of action of selected other NAs.

The efficiency of concurrent chemo-radiotherapy can greatly benefit from increased knowledge about mechanisms of action of radiosensitizers. We hope that the information generated as part of the present thesis will assist in the identification and selection of drugs able to maximize the radiation response of tumors and the optimization of treatment schedules.

3 Materials and Methods

3.1 Materials

Table 3.1: Laboratory Apparatuses

Laboratory Apparatus	Model	Manufacturer
Cell counter	Multisizer™ 3	Beckman Coulter Inc.

Cell Sorter	Epics Altra	Beckman Coulter Inc.
Centrifuge	Multifuge 3 S-R	Heraeus
Centrifuge	Avanti J-20XP	Beckman Coulter Inc.
Centrifuge	Tabletop GS-6R	Beckman Coulter Inc.
Elutriation Centrifuge	Beckman J2-21M centrifuge	Beckman Coulter Inc.
CO2- incubator	Hera Cell 240	Heraeus
Confocal Microscope	TCS-SP5	Leica Microsystems
Dry blotting system	iBlot	Invitrogen
Flow Cytometer	Coulter XL-MCL	Beckman Coulter Inc.
Flow Cytometer	Gallios	Beckman Coulter Inc.
Imaging scanner	Typhoon 9400	GE Healthcare
Infrared imaging system	Odissey	LI-COR
Laboratory microscope	Inverted phase contrast	Olympus
Laminar Flow Hood	Hera safe	Heraeus
Liquid Scintillation counter	TriCarb1900 TR	Packard
Magnetic stirrer	MR Hei-Mix L	Heidolph
Microtiter Pipettes	Rainin	
Mini centrifuge	Biofuge fresco	Heraeus

Molecular Imager	VersaDoc	Bio-Rad
Electroporation device	Nucleofector I	Lonza AG
pH-Meter	WTW	InoLab
Photometer	Nanodrop	Thermo Scientific
Photometer	UV-2401 PC	Shimadzu
Pipet Aid	Express	Falcon
Rocky Shaker	3D	Peter Oehmen
SDS PAGE equipment	Mini Protean	Bio-Rad
X-ray tube	Isovolt 320HS	General Electric-Pantak

Table 3.2: Chemicals

Chemical	Provider
1-β-D-arabinofuranosylcytosine	Sigma-Aldrich, Steinheim, Germany
2-Mercaptoethanol	Sigma-Aldrich, Steinheim, Germany
2´-deoxy-2´,2´-difluorocytidine	LC Laboratories, USA
9-β-D-arabinofuranosyl-2-fluoro-adenine	Metkinen, Finland
9-β-D-arabinofuranosyladenosine	TCI America, USA
Aphidicolin	SERVA, Heidelberg
Boric acid	Roth, Karlsruhe, Germany
BSA [Bovine serum albumin fraction V]	Roth, Karlsruhe, Germany
Bromophenol blue	Sigma-Aldrich, Steinheim, Germany

Coomassie brilliant blue R 250	SERVA Electrophoresis GmbH, Heidelberg, Germany
Crystal violet	Merck, Darmstadt, Germany
DAPI	Sigma-Aldrich, Steinheim, Germany
Dichlorodimethylsilane	Merck, Darmstadt, Germany
DMSO [Dimethyl sulfoxide]	Sigma-Aldrich, Steinheim, Germany
DMEM [Dulbecco's Modified Eagle Medium]	Gibco™, Invitrogen, Karlsruhe, Germany
DTT [Dithiothreitol]	Roth, Karlsruhe, Germany
EtOH [Ethanol]	Sigma-Aldrich, Steinheim, Germany
EtBr [Ethidium bromide]	Roth, Karlsruhe, Germany
EDTA [Ethylenediaminetetraacetic acid]	Roth, Karlsruhe, Germany
FBS [Fetal bovine serum]	Biochrom, Berlin, Germany; Gibco™, Invitrogen, Karlsruhe, Germany
FBS [Fetal bovine serum]	PAA, Coelbe, Germany
FBS [Fetal bovine serum]	Gibco™, Invitrogen, Karlsruhe, Germany
HEPES	Roth, Karlsruhe, Germany
Hydroxyurea	Sigma-Aldrich, Steinheim, Germany
Isopropanol	Sigma-Aldrich, Steinheim, Germany
KCl	Roth, Karlsruhe, Germany
KH2PO4	Roth, Karlsruhe, Germany
KOH	Roth, Karlsruhe, Germany
LMA [Low melting agarose]	Roth, Karlsruhe, Germany
Mc Coy's 5A medium	Sigma-Aldrich, Steinheim, Germany
Methanol	Sigma-Aldrich, Steinheim, Germany
MgCl2	Merck, Darmstadt, Germany
NaCl	Roth, Karlsruhe, Germany

NaHCO3	Roth, Karlsruhe, Germany
NaH2PO4	Roth, Karlsruhe, Germany
Na2HPO4	Roth, Karlsruhe, Germany
NLS [N-lauroyl sarcosine]	Merck, Heidelberg, Germany
Non-fat dry milk	Roth, Karlsruhe, Germany
NU7441	Tocris Bioscience, Ellisville, MO, USA
Paraformaldehyde	Honeywell Specialty Chemicals GmbH, Seelze, Germany
Penicillin	Sigma-Aldrich, Steinheim, Germany
Phenylmethanesulfonylfluoride	Roth, Karlsruhe, Germany
Phosphoric acid	Roth, Karlsruhe, Germany
Poly-L-lysine	Biochrom AG, Berlin, Germany
ProLong® Gold antifade reagent	Invitrogen, Karlsruhe, Germany
PI [Propidium iodide]	Sigma-Aldrich, Steinheim, Germany
Protease from *S. griseus*	Sigma-Aldrich, Steinheim, Germany
Protease inhibitor cocktail	Sigma-Aldrich, Steinheim, Germany
Puromycin	Sigma-Aldrich, Steinheim, Germany
RIPA buffer	Thermo Scientific, Schwerte, Germany
RNase A	Sigma-Aldrich, Steinheim, Germany
Scintillation Cocktail UniSafe1	(Zinsser Analytic)
SEAKEM LE® Agarose	Lonza
SeeBlue plus2 pre-stained protein ladder	Invitrogen, Karlsruhe, Germany
SDS [Sodium dodecyl sulfate]	Roth, Karlsruhe, Germany
Streptomycin	Calbiochem, Invitrogen, Karlsruhe, Germany
Tetramethylethylenediamine	Sigma-Aldrich, Steinheim, Germany

Trichloric acid	Roth, Karlsruhe, Germany
TRIS [Tris(hydroxymethyl)aminomethane]	Roth, Karlsruhe, Germany
Tris-HCl	Roth, Karlsruhe, Germany
Triton X-100	Sigma-Aldrich, Steinheim, Germany
Trypsin	Biochrom AG, Berlin, Germany
Tween 20	Roth, Karlsruhe, Germany

Table 3.3: Software

Software	Provider	Use
ImageQuant™ 5.0	GE Healthcare Life Sciences, USA	Quantification PFGE Gels
SigmaPlot® 11.0	Systat Software, USA	Graphic Presentation, Curve fitting
ImarisXT® 6.0	Bitplane Scientific Software, Switzerland	Immunofluorescence analysis (Foci)
Microsoft Excel 2010®	Microsoft Corp., USA	Data analysis and calculations
Wincycle™	Phoenix Flow Systems, USA	Cell cycle analysis
Kaluza 1.2	Beckman Coulter Inc., USA	Flow Cytometry analysis (Gallios)
EXPO32™ MultiComp V1.2	Beckman Coulter Inc., USA	Flow Cytometry analysis (XL-MCL/ALTRA)
Adobe® Creative Suite® 5.5	Adobe Systems Inc., USA	Illustrations, presentation, cropping

ApE A plasmid editor V1.17	Freeware, M.W. Davis	Sequence viewing/editing/alignments
EndNote X4	Thomson Reuters	Literature Bibliography

3.2 Methods

3.2.1 Cell culture

3.2.1.1 Cell lines and passage

A549 human non-small cell epithelial lung carcinoma cells (American Type Culture Collection; CCL-185^{TM}; positive for p53) were maintained in McCoy´s 5A medium. Stably transfected U2OS human Osteosarcoma cell lines (kindly provided by Jeremy Stark, Ph.D.; Beckman Research Institute of City of Hope, Duarte, CA) carrying different reporter substrates (279A/EJ2-GFP; 280A/EJ5-GFP; 282C/DR-GFP; 283C/SA-GFP) for the repair of I-SceI induced DSB were cultured in McCoy´s 5A medium containing 2 µg/ml puromycin. HCT116 human colon carcinoma cell lines were cultured in McCoy´s 5A medium. The following HCT116 cell lines were used in these studies: HCT116 (HCT116 WT), as well as HCT116 Lig4$^{-/-}$ (HCT116 Lig4) (Fattah, 2010) and HCT116 DNA-PKcs$^{-/-}$ (HCT116 DNA-PK) (Ruis, 2008) derivative knockout Mouse embryonic fibroblasts (MEF) were cultured in Dulbecco´s modified Eagle medium DMEM. The following MEF cell lines were used in these studies: p53$^{-/-}$/Lig4$^{+/+}$ (MEF Lig4$^{+/+}$), p53$^{-/-}$/Lig4$^{-/-}$ (MEF Lig4$^{-/-}$) (kind gift of Dr. F. Alt; (Frank, 2000)). CHO cell lines were cultured in DMEM. All growth media were supplemented with 10% fetal bovine serum (FBS) as well as 100 µg/ml penicillin and 100 µg/ml streptomycin. All cell lines were grown as monolayer cultures and incubated at 37°C in a humidified atmosphere containing 5% CO_2 and 95% air. For passaging or collection of cells for experiments, dishes were washed with phosphate buffered saline (PBS) and trypsinized at 37°C for 3-5 min using a solution of 0.05% Trypsin. Human cell lines were passaged after 3 to 4 days, while the faster growing rodent cell lines were passaged every second day. Intervals between passages were kept regular and fixed cell numbers of cells were plated for a given cell

line and interval. Cell numbers were determined by counting in a Beckman Coulter Cell counter (Multisizer™ 3). Confluence was avoided during passage and all cells used in experiments were in the exponential phase of growth unless stated otherwise (experiments with plateau phase or serum deprived cells). Cell cycle distribution of cells in passage was regularly checked by flow cytometry after staining with propidium iodide.

Table 3.4: Cell lines

Cell line name	species	Cell type
A549	*Homo sapiens*	Alveolar adenocarcinoma
HCT116 WT	*Homo sapiens*	Colon carcinoma
HCT116 LIG4$^{-/-}$	*Homo sapiens*	Colon carcinoma
HCT116 DNA-PKcs$^{-/-}$	*Homo sapiens*	Colon carcinoma
U2OS 280A	*Homo sapiens*	Osteosarcoma
U2OS 282C	*Homo sapiens*	Osteosarcoma
U2OS 283C	*Homo sapiens*	Osteosarcoma
U2OS EJ-DR	*Homo sapiens*	Osteosarcoma
MEF	*Mus musculus*	Embryonal fibroblasts
MEF Lig4$^{-/-}$	*Mus musculus*	Embryonal fibroblasts
DRaa40	*Cricetulus griseus*	Ovarian

3.2.1.2 Induction of a plateau-phase like growth state by serum deprivation

In a number of experiments we purposefully did not use cell cultures in the exponential phase of growth, but cultures that retained only very low levels of proliferative activity. In regular cultures this growth state is attained when cells are grown for a prolonged period of time without medium change. Growth factors that drive the entry of cells into the cell cycle are introduced into the culture medium by addition of FBS. Those factors become gradually depleted by cellular uptake. When growth factor levels become too low, cells exit the division cycle. This state is also referred to as G0 (in analogy to the gap phases of the cell cycle) or quiescence. It is not to be confused with terminal differentiation, as it is reversible upon stimulation with growth factors.

In many cell lines growing into a plateau phase is accompanied by a high accumulation of cells with G1 DNA content. This however is not a universal phenomenon, as especially cancer cell lines can be either relatively independent of growth factor regulation, or capable of their own growth factor production and secretion. Plateau phase cultures are preferable as model system over exponential cultures for a number of questions, as the vast majority of cells in an adult human body is in a resting, post-mitotic state. Also in tumor tissue usually not all cells are continuously, actively dividing (Moore and Lyle, 2011).

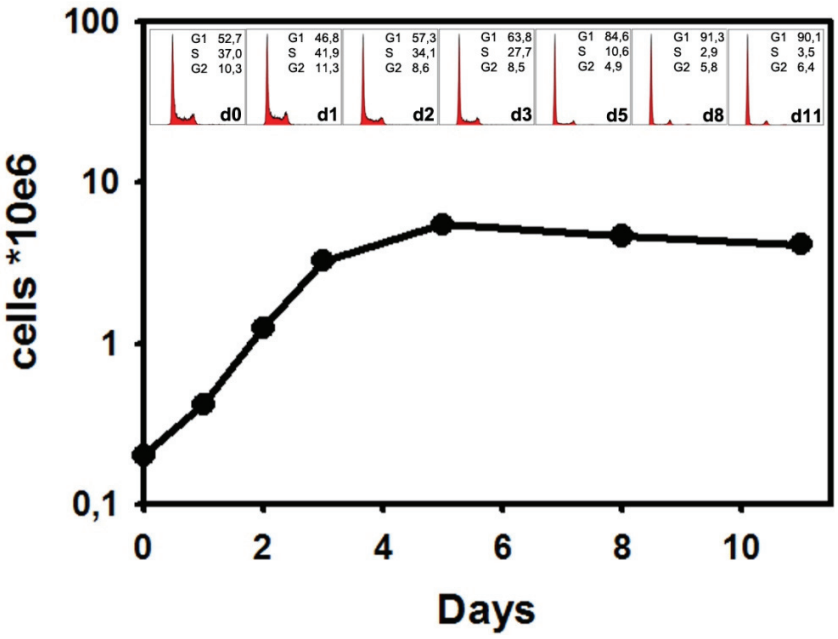

Figure 12 Growth curve of A549 cells. A549 cells were plated at a density of $0.2*10^6$ in 5 ml per petri dish (60mm diameter) at day 0 (d0). Cells were counted every 24h and samples were fixed for later analysis of DNA content by PI staining. Red histograms show the result of PI flow cytometry. Black dots and line: Cell number/dish as determined by counting in a Beckmann Coulter cell counter.

When cells are grown into the plateau phase, small deviations in the initial cell number can cause substantial differences in the time when cells reach this phase. For reasons of accumulation of metabolic end products and dead cell remnants however, it is desirable to use cells that are in the early plateau phase. The variations mentioned above make it difficult to obtain cell populations with the same plateau state quality at a fixed time point (e.g. equal cell cycle distribution).

Since the plateau phase state derives from growth factor exhaustion, a plateau phase-like growth state can also be induced by depriving an exponentially growing culture from growth factors. Besides being time saving, such an approach creates defined conditions and ensures higher reproducibility. We employed a protocol that involved growing cells for 2 days under standard conditions for exponential culture. After 48h, medium containing serum was removed and replaced by medium without serum (i.e. free of growth factors). After 24h of serum deprivation cells were used in the respective experiments. Cells were continuously kept in serum free medium throughout the whole experiment. All experiments with non-cycling populations in this work were performed using this serum deprivation protocol. For this reason, the terms plateau phase cells and serum deprived cells are used interchangeably here.

3.2.1.3 Cell cycle analysis by Propidium iodide staining

Propidium iodide (PI) is a DNA intercalating dye that exhibits strongly increased fluorescence when bound to nucleic acids. It is not cell membrane permeable and binds to DNA as well as RNA. Thus, for measurements of DNA content, cells have to be permeabilized and treated with RNAse. Cells are fixed and permeabilized by resuspension in cold EtOH 70% (4°C). After fixation cells can be stored at 4°C for a prolonged time. Before measurement cells are spun down, EtOH is aspirated and the pellet is resuspended in PI staining buffer (PBS, 40µg/ml PI, 62µg/ml RNAse) and incubated for 15 min at 37°C in a water bath. For cell cycle determination routinely $1x10^4$ cells were measured per sample.

3.2.2 Flow cytometry

Flow cytometry analysis of cells exhibiting a fluorescent signal, also known as fluorescence activated cell sorting or in short FACS, is a method to rapidly measure high numbers of cells in a single cell suspension. Sample cells are driven into a capillary, hydro-dynamically focused and transported within a sheath stream through the light path of an excitation laser. Emission light of excited fluorophores and scattered incident light

are collected by photomultiplier tubes (PMT) that amplify the signal. Scattered incident light provides information about size and granularity of cells (forward and side scatter). Incident light is selectively removed by a long pass filter (typically 488 nm LP) before reaching the PMTs assigned for fluorescence signal detection.

Flow cytometry analysis of cells was done using a Beckman Coulter XL-MCL flow cytometer equipped with an Argon ion laser (488 nm) and a Beckman-Coulter Gallios flow cytometer equipped with a solid state laser (488 nm). Analysis of experiment repeats was always performed with the same flow cytometer. Emission of green fluorescent protein (GFP) was measured using a 525 nm bandpass filter when measured alone, or a 510 nm bandpass filter when measured together with DsRed2. Emission of yellow fluorescent protein (YFP) was measured using a 550 nm bandpass filter and emission of dsRed2 was collected using a 610 nm bandpass filter. Propidium iodide (PI) was routinely measured with a 620 nm bandpass filter. Data acquired with the XL-MCL flow cytometer were analyzed in the EXPO32^{TM} MultiComp V1.2 software. Data acquired with the Gallios flow cytometer were analyzed in the Kaluza 1.2 software. Detector settings (PMT gain) were chosen according to the application. Compensation was not required for most measurements. In experiments with multiple fluorochromes exhibiting emission overlap (GFP/YFP and GFP/dsRed2) compensation was done using monochrome control samples.

3.2.3 X-Irradiation

X-irradiation of cells was performed using an X-ray tube (General Electric-Pantak) operated at 320kV, 10 mA with a 1.65 mm aluminium filter. The distance of the X-ray tube to the irradiation table was adjusted according to the cell culture vessel format used in the experiment. This adjustment was done in order to achieve homogenous coverage of the target area by the radiation field. 60 mm and 30 mm diameter petri dishes were irradiated at a distance of 50 cm, while cells grown on 100 mm petri dishes were irradiated at a distance of 75 cm. Rotation of the irradiation table during exposure compensated for the intensity variations within the radiation field, ensuring homogenous

irradiation. The dose rate at 50 cm was ~2.7 Gy/min, and at 75 cm ~1.3 Gy/min. Radiation dose was confirmed at regular intervals using Fricke's chemical dosimetry.

3.2.4 Transfection of nucleic acids

The term transfection describes the introduction of nucleic acids into cells by non-viral methods. The most common approaches employed for the transfection of cells are usage of Lipid based transfection reagents (e.g. Lipofectamine), cationic Polymers (e.g. Polyethylenimin) or electroporation based methods (e.g. Nucleofection). In this work Nucleofection™ was exclusively used for the transfection of cells. Depending on the type of experiment $1x10^6$ - $6x10^6$ cells were used per transfection reaction. No differences in transfection efficiency could be observed for cell numbers up to $8x10^6$ cells/reaction (highest cell number tested) with Plasmid DNA, or in knockdown efficiency up to $12x10^6$ cells/reaction (highest cell number tested) for the transfection of siRNAs. Cells were collected for nucleofection by trypsinization and pelleted for 5 min at 1500 rpm. The supernatant was aspirated and the pellet resuspended in 100 µl of custom nucleofection buffer (80 mM NaCl, 5 mM KCl, 12 mM Glucose, 25 mM HEPES, 20mM $MgCl_2$, 0.4 mM $Ca(NO_3)_2$, 40 mM Na2HPO4/NaH2PO4) and transferred in an electroporation cuvette. Nucleofection program was chosen according to the cell line (Table 3.5). After transfection cells were taken up in pre-warmed (37°C) growth medium, plated out and returned to the incubator. Measurements were taken, depending on the experimental system, after 24h, 48h or 72h hours using flow cytometry.

Table 3.5: Nucleofector Programs

Cell type	Nucleofector Program
A549	**X-05**
U2OS	**X-01**
CHO	**U23**

Table 3.6: siRNAs

siRNA	Target Sequence	Provider
GFP-22	CGG CAA GCT GAC CCT GAA GTT CAT	Qiagen
Luciferase GL2	AAC GTA CGC GGA ATA CTT CGA	Qiagen
Hs_BRCA2_7	TTG GAG GAA TAT CGT AGG TAA	Qiagen
Hs_RAD52_6	TGG GCC CAG AAT ACA TAA GTA	Qiagen
Hs_RAD51_7	AAG GGA ATT AGT GAA GCC AAA	Qiagen

3.2.5 Repair-outcome-specific chromosomal reporters

DRaa-40 were obtained from Maria Jasin, Ph.D. (Memorial Sloan Kettering Cancer Center, New York, USA). These cells were derived from the CHO cell line AA8 by stable integration of the DR-GFP reporter construct (Pierce, 1999).

A panel of four stably transfected human U2OS cell lines was obtained from Jeremy Stark, Ph.D. (Beckman Research Institute of City of Hope, Duarte, USA) and used to assay the influence of several drugs on the repair efficiency of distinct pathways of DSB repair (Pierce, 1999; Stark, 2004; Bennardo, 2008; Bennardo, 2009; Gunn and Stark, 2012). These assays are based on the reconstitution of a reporter gene by repair of an endonuclease induced chromosomal DSB. Each of the four U2OS cell lines used within this study carries a different reporter construct stably integrated into their genomes. Each of those constructs contains one or two recognition sites for the homing endonuclease I-SceI that has no naturally occurring target sites within mammalian genomes. None of those constructs generates a signal without having been processed for DSB repair resulting in a specific recombination outcome. Expression of I-SceI from a plasmid vector results in the creation of a DSB at its cutting site. Although this DSB may

be repaired by any pathway of DSB repair, only repair events that result in the restoration of a functional EGFP expression cassette are detected.

The DR-GFP construct (integrated into U2OS 282C, DRaa40 an EJ-DR) consists of two non-functional, direct repeat EGFP Sequences. The first consists of a modified eGFP gene with an I-SceI site containing a premature stop codon (SceGFP), the second is a 3´- truncated modified EGFP ORF (iGFP). Repair via HRR (more specifically short tract gene conversion) results in the generation of a functional EGFP-ORF from DR-GFP (Figure 17 A & Figure 20 A).

The SA-GFP construct (integrated into U2OS 283C) harbors two direct repeats of truncated EGFP-ORFs. The first of the two repeats is truncated at the 3´-end (5´-GFP) the second is truncated at the 5´-end (3´-GFP) and contains an I-SceI site. Signal generation through HRR repair of this construct is prevented by a premature stop codon at the 3´-end of the first ORF (5´-GFP). Upon repair by SSA a functional EGFP gene is reconstituted (Figure 21 A).

The EJ5- GFP construct consists of a CAG promoter (chicken beta-actin promoter with CMV enhancer) that is separated from a full length GFP open reading frame by a puromycin (Puro) gene (Figure 22 A). The Puro gene is flanked by two I-SceI sites in tandem orientation. DSBs induced by I-SceI in this construct can be directly repaired using the proximal ends, thus restoring the two original I-SceI sites. Alternatively, it is possible that the intervening DNA is lost and rejoining occurs between the distal ends, which results in the loss of the Puro gene and one or both of the I-SceI sites. GFP expression is only possible when distal ends are joined and the CAG promoter is brought into proximity of the GFP gene.

U2OS EJ-DR cells were obtained from the Lab of Ranjit S. Bindra, MD, Ph.D. (Smilow cancer hospital, Yale, USA) (Bindra, 2013). These cells were used to examine the influence of NAs on the general mutagenicity of DSB repair. The EJ-RFP system functions after a different principle than the three constructs described above. The EJ-RFP system consists of two integration cassettes that are randomly introduced at different locations in the genome (Figure 23 A). One cassette consists of a tetracycline repressor gene under the control of a constitutively active promoter. The TetR gene

contains a recognition site for the I-SceI endonuclease. The other cassette is a DsRed gene containing several TetR binding sites. Under non inducing conditions TetR is expressed and binds to its binding sites in the DsRed gene, resulting in suppression of gene expression. Upon expression of I-SceI a DSB can be induced in the TetR gene. If this DSB is repaired without any sequence alterations, TetR continues to be expressed. If repair of the DSB results in loss of sequence or a frame shift no functional TetR protein will be expressed. As a consequence, cells that have undergone mutagenic repair will eventually develop red fluorescence. EJ-DR cell also contained an integration of the DR-GFP construct. However, since measurements of the EJ-RFP signal had to be taken 4 days after transfection, data that concomitantly accrued from the DR-GFP integrate did not yield meaningful information with regard to short term NA treatment promptly after transfection (see Discussion 5.3.3 and Figure 37).

I-SceI expression in the U2OS cells was achieved by transient transfection of pCMV-3xNLS-ISceI (Figure 17 A). Transfection was performed by nucleofection. After transfection, cells were allowed to re-attach for 1.5 h or 3h before drug treatment. Drug treatment lasted for 4 h unless indicated otherwise. Cells were collected and measured by flow cytometry 24 h after transfection unless indicated otherwise. FACS data was analyzed in the Kaluzaa 1.2 software and the percentage of GFP positive cells was determined. Results are expressed as percent repair efficiency of I-SceI transfected controls (no drug treatment). Variations in transfection efficiency could be excluded, as all cells used in one experiment were transfected together in a single reaction and subsequently distributed to several dishes before drug treatment.

3.2.6 Clonogenic survival assay

Clonogenic survival assays determine the reproductive integrity of cells. To allow the formation of isolated colonies arising from a single founder cell, test cells have to be plated at low density. To this end cells were plated from a single cell suspension aiming for 30-150 colonies/dish. With increasing expected cell killing (i.e. higher doses of IR or increasing drug concentrations) the number of plated cells was increased. In this work clonogenic survival assays were used to investigate the radiosensitizing effects of ara-A

and other drugs. A549 cells were grown for 2 days and collected in the exponential phase of growth at the day of the experiment. Survival data obtained at different doses of IR and drug treatment with different concentrations was always normalized to the survival of non-irradiated (0 Gy) cells treated with the same drug concentration. Two slightly different protocols were followed for these treatments:

Protocol I: Cells were plated with the respective concentrations of ara-A and immediately irradiated without significant pre-incubation with the drug (Figure 14 A).

Protocol II: Cells were plated and allowed to attach for 1.5-2 hours. Drugs were added and cells were pre-incubated for a defined period of time before irradiation (Figure 14 B, Figure 16 C, Figure 30 B). Length of pre-treatment was either 15 min (Figure 16 C) or 40 min (Figure 14 B and Figure 30 B), depending on the design and scale of the respective experiments. Within a set of experiments pre-treatment times were always identical.

There were no significant differences between results obtained with the two protocols or different length of pre-treatment. In all cases the medium containing ara-A was removed 4 h after irradiation, the cells were washed twice with medium and then supplied with fresh growth medium containing 10% FBS. The cells were kept at 37 °C, 5% CO_2 for 9-10 days and then stained for counting (1% crystal violet in 70% EtOH). Colonies that comprised 50 or more cells were scored. Curves were fitted to data using the linear-quadratic model.

3.2.7 Pulsed-field gel electrophoresis

Pulsed-field Gel electrophoresis (PFGE) is a method that allows the physical separation of large pieces of DNA within a gel matrix. Conventional constant field agarose gel electrophoresis allows the efficient separation of DNA fragments of 100-200 base pairs (bp) up to approximately 50 kbp. PFGE overcomes this size limit by applying an alternating electrical field and allows the resolution of DNA molecules up to 10 Mbp (Gardiner, 1991; Gurrieri, 1999). In this work asymmetric field inversion gel electrophoresis (AFIGE), a PFGE variation, was used to investigate the repair of DSB in irradiated cells. To this end, cells were embedded in low melting agarose (LMA), cut into

equally sized cylindrical pieces (plugs), lysed, loaded on a gel and subjected to the alternating electrical field for 40h. The amount of DNA that was able to escape the plug and migrate into the gel during the run provides a measure of DSB present in the assayed population.

DSB are induced in a linear fashion proportionally to the dose of IR. However, DNA release in PFGE can vary depending on cell line and cell cycle status of the used culture. To create a standard curve a dose response (DR) was determined within each experiment. Cells were collected, pelleted and resuspended in cold serum-free HEPES-buffered medium at a concentration of 6 x 10^6 cells/ml. This cell suspension was mixed with an equal volume of pre-warmed (50°C) serum-free medium containing 1% low melting agarose (LMA) to a final concentration of 3x10^6 cells/ml and poured into round glass capillaries for polymerization. The solidified agarose with the cell suspension was subsequently cut into plugs containing approximately 1.5 x 10^5 cells/plug. DR plugs were placed in 60 mm petri dishes containing 3.5 ml cold HEPES-buffered serum-free medium and X-irradiated on ice. X-ray doses used for DR curves were either from 5 Gy – 20 Gy in steps of 5 Gy, or from 10 Gy to 40 Gy in steps of 10 Gy. Irradiated plugs were immediately placed in cold lysis buffer (10 mM Tris, 50 mM NaCl, 100 mM EDTA, 2% N-lauryl sarcosine, pH 7.6, 0.2mg/ml protease), and incubated at 4°C for 30 min before placing them at 50°C for 18h.

For the evaluation of DSB repair kinetics after IR attached cells were irradiated on ice (unless stated otherwise) with 20 Gy of X-rays. After irradiation cold medium was replaced by fresh pre-warmed growth medium (42 °C) to avoid time lag due to prolonged warm up of chilled medium. In drug treatment experiments the replacement medium contained the same concentrations as pre-treatment medium. After each repair time interval cells were collected by trypsinization, embedded in agarose plugs and lysed as described above. After lysis, plugs were washed for 1 h at 37°C in washing buffer (10 mM Tris, 100 mM EDTA, 50 mM NaCl, pH 7.6) and then treated with 0.1 mg/ml RNase A for 1 h in washing buffer at 37°C. For determination of the background-DNA-release, plugs were prepared from otherwise identically treated non-irradiated cells at different time points (typically 2h or 4h and 8h).

Plugs were loaded on 0.5% agarose gels (SeaKem® LE Agarose, Lonza) pre-stained with 0.7 µg/ml EtBr and gel slots were sealed with 1% Agarose. The gels were run in 0.5 x TBE (45 mM Tris, pH 8.2, 45 mM Boric Acid, 1 mM EDTA) in Horizon 20x25 gel boxes with circulating, continuously cooled buffer to ensure a stable temperature of approx. 10 °C during the whole run.

The opposing electrical fields for AFIGE were provided by two power supplies (Bio-Rad) connected to a custom build switching unit. Run parameters were set to cycles of 50 V (1.25 V/cm) for 900 s in the direction of DNA migration (forward) alternating with cycles of 200 V (5.0 V/cm) for 75 s in the reverse direction for a total of 40 hours. Afterwards gels were scanned with a Typhoon 9400 imaging device (GE Healthcare) and analyzed using the ImageQuant™ 5.0 software (GE Healthcare).

The fraction of DNA released (FDR) was calculated by dividing the signal of DNA released into the gel (lane) by the total signal (lane + plug). The FDR values of irradiated samples were corrected by the background values of non-irradiated control cells (see above). Using FDR values derived from the linear DR standard curves a dose equivalent (DEQ) in Gy was calculated for the repair kinetics (RK) data points. DEQ was plotted against repair time and curve fitting was performed in SigmaPlot 11.0 software using an exponential decay algorithm assuming a fast and slow component in the RK curves.

3.2.8 PFGE with sorted cell populations

Experiments with cell populations sorted by flow cytometry generally followed the protocol for PFGE described above with some adjustments as laid out below. Due to the large number of cells required per repair time point, sorting is a time consuming procedure that only allows the processing of a few samples per day. Thus the cells that were collected at each time point on the day of the experiment were frozen for later sorting. Freezing was done by resuspending washed, pelleted cells in cold freezing solution A (5mM KH2PO4, 25mM KOH, 30mM NaCl, 20mM L (+) lactic acid, 5mM Dextrose, 0.5mM MgCl2, 200mM Sorbitol in Milli-Q H2O) and gently mixing this suspension with an equal volume of freezing solution B (Freezing solution A with 20%

DMSO). Cells were then transferred to -150 °C for snap freezing and storage. Controls were prepared before freezing and every following step of the procedure. For sorting, aliquots of cells were quickly thawed and suspended in cold growth medium. The thawed cells were stained with propidium iodide (PI) in a permeabilizing solution (PI 40 µg/ml, Tris 0.1M, NaCl 0.1M, MgCl2 5mM, Triton X-100 0.05%) sorted according to DNA content in a Beckman-Coulter Epics Altra Flow Cytometer. Several measures had to be taken to optimize cell recovery. Cells were collected in tubes pre-coated with Dichlorodimethylsilane (Merck, 2% solution in 1,1,1-trichloroethane) into 0.5 ml of heat treated fetal bovine serum. Sheath fluid (phosphate-buffered saline, PBS) and collection tubes were continuously chilled (10 °C) during sorting. Numbers of deposited cells were reconfirmed with manual counting in a Rosenthal chamber. Plugs for PFGE were prepared as described above, with the exception that cell numbers of sorted populations were adjusted to contain 1 x 10^5 cells/plug for G1 populations, and 0.5 x 10^5 cells/plug for G2 populations - to ensure equal amounts of DNA per plug.

3.2.9 Immunofluorescence staining

For immunofluorescence detection of Rad51 foci in A549 cells were grown for two days on glass coverslips in 30 mm petri dishes aiming for a total number of 500.000 cells per dish. Prior to irradiation cells were subjected to a 15 min pulse of 10 µM 5-ethynyl-2´-deoxyuridine (EdU). This was done in order to enable identification of cells that were synthesizing DNA at the time of irradiation, i.e. S-Phase cells. Immediately before irradiation EdU was washed away and cells were supplied with fresh medium. Cells were irradiated with 4 Gy X-rays and kept at 37 °C for, 5% CO_2 for 3h. After incubation, cells were briefly washed with PBS and fixed with 2% PFA for 15 min. Fixed cells were washed with PBS again and permeabilized with 0.5% Triton X-100 in 100 mM Tris, 50 mM EDTA. After permeabilization cells were washed twice with 3% BSA. Incorporated EdU was stained with the Click-iT® EdU Alexa Fluor® 647 imaging kit according to manufacturer's instructions. Click chemistry allows the addition of a fluorophore to EdU incorporated in DNA without the need for denaturation. A Click reaction is a copper-catalyzed covalent reaction between an azide and an alkyne. In this application, the EdU

carries the alkyne and the Alexa Fluor® dye presents the azide (Salic and Mitchison, 2008; Invitrogen, 2011). Briefly, a reaction cocktail was prepared containing Copper sulfate (CuSO4), Alexa Fluor® 647 azide and the buffer and additive provided in the kit. Cells grown on coverslips were placed on 100 µl drops of the reaction cocktail on Parafilm (Pechiney Plastic Packaging) for 30 min and protected from light. Afterwards cells were washed again in 3% BSA and then incubated for one hour in a blocking solution containing 0,2 % gelatin and 0,5 % BSA fraction V in PBS. Cells were then incubated with primary antibody (Ab) in blocking solution overnight, using mouse monoclonal IgG2b Rad51 14B4 (Genetex) and rabbit polyclonal IgG cyclin B1 H-433 (Santa Cruz). Incubation with secondary Ab for one hour was performed the next day after triple washing with PBS. Rad51 was detected using Alexa 488 polyclonal goat anti-mouse IgG and cyclin B1 was detected using a polyclonal Alexa 568 conjugated anti rabbit IgG antibody from goat (both Invitrogen). Finally the coverslips were incubated with 4',6-diamidino-2-phenylindole (DAPI) for staining of DNA and mounted on microscopic slides with ProLong® Gold antifade reagent (Invitrogen). Slides were stored in the dark for at least 24h before analysis by confocal laser scanning microscopy.

Immunofluorescence detection of various IRIF in serum deprived MEF Lig4$^{-/-}$ was performed using the same antibody staining protocols using antibodies and dilutions as stated in Table 3.7, but without labeling with EdU.

Table 3.7: Antibodies Immunofluorescence

IF Primary Ab	Host/ type	specificity	Dilution	Provider
Cyclin B1	Rabbit polyclonal	Human	1:100	Santa Cruz
Rad51 (14B4)	Mouse monoclonal	Human	1:400	Genetex
gH2AX (pS139)	Mouse monoclonal	Human, mouse	1:200	Abcam
53BP1 (H-300)	Rabbit polyclonal	Human, mouse	1:200	Santa Cruz
pATM-S1981 (10H11.E12)	Mouse monoclonal	Human, mouse	1:400	Cell Signaling
IF Secondary AB	**Host/ type**	**Specificity**		**Provider**
Alexa488	goat polyclonal	Mouse IgG	1:400	Invitrogen
Alexa568	goat polyclonal	Rabbit IgG	1:400	Invitrogen
Alexa633	goat polyclonal	Rabbit IgG	1:400	Invitrogen

3.2.10 SDS-PAGE

Denaturing SDS-Polyacrylamide gel electrophoresis allows the separation of proteins according to their molecular weight in a unidirectional electrical field. Cellular protein extracts for SDS-PAGE were prepared using RIPA buffer with the addition of a protease inhibitor cocktail. SDS-PAGE gels consisted of a 5% stacking and a 10% resolving gel, which were cast into Bio-Rad mini gel stands. For loading 20-50 µg (depending on the protein to be detected) cell extracts were mixed 1:1 with 2x Laemmli Buffer, denatured for 5 min at 96 °C and centrifuged briefly at 13000 rpm. For electrophoresis a constant voltage of 100 V was set for 2 h.

3.2.10.1 Western blot

During Western blotting proteins are transferred from a SDS-polyacrylamide gel onto a nitrocellulose membrane. Transfer was performed using an iBlot® dry blotting system (Invitrogen). For transfer pre-assembled blotting stacks (Invitrogen) containing a nitrocellulose membrane were used. After transfer the membrane was incubated for 2 h in 5% non-fat dry milk in 1 x TBS-T (0.05% Tween20 in 1 x PBS). For immunodetection the membranes were incubated overnight at 4 °C with primary Ab. After washing three times for 10 min in PBS-T the secondary Ab was incubated for 1.5 h and the membrane was again washed three times in PBS-T prior to detection. The Odyssey® Infrared Imaging System from LI-COR Biosciences was used for detection and analysis.

Table 3.8: Antibodies Western blot

WB Primary Ab	Host/ type	specificity	Dilution	Provider
BRCA2 (3E6)	Mouse monoclonal	Human	1:500	GeneTex
Rad51 (Ab-1)	Rabbit polyclonal	Human	1:2000	Calbiochem
Rad52 (F-7)	Mouse monoclonal	Human	1:500	SantaCruz
Ku80 (H-300)	Rabbit polyclonal	Human	1:400	SantaCruz
GAPDH (MAB374)	Mouse monoclonal	Human	1:10000	Millipore
WB Secondary Antibody	**Host/ type**	**Specificity**	**Dilution**	**Provider**
IRDye 800CW	Goat polyclonal	rabbit	1:10000	LI-COR
IRDye 800CW	Goat polyclonal	mouse	1:10000	LI-COR
IRDye 680LT	Goat polyclonal	mouse	1:10000	LI-COR
IRDye 680LT	Goat polyclonal	rabbit	1:10000	LI-COR

3.2.11 Confocal laser scanning microscopy (CLSM) and foci quantification

CLSM was performed on a LEICA TCS-SP5 confocal microscope to generate high resolution three dimensional image data of the stained cells. A key feature of a confocal microscope is the pinhole in front of the optical detector, a photo multiplier tube (PMT), that blocks out emission light that originates from all other points within the sample (out-of-focus light) but the points in the focal plane of the objective. Thus a considerable increase in optical resolution and contrast as compared to conventional fluorescence microscopy is achieved. In CLSM the sample is scanned by a focused laser beam that moves over the specimen in lines and only illuminates a small focal volume of the sample at any given time. Confocal scanning in steps of 0.5 µM along the Z-Axis through the whole specimen was performed to obtain a stack of optical sections (Z-stack). These pictures were used to create a three-dimensional image of the spatial structure of the investigated specimen, which was saved as LIF file and used for foci analysis. For data presentation, image stacks were merged into a single two-dimensional picture, the maximum intensity projection (MIP), and exported as TIFF files. For each slide at least 5 fields were analyzed, with an average of 120 S- and 20 G2-phase cells per sample. Parameters and settings used for CSLM and foci analysis are summarized in Table 3.9.

Foci were scored using the ImarisXT® 6.0 Software. For this purpose LIF files were loaded into the Imaris software and processed using embedded MatLab features. Fluorescent spots with a diameter above 0.5 µm and intensity above a set gray value threshold, which was kept constant within experiments, were identified as foci and grouped into object clouds within each nucleus. The threshold values were kept identical throughout all experiments. The number of foci within each single nucleus was recorded and average foci numbers were calculated. It was discriminated between cells in G1, S or G2 phase based on the staining of cyclin B1 and EdU incorporation.

Table 3.9: Microscope settings and parameters

Hardware	**Type**
Microscope	Leica TCS-SP5
Objective	HCX PL APO lambda blue; 63.0x1.4 OIL UV
Acquisition parameter	**Mode**
Scan direction	Bidirectional
Zoom	1
Speed	400 Hz
Resolution	1024x1024
Excitation laser	**Intensity setting**
405 nm	25 %
488 nm	10 %
561 nm	20 %
633 nm	20 %
Detector Range	**PMT voltage / Offset**
415 nm – 490 nm	700.8 / -4 %
505 nm – 547 nm	636.0 / -3.5 %
587 nm – 621 nm	750.2 / -4,9 %
657 nm – 684 nm	600.6 / -2 %

Imaris parameter	Value
Minimal spot size	0.5 µm

3.2.12 In vivo replication assay

Inhibition of cellular DNA synthesis by various drug treatments was assayed by incorporation of tritium labeled thymidine (^{3}H-thymidine). A549 Cells were grown in 25 cm^2 flasks under standard tissue culture conditions (37 °C, 5% CO_2) with caps loosely screwed on for 24 h. One day before the experiment caps were fastened and flasks transferred to a warm room (37 °C) with normal atmosphere for another 24 h. All further steps of the experiment were performed in the warm room, to avoid decrease of replicative activity caused by temperature fluctuations. Drugs were added 30 min prior addition of the ^{3}H-thymidine pulse. Controls were treated with the respective solvent. ^{3}H-thymidine was added to the drug containing medium to a concentration of 0,5 µCi/ml. Radioactive medium was removed 20 min later, cells were washed with ice cold PBS and trypsinized. The collected cells were kept on ice until further processing. Cells were counted with the Multisizer™ 3 cell counter (Beckman coulter) for later normalization to allow comparisons between samples. Cells were sucked onto a glass microfibre filter (Whatman™, GF/A, 25 mm) using a vacuum manifold. Trichloroacetic acid was added to the filters and incubated for approximately 5 min before being sucked through. The filters were washed with Millipore water and sucked dry. Subsequently the filters were transferred to the bottom of scintillation vials. To each vial 0.5 ml of 0.5 N NaOH were added and incubated overnight at 65°C. On the following day 0.5 ml 0.5 N HCl were added to each vial. Lastly, 10 ml of a scintillation cocktail (Unisafe 1, Zinsser Analytic) was added and the vials were mixed thoroughly using a vortex mixer. Measurements were taken in a Tri-Carb Liquid Scintillation Counter 1900 TR (Packard) 6 h to 24 h later.

4 Results

4.1 Inhibition of DNA replication in A549 cells

One of the most prominent biological effects of ara-A in mammalian cells is inhibition of DNA replication. To determine the concentrations required to achieve effective inhibition at this endpoint we performed DNA replication assays with A549 lung carcinoma cells.

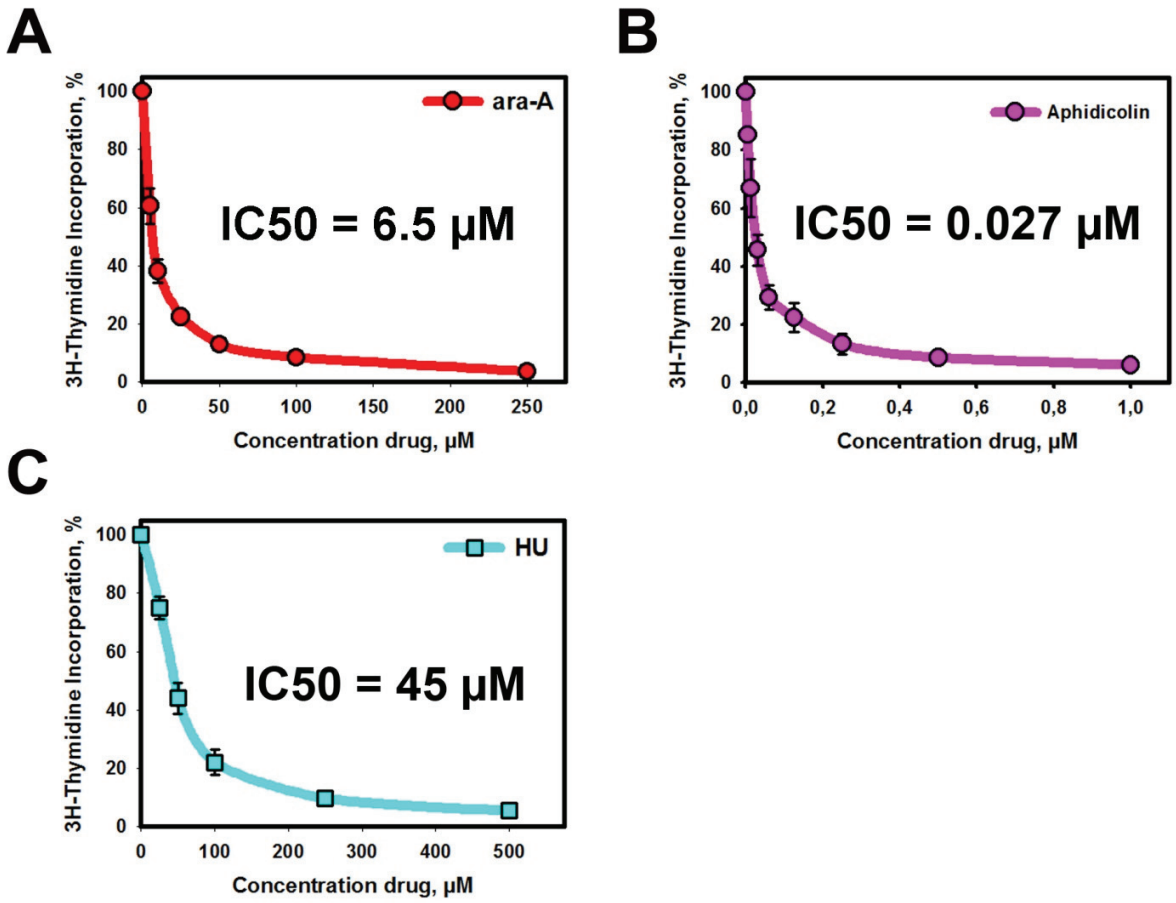

Figure 13 Measurement of DNA replication by ^{3}H-thymidine incorporation in A549 cells. A) Effect of ara-A treatment on DNA replication. Data points show the mean and standard deviation (s.d.) of three independent experiments. **B)** Effect of aphidicolin treatment on DNA replication. Data points show the mean and standard deviation (s.d.) of three independent experiments. **C)** Effect of hydroxyurea (HU) treatment on DNA replication. Data points show the mean and standard deviation (s.d.) of three independent experiments. Bold text in each graph indicates the IC50 values for DNA replication inhibition.

We also compared the inhibition of replication exerted by ara-A in this assay to the inhibition by two non-NA replication inhibitors. Specifically, we used hydroxyurea (HU), a small molecule known to inhibit RnR, and aphidicolin, an inhibitor of DNA polymerases (α,δ & ε).Replication was assayed by incorporation of tritium labeled thymidine (3H-thymidine). Inhibitors were added 30 min prior to a 20 min pulse treatment with 3H-thymidine. Subsequently cells were lysed and incorporation of 3H-thymidine was measured in a liquid scintillation counter.

Figure 13 shows the results obtained with the replication inhibitors normalized to controls incubated without drug. The concentration at which 50% of the maximum inhibition of replication was achieved ($IC50_{repl}$) was determined. Figure 13 A shows the inhibition of DNA replication by ara-A in A549 cells. An $IC50_{repl}$ of 6.25 µM was determined. Aphidicolin proved to be the most effective inhibitor of DNA replication in our experiments with an $IC50_{repl}$ of 0.027 µM (Figure 13 C). Much higher concentrations of HU were required to achieve comparable inhibition of replication ($IC50_{repl}$= 45 µM; Figure 13 D).

4.2 Radiosensitization of cycling A549 cells by ara-A

Having established the effectiveness of ara-A in our cell system, we next investigated the potential of ara-A to sensitize cycling A549 cells to IR. Cells were routinely maintained in the exponential phase of growth. For experiments, A549 cells were grown for 2 days and collected by trypsinization while still in the exponential phase of growth. Cells were plated at numbers (estimates from available survival data) aiming for 30-150 colonies/dish after exposure to pre-defined radiation doses. Two slightly different protocols for survival assays with drug treatment and irradiation were applied within this work (protocols I and II; see Materials and Methods), that vary with regard to cell attachment time and drug pre-incubation before irradiation. Both protocols yielded comparable results. Figure 14 A (protocol I) shows strong radiosensitization of A549 cells by 250 µM, 500 µM and 1000 µM of ara-A that increased with increasing drug

concentration. At concentrations of 500 µM and above a shoulderless survival curve was obtained.

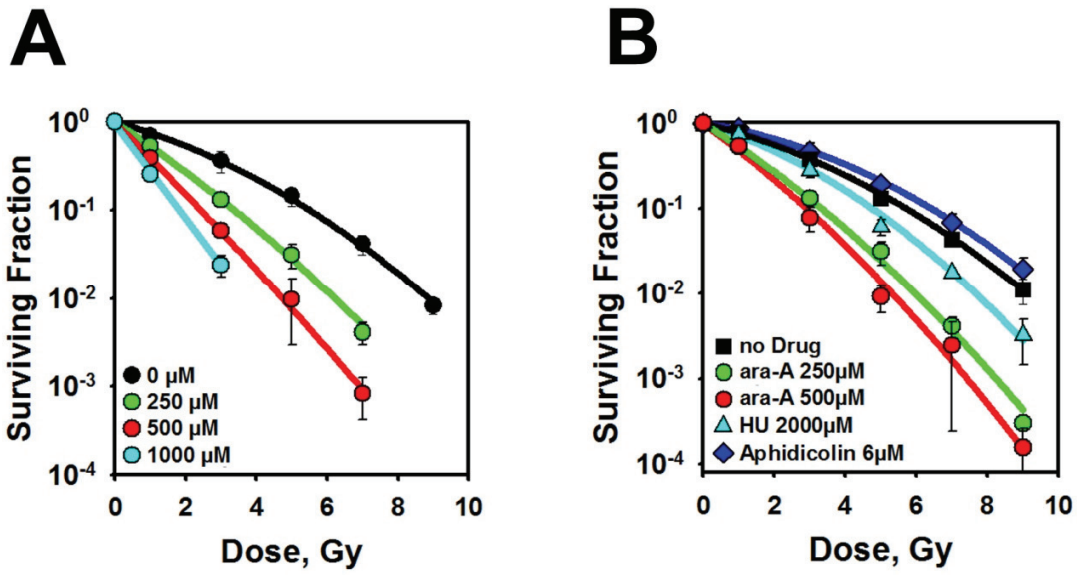

Figure 14 Effect of ara-A on the radiosensitivity to killing of A549 cells. A) Exponentially growing A549 cells were exposed to the indicated doses of ara-A for 4 h after IR. Plating efficiency (PE) was 0.68, 0.55, 0.42 and 0.29 for cells exposed to 0, 250, 500, and 1000 µM, respectively. Black circles represent cells treated with 0 µM ara-A, green circles cells treated with 250 µM ara-A, red circles cells treated with 500 µM ara-A and blue circles cells treated with 1000 µM ara-A. The results shown represent the mean and standard error calculated from three independent experiments, each including double determinations. **B)** Comparison of radiosensitization by 4h post-irradiation treatment with ara-A and other DNA replication inhibitors in exponentially growing A549 cells. Red circles, ara-A (500 µM); green circles ara-A (250 µM); light blue triangles, HU (2000 µM); dark blue diamonds, aphidicolin (6 µM); black squares, control (no drug treatment). The results shown represent the mean and standard error calculated from three independent experiments, each including double determinations.

Sensitizer enhancement ratios (SER) were calculated for radiosensitization by ara-A. Two different approaches were employed for this calculation: 1. SER was determined at at a fixed dose of 2 Gy by dividing the fraction of surviving cells (SF2) without drug

treatment by that measured with ara-A treated cells. 2. SER was determined at a fixed cell survival of 37% (the survival fraction at which statistically each cell within a population has received on average one lethal hit) by dividing the corresponding radiation dose of untreated cells to that of treated cells. The SER calculated for 500 µM ara-A was 3.7 based on SF2 and 2.9 based on 37% survival (Table 1).

Table 4.1: Quantification of ara-A mediated radiosensitization. Sensitizer enhancement ratios (SER) were calculated for the survival of A549 cells at 2 Gy (SF2), as well as for the radiation dose where cell survival was 37% (37%sv).

Conc. Ara-A	SER (SF2)	SER (37%sv)
250 µM	2.0	1.9
500 µM	3.7	2.9
1000 µM	7.9	3.8

This observation was in agreement with earlier results showing radiosensitization of rodent and human cell lines (in the plateau and the exponential phases of growth, respectively) by treatment with ara-A. Since ara-A effectively inhibits DNA replication we inquired whether radiosensitization by ara-A may be attributable to inhibition of this cellular function alone. To answer this question we compared radiosensitization elicited by post-irradiation treatment with ara-A with the radiosensitizing effects of HU and aphidicolin (Figure 14 B; Protocol II, 40 min pre-incubation). Since these compounds inhibit DNA replication with widely different efficiencies we used the $IC50_{repl}$ values as orientation for the comparison of the radiosensitizing effect. We observed that aphidicolin at 6 µM (~220-fold $IC50_{repl}$) did not sensitize cells to IR at all. In contrast, ara-

A at 250 µM (40-fold $IC50_{repl}$) and 500 µM (80-fold $IC50_{repl}$) caused marked radiosensitization of A549 cells. HU at 2000 µM (~45-fold $IC50_{repl}$) did cause radiosensitization in these cycling cells, but the effect was only modest compared to the effect of ara-A. From this result we concluded that effects beyond DNA replication inhibition must underpin the radiosensitizing effect of ara-A, which should be more specific than global inhibition of DNA replication. We hypothesized that the drug somehow interferes with the repair of IR-induced DSB. Although inhibition of DNA synthesis alone appears not to be sufficient to explain the radiosensitizing effect of ara-A, it may well play a role in the interference with DSB repair. Pathways of HRR are the only DSB repair mechanisms known to involve extensive DNA synthesis. Thus, we decided to first investigate possible interactions of ara-A with HRR.

4.3 Impact of ara-A treatment on HRR

4.3.1 Inhibition of IR induced RAD51 foci formation by ara-A

Rad51 is the central recombinase in HRR that forms a nucleoprotein filament on the resected DNA ends during the repair process. Accumulation of Rad51 at sites of DSB can be visualized by immunofluorescence staining as discrete foci. These foci form and decay with characteristic kinetics upon exposure of cells to IR. Scoring of Rad51 foci is widely used as a surrogate marked of HRR function. We applied this method to investigate possible interference of ara-A with HRR.

We used exponentially growing A549 cells and selected a radiation dose (4 Gy) and time point of observation (3 h) known to produce maximum numbers of Rad51 foci (previous unpublished work from our group). In addition to Rad51 staining, we included additional staining protocols allowing the assignment of each cell in a particular phase of the cell cycle. Expression of cyclin B1 is regulated differentially throughout the cell cycle: Expression starts in S-phase and continues in G2. However, staining with cyclin B1 is not sufficient for a reliable assignment of cells in G1, G2 and S cells. Expression of cyclin B1 is weak in early- to mid-S phase cells, but remains high between late-S and G2 phase. Therefore, to improve the discriminatory power of our assay we also included

incorporation and staining of EdU. EdU is an analog of thymidine that was recently developed as an alternative for BrdU for the detection of S-phase cells in a proliferating cell population (Cappella, 2008). EdU like BrdU is incorporated into DNA without inhibiting DNA replication. However, for detection of BrdU, DNA must be denatured in order to grant the required antibodies access to the incorporated BrdU nucleotides. Detection of EdU on the other hand is based upon a chemical reaction whereby a fluorophore is coupled covalently to the incorporated nucleotide without the need for DNA denaturation. Together, EdU and Cyclin B1 staining allowed for an unambiguous assignment of each analyzed cell in a phase of the cell cycle. EdU positive cells were identified as being in S-phase at the time of irradiation and were analyzed either during S-phase or in the subsequent G2–phase of the cell cycle. Cells that were positive for cyclin B1 but negative for EdU were scored as being in G2 during the time of irradiation and remaining in G2 in the following repair time interval. Cyclin B1 and EdU negative cells were scored as being in G1 at the time of irradiation. G1 cells were not scored in the context of the present set of experiments, as G1 cells fail to develop Rad51 foci after IR (Figure 15 A).

Our labeling strategy allowed us to stringently discriminate G1, S and G2 phase cells from each other and allowed us to analyze a large number of S-phase cells (385 (+/-106); n= 3). However, the number of G2 cells that could be analyzed was relatively small (61 (+/-19); n= 3). This is mainly due to two factors: First, in an exponentially growing culture of A549 cells, the number of cells in G2 is typically only about a quarter of the number of cells in S. Second, in our experiments cells were fixed 3h after irradiation, a time during which a large proportion of cells that were in G2 could have entered mitosis without irradiation. However, irradiation with a dose of 4 Gy is expected to induce a G2 block that would prevent most G2 cells from progressing into mitosis. Nevertheless, more cells may have escaped the G2/M checkpoint activation than expected. This could explain why we did not only find 4 times more S-phase cells, but about 6 times more.

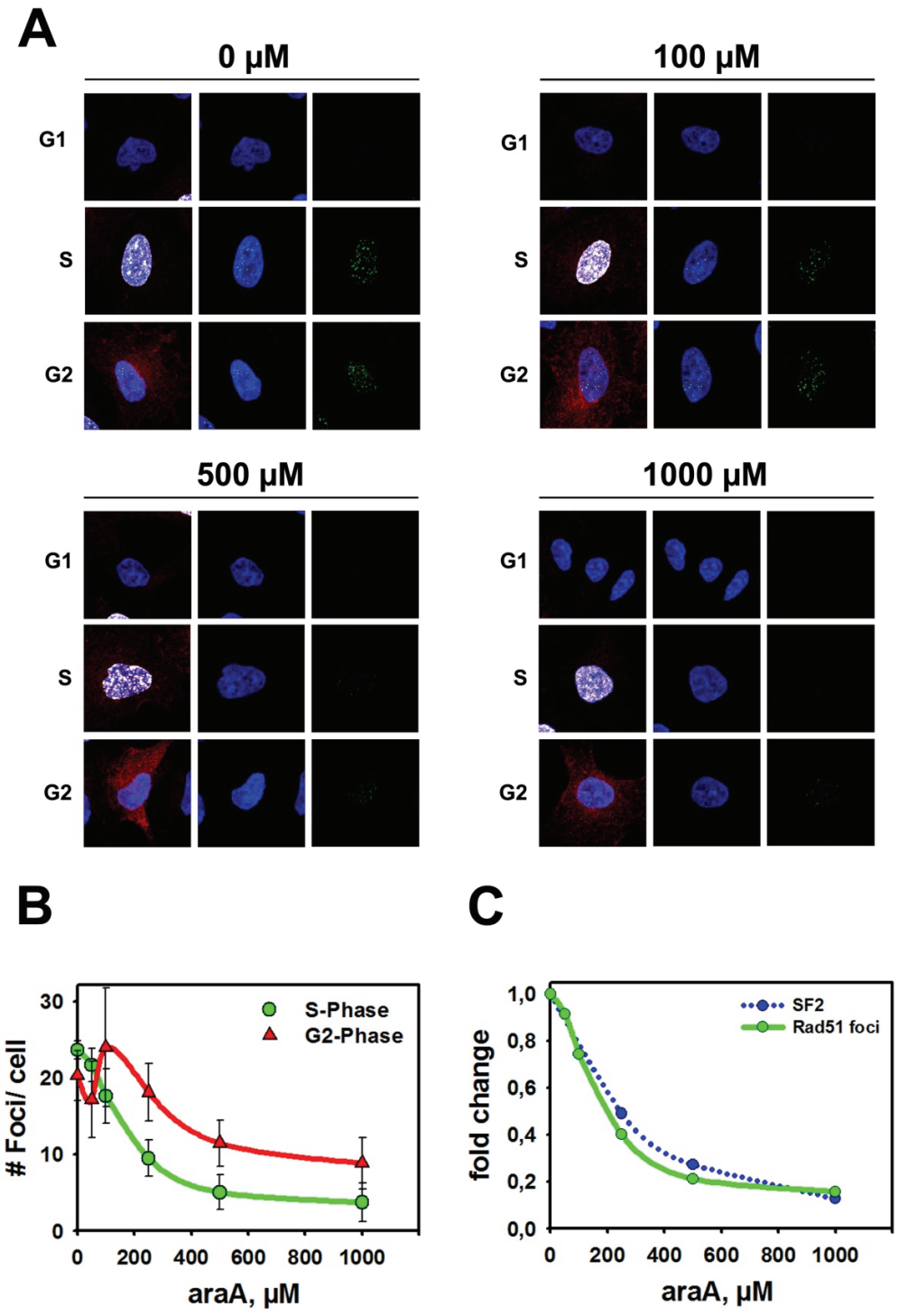

Figure 15 Inhibition of Rad51 foci formation in A549 cells by ara-A. Cells were fixed and stained 3 h after exposure of exponentially growing A549 cells to 4 Gy X-rays and treatment with different concentrations of ara-A. To label cells in S-phase, cultures were exposed to an EdU pulse (15 min) just before irradiation. Late-S and G2-cells were identified by staining for Cyclin B1. **A)** Split channel

representation of confocal microscopy immunofluorescence images. Micro molar indications above the individual blocks show the respective ara-A concentration. The left column of each block shows an overlay of DAPI (blue), EdU (white), Cyclin B1 (red) and Rad51 (green) staining. The middle column shows an overlay of DAPI (blue) and Rad51 (green) staining. The right column shows Rad51 staining alone (green). **B)** Number of Rad51 foci scored in S-phase (green circles and line) and G2-Phase cells (red circles and line) as a function of ara-A concentration. Mean foci number and s.e.m. from 3 independent experiments are shown. Each S-phase data point represents a total of 384 (±105) cells (~130 S-phase cells were analyzed for each concentration in every experiment). Each G2 data point represents of 61 (±19) cells on average in 3 independent experiments (~20 G2-phase cells were analyzed for each concentration in every experiment). **C)** Comparison of the concentration dependency of survival of A549 cells at 2 Gy (post-irradiation treatment with ara-A for 4 h) and Rad51 foci suppression in A549 by ara-A. Curves were derived from the data presented in Figure 14 and Figure 15 B.

Quantitative analysis of immunofluorescence images revealed a marked reduction in the number of Rad51 foci in ara-A treated cells irradiated during the S-phase (Figure 15 B; green circles). Half maximum inhibition of Rad51 foci formation was about 165 µM ara-A and Rad51 foci formation almost ceased above 500 µM. The ara-A concentration-Rad51 foci-effect relationship is very similar to that of radiosensitization to killing at 2 Gy, which implies a cause-effect relationship between these two endpoints (Figure 15 C).

Higher concentrations of ara-A appeared to be required in G2 to reduce the number of Rad51 foci to similar levels like in S-phase cells. Nevertheless, the reduction of Rad51 foci formation in ara-A treated G2-phase cells followed a similar trend. At concentrations above 250 µM a strong reduction was observed in the number of Rad51 foci and more than 50% inhibition was achieved at 1000 µM ara-A (Figure 15 B; red triangles and line). We concluded therefore that ara-A must exert a strong inhibitory effect on HRR. Figure 15 C shows the normalized number of Rad51 foci (S + G2) and the normalized survival at 2 Gy, both plotted against the ara-A concentration. The curves show an almost identical course in dependence of drug concentration, suggestive of an underlying cause-effect relationship.

4.3.2 Proficiency in HRR is a prerequisite for radiosensitization by ara-A

Results obtained by scoring Rad51 foci prompted us to hypothesize that inhibition of HRR may constitute an important mechanism of radiosensitization by ara-A. If inhibition of HRR was a major mechanism of radiosensitization, sensitization of cells already deficient for HRR should be reduced as compared to HRR proficient cells. Maximum suppression of HRR would theoretically be achieved in the absence of Rad51 (see also Figure 19). Since knockout of Rad51 is lethal in mice as well as in human cell lines, we attempted to induce a transient deficiency in HRR by RNAi mediated knockdown of Rad51. In order to enable direct comparisons with the already available cell survival measurements (see above), we used A549 cells to carry out these knockdown experiments. We used the same siRNA against Rad51 used in the DR-GFP experiments and as a negative control a siRNA against GFP. Cells were grown for 48 h before transfection with the respective siRNA. After transfection cells were cultured for another 24h before collection and processing for plating and irradiation for colony formation. Cells were left for 1.5h to attach before addition of ara-A. Cells were pre-incubated with the drug for 45 min before irradiation and the drug was washed away 4h later (Protocol II). Cellular levels of Rad51 protein were monitored by western blotting and proved to be reduced by more than 90% after transfection of the corresponding siRNA (Figure 16 A). Plating efficiency (PE) of cells transfected with siRNA targeting GFP was equal to that commonly found for untreated A549 cells. Furthermore, cells transfected with this control exhibited normal radiosensitivity to killing and were radiosensitized by ara-A to the same extend as untransfected cells in previous experiments.

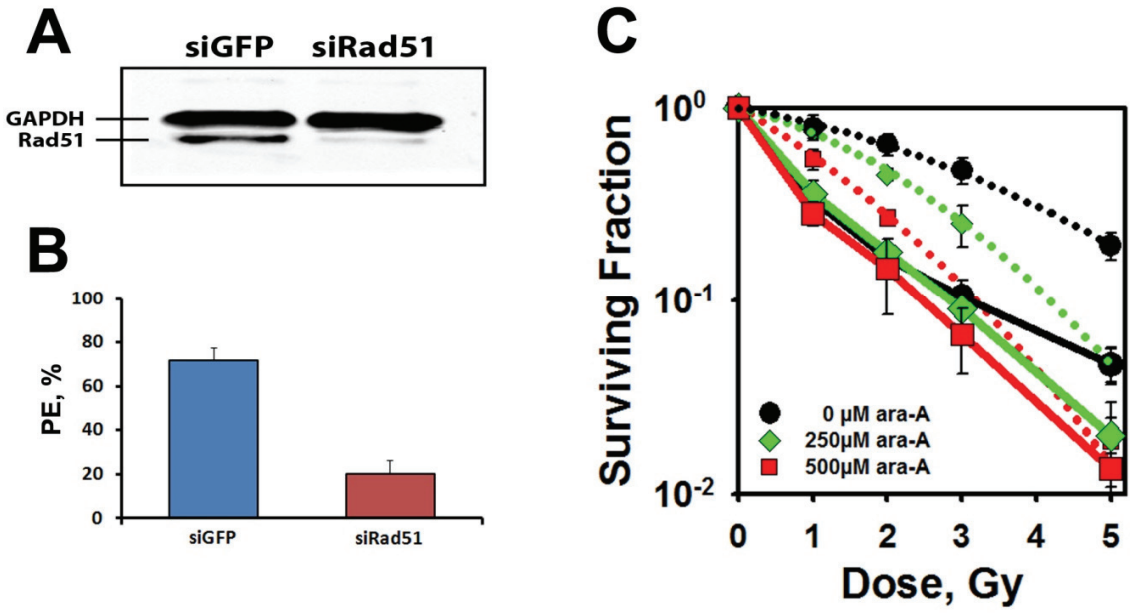

Figure 16 Requirement of HRR for the radiosensitization by ara-A. A) Detection of RAD51 protein in A549 cells 48h after transfection with either control (siGFP) or Rad51 (siRad51) siRNAs. GAPDH was used as a loading control. Detection of RAD51 and GAPDH was performed simultaneously using secondary antibodies with two different infrared dyes. Rad51 protein was reduced by more than 90% through RNAi. **B)** Plating efficiencies (PE) of siRNA transfected A549 cells. Cells transfected with the control siRNA exhibit the same PE typical for untransfected A549 cells. Cells transfected with siRad51 showed a decreased PE of about 20%. Bars show mean and s.d. from 3 independent experiments. **C)** Radiosensitivity of siRNA transfected cells treated with different concentrations of ara-A. *Dotted lines:* Cells transfected with siGFP. *Solid lines:* Cells transfected with siRad51. *Black circles and curves:* No ara-A treatment. *Green diamonds and curves:* Treatment with 250 µM ara-A. *Red squares and curves:* Treatment with 500 µM ara-A. Plots show mean and s.d. of 3 independent experiments.

This confirmed that the transfection procedure itself had no significant impact on the viability and radiosensitivity of cells. On the other hand, we found that the PE of cells transfected with siRNA against Rad51 was reduced (20% +/- 6% vs. 72% +/- 6) (Figure 16 B). This was not unexpected, as cells deprived of key HRR factors have been shown to display reduced PE (Feng, 2011; Liu, 2011; Short, 2011; Jensen, 2013). Importantly, cells treated with siRNA against Rad51 were significantly more radiosensitive than the corresponding controls. This is in agreement with the radiosensitive phenotype shown by others after Rad51 knockdown and confirms that cells retaining their ability to form

colonies after transfection of Rad51 siRNA do not represent an untransfected subpopulation (Liu, 2011; Short, 2011). In Rad51 depleted cells treatment with ara-A failed to further increase the radiosensitivity at most irradiation doses (Figure 16 C). Only at the highest radiation dose used in these experiments (5 Gy) we observed a significant (p= 0.006) radiosensitization by ara-A. However, the shape of the survival curve and the observed increase in radioresistance makes it likely that this radiosensitization derived from a small subpopulation that retained more HRR function than the bulk of cells. We concluded that HRR proficiency is a pre-requisite for efficient ara-A mediated radiosensitization.

4.3.3 Effects of ara-A on homology directed repair in reporter gene assays

4.3.3.1 Effects of ara-A on HRR

Several cellular reporter gene systems exist that claim to provide a measure for the activity of specific DSB repair pathways. To further investigate inhibition of HRR by ara-A we employed cell lines bearing stable integrations of a repair reporter construct that is designed to detect events that can arise due to the activity of the SDSA sub-pathway of HRR. This construct, DR-GFP, consists of two modified GFP gene sequences oriented as **d**irect **r**epeats (hence the name DR-GFP; see Figure 17 A). The first of the two sequences is a full length GFP gene (SceGFP), which is disrupted by an I-SceI site and a premature Stop-codon. It is followed by a 3´ truncated **i**nactive copy of GFP (iGFP). Functional GFP cannot be expressed from any of the two GFP gene sequences in the construct. Upon expression of the I-SceI endonuclease a DSB is introduced in the SceGFP gene. If this DSB is repaired by HRR using iGFP as donor sequence, the I-SceI site and the premature Stop-codon in the SceGFP gene will be replaced by functional GFP sequences. Such a gene conversion event results in the reconstitution of a functional GFP gene. Cells that have undergone this form of repair can be easily detected by flow cytometry due to the resulting GFP fluorescence.

A CHO cell line, Draa40, carrying the DR-GFP construct was immediately available to us. Initial experiments were carried out using the following experimental protocol: CHO cells were transfected with the I-SceI expression plasmid (pCMV3xNLSI-SceI; Figure **17** A) using electroporation (Nucleofector; Lonza), which requires cell trypsinization and the generation of a suspension with high cell concentration. After transfection cells were plated with normal growth medium and incubated for 3h at under standard culture conditions to allow for reattachment of cells and the expression of I-SceI. Three hours later, ara-A was added and the cells were maintained with the drug for an additional 4h. At the end of the treatment time interval, drug-containing medium was removed and cells were washed and supplemented with fresh growth medium. Cells were collected 24h after transfection for analysis by flow cytometry (Figure 17 B).

Using this protocol we first investigated the concentration-dependent effects of ara-A on HRR. Ara-A is significantly more toxic to CHO than to human cells. Therefore we chose 500 µM ara-A to be the upper concentration limit. We found a strong correlation between increasing ara-A concentration and decreasing proportion of cells developing green fluorescence, indicating inhibition of HRR (Figure 17 C).

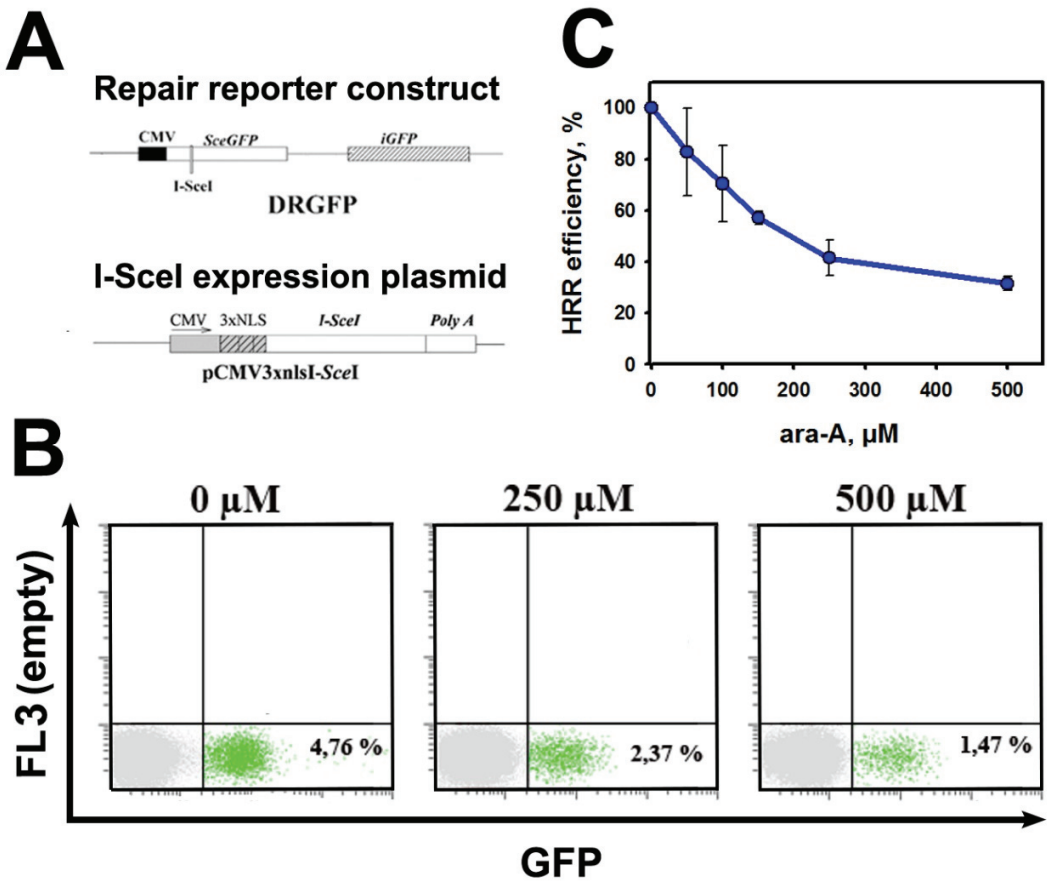

Figure 17 Suppression of HRR in DRaa40 cells harboring the DR-GFP reporter. A) Schematic of the stably integrated DR-GFP reporter construct and the I-SceI expression plasmid used to induce DSB in transfected cells. **B)** Representative flow cytometry dot plots of DRaa40 cells treated with different concentrations of ara-A. GFP was measured in fluorescence channel 1 (FL1). For better depiction of the positive populations, the GFP signal was plotted aginst signal recorded in FL3, for which no stain is included and in which cells showed very low autofluorescence. **C)** Graphical representation of HRR efficiency as a function of ara-A concentration (treatment 3h-7h after transfection) in DRaa40 cells. Data points show the mean and s.d. from 3 independent experiments.

At 500 µM ara-A suppressed HRR by about 70% (Figure 17 B&C). We next sought to determine whether there is a temporal relationship between HRR inhibition and the position of the treatment time window. We performed experiments in which we compared the effect of the default 3-7h post-transfection treatment to equal duration treatments applied at later times after transfection. We found that inhibition was

significantly weaker (p= 0.002) when the treatment was initiated 7h after transfection, and not present when treatment started 20h post transfection (Figure 18).

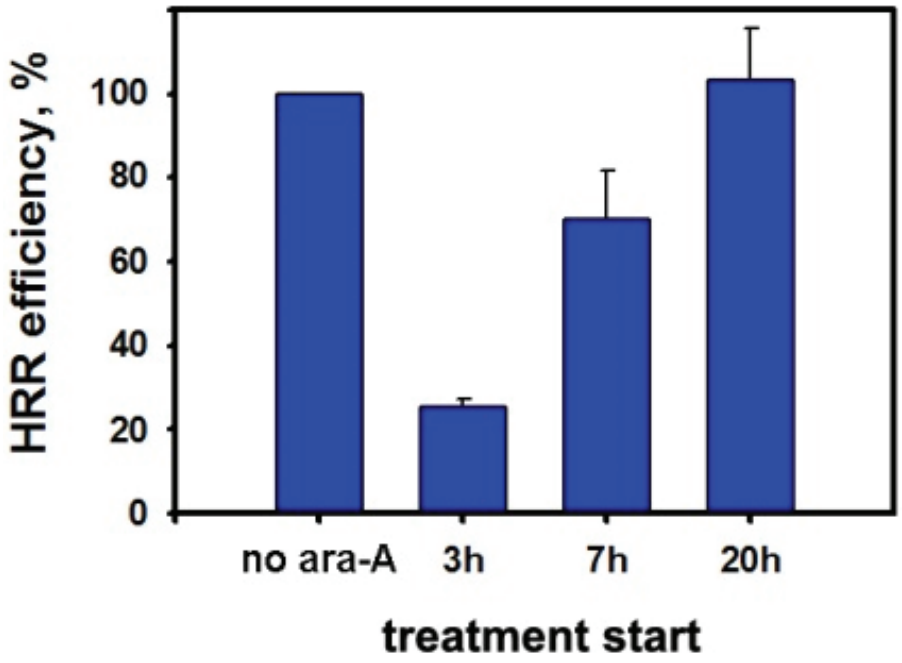

Figure 18 Time dependence of the effect of ara-A in DRaa40 cells (DR-GFP). A) Effect of a shift of the 4h treatment window to later times after transfection. Cells were treated with 500 μM ara-A for 4h. X-axis categories indicate the time of treatment start after transfection of the I-SceI plasmid. Data shown represent the mean and s.d. from three independent experiments.

When the human osteosarcoma cell line U2OS 282C, which also carries the DR-GFP construct, became available to us, we switched to this more relevant human cell system. The switch to a human system also gave us the opportunity to validate the assay by silencing of various factors implicated in HRR with siRNAs designed to target human transcripts. As a negative control we used a siRNA against Luciferase (Ctrl). Cells were transfected with siRNA using nucleofection and incubated for 24h under standard culturing conditions before transfection with the I-SceI expression vector. Another 24h later (48h after siRNA transfection) cells were collected and analyzed by flow cytometry. The efficiency of the knockdowns was confirmed at the protein level by western blotting (Figure 19 and (Costantino, 2013)). Knockdown of both, BRCA2 and Rad51, lead to a

strong and highly significant reduction of HRR in this system (Figure 20 B). Silencing of Rad51, as expected, had the strongest effect reducing the frequency of gene conversion events by more than 98 % (p= 0.00004). Silencing of BRCA2, which is known to play an important role in loading Rad51 onto ssDNA, resulted in a decrease of HRR events by almost 80 % (p= 0.017). Rad52 is a crucial factor for HRR in yeast, but is not essential for this process in human cells, probably due to a functional redundancy with BRCA2 (Feng, 2011). Accordingly, Rad52 knockdown is associated with a reduction of HRR by only approximately 25 %, but which was still significant (p= 0.049) (Figure 19 B).

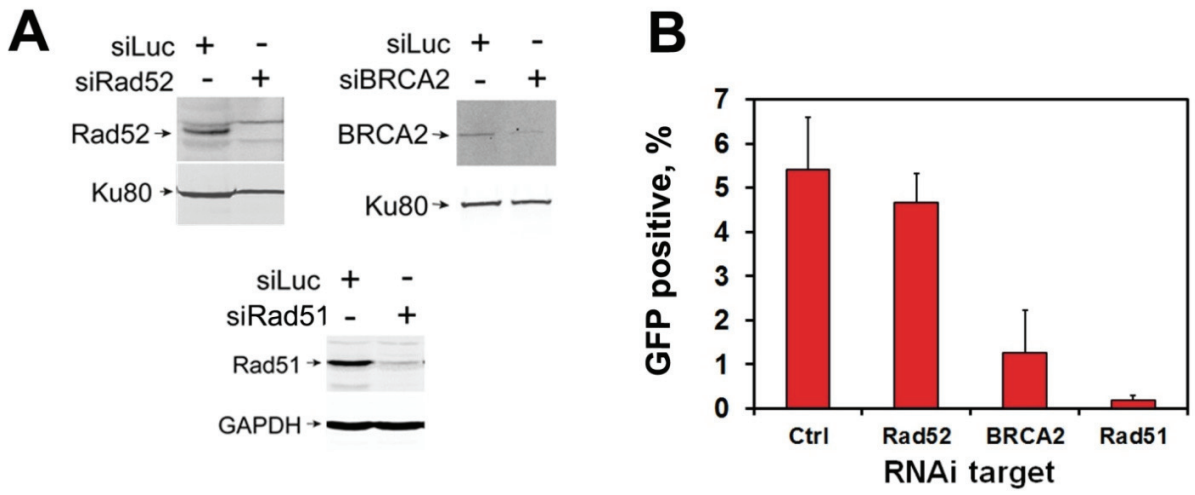

Figure 19 Knockdown of components of HRR in U2OS 282C cells (DR-GFP). **A)** Detection of protein levels by western blot. (Transfection and sampling were conducted by Simon Magin; gel runs, blotting and detection by Dr. Emil Mladenov). Upper left panel: RNAi of Rad52; knockdown>90%. Ku80 was used as loading control. Upper right panel: RNAi of BRCA2; knockdown~65%; loading control Ku80. Lower panel: RNAi of Rad51; knockdown 87%; loading control GAPDH. **B)** Quantification of GFP positive cells 24h after I-SceI-plasmid transfection and 48h after siRNA transfection. Bars show mean and s.d. of multiple experiments. Ctrl n=4; Rad52 n=5; BRCA2 n=3; Rad51 n=6.

Having confirmed the validity of U2OS 282C cells as a test system for HRR, we proceeded to test the effects of ara-A on HRR in human cells. Based on additional experimentation for optimization (Figure 35) we slightly modified the treatment protocol used in previous experiments and preponed drug-addition to 1.5h after transfection of

the I-SceI expression plasmid. After 4h of incubation with ara-A the medium was removed, cells were washed twice and supplied with fresh medium. Cells were analyzed by flow cytometry 24h after transfection.

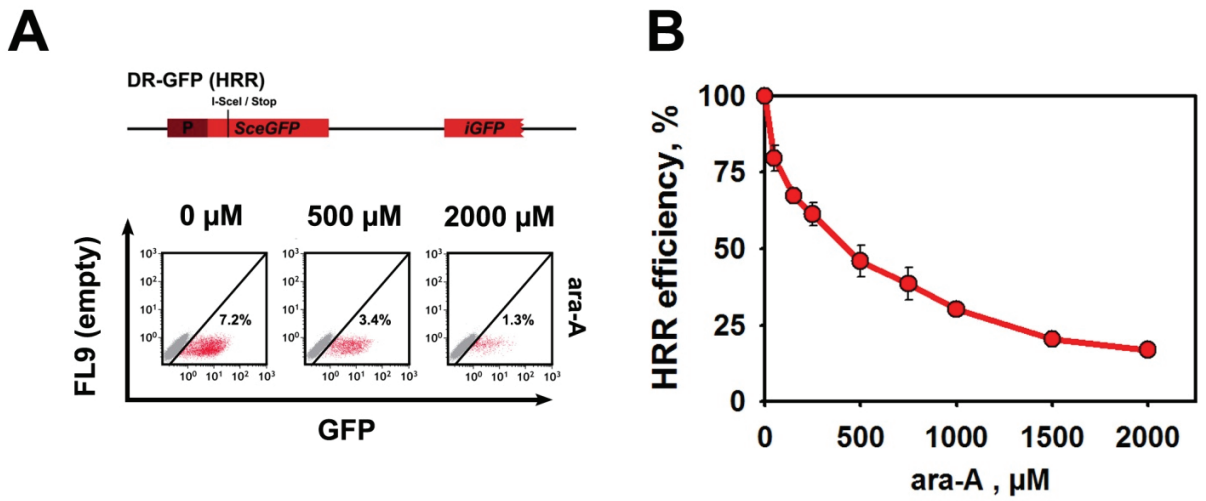

Figure 20 Inhibition of HRR by ara-A in U2OS 282C cells. A) *Top:* Schematic of DR-GFP construct present as single copy in this cell line. *Bottom:* representative flow cytrometry dot plots of samples treated with different concentrations of ara-A. **B)** Titration of ara-A effect on HRR as measured 24h after transfection with the I-SceI expression plasmid. Data points represent mean and s.d. from 3-5 independent experiments.

Incubation of U2OS 282C with ara-A for 4h resulted in a clear, concentration dependent decrease of the frequency of gene conversion events (Figure 20 A&C). These results confirmed the observations made with immunofluorescence staining of IR induced Rad51 foci. We concluded that ara-A exerts a strong inhibitory effect on HRR.

4.3.3.2 Effects of ara-A on SSA

Besides HRR, SSA is the other homology directed process for the repair of DSB. SSA repairs DSB by the intramolecular annealing of homologous sequences (see Introduction). Thus, there is no conceptual requirement for the presence of a sister chromatid or *de novo* synthesis of DNA. SSA frequently leads to the creation of large deletions and must be considered a highly error prone rejoining process. To investigate potential effects of ara-A on SSA we employed another repair reporter system.

The SA-GFP construct consists of two consecutive truncated GFP-ORFs separated by 2,7kb (Figure 21 A). The two sequences share 266nt of homology (Gunn and Stark, 2012). The first ORF (5´-GFP) is truncated at its 3´-end the second (3´-GFP) is truncated at its 5´-end and harbors an I-SceI site. Signal generation after repair by HRR is hampered by a premature stop codon at the 3´-end of the first ORF (5´-GFP). Upon repair by SSA a functional GFP gene is reconstituted.

We obtained a U2OS cell line (283C) which carries this construct stably integrated into its genome. First we wanted to evaluate this system in a similar manner as we did for the DR-GFP cell line 282C. The protein repertoire required for SSA in mammalian cells has not been very well characterized, but it is known that a functional HRR pathway strongly suppresses SSA events (Tutt, 2001; Stark, 2002). Therefore we decided to knock down the same set of proteins involved in HRR that was used in the evaluation of DR-GFP in U2OS 282C. Efficiency of knockdowns was equivalent to those achieved in U2OS 282C cells (compare Figure 19 A).

Consistent with the reported suppression of SSA by HRR, knockdown of the key HRR factors BRCA2 and Rad51 resulted in an increase in the frequency of SSA events in our experiments by about 400% and 500% respectively (Figure 21 B). Knockdown of Rad52, which had only shown mild effects on HRR, resulted in a reduction of SSA by approximately 55%. This suggests a more important role for Rad52 in SSA than in HRR in human cells and is in line with findings by other groups (Stark, 2004). Together these results seemed to confirm the validity of the SA-GFP system in U2OS 283C cells. We investigated the effects of ara-A on SSA using the same treatment plan as in experiments with the DR-GFP construct in 282C cells.

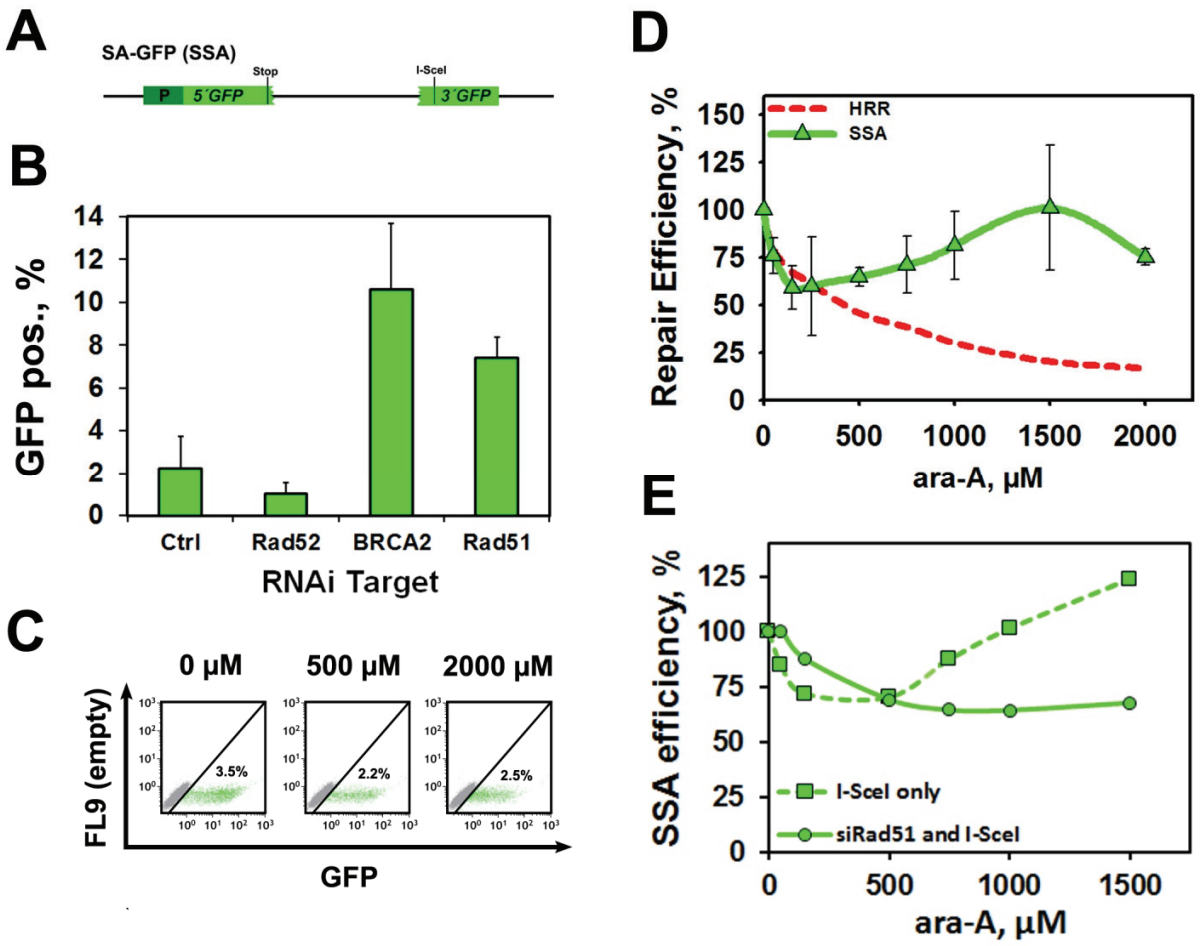

Figure 21 Effects of ara-A on SSA mediated repair in U2OS 283C cells (SA-GFP). A) Schematic of the SA-GFP construct. **B)** Effect of knockdown of several HRR factors on the SSA mediated repair of SA-GFP. Knockdown of BRCA2 and Rad51 lead to a dramatic increase in the proportion of GFP positive cells. **C)** Representative FACS plots of samples treated with different concentrations of ara-A measured 24h after transfection with the I-SceI expression plasmid. **D)** Titration of the effect of ara-A on SSA mediated repair, measured by flow cytometry 24h after transfection of the I-SceI expression plasmid. The dashed red line is a reproduction of the curve showing the effect of ara-A on HRR from Figure 20 C. Data points represent mean and s.d. from 3 independent experiments. **E)** Increase of SSA at higher concentrations of ara-A is dependent on inhibition of HRR. In cells that have been rendered deficient for HRR by RNAi of Rad51 no increase in SSA occurs at higher concentrations. Cells were transfected with siRNA for 48h and I-SceI was expressed for 24h prior to analysis. Data is normalized to the respective control without ara-A treatment. *Circles and solid line:* Cells silenced for Rad51. *Squares and dashed line:* Cells only transfected with I-SceI expression plasmid 24h prior to analysis. Plot represents data from one experiment.

Interestingly, we found that after an initial reduction of the efficiency of SSA at ara-A concentrations up to 150 µM, the frequency of GFP positive cells increased again at higher concentrations of ara-A (Figure 21 C&D) leading to full recovery at around 1500 µM ara-A. We speculated that this recovery of SSA at higher concentrations resulted from relieve of suppression mediated by Rad51 dependent HRR. We tested this hypothesis by silencing of Rad51 before subjecting U2OS 283C cells to ara-A treatment (Figure 21 E). As predicted, knockdown of Rad51 before induction of the DSB resulted again in a strong increase of repair by SSA compared to cells that were only transfected with the I-SceI expression plasmid (compare Figure 21 B). For better comparability values from Rad51 knockdown cells and cells left untreated before I-SceI expression were normalized to their respective controls (Figure 21 E). No recovery of SSA at higher concentrations was observed in cells deprived of Rad51, but SSA could still be reduced by about a third (Figure 21 E). This confirmed that the observed increase of SSA at higher concentrations of ara-A stemmed from the concomitant inhibition of HRR. Furthermore this result indicated that only a fraction of SSA events is sensitive to inhibition by ara-A, while about two thirds of SSA events are not.

4.4 Impact of ara-A treatment on NHEJ

4.4.1 Non-homologous rejoining of distal ends in paired DSB

Taken together the above results suggested an important role of HRR inhibition in the ara-A-mediated radiosensitization of cycling cells. However, a large amount of data from earlier studies showed strong inhibition of the repair of potentially lethal damage (PLD) by ara-A in non-cycling plateau phase cultures. Since the cell types used in most of these studies show extensive accumulation of cells with G1-DNA content in the plateau phase of growth, PLD inhibition in these populations cannot be explained by invoking inhibition of HRR. Therefore we inquired whether there may be other DSB repair pathways that are inhibited by ara-A.

The above results obtained with the SA-GFP construct indicated that mutagenic repair pathways may benefit from ara-A treatment under certain circumstances. SSA represents a homology dependent mode of mutagenic repair that results in the introduction of large deletions. Stark and colleagues have developed a reporter construct, EJ-5GFP, that also allows the measurement of non-homologous rejoining events associated with extensive deletions. The EJ5-GFP construct (integrated into U2OS 280A) consists of an intact EGFP ORF which is separated from its promoter by an interspersed puromycin resistance gene (Puro). In its uncut form only Puro is expressed. The Puro gene is flanked by two I-SceI sites. Upon cleavage at these sites rejoining can take place either between the proximal ends, leaving Puro in its place, or between the distal ends (distal end joining), resulting in excision of Puro and enabling expression of EGFP (Figure 22 A). This construct was stably integrated in U2OS cells resulting in the creation of the derivative cell line U2OS 280A.

The fidelity of the DNA-PK dependent pathway of NHEJ (D-NHEJ) is known to be higher than that of B-NHEJ, which is also frequently associated with large sequence losses. Therefore, we used chemical inhibition of DNA-PKcs to test if the EJ5-GFP can be used as an assay for the fidelity of NHEJ. NU7441 is a specific inhibitor of DNA-PKcs and induces a strong DSB repair defect in D-NHEJ proficient cells (Figure 38). Cells transfected with the I-SceI expression plasmid were treated with increasing concentrations of NU7441 for 6h after transfection. The proportion of GFP positive cells increased with increasing concentration reaching a plateau at approximately 5 μM (Figure 22 B). Perturbation of D-NHEJ by inhibition of DNA-PKcs resulted in an increase from 12% GFP positive cells in the untreated control to more than 20% in cells treated with 5 μM or more of Nu7441. We concluded that the use of distal over proximal ends in the repair of I-SceI induced tandem DSBs is indicative of compromised D-NHEJ, which is compensated for by B-NHEJ.

We proceeded to also perform experiments similar to those carried out with U2OS cells carrying the DR-GFP and SA-GFP constructs. We found that a 4h treatment with ara-A resulted, after a small decrease at lower concentrations (50 μM and 150 μM), in a concentration dependent increase in the proportion of GFP positive cells in the U2OS 280A cell line (Figure 22 C&D). This increase was found to be significant at all

concentrations above 250 µM ($p<0.05$). At 2000 µM ara-A, joining of distal ends increased to 130% (+-22%) of controls. Figure 22 D also shows the results obtained with the DR-GFP and SA-GFP constructs as dashed lines.

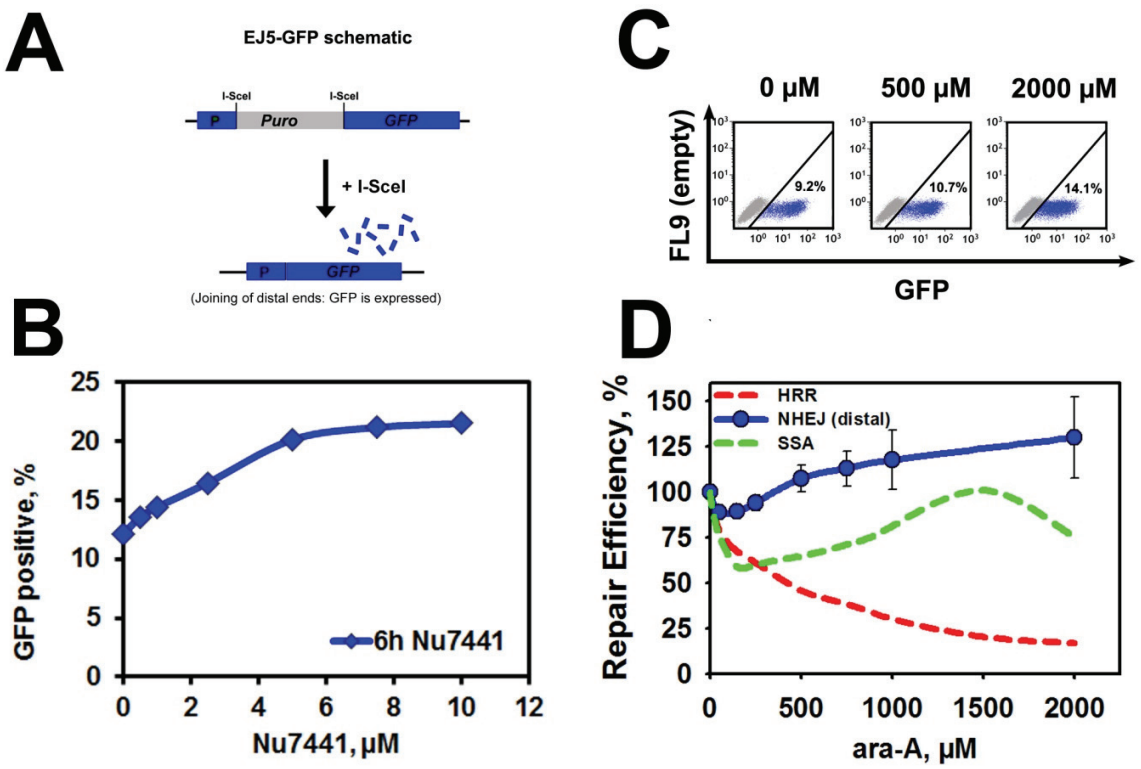

Figure 22 Effect of ara-A on the joining of distal ends in U2OS 280A (EJ5-GFP). A) Schematic of the EJ5-GFP construct. **B)** Effect of DNA-PKcs inhibition on the joining of distal ends. Cells were rendered deficient in D-NHEJ by treatment with the DNA-PKcs inhibitor Nu7441 for 6h. The inhibition resulted in a strong increase in the frequency of distal–end joining. Plot represents data from one experiment. An experiment with different treatment schedule yielding qualitatively equivalent results is presented in the appendix (Figure 39). **C)** Representative dot plots of U2OS 280A cells treated with different concentrations of ara-A. Flow cytometry was performed 24h after transfection of the I-SceI expression plasmid. **D)** Titration of the effect of ara-A on the use of distal ends for the repair of a DSB. Blue circles and line represent the mean and s.d. of three independent experiments with U2OS 280A cells and ara-A. The dashed red line shows the effect of ara-A on HRR and has been transferred from Figure 20 C. The dashed green line shows the effect of ara-A on SSA and has been transferred from Figure 21 D.

Taken together the results obtained with these DSB repair reporter constructs indicated that ara-A elicits a clear inhibition of the faithful HRR pathway, while mutagenic repair pathways like the rejoining of distal DSB ends or SSA appear to be favored and show enhancement.

4.4.2 The effect of ara-A on mutagenic repair in the EJ-RFP system

The EJ5-GFP construct allows the detection of a very specific repair event by NHEJ that results in the elimination of the intervening sequence between two I-SceI sites. This can be interpreted as an indicator for the tendency of a cell to perform mutagenic repair. However, the repair events that result in signal generation in this reporter system represent only a very small part of the spectrum of possible mutagenic NHEJ events.

A repair reporter system that allows the detection of the majority of mutagenic events was developed by Bindra et al. (Bindra, 2013) and stably integrated into U2OS cells. The resulting cell line was named U2OS EJ-DR. The EJ-RFP system consists of a tetracycline repressor gene and an independent DsRed gene containing several TetR binding sites (Figure 23 A). Expression of the DsREd gene is constitutively repressed. The TetR gene contains an I-SceI site that is cut upon expression of I-SceI in the cells. If the resulting DSB is repaired with mutagenic consequences the TetR gene is disrupted and a DsRed signal can develop. This requires clearance of the remaining TetR protein and subsequent expression of the DsRed gene. In addition maturation of DsRed protein requires more time than the maturation of GFP proteins (Magin, 2013). These factors are reflected by the slow kinetics of appearance of red fluorescent signal in the cell population (Figure 37 A&B). DsRed positive cells starts to appear 3 days after transfection of the I-SceI plasmid and after 4 days a robust population had built up (Figure 37 A&B). Thus, measurements using this system could not be performed after 24h as in the other reporter cell lines, but had to be carried out 96h after transfection.

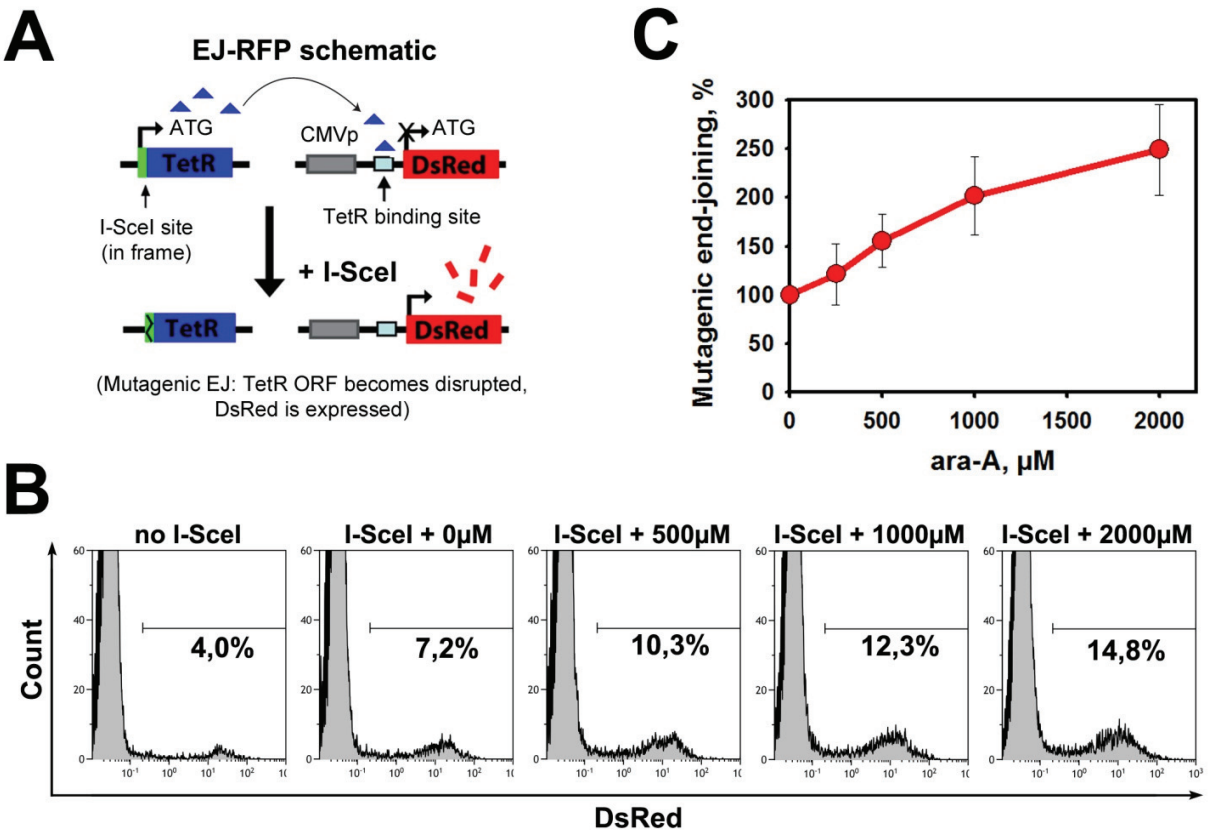

Figure 23 Effect of ara-A on mutagenic DSB repair pathways in U2OS EJ-DR cells. A) Schematic of the EJ-RFP system. **B)** DsRed expression in EJ-DR cells 96h after transfection. Non-transfected cells (no I-SceI) have a substantial background of DsRed positive cells. Transfection of I-SceI causes an increase in the portion of DsRed positive cells (I-SceI + 0µM). Treatment with ara-A increased the fraction of DsRed positive cells significantly ($p < 0.05$) above 250µM (I-SceI 500µM-2000µM). Y-Axis was limited to a fixed value to allow better comparison of the fraction of positive cells. Equal amounts of cells were measured for each sample ($1.5*10^4$). **C)** Effect of ara-A treatment on mutagenic end-joining in EJ-DR cells 96h after transfection of the I-SceI expression plasmid. Measured values were corrected for background and normalized to the corrected control (0µM). Data points represent mean and s.d. from three independent experiments.

Unlike the other reporter cell lines introduced so far the EJ-DR cells possessed a significant background, i.e. cells with fluorescent signal without induction of I-SceI (between 1.5%-5% of the total population; Figure 23 B). Therefore, measured values were corrected by the background detected in untransfected cells and normalized to the number of DsRed positive cells in the control (I-SceI transfected without drug treatment).

We observed that in cells that were treated with ara-A for a four hour period after transfection, the proportion of cells showing red fluorescence was elevated (Figure 23 C). With rising concentrations of ara-A the amount of mutagenic repair of the I-SceI induced DSB appeared to increase. At a concentration of 2000 µM the corrected portion of DsRed positive cells was 250% of the control (Figure 23 C).

4.4.3 Effect of ara-A on DSB repair kinetics in D-NHEJ proficient cells

Results from experiments involving the SA-GFP, EJ5-GFP and EJ-RFP constructs suggested that treatment with ara-A induces a shift towards more mutagenic modes of DSB repair. While for SA-GFP the responsible repair pathway is clear (SSA), for EJ5-GFP and EJ-RFP interpretation is less unequivocal. However, results obtained with Nu7441 in U2OS 280A cells prompted us to hypothesize that signal generation in the EJ5-GFP construct is indicative of B-NHEJ activity. We asked whether this shift towards mutagenicity and putative promotion of B-NHEJ, as well as inhibition of HRR would be reflected in the kinetics of DSB repair in cells treated with ara-A.

PFGE is a method that allows the physical detection of DSB in DNA. The amount of DSB and the kinetics of their repair are measured in the pooled total DNA of irradiated cell populations. The method is described in detail under Materials and Methods. Briefly, cells are embedded in small agarose blocks (plugs), which are loaded onto agarose gels that are subjected to an alternating electrical field for long run times (40 hours). DSB reduce the molecular weight of DNA and generate DNA fragments that can migrate from the plug into the gel. Higher molecular weight chromosomal DNA remains trapped within the plug.

To obtain a measure for the amount of DSB present in a sample, the fluorescence signal generated by the stained DNA that leaves the plug and enters the lane is divided by the total signal of the same sample (plug + gel lane signal). This ratio is termed the fraction of DNA released (FDR). A linear relationship exists between FDR and radiation dose (Figure 24 B). Dose response curves (DR) are generated with samples that are irradiated with different doses of X-rays, but are not allowed to repair before processing. The DR data is used to express the FDR of cells that were allowed to repair as radiation

dose equivalents (DEQ). In this way repair kinetics (RK) are obtained that start (0 h) with a total DSB load equivalent to the initially delivered radiation dose (here 20 Gy). In repair proficient cells the kinetics of repair, as seen by the decline in DEQ, is biphasic. A fast component repairs ~80% of DSB within 0.5h-1h after irradiation and is followed by a second one that removes the remaining DSB within 4h-8h after IR.

It is well known that some pathways of DSB repair operate with varying efficiencies depending on the growth state and phase of the cell cycle. HRR for example can only operate during the S an G2 phase, while B-NHEJ is known to be inhibited in the plateau phase of growth but enhanced in G2 (Wu, 2008b; Singh, 2011) (see Introduction). Thus, it is possible that repair pathway specific effects of ara-A would be masked by the distribution of cells over all phases of the cell cycle when using asynchronous samples.

To overcome this complication we combined FACS with PFGE. In this way we could analyze populations highly enriched in G1 or G2 phase cells (Figure 24 A). Separate DR curves were prepared for asynchronous, G1 and G2 cells. G1 and G2 phase cells show a higher FDR per Gy than asynchronous cells (Figure 24 B). This is due to the S-phase cells present in the asynchronous population, which are known to display a lower FDR per Gy due to replication associated DNA structures (Latz, 1996; Dewey, 1997).

Treatment with 1 mM ara-A did not change the kinetics of DSB repair in asynchronous cells (Figure 24 C). Excellent purities were achieved for cells sorted in G1 and G2 from exponentially growing cultures. For G1 cells an enrichment of 95.8% +/- 2.0% and for G2 cells an enrichment of 81.1% +/- 6% was achieved. These purity levels were maintained for all populations sorted at the different repair time points; the cell cycle analysis is shown in the right panels of Figure 24 C, D and E. Neither G1 nor G2 cells showed inhibition of DSB repair after incubation with 1 mM ara-A.

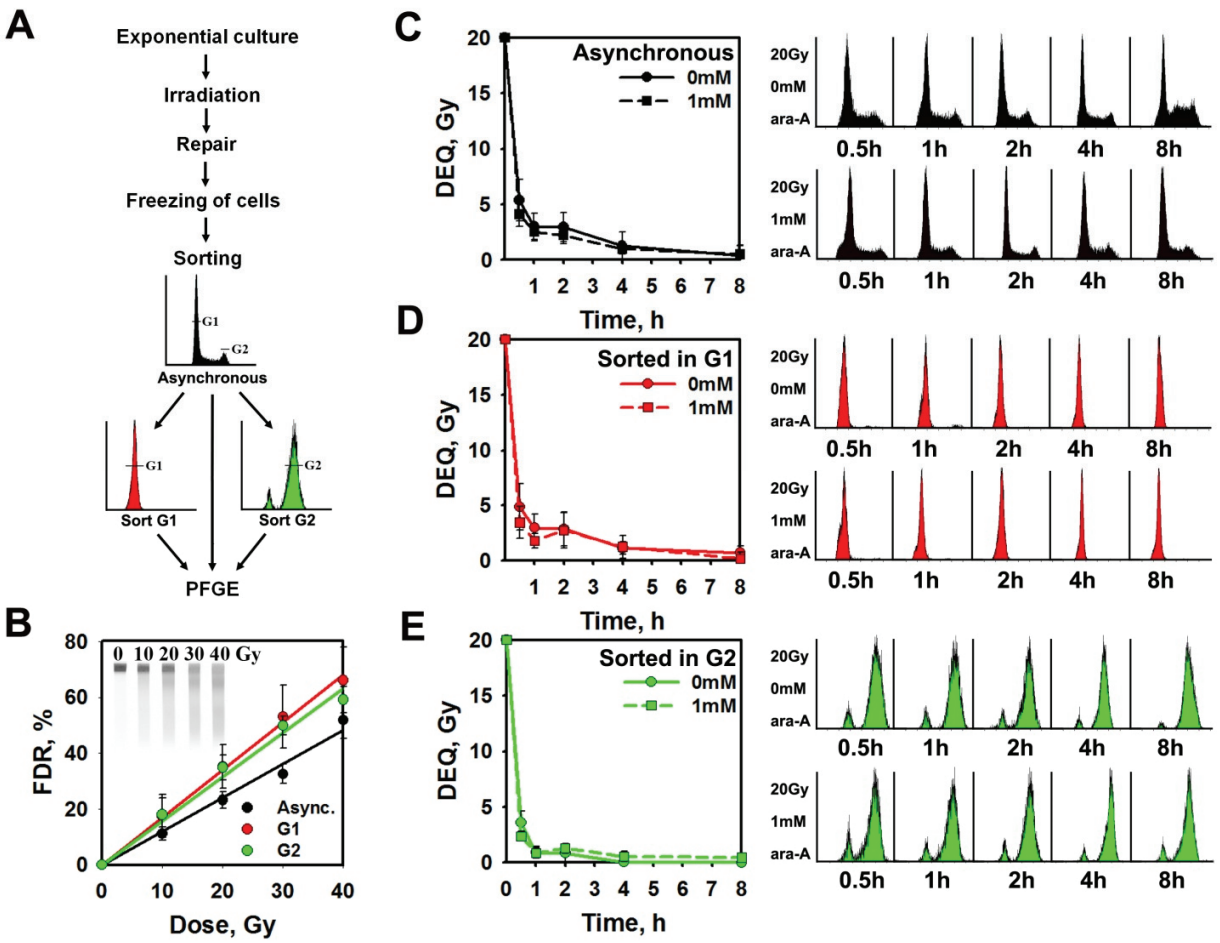

Figure 24 DSB repair by PFGE in sorted G1 and G2 A549 cells. A) Outline of the experimental work-flow. **B)** Dose response (DR) curves for the induction of DSBs in sorted G1- and G2-phase cells, as well as in the asynchronous populations. Black circles, asynchronous cells; red circles, sorted G1 cells; green circles, sorted G2 cells. In the upper left corner an image of a typical DR on a PFGE gel is shown. **C)** Results for the asynchronous cell population. *Left panel:* DSB repair kinetics measured in the presence (1 mM; dashed line), or absence (0 mM; solid line) of ara-A. *Right panel:* Representative flow cytometry histograms of cell populations collected at different times after IR. **D)** As in C for cells sorted in G1-phase. **E)** As in C for cells sorted in the G2-phase. All graphs depict the mean and s.d. from 6-8 determinations from 2 independent experiments. FDR = fraction of DNA released; DEQ = Dose equivalent.

The careful approach and the accuracy of the obtained results allowed us to exclude confounding factors of PFGE technology as the reason why inhibition of DSB repair after incubation with ara-A could not be detected. D-NHEJ, unlike HRR and B-NHEJ, is

believed to operate with unaltered efficiency in G1, S and G2. Moreover, D-NHEJ is commonly regarded to be the dominant pathway of DSB repair throughout the cell cycle. If the great majority of DSB is repaired by D-NHEJ under the conditions employed for PFGE, interference of the drug with one of the remaining repair pathways or a partial shift to other pathways may be missed. This interpretation is supported by the observation that HRR mutants show in similar experiments no DSB repair defect, despite their increased radiosensitivity to killing (Wang, 2001a; Iliakis, 2004). Furthermore it is not clear if a shift to B-NHEJ in D-NHEJ proficient cells would necessitate a slowdown of repair.

4.4.4 Effect of ara-A on DSB repair in D-NHEJ deficient cells

Since we couldn´t detect any effect of ara-A on the kinetics of DSB repair in D-NHEJ proficient cells we inquired if the same was true for D-NHEJ deficient cell lines. The activity of B-NHEJ becomes dominant in cells where core components of the classical, DNA-PKcs dependent pathway are dysfunctional or not present. Repair of DSB that is observable in these cells is chiefly carried out by B-NHEJ (Dibiase, 2000; Perrault, 2004). We reasoned that in these cells alterations of the activity of B-NHEJ may be more apparent.

For this purpose we utilized the human colorectal cancer cell line HCT116 (WT) and its two derivative knockout mutants HCT116 Lig4$^{-/-}$ and HCT116 DNA-PKcs$^{-/-}$. We performed experiments with exponentially growing as well as with serum deprived cells. B-NHEJ is known to be suppressed under the latter condition (Singh, 2011) and we were curious to see if there might be differential effects. For serum deprivation we employed the protocol as described in Material and Methods (3.2.1.2). Briefly, cells were grown for 2 days. Then medium containing serum was removed and replaced by medium without serum. Another 24h later, cells were used in the experiment, during which they were continuously kept without serum. We used a treatment with 500 µM of ara-A for all cell lines. Cells were treated until they were collected at the respective time points for further processing.

In exponentially growing cells ara-A treatment did not alter the repair kinetics of the WT, but enhanced the repair of DSB in Lig4 knockout cells (Figure 25 A). Repair in ara-A

treated Lig4$^{-/-}$ cells was increased by a dose equivalent of 5 Gy compared to the untreated Lig4$^{-/-}$ cells at 0.5h, but progressed with similar kinetics afterwards, keeping a constant gap (delta DEQ= 4-5 Gy) (Figure 25 A). Ara-A treated DNA-PKcs knockout cells repaired quicker initially, but repair progressed faster in the untreated DNA-PKcs$^{-/-}$ cells between 1h and 4h (Figure 25 A). At 8h treated and untreated DNA-PK cs$^{-/-}$ cells had the same amount of residual DSB. Interestingly the curves of ara-A treated Lig4$^{-/-}$ and DNA-PKcs$^{-/-}$ cells were fully congruent (Figure 25 A).

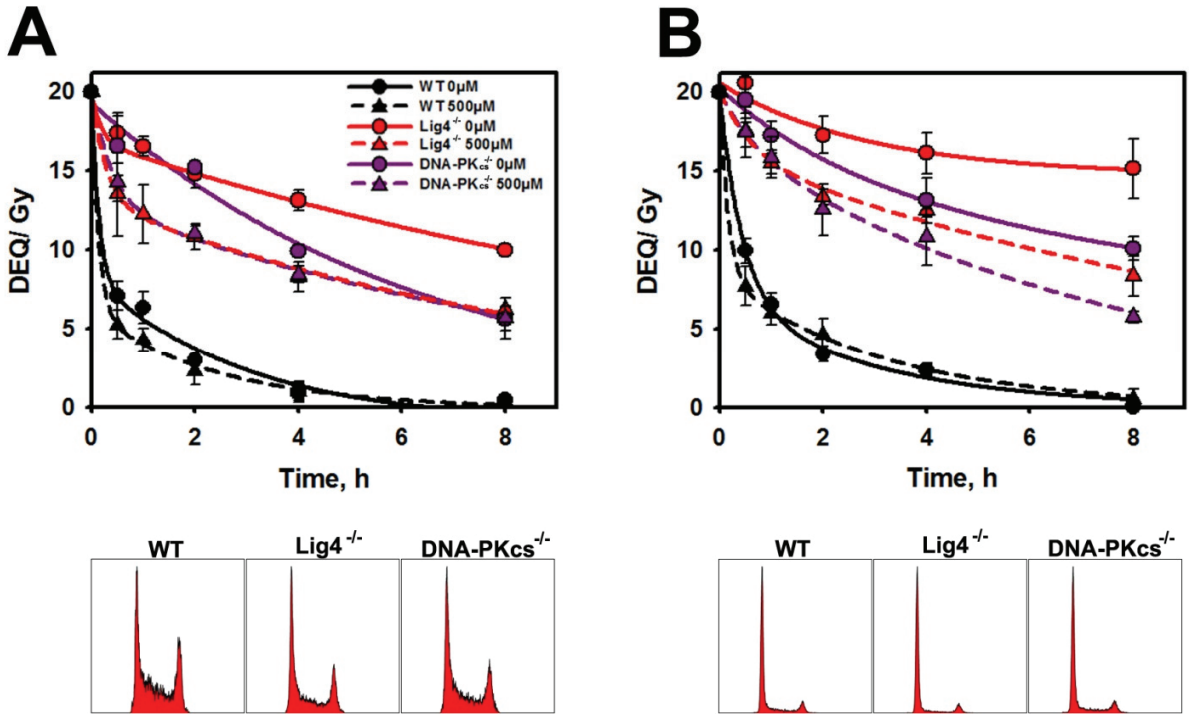

Figure 25 Enhancement of DSB repair in D-NHEJ deficient human cells. **A)** *Top Panel:* Exponentially growing HCT116 wild type (WT), Ligase 4 knockout (Lig4$^{-/-}$) and DNA-PKcs knockout (DNA-PKcs$^{-/-}$) cells were irradiated with 20 Gy X-rays and left to repair without or with 500 µM ara-A. The amount of DSB was determined by PFGE. *Black circles and solid line:* HCT116 WT without ara-A. *Black triangles and dashed line:* HCT116 WT treated with 500 µM ara-A. *Red circles and solid line:* HCT116 Lig4$^{-/-}$ without ara-A (0 µM). *Red triangles and dashed line:* HCT116 Lig4$^{-/-}$ treated with 500 µM ara-A. *Violet circles and solid line:* HCT116 DNA-PKcs$^{-/-}$ without ara-A (0 µM). *Violet triangles and dashed line:* HCT116 DNA-PKcs$^{-/-}$ treated with 500 µM ara-A. Data Points represent mean and s.d. from triple determination from one experiment. *Bottom Panel:* Cell cycle distributions of the starting populations of the three used cell lines. **B)** As in (A), but for serum deprived cells.

Under conditions of serum deprivation, DSB repair kinetics of WT cells were minimally slower than in exponentially growing cells, but were not altered by ara-A treatment (Figure 25 B). In line with the expectations the repair of DSB by the two knockout cell lines was substantially decreased in serum deprived cultures due to suppression of B-NHEJ (Figure 25 B). Treatment with 500 µM ara-A clearly increased the efficiency of B-NHEJ in Lig4$^{-/-}$ cells (Figure 25 B). After 8h, ara-A treated cells had repaired 52% of the initial DSB load. Untreated Lig4 on the other hand still retained more than 75% of the initial DSB (delta DEQ= 6.8). The difference was smaller in DNA-PKcs knockout cells (Figure 25 B), but present in contrast to exponentially growing cells. After 8h ara-A treated DNA-PK cells only retained DSB corresponding to a DEQ of 5.7 Gy. Untreated DNA-PK cells on the other hand retained DSB corresponding to a DEQ of 10.1 Gy (delta DEQ= 4.4).

PFGE experiments with HCT116 WT, Lig4$^{-/-}$ and DNA-PKcs$^{-/-}$ cells showed that ara-A modulates DSB repair in D-NHEJ deficient cells in the exponential phase of growth, as well as under serum deprivation. These results confirmed that ara-A treatment can positively regulate B-NHEJ. They also showed that promotion of B-NHEJ, compared to the untreated controls, was more pronounced when B-NHEJ was suppressed by serum deprivation.

4.4.5 Relieve of serum deprivation-induced inhibition of B-NHEJ by ara-A

In the light of the above results obtained with HCT116 cells we progressed to another system that reproducibly provides very strong inhibition of B-NHEJ under conditions of serum deprivation. MEF with a knockout for both alleles of Lig4 (MEF Lig4$^{-/-}$) have been extensively used in our institute. Under serum deprivation they frequently showed an almost full lack of DSB repair. To confirm that these standard could be met within this line of investigation we aimed to reproduce these PFGE results. We used exponentially growing, as well as serum-deprived cultures of MEF Lig4$^{-/-}$ and the parental MEF Lig4$^{+/+}$ for comparison. Exponentially growing Lig4$^{-/-}$ MEFs showed a pronounced DSB repair defect while the parental cells repaired efficiently (**Figure** B). Still within 2h after

irradiation about 50% of the breaks were repaired in MEF Lig4$^{-/-}$ cells, reflecting the activity of B-NHEJ.

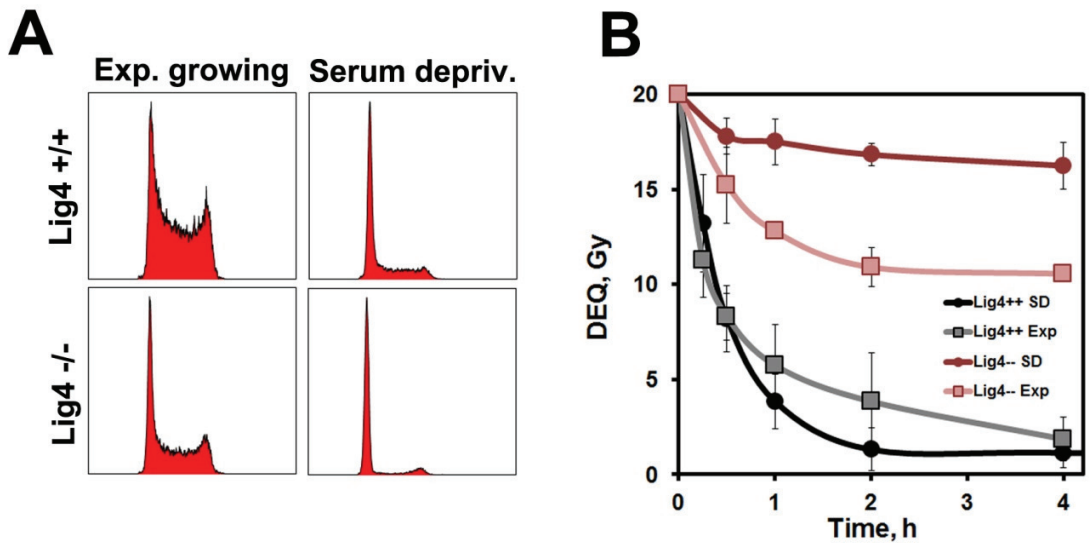

Figure 26 DSB repair by PFGE in exponentially growing and serum deprived MEF. A) Cell cycle distributions determined by FACS. **B)** DSB repair kinetics of MEF Lig4$^{-/-}$ and MEF Lig4$^{+/+}$ cells. *Grey squares and line:* Exponentially growing MEF Lig4$^{+/+}$ cells. *Black circles and line:* Serum deprived MEF Lig4$^{+/+}$ cells. *Light red squares and line:* Exponentially growing MEF Lig4$^{-/-}$ cells. *Dark red circles and line:* Serum deprived MEF Lig4$^{-/-}$ cells. Data points of MEF Lig4$^{+/+}$ cells and exponentially growing MEF Lig4$^{-/-}$ cells represent mean and s.d. of triple determinations from one experiment. Data points of serum deprived MEF Lig4$^{-/-}$ represent mean and s.d. of 4 independent experiments with triple determinations each.

A plateau phase like state could be induced very efficiently in these cells by serum deprivation and resulted in accumulation of cells with G1 DNA content (Figure A). As a result of this, an almost complete inhibition of DSB repair was observed in serum deprived MEF Lig4$^{-/-}$ cells (Figure 26 B). In contrast serum deprivation did not significantly alter DSB repair kinetics in MEF Lig4$^{+/+}$ cells (Figure 26 B).

We found that exponentially growing MEF Lig4$^{+/+}$ and MEF Lig4$^{-/-}$ cells were very sensitive to ara-A treatment, which lead to extensive cell death and unacceptably high levels of background at longer treatment times in PFGE experiments (Data not shown). Therefore we decided to only use serum deprived Lig4$^{-/-}$ cells for further experiments, where toxicity was not a problem (Figure 27 A; lower panel controls 4h). Cultures of serum deprived Lig4$^{-/-}$ MEFs were irradiated with 20 Gy X-rays and treated with 250µM ara-A or solvent and left to repair for different time intervals. As expected the untreated

cells showed impaired DSB repair (Figure 27 A). Astoundingly cells treated with 250 µM ara-A showed repair kinetics almost equal to repair in MEF Lig4$^{+/+}$ cells (compare Figure 27 A and Figure 26 B).

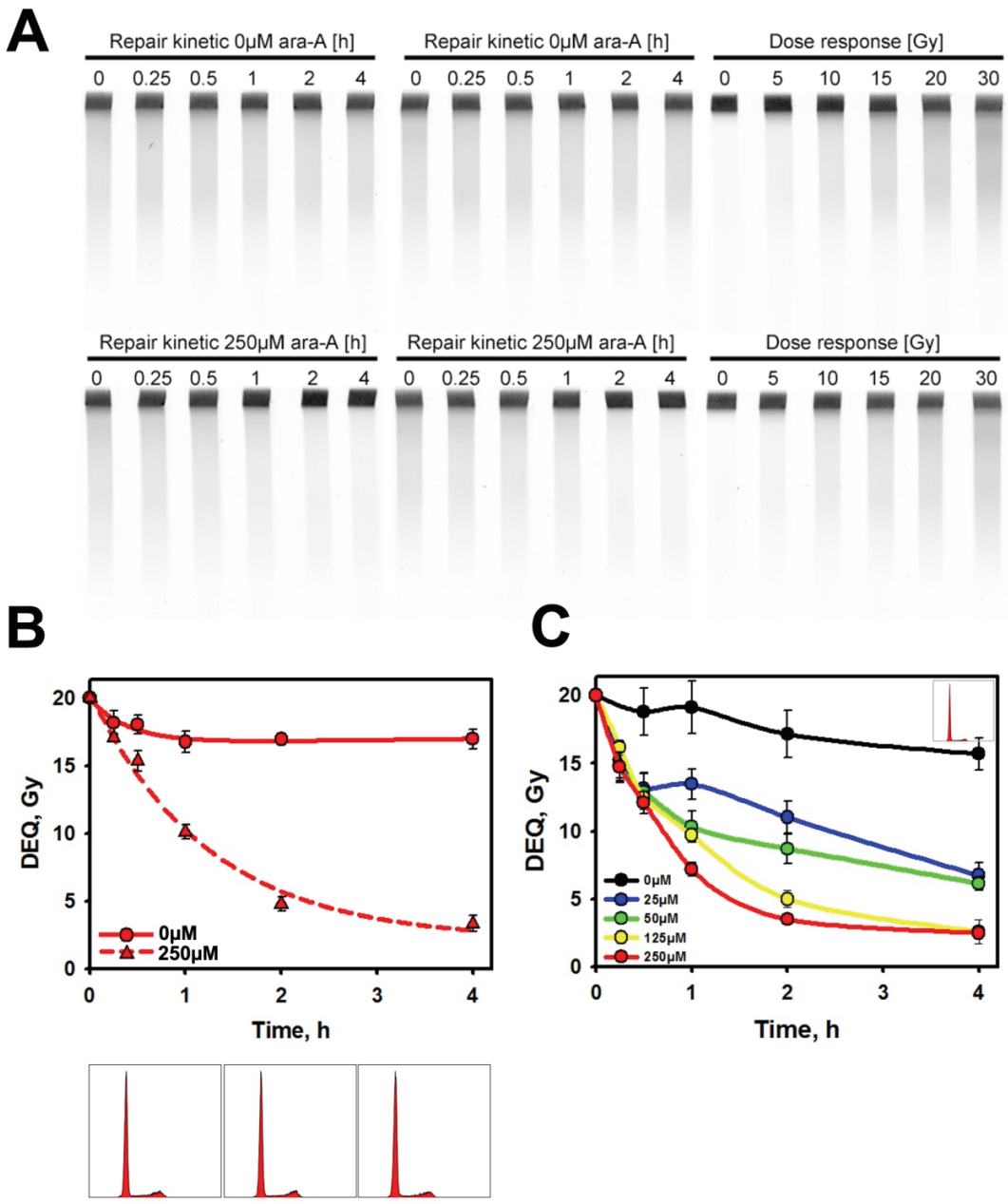

Figure 27 Ara-A treatment reactivates DSB repair in serum deprived Lig4$^{-/-}$ cells. A) *Top:* DSB repair kinetics measured by PFGE in serum deprived Lig4$^{-/-}$ cells. Cells were irradiated with 20 Gy and repair followed for 4h. Untreated cells hardly show any repair of DSB. Treatment with 250 µM enables efficient

repair which is almost complete after 4h. Data points represent mean and s.d. of triple determinations from one experiment. *Bottom:* Cell cycle distributions determined by FACS of cells stained for DNA content with PI. Treatment with ara-A did not cause any changes in the flow cytometry histograms. **B)** Titration of B-NHEJ enhancement by ara-A. DSB repair kinetics measured by PFGE in serum deprived MEF Lig4$^{-/-}$ cells. Cells were irradiated with 20 Gy and repair followed for 4h. Cells were either left untreated (0 µM), or treated with 25 µM (blue symbols and line), 50 µM (green symbols and line), 125 µM (yellow symbols and line) or 250 µM (red symbols and line). *Upper right corner of the graph:* Cell cycle distribution of the starting population determined. Data points represent mean and s.d. of triple determinations from one experiment.

This effect surpassed our expectations by far. We inquired whether lower concentrations of ara-A elicit similar effects. We found that ara-A concentrations between 25 µM and 250 µM all strongly increased the efficiency of B-NHEJ (Figure 27 B). Interestingly all concentrations showed almost identical enhancement of DSB repair up to 30 min after irradiation. At later times, however, the effect clearly increased with rising concentrations (Figure 27 B). Yet, even 25 µM and 50 µM ara-A were sufficient to reduce residual DSB after 4h of repair by a factor of two compared to the untreated control (0 µM). After treatment with 125 and 250 µM respectively, cells had repaired 87.5% of the initial damage, while the untreated control had repaired only 23,5% (delta DEQ= 12,8).

These results strongly supported the notion that ara-A treatment enhances B-NHEJ efficiency. Furthermore they suggested that ara-A interferes with the mechanism that suppresses B-NHEJ in the plateau phase of growth respectively under serum deprivation.

4.4.6 Analysis of IR induced foci in serum deprived MEF Lig4$^{-/-}$

To further investigate the effect of B-NHEJ enhancement by ara-A we employed immunofluorescence combined with confocal microscopy to analyze DSB repair at low radiation doses. We selected proteins and modifications involved in the DNA damage response with the property of forming IRIF upon exposure to IR. One post-translational protein (PTM) modification we studied was the phosphorylation of Serine 139 (S139) of the histone variant H2AX. This PTM is commonly used as a surrogate marker for DSB

and is also known as γH2AX. Foci of γH2AX form in large chromatin domains around DSB.

Recruitment of the protein 53BP1 to the sites of DSB is another assay that has been regularly used to monitor the repair of DSB. Both of these markers can be used to assess the capability of a cell to repair DSB.

Another protein modification occurring after IR is the phosphorylation of Serine 1981 (S1981) of ATM (pATM). ATM is a central kinase in IR induced DNA damage signaling and requires this phosphorylation for activation. pATM accumulates at sites of DSB where it can also be detected as IRIF. We aimed to analyze the assembly and the kinetics of decay of foci formed by these proteins in serum deprived Lig4$^{-/-}$ MEFs.

In cells that were not treated with ara-A, foci of γH2AX persisted virtually unchanged from 1h (49.0 (+/- 13.7)) up to 24h (45.2 (+/- 8.4)) after exposure to 1 Gy (Figure 28 A). However, serum deprived MEF Lig4$^{-/-}$ cells that were treated with 250 µM ara-A developed a pan-nuclear γH2AX staining that grew in intensity with time (Figure B). After 4h 90% of cells exhibited pan-nuclear staining and 8h and later 100% of cells showed this staining pattern (Figure 28 D), which made a meaningful quantitative analysis of γH2AX foci impossible. Similarly, 98% of non-irradiated cells showed pan-nuclear staining for γH2AX after 24h (Figure 28 C). However, the intensity of the staining in non-irradiated cells did not reach the glaring intensity found for irradiated cells treated with ara-A. Still, pan-nuclear γH2AX staining was not exclusively observed in ara-A treated cells. In untreated cells with or without irradiation an average percentage of 16.3% (+/- 3.3%) of cells with pan-nuclear staining could be observed (Figure 28 A, C&D).

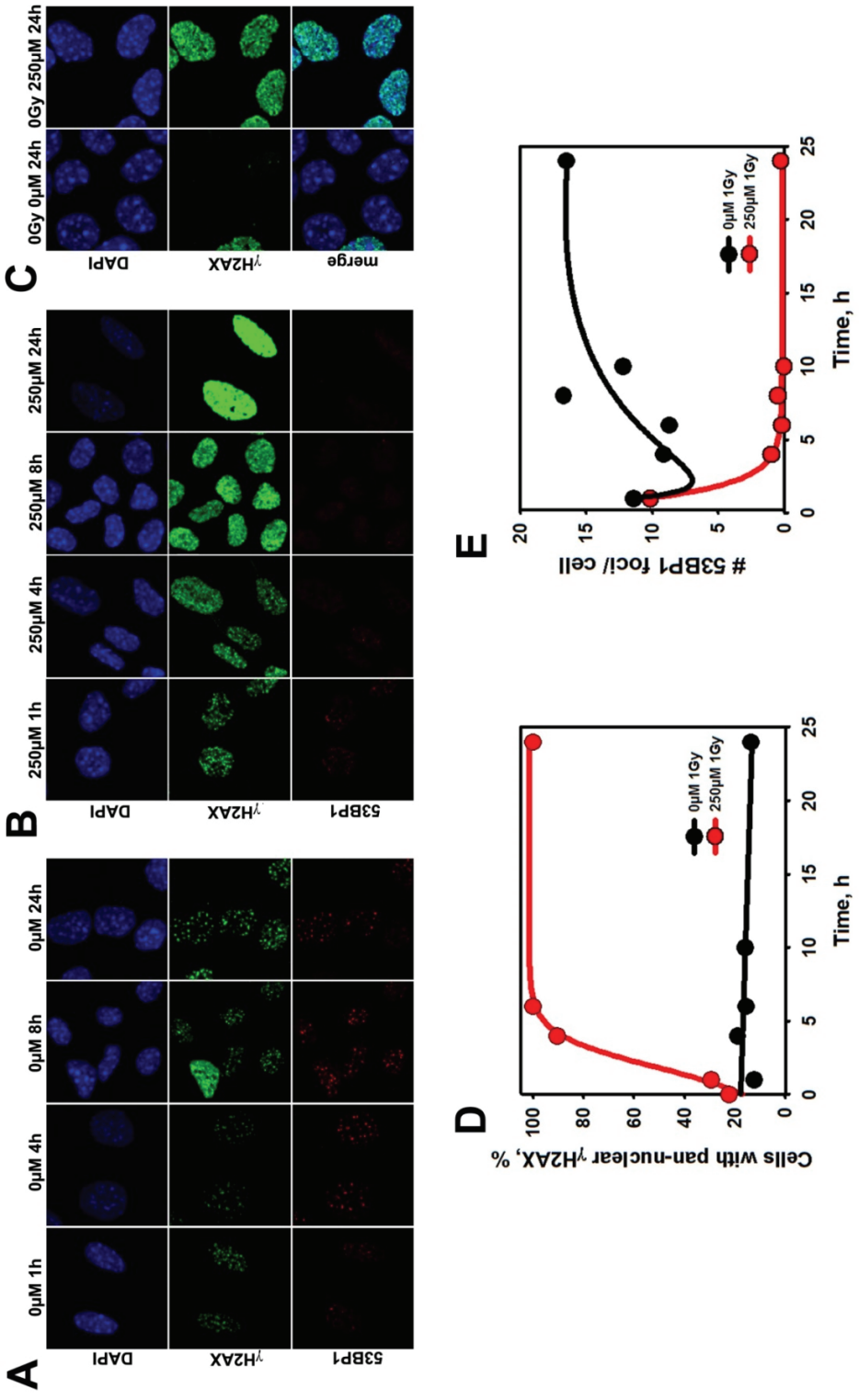

Figure 28 Quantification of γH2AX and 53BP1 foci in serum deprived Lig4$^{-/-}$ MEFs. A) Serum deprived Lig4$^{-/-}$ MEFs exposed to 1 Gy and left without further treatment until fixation. Maximum intensity projection (MIP) representations of Z-stacks recorded by confocal laser scanning microscopy (CLSM) of

immunofluorescent (IF) stained fixed cell samples. Cells were stained for DNA with DAPI (blue, top row), with an antibody against γH2AX (green, middle row) and an antibody against 53BP1 (red, bottom row). Pictures of cells fixed after 1h (1st column), 4h (2nd column), 8h (3rd column) and 24h (4th column) are shown. **B)** Serum deprived Lig4$^{-/-}$ MEFs exposed to 1 Gy X-rays and treated with 250 µM ara-A until fixation. MIP representations of Z-stacks recorded by CLSM of IF stained fixed cell samples. Cells were stained for DNA with DAPI (blue, top row), with an antibody against γH2AX (green, middle row) and an antibody against 53BP1 (red, bottom row). Pictures of cells fixed after 1h (1st column), 4h (2nd column), 8h (3rd column) and 24h (4th column) are shown. **C)** Non-irradiated serum deprived Lig4$^{-/-}$ MEFs left without ara-A (left column) or treated with 250 µM ara-A (right column) for 24h. Samples were fixed at the latest time point (24h) together with irradiated cells. MIP representations of Z-stacks recorded by CLSM. Cells were stained for DNA with DAPI (blue, top row) and with an antibody against γH2AX (green, middle row). The bottom row shows an overlay of the DAPI and the γH2AX stain. **D)** Quantification of the proportion of cells with pan-nuclear γH2AX staining in cells left without ara-A after irradiation (0 µM; black circles and line) and treated with 250 µM ara-A (red circles and line). **E)** Quantification of 53BP1 foci per nucleus. *Black circles and line:* cells left without ara-A after irradiation (0 µM). *Red circles and line:* Cells treated with 250 µM ara-A after irradiation. Data points represent the mean of all cells (51 (+/-17) per time point) analyzed in one experiment.

Foci of 53BP1 on the other hand were, when detectable, always present in the form of distinct, quantifiable dots in ara-A treated and untreated cells (Figure 28 A&B). The initial number of average 53BP1 foci per cell was very similar (11.4 and 10.1 foci per cell) under both conditions. In cells without ara-A, 53BP1 foci persisted up to 24h after irradiation with a tendency to even slightly increase (Figure 28 A&E). In contrast, in cells treated with 250 µM ara-A 53BP1 foci quickly disappeared (Figure 28 B&E). After 4h only about 1 focus per cell could be detected on average. After 24h the number had decreased to 0.25 foci per cell on average (Figure 28 E). Interestingly, pan-nuclear γH2AX staining and the formation of 53BP1 foci seemed not to be mutually exclusive per se, at least in untreated cells (compare Figure 28 A; 0 µM 8h: pan nuclear γH2AX staining in cell with clear and bright 53BP1 foci). Still, most cells exhibiting pan-nuclear γH2AX staining showed fewer or no 53BP1 foci.

Detection of pATM after irradiation with 1 Gy revealed bright, punctate nuclear foci (Figure 29 A&B). The initial number of pATM 1h after irradiation was virtually identical in ara-A treated (60.8 (+/-15.6)) and untreated cells (60.6(+/-12.7)) (Figure 29 C). In

untreated cells a slow decay of pATM foci was observable (Figure 29 C). After 24h cells retained approximately half of the initial foci (27.9 (+/-6.7)), which were still visible as clearly defined, bright spots (Figure 29 A&C). In cells that were treated with 250 µM ara-A decay of pATM foci proceeded much faster, with approximately 50% of foci being lost after 8h (residual foci 8h: 27.3 (+/- 20.6)) (Figure 29 B&C). This resulted in complete disappearance of pATM foci 24h after irradiation (Figure 29 B&C). Cells that lost the discrete protein foci retained a weaker, diffuse nuclear staining (Figure 29 B).

We concluded that the complete disappearance of 53BP1 and pATM foci with time in serum deprived MEF Lig4$^{-/-}$ cells, was indicative of complete repair of DSB. This supported data showing enhanced repair of those cells in PFGE experiments. Pan-nuclear staining with γH2AX and to a lesser degree of pATM after treatment with ara-A require further investigation.

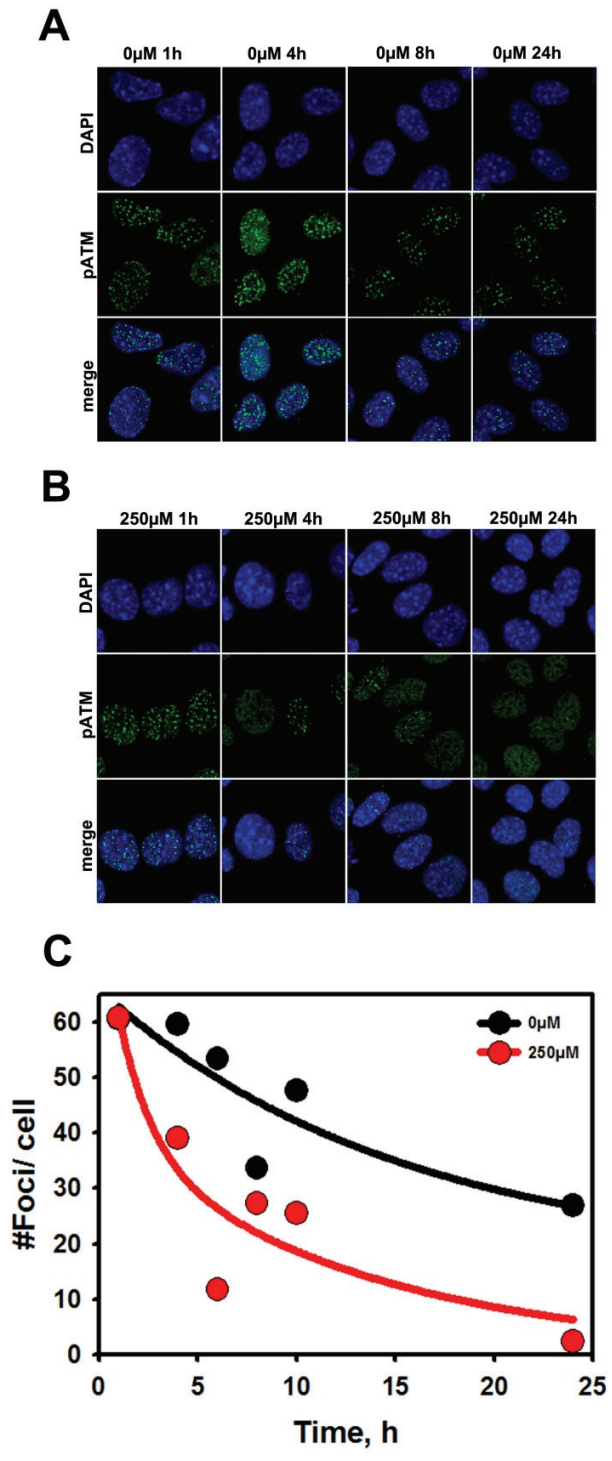

Figure 29 Quantification of pATM-S1981 Foci in serum deprived Lig4$^{-/-}$ MEFs. A) Serum deprived Lig4$^{-/-}$ MEFs exposed to 1 Gy X-rays. Maximum intensity projection (MIP) representations of Z-stacks recorded by confocal laser scanning microscopy (CLSM) of immunofluorescent (IF) stained fixed cell

samples. Cells were stained for DNA with DAPI (blue, top row) and with an antibody against pATM-S1981 (pATM; green, middle row). The bottom row shows a merged picture of the DNA and pATM stains. Pictures of cells fixed after 1h (1st column), 4h (2nd column), 8h (3rd column) and 24h (4th column) are shown. **B)** Serum deprived Lig4$^{-/-}$ MEFs exposed to 1 Gy X-rays and treated with 250 µM ara-A until fixation. MIP representations of Z-stacks recorded CLSM. Cells were stained for DNA with DAPI (blue, top row) and with an antibody against pATM-S1981 (pATM; green, middle row). The bottom row shows a merged picture of the DNA and pATM stains. Pictures of cells fixed after 1h (1st column), 4h (2nd column), 8h (3rd column) and 24h (4th column) are shown. **C)** Quantification of pATM foci in irradiated cells with or without ara-A. *Black circles and line:* cells left without ara-A after irradiation (0 µM). *Red circles and line:* Cells treated with 250 µM ara-A after irradiation. Data points represent the mean of all cells (43 (+/-8) per time point) analyzed in one experiment.

4.5 Effects of other NAs on radiosensitivity and DSB repair

4.5.1 Effects on the survival of A549 cells

The interesting results obtained with ara-A motivated us to expand our study to include other NAs. We decided to use fludarabine, ara-C and gemcitabine. Fludarabine, an adenosine analog, is a fluorinated derivative of ara-A. Ara-C is an analog of cytosine and gemcitabine the di-fluorinated derivative (Figure 1). Both of these compounds are significantly more cytotoxic than ara-A and fludarabine and effectively inhibit DNA replication at much lower concentrations (Figure 30 A and Figure 42). Fludarabine and gemcitabine have both been reported to possess radiosensitizing potential. Ara-C on the other hand is generally not regarded as a radiosensitizer.

We performed survival experiments in A549 cells as described above for ara-A using a 40 min pre-incubation and a 4h post-irradiation treatment (protocol II). From preliminary experiments we selected concentrations of the respective drug that yielded plating efficiencies no lower than 40% -50% of the control. This data had shown that in the case of ara-C, although only moderately toxic at doses below 100 µM, toxicity increased drastically at concentrations above 250 µM. Therefore concentrations below 100 µM were used. Two concentrations were tested for ara-C (10 µM and 50 µM) and gemcitabine (1 µM and 10 µM). Fludarabine, which had shown toxicity very similar to

ara-A, was used at the same concentration as the latter (500 µM). Predictions for PE reduction were met well by the results obtained (Figure 30 A).

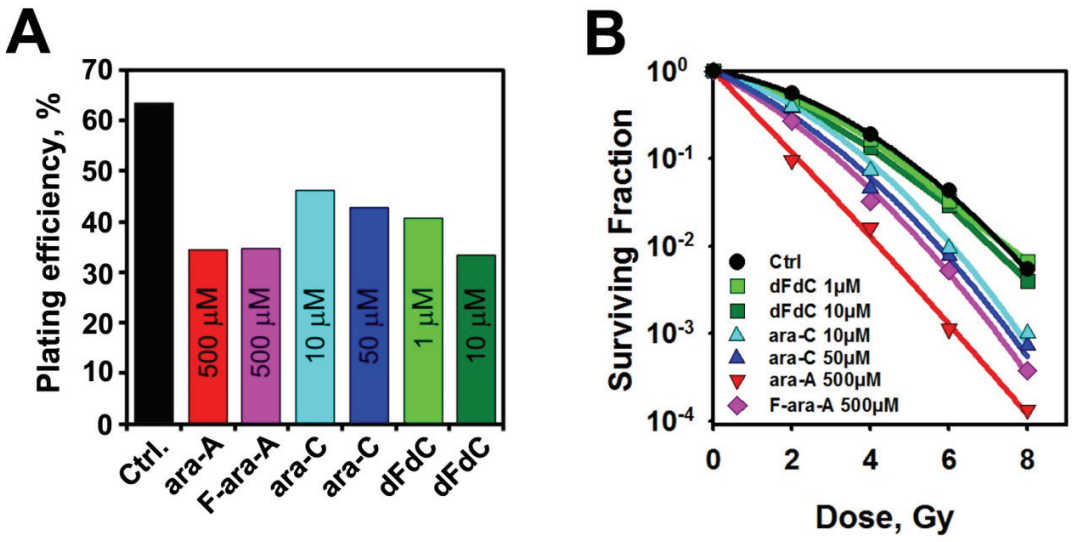

Figure 30 Comparison of radiosensitization by post-irradiation treatment with different NAs. A) Plating efficiencies for colony formation of exponentially growing A549 cells treated with different concentrations of NAs for 4h. Bars represent the mean of two independent experiments, each including double determinations. **B)** Survival of exponentially growing A549 cells after exposure to different doses of X-rays and the indicated concentrations of NA drugs for 4 h after IR. Red triangles, ara-A (500 µM); pink diamonds, fludarabine (F-ara-A; 500 µM); light blue triangles, ara-C (10 µM); dark blue triangles, ara-C (50 µM); light green squares, dFdC (1 µM); dark green squares, dFdC (10 µM); black circles, control (no drug treatment). Survival data is normalized to the corresponding unirradiated controls (compare panel A). The results shown represent the mean of two independent experiments, each including double determinations. A third experiment using different concentrations yielded similar results.

Treatment with 500 µM Ara-A resulted in a steep, shoulderless survival curve as expected (Figure 30 B). Fludarabine at the same concentration did sensitize the A549 cells, but to a lesser degree than ara-A (Figure 30 B). Unexpectedly, treatment with ara-C showed radiosensitization similar to fludarabine (Figure 30 B). There was only a very small increase in radiosensitization between treatment with 10 µM and 50 µM ara-C. We were surprised at first not to find radiosensitization by gemcitabine (Figure 30 B). However, an in-depth literature research revealed that results reporting

radiosensitization by gemcitabine generally use long pre-incubations (e.g. 16-32h) with the drug (Shewach, 1994; Rosier, 1999; Pauwels, 2003). On the other hand, studies that also test the effect of post-irradiation treatment don´t find radiosensitization (Shewach, 1994). Thus, our finding is in accordance with the existing literature.

We concluded that post-irradiation treatment with gemcitabine is not sufficient to induce radiosensitization in A549 cells. Ara-C had some radiosensitizing potential in our hands, albeit distinctly weaker than ara-A. Fludarabine also proved to be a weaker radiosensitizer than ara-A in A549 cells.

4.5.2 Effects on ara-C and fludarabine on HRR, SSA and distal NHEJ

We decided to exploit the reporter assays, which we had used to measure the influence of ara-A on different pathways of DSB repair, to further evaluate the effects of ara-C and fludarabine, for which we had found radiosensitization as a post-treatment. We also included aphidicolin and HU as controls in these experiments.

Both compounds inhibit replication, but show no or only weak radiosensitizing potential (compare Figure 13 B&C and Figure 14 B). HU inhibits replication in a range comparable to ara-A ($IC50_{repl} > 5$ µM), while aphidicolin inhibits DNA replication at much lower concentrations, in a range comparable to that of ara-C ($IC50_{repl} < 0.3$ µM).

These controls were intended to confirm that transient inhibition of DNA replication alone was not sufficient to cause major changes in the read out of the reporter assays. Treatment conditions in these experiments were as described for ara-A above.

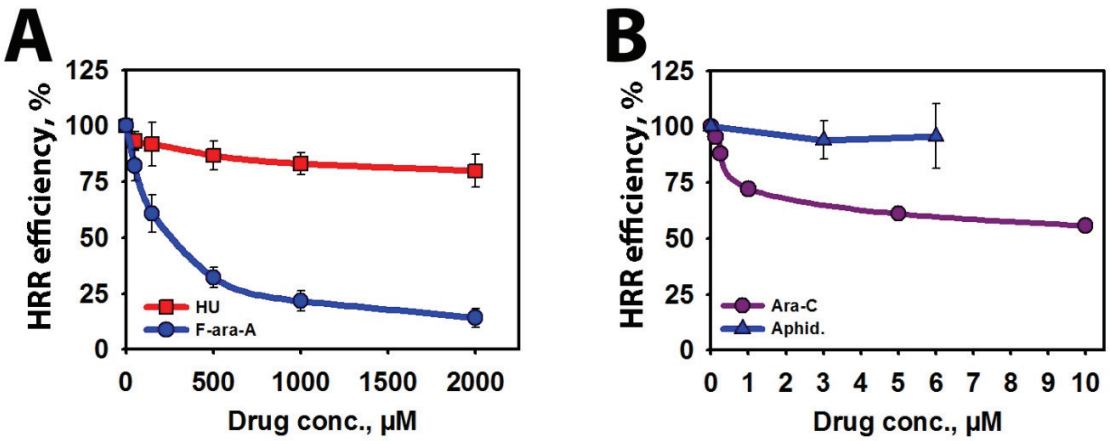

Figure 31 Effect of fludarabine and ara-C on HRR in U2OS 282C cells (DR-GFP).

A) Effects of fludarabine (F-ara-A) and hydroxyurea (HU) on HRR. *Blue circles and line:* F-ara-A. *Red squares and line:* HU. Data points represent mean and s.d. from three independent experiments. **B)** Effects of ara-C and aphidicolin on HRR. *Dark pink circlesand line:* Ara-C. Plot shows the mean from two independent experiments *Blue triangles and line:* Aphidicolin. Data points represent mean and s.d. from three independent experiments.

We started by testing the effects of fludarabine and ara-C on HRR using the U2OS 282C cells, which carry the DR-GFP construct. Fludarabine proved to be an effective inhibitor of HRR with a concentration-effect relationship very similar to ara-A (Figure 31 A). Incubation with HU, even at 2000 µM, on the other hand, had only a very small effect on HRR (Figure 31 A). Aphidicolin also failed to inhibit HRR in U2OS 282C cells. Treatment with ara-C showed substantial but comparatively weak inhibition, reducing HRR by almost 45 % at a concentration of 10 µM (Figure 31 B). Since neither HU nor aphidicolin inhibited HRR despite their strong effects on DNA replication, we concluded that inhibition of replication per se was not sufficient to suppress HRR.

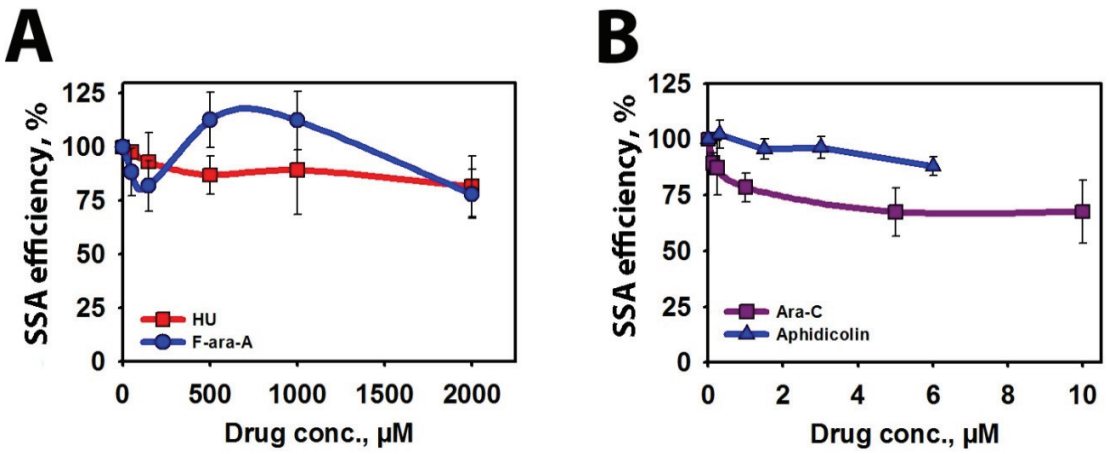

Figure 32 Effect of fludarabine and ara-C on SSA in U2OS 283C cells (SA-GFP).

A) Effects of fludarabine (F-ara-A) and hydroxyurea (HU) on SSA. Blue circles and line: F-ara-A. Red squares and line: HU. Data points represent mean and s.d. from three independent experiments. **B)** Effects of ara-C and aphidicolin on SSA. Dark pink squares and line: Ara-C. Blue triangles and line: Aphidicolin. Data points represent mean and s.d. from three independent experiments.

We proceeded to test fludarabine and ara-C in the U2OS 283C cells, to investigate their effect on the efficiency of SSA. Fludarabine treatment again resulted in a response similar to that of ara-A. After an initial decrease of SSA mediated repair, there was an increase at higher concentration, which was again abolished at very high concentrations (Figure 32; Figure 31 A). In contrast to ara-A, fludarabine lead to an effective net increase of SSA at concentrations between 500 and 1000 µM. HU again showed only little effect (Figure 32 A) and similar behavior was observed for aphidicolin. This drug only had a small impact on SSA, reducing its efficiency to 88% (+/- 4%) of control at 6 µM (Figure 32 B). Ara-C had a stronger effect, reducing SSA by more than 30% to 68% (+/- 11%) at 5 µM, but did not inhibit the pathway further at 10 µM (Figure 32 B).

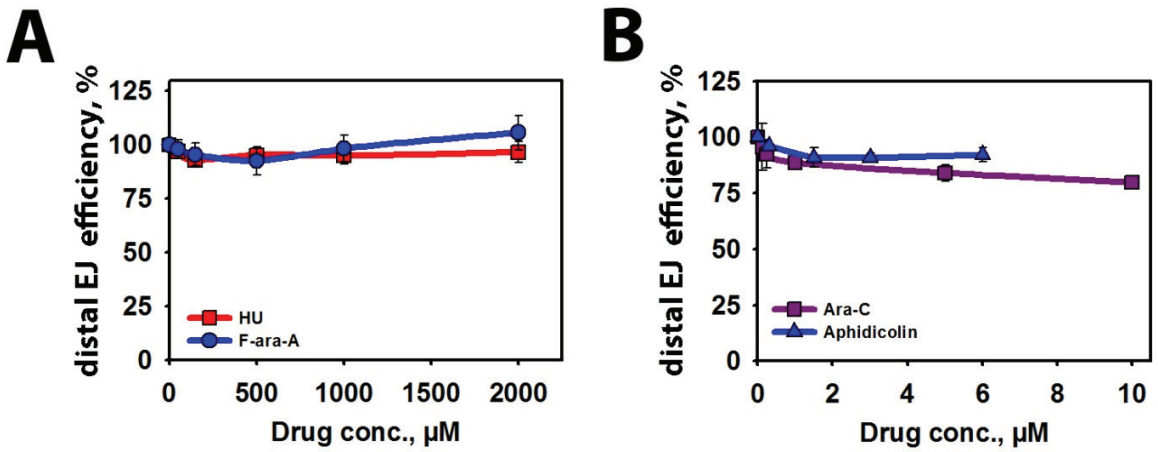

Figure 33 Effect of fludarabine and ara-C on the joining of distal ends of two DSB (EJ5-GFP). A) Effects of fludarabine (F-ara-A) and hydroxyurea (HU) on distal-end joining. *Blue circles and line:* F-ara-A. *Red squares and line:* HU. Data points represent mean and s.d. from three independent experiments. **B)** Effects of ara-C and aphidicolin on distal-end joining. *Dark pink squares and line:* Ara-C. *Blue triangles and line:* Aphidicolin. Data points represent mean and s.d. from three independent experiments.

We concluded this analysis with the EJ5-GFP construct in U2OS 280A to measure the joining of distal ends of DSB. The effects of HU and fludarabine on the joining of distal ends seemed negligible. However, there is a small trend for distal end-joining to increase at higher concentrations of fludarabine (Figure 33 A). Aphidicolin and ara-C also had only small effects on the readout of this assay. Aphidicolin caused a reduction of 8% in the rejoining of distal ends at 6 µM, while ara-C reduced the efficiency of this repair mode to 80% (+/- 1.8%) of the controls at 10 µM (Figure 31 B).

We concluded that inhibition of DNA synthesis by HU and aphidicolin had no important effects on the overall efficiency of any of the repair pathways or modes tested with this panel of cell lines. The profile of fludarabine for the modulation of repair pathway efficiencies was similar to that of ara-A, albeit with a much less pronounced effect on the joining of distal ends and a more pronounced effect on SSA. Ara-C was different from fludarabine and ara-A, as it uniformly reduced all types of repair events in these reporter

assays. The reductions elicited by ara-C were quiet moderate, ranging from 20% - 40%, but consistent.

4.5.3 Effects on mutagenic repair in EJ-DR cells

The differences in the action of fludarabine and ara-C on specific repair outcomes we had found were intriguing. We wondered how the individual drugs would influence the overall fidelity of DSB repair. To address this question we conducted experiments using the U2OS EJ-DR cell line. We used the same conditions as described for experiments with ara-A. In this series of experiments we increased the tested ara-C concentrations to 100 µM, to investigate if we would find more pronounced effects at higher concentrations. Fludarabine caused an increase of mutagenic end joining to about 150% of the controls at concentrations above 500 µM (Figure 34 A). Ara-C on the other hand caused a small reduction (about 20%) of mutagenic repair (Figure 34 B). However, this reduction was significant only at 1 µM (p= 0.001).

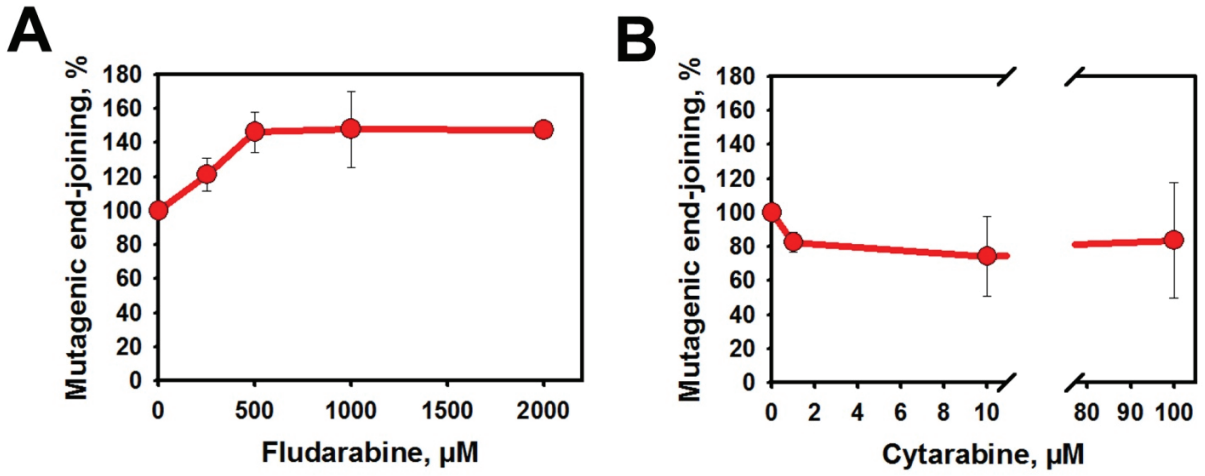

Figure 34 Effect of fludarabine and ara-C in U2OS EJ-DR cells (EJ-RFP).

A) Effect of treatment with fludarabine (4h starting 1.5h after transfection) on mutagenic end-joining. Flow cytometry analysis was performed four days after transfection with the I-SceI expression plasmid. Data points represent mean and s.d. from 3 independent experiments. **B)** As in (A) but with ara-C.

We concluded that Fludarabine behaved similar to ara-A in I-SceI reporter assays, but showed some differences in the strength of effects on individual repair pathways. Notably, fludarabine had lesser potential to increase distal-end joining and the overall mutagenicity of repair. Ara-C on the other hand did not have a positive influence on any of the examined repair pathways. Instead it showed small to moderate reduction of all repair outcomes.

5 Discussion

5.1 Design of this study and general considerations

It was our aim to investigate mechanisms of radiosensitization by NAs using ara-A as a model compound. We focused on possible interactions of ara-A with pathways of DSB repair. A well- known characteristic of this deoxyadenosine analog is its inhibitory effect on mammalian DNA replication (Plunkett, 1974; Muller, 1975; Kufe, 1983; Ohno, 1989). Most of the results previously reporting radiosensitization by ara-A were generated using cultures in the plateau phase of growth (Iliakis, 1980; Iliakis and Bryant, 1983; Iliakis and Ngo, 1985; Iliakis, 1989b; Little, 1989). Plateau-phase conditions conveniently circumvent complications frequently generated when treating an actively growing culture with substances that have cell cycle phase specific effects. In the case of an S-phase inhibitor these complications include S-phase specific cytotoxicity and changes in the cell cycle distribution that may modify the outcome of many types of experiments.

Despite the difficulties in experimentation and the interpretation of data that are associated with the usage of asynchronous cell populations, we decided to use exponentially growing cells for a large part of this work. One rational for this decision was that also within a tumor, cells can be found distributed in all phases of the cell cycle. A second important reason was that we wanted to investigate the effects of this drug on all known pathways of DSB repair. Since the activity of some repair pathways, especially HRR, but also B-NHEJ, underlie cell cycle dependent control mechanisms the use of

proliferating cultures was without alternative (Shrivastav, 2008; Escribano-Diaz, 2013). However, it was essential for us to have controls that allowed us to differentiate between effects that were primarily due to inhibition of replication and other, not directly replication linked effects. For this reason we included two non-nucleoside replication inhibitors in our studies. Aphidicolin is a tetracyclic fungal metabolite that inhibits the DNA polymerases α, δ and ε by direct binding (Ikegami, 1978; Ohashi, 1978). Hydroxyurea (HU) is a hydroxylated analog of urea that acts by inhibiting the enzyme ribonucleotide reductase (RnR), which results in deregulation and depletion of deoxynucleotide pools (Chapman and Kinsella, 2011). Ara-A on the other hand can be incorporated into DNA and inhibits the DNA polymerases α and β, as well as the enzymes primase and RnR (Dicioccio and Srivastava, 1977; Chang and Cheng, 1980; Kuchta and Willhelm, 1991).

5.2 Inhibition of replication and sensitization of cycling cells

The two control compounds and ara-A all have different, albeit partially overlapping, modes of action and are effective as replication inhibitors in different concentration ranges. We performed replication assays to assess their inhibitory activity. The results of these assays were used to calculate IC50 values for replication ($IC50_{repl}$), which enabled us to use the control compounds at equal-effect or higher concentrations than ara-A (Figure 13). Exponentially growing cells were sensitized very efficiently to IR by ara-A treatment (Figure 14 A). We compared the radiosensitizing effect of ara-A at 40 and 80 times $IC50_{repl}$ to the survival of cells that had been treated with HU at 45 times $IC50_{repl}$ or aphidicolin at 220 times $IC50_{repl}$ (Figure 14 B). Aphidicolin did not elicit any radiosensitization in treated cells. HU treatment caused some radiosensitization, which was much weaker than that caused by ara-A.

These experiments confirmed that radiosensitization by ara-A cannot solely be attributed to inhibition of replication during the treatment period. HU has been implicated as radiosensitizer and a number of clinical studies had been initiated in the 1960s and 70s, before interest declined again due to controversial results.The comparatively weak

sensitization that was caused by HU is likely to be related to the role of RnR in radiation response and possibly DNA repair (Chapman and Kinsella, 2011).

RnR is a tetrameric complex consisting of two subunits named R1 and R2. R1 is the larger, regulatory subunit, which is expressed constitutively throughout the cell cycle. The expression of the R2 subunit is cell cycle dependent, with highest levels reached in the S-phase (Kuo and Kinsella, 1998). Importantly, relatively recently an alternative R2 subunit, named p53R2, was discovered. This subunit is not cell cycle regulated, but becomes induced transcriptionally after exposure to IR (Tanaka, 2000). This finding suggests some replication independent functions of RnR in the response to IR. Ara-A is known to have an inhibitory effect on RnR as well (Moore and Cohen, 1967; Chang and Cheng, 1980). Thus, inhibition of RnR may also play a role in the radiosensitization by ara-A. However, the small radiosensitization elicited by HU suggests that the contribution of this mechanism to the overall radiosensitization by ara-A will be small.

The highly efficient radiosensitization by ara-A demonstrated in survival assays strongly suggested an interference of this drug with pathways of DSB repair. We applied various techniques for the detection of DSB and the measurement of their repair in this study. Each of these methods has its individual strength and weaknesses. These will be discussed comparatively in the next section, before proceeding to the discussion of the actual results.

5.3 Methods for the measurement of DSB repair

5.3.1 PFGE

PFGE is a physical method for the detection of DSB (Gardiner, 1991; Gurrieri, 1999). The amount of DSB and the kinetics of their repair are measured in the pooled total DNA of irradiated cell populations. For this end cells have to be exposed to high doses of IR and are incubated for different times afterwards. In this study 20 Gy were used as a standard induction dose. The clear advantage of PFGE is that it directly measures the actual physical presence of DSB within the genomes of cells and therefore can

accurately describe the kinetics with which they are rejoined. However, it cannot yield information about the repair pathways that conduct this repair. Switches in repair pathways that don´t significantly change the overall rate of repair will go unnoticed in PFGE experiments. Evidence from genetic studies indicates that repair as it is measured by PFGE in repair proficient cells mostly represents D-NHEJ, while in D-NHEJ deficient cells the observed DSB repair can almost entirely be attributed to B-NHEJ (Dibiase, 2000; Perrault, 2004). HRR seems to play hardly any role in the repair that is detected by PFGE in D-NHEJ proficient as well as in D-NHEJ deficient cells (Wang, 2001a; Iliakis, 2004). This may also partly be due to a limitation of PFGE, which is the requirement for high doses of IR to allow sufficient resolution. Experiments with lower initial doses than 10 Gy become very difficult to analyze. This can be a problem, as radiation dose may also be a factor determining repair pathway choice (Sasaki, 2013). Finally, bulk analysis of cells in the standard application of this method means that distinct behavior of sub populations cannot be identified and distinguished. This includes cells from different phases of the cell cycle, which are known to show very different repair repertoires and potentials. However, in this study we could overcome the latter limitation by usage of a sophisticated combination of cell sorting and PFGE.

5.3.2 IRIF

The analysis of ionizing radiation induced protein foci (IRIF) by immunofluorescence microscopy offers a much higher sensitivity with regard to the required dose and number of DSB than PFGE. Foci analysis enables the use of doses as low as 0.01 Gy for the production of statistically significant results (Markova, 2007). It also allows analysis on a single cell level, including discrimination by cell cycle phase or other criteria. However it is not only advantageous, as it lacks the direct physical evidence for the presence of a DSB. While the number of γH2AX foci for examples that is found after a given does correlates very well with the theoretically predicted and with other methods verified numbers, it has become evident that there are substantial timely differences between the kinetics of the disappearance of physical DSB and the generation and decay of IRIF (Markova, 2007; Kinner, 2008). The number of γH2AX foci for peaks about 1h after

irradiation in wild type cells, a time at which more than half of the DSB are already rejoined in repair proficient cells, as we know from physical methods like PFGE (see Figure 24, Figure 25 and Figure 26). Thus counting of foci may be used for the estimation of damage induction and residual damage, but caution must be exercised when drawing conclusions for the kinetics of repair, as the presence of a focus does not necessarily signify the presence of a physical break. Additionally it has been shown that phosphorylation of γH2AX does not exclusively occur only after DSB induction, but can be induced by other factors as well (Tu, 2013). Nonetheless, analysis of IRIF is a valid approach for the investigation of some aspects of DSB repair, particularly because it offers the opportunity to gain mechanistic insights into how breaks become repaired.

5.3.3 The use of I-SceI reporter assays for the assessment of DSB repair pathway activities

Repair reporter constructs carrying recognition sites for rare cutting endonucleases that are stably integrated into the genome can be used to assay the frequency of specific repair events. In this type of reporter assay the expression of a site specific endonuclease (here I-SceI) leads to the introduction of a DSB in the reporter construct. The design of the construct is such, that only a special type of repair outcome, often specific to a single repair pathway, results in generation of a signal (Gunn and Stark, 2012). These I-SceI reporter assays are widely used to measure the efficiency of different pathways of DSB repair.

However, important differences to the repair of IR induced DSB have to be considered when working with these assays. These are mainly the different time frame of damage induction and the chemical composition of the breaks:

At the dose rates used in this study DSB are induced by IR in a manner of seconds or minutes. In the case of DSB induction by I-SceI, several steps precede the cutting: After transfection the I-SceI gene needs to be transcribed, the mRNA translated and the resulting enzyme has to translocate to the nucleus and find its cutting site. Moreover, once expressed I-SceI remains present and active within the cell. Additionally, more I-

SceI will continuously be expressed as long as the plasmid remains intact. Work from our group has shown that the levels of I-SceI protein in transfected cells remain constant up to 72h at least (Schipler, 2013). In the same study foci of 53BP1 were shown to be present for longer than 24h in repair proficient cells transfected with an I-SceI expression plasmid, indicating ongoing cutting of I-SceI sites (Schipler, 2013). Thus, DSB can be induced over a long period of time, possibly several days, in I-SceI inducible reporter assays.

The chemical nature of the ends of DSB induced by either IR or I-SceI is very different. While IR induced DSB usually harbor chemically modified ends that prohibit ligation without further processing (Figure 4 B&C), DSB introduced by I-SceI can readily be religated due to the presence of unaltered 3´-OH and 5´-phosphate groups and complementary overhangs (Figure 4 A) ((Magin, 2013; Schipler and Iliakis, 2013)). Simple religation of an I-SceI induced DSB will result in reconstitution of the I-SceI site without generation of a signal. This regenerated site is again susceptible to cutting by the restriction enzyme, which may result in cycles of repeated cutting and religation. These cycles will be ended only when either a signal generating event occurs or the I-SceI site is disrupted by another repair outcome. This can lead to under- or overestimation of the activity of different repair pathways and creates further uncertainty with regard to the time when damage induction and repair occur.

When conditions are tested that themselves last or can be sustained for prolonged times (e.g. knockdown or knockout of genes or treatments with low cytotoxicity), the continuous damage induction in I-SceI reporter assays does not present a major problem. However, treatment with many drugs, including NAs, is limited by cytotoxity that increases with time. Furthermore, cell cycle phase specific drugs can elicit changes in the cell cycle distribution that could bias readings conducted at later times. Indeed we have found that such effects can lead to deceptive results when measurements are taken at 48h-72h after short term drug treatment (Figure 36 and Figure 37). Therefore, to avoid complications that would be associated with short term drug treatment and this inherent characteristic of the I-SceI system, we limited the observation time to 24h in this study where possible.

Taken together, I-SceI reporter assays allow the measurement of specific repair outcomes indicative of DSB repair pathway activity. These results can provide valuable information about the effect of various treatments on these pathways. However, due to the different kinetics of DSB induction and the distinct chemical characteristics of the breaks caution has to be exercised when interpreting results and drawing direct comparisons to the effect of IR.

In summary, each of the methods discussed above is able to provide a different kind of information about DSB repair. PFGE shows the actual presence of breaks, detection of IRIF by immunofluorescence sheds light on cellular responses to DSB and signaling, while I-SceI reporter assays provide information about how repair of some breaks has been completed. Each of these methods has its own limitations and peculiarities, knowledge about which is required for meaningful interpretation. Thus, data generated with each of those methods as individual piece of information has to be interpreted with care and under consideration of these limitations. Combination of information generated with multiple methods greatly strengthens the certainty with which conclusions can be drawn and broadens the scope of observations. Therefore we tried to address all question that arose in this study with a combination of methods.

5.4 Effects of ara-A on HRR

5.4.1 Effect of ara-A on IR induced Rad51 foci formation

Since ara-A is an efficient inhibitor of replication we wondered if it may also effect mechansims of DSB repair that require substantial DNA synthesis. We used antibody staining and analysis by confocal microscopy to score Rad51 foci as a surrogate for ongoing HRR. We included cyclin B1 (CycB1) staining and labelling with EdU to enable the definitive discrimination of cells in G1, S and G2.

EdU incorporation itself had no influence on Rad51 foci formation. The maximum number of Rad51 foci and the time when the maximal number of foci is reached for a given dose are dependent on the applied dose of IR. Studies in our group have shown that the maximum number of Rad51 foci is reached at 4 Gy and that this maximum

occurs at about 3h after irradiation. Thus, we chose 4 Gy as the test dose, to induce a maximum number of Rad51 foci.

The results of these experiments clearly showed that the formation of Rad51 foci could efficiently be suppressed by ara-A treatment. Rad51 foci formation was almost fully abrogated at 1000 µM ara-A in S-phase cells and showed strong reduction in G2 cells (Figure 15 B). The requirement of higher concentrations of ara-A in G2 to reduce the level of Rad51 foci to similar numbers as in S-phase cells may either indicate an initial resistance of HRR to ara-A in the G2 phase, or could be related to higher absolute numbers of DSB in G2-cells that are repaired by HRR. Induction of DSB is proportional to DNA amount and thus is expected to be higher in G2 than in S-phase cells. In any case, from 100 µM onwards the curve for G2-cells followed an almost identical course as the curve for S-phase cells, suggesting a similar cause-effect relationship.

These results showing suppression of IR induced Rad51 foci formation by treatment with ara-A, strongly indicated that successful execution of HRR was directly inhibited by this drug. Furthermore, the suppression of Rad51 foci formation caused by ara-A correlated very well with the radiosensitization elicited by ara-A in cycling A549 cells (Figure 15 C). Therefore we decided to test the importance of HRR inhibition in ara-A mediated radiosensitization in clonogenic survival assays.

5.4.2 Survival with Rad51 silenced cells

If inhibition of HRR was a major mechanism of radiosensitization, the sensitization of cells already deficient for HRR should be reduced as compared to HRR proficient cells. Knockout of Rad51 is embryonic lethal in mice and Rad51 knockout cell lines are not viable. However, work by others indicated that transient silencing of Rad51 allows cells to remain viable (Liu, 2011; Short, 2011). Therefore we decided to induce HRR deficiency in A549 cells via knock down of Rad51 by RNAi. As control population we used cells that were transfected with a siRNA against GFP. We found that Rad51 silenced cells retained a PE of 20% (Figure 16 B). This represented a considerable reduction compared to the control, but was expected and similar to reductions in PE after Rad51 knockdown reported by others (Liu, 2011; Short, 2011). This reduction in

viability is likely due to functions of Rad51 in replication (Sonoda, 1998; Daboussi, 2008; Petermann, 2010).

Rad51 knockdown cells were much more radiosensitive than the controls. This as well was in accordance with results reported by others and confirmed that cells that retained viability still represented successfully transfected cells (Liu, 2011; Short, 2011). Importantly, treatment with ara-A did not further increase the radiosensitivity of those cells. Only at 5 Gy, which was the highest dose used in these experiments, some sensitization seemed to occur. It is important to note though, that the curve of the Rad51 knockdown cells flattens out at this dose, displaying a resistance tail (Figure 16 C). This type of curvature occurs typically when radioresistant subpopulations start to dominate the shape of the survival curve. The higher the radiation dose, the smaller is the number of cells that survive. Sensitive cells become inactivated first, while more radioresistant cells may remain clonogenic at higher doses. A very small subpopulation of resistant cells will have hardly any impact on the course of the survival curve at lower doses, but will determine its shape almost entirely at higher doses (Iliakis and Okayasu, 1990). It is likely that the resistance tail of the survival curve of Rad51 knockdown cells is largely due to cells in which silencing was less efficient than in the bulk of the population. Those cells would still be at least partially proficient for HRR and thus also susceptible to sensitization by an HRR inhibitor. We concluded that inhibition of HRR indeed is an important factor in ara-A mediated radiosensitization in cycling cells.

5.4.3 Effect of ara-A on HRR of the DR-GFP reporter construct

Initially only a CHO cell line, DRaa40, carrying a reporter for HRR (DR-GFP) was available to us. Development of a GFP signal in this system is indicative of successfully completed HRR (Figure 17 B) (Pierce, 1999). For experiments cells were transfected with an expression plasmid for the I-SceI endonuclease and were exposed to different concentrations of ara-A three hours later. After a four hour treatment the drug was removed. 24h after transfection the cells were collected and analyzed by flow cytometry. Treatment with ara-A strongly suppressed HRR in this system, showing 70% inhibition at a concentration of 500 µM (Figure 17 C).

At a later time we were able to obtain human cell lines (U2OS) carrying DR-GFP and other reporter constructs. Knockdown of several proteins implicated in HRR in the cell line harboring DR-GFP (U2OS 282C) confirmed the validity of this reporter as test system for HRR (Figure 19). Ara-A proved to be a very effective inhibitor of HRR of the DR-GFP construct in these human cells as well. The concentrations that were required to achieve equal suppression were higher than in DRaa40 cells (1000 µM vs. 500 µM for 70% inhibition), which is in accordance with the higher toxicity this compound is known to show in rodent cells (Juranka and Chan, 1980).

Taken together, suppression of Rad51 foci formation, lack of radiosensitization after knockdown of Rad51 in human A549 cells and inhibition of HRR measured by the DR-GFP reporter in CHO and human U2OS cells confirm strong inhibition of HRR by ara-A. So far the exact molecular mechanisms that cause this inhibition remain unknown. The multistep process of HRR can be envisioned to be inhibited at several stages. This includes the resection of DSB ends that creates the ssDNA intermediate, formation of the Rad51 nucleoprotein filament, search for homology, elongation of the invading strand upon synapsis or resolution of recombinational structures and final ligation (Li and Heyer, 2008). Considering the effects of ara-A as an inhibitor of replication, inhibition of repair synthesis seems like an obvious mechanism for inhibition of this repair pathway. For ara-A inhibition of polymerase alpha/primase and polymerase beta has been reported (Dicioccio and Srivastava, 1977; Kuchta and Willhelm, 1991). A main mechanism of replication inhibition by ara-A is inhibition of RNA primer synthesis for lagging strand synthesis by the primase enzyme (Kuchta and Willhelm, 1991). However, primer synthesis is not required in HRR as the invading strand serves to prime DNA synthesis. Furthermore, multiple polymerases have been implicated to promote HRR, including the Polymerases beta, delta, eta, zeta and REV1 (Canitrot, 2004; Maloisel, 2008; Kane, 2012; Sharma, 2012). Moreover the Polymerase delta subunit POLD3 (POL32 in yeast) has been shown to play an important role in the BIR pathway of HRR (Costantino, 2014). Except for Polymerase beta for none of the other polymerases listed an inhibition by ara-A has been reported. Additionally, the presence of several trans-lesion synthesis polymerases (zeta, eta and REV1) in this list suggests that HRR may possess the flexibility to bypass disturbances, like incorporated NAs, in template DNA.

Incorporation of ara-A during repair synthesis itself may hamper completion of HRR. However, the amount of DNA synthesis required during most HRR events is limited (several hundred bases) and it is unclear if incorporation of ara-A could be sufficient to obviate its completion, since it does not act as a chain terminator (Plunkett, 1974; Muller, 1975; Kufe, 1983; Ohno, 1989). Therefore inhibition of DNA synthesis cannot readily be assumed to underlie inhibition of HRR. The strong suppression of Rad51 foci formation observed under ara-A treatment may indicate that suppression of HRR takes place at an even earlier stage, like the resection of break ends or loading of Rad51 on ssDNA. Further studies are required to clearly identifiy the molecular mechanisms of the inhibition of HRR by ara-A. However, first evidence helping to eliminate one candidate process came from the usage of another reporter cell line.

5.4.4 Effect of ara-A on SSA

Using the SA-GFP construct integrated into U2OS 283C cells, we examined the effect of ara-A on the mutagenic SSA pathway. Silencing of HRR factors in the SA-GFP system resulted in a massive increase of SSA events. This impressively demonstrated the suppression of SSA that is mediated by HRR and has also been reported previously (Tutt, 2001; Stark, 2004; Mansour, 2008). We found that SSA could be partially inhibited by ara-A, but also benefited from inhibition of HRR at higher concentrations of ara-A. We showed that this recovery of SSA derived from an ara-A mediated release of SSA from the suppression exerted by HRR. This result gave further indirect evidence for inhibition of HRR by ara-A. It is interesting that ara-A could reduce SSA efficiency only by around 30%. This means that the majority of SSA events is resistant to ara-A. Since all SSA events are dependent on extensive end-resection, this indicates that end resection is not inhibited by ara-A. Thus inhibition of end-resection can likely be excluded as a potential mechanism for the inhibition of HRR.

5.5 Effects of ara-A on NHEJ

5.5.1 Effect of ara-A on distal end-joining

Another repair reporter system, the EJ5-GFP construct integrated into U2OS 280A cells, allowed the analysis of the effect of ara-A on a specific subtype of NHEJ events. This construct does not simply measure the repair of a single I-SceI-induced DSB, but involves induction and misrepair of two DSB. Each of these DSB can either be repaired by rejoining of the proximate ends, or by rejoining of one end from the first and one from the second DSB (distal ends). Rejoining of distal ends results in the loss of the large (~1.8kb) intervening fragment, but enables expression of a GFP gene. Thus, signal generating events in this system have to be considered as a highly mutagenic form of NHEJ. Therefore, this assay should be expected not to measure the activity of the classical DNA-PK dependent pathway of NHEJ (D-NHEJ), but rather that of backup pathways of NHEJ (B-NHEJ). To confirm this interpretation we inhibited DNA-PKcs, a central component of D-NHEJ, with the specific inhibitor NU7441. Measurements by PFGE (Figure 38) or the phosphorylation of H2AX (Shaheen, 2011) show that treatment with this inhibitor induces a substantial defect in the repair of DSB, clearly demonstrating an inhibition of D-NHEJ. In U2OS cells harboring the EJ5-GFP construct on the other hand, treatment with NU7441 almost doubled the usage of distal ends (Figure 22 and Figure 39). This finding is in accordance with similar reports from others (Gunn, 2011).

Treatment with ara-A caused distal-end joining events to increase by 30%. We interpreted this finding as an indication for increased activity of backup NHEJ. Taken together, the results obtained with this set of reporter cell lines indicated that HRR is inhibited by ara-A, while mutagenic pathways of homology directed (SSA) or NHEJ benefit from ara-A treatment.

5.5.2 Effect of ara-A on mutagenic DSB repair in the EJ-RFP system

To further investigate whether repair by B-NHEJ is really promoted by ara-A, we employed another reporter cell system. The EJ-RFP system was recently developed in the group of Dr. Simon Powell (Bindra, 2013). In contrast to the previously used

reporters, in this system the expression of a signal is not based on the generation of a functional gene by one certain, predefined repair event. Instead, the disruption of a gene by any kind of mutagenic repair leads to generation of a signal. The different way of signal generation is mirrored in delayed appearance of the signal as compared to the I-SceI reporter assays above. This necessitated measurement after 96h instead of 24h after transfection of the I-SceI plasmid. Treatment with ara-A resulted in a 2.5-fold increase of the DsRed signal compared to untreated controls. This showed that ara-A greatly promotes the mutagenic repair of DSB. In contrast to NU7441 there is no evidence so far for any impairment of D-NHEJ by ara-A. To address the question if ara-A may have an inhibitory effect on D-NHEJ we examined its influence on the kinetics of DSB repair in D-NHEJ proficient A549 cells by PFGE. Furthermore, we were interested to see if the inhibition of HRR that is mediated by ara-A may be detectable in this assay.

5.5.3 PFGE of sorted G1 and G2 cells from an exponentially growing culture

We used pulsed field gel electrophoresis (PFGE) to measure the repair of DSB in the genome of X-irradiated A549 cells. As discussed above (5.3.1) DSB repair as it can be observed by PFGE in repair proficient asynchronous cell populations is mainly due to the activity of D-NHEJ, which is generally assumed to be the dominant pathway of DSB repair throughout the cell cycle (Dibiase, 2000; Wang, 2001a; Iliakis, 2004; Perrault, 2004; Mladenov and Iliakis, 2011). However, since HRR as well as B-NHEJ show strong cell cycle dependence in their activity, which is absent or lower in G1 and higher in G2, we reasoned that it might be possible to see their influence when G1 and S/G2 cells were analyzed separately (San Filippo, 2008; Wu, 2008a; Wu, 2008b; Heyer, 2010).

Thus, we decided to irradiate and treat cells as exponentially growing cultures, but sort cells by FACS in different phases of the cell cycle for later analysis by PFGE. DNA from cells in the S-phase of the cell cycle has different characteristics of release migration in a gel, than G1 and G2 cells. This differential DNA release is related to S-phase specific DNA structures (Latz, 1996; Dewey, 1997). Thus, it was necessary to prepare separate dose response curves for each category.

Since S-phase cells are themselves a heterogeneous population with regard to their progress in DNA replication and the related potential to perform HRR, we decided to concentrate on G1 and G2 cells. These represent two extremes of the cell cycle with G1 cells putatively having 0% potential and G2 cells theoretically having 100% potential to perform HRR. Cell sorting gave us the best possible purity (Figure 24). G1 cells could be enriched >95% and G2>80%. It is not possible to achieve the same purity for G2 as for G1, because the broader distribution of the G2 peak partially overlaps with cells in late S-phase (and vice versa). Additionally, the smaller number of G2 cells precludes overly restrictive gating, due to the large cell numbers that were required for the analysis. A purity of >80% G2 cells however is a better enrichment than can be achieved with any other non-chemical method in this cell system. The cleanliness of those preparations is also reflected by the dose response curves of the G1 and G2 fractions (Figure 24 B). Both G1 and G2 cell dose responses are steeper than the curve of the asynchronous cells, due to the absence of S-phase cells. G1 and G2 cell dose responses are almost superimposable, only the G2 is minimally lower due to the slightly higher S-phase contamination.

The results of this experiment clearly showed that neither in the asynchronous population, nor in G1 or G2 cells from the same exponentially growing culture, the kinetics of DSB repair were altered by ara-A in any way. This suggested that the inability to detect defects in HRR in asynchronous cell populations by PFGE (Wang, 2001a; Iliakis, 2004), which we had hoped to overcome by our sorting strategy, was not only due to masking effects of cells in other phases of the cell cycle. Importantly, novel, thus far unpuplished findings from our group demonstrate that the contribution of HRR to the total load of repair is diminished with increasing radiation dose. These results indicate that the contribution of HRR drops from as much as 70% at 0.25 Gy to about 15% at 2 Gy. This ratio is further reduced at a slower rate at even higher doses. At the dose of 20 Gy applied in our PFGE experiments, the fraction of DSB that remains destined for repair by HRR can be expected to be minuscule. Thus, the high doses required to achieve satisfying resolution in PFGE experiments reduce the contribution of HRR to the overall repair of DSB and thus render PFGE inappropriate for the investigation of the role of this pathway in DSB repair.

However, an important motivation to conduct these experiments had also been to observe potential signs of a shift from relatively accurate D-NHEJ to more error-prone B-NHEJ as it had been indicated by I-SceI reporter assays. B-NHEJ as it can be observed in D-NHEJ deficient cells operates with slower kinetics than D-NHEJ. The repair kinetics in our experiments yielded no indication for a shift from a fast to a slower process. We concluded, that if B-NHEJ took a greater part in the repair of DSB in those cells when treated with ara-A, this form of B-NHEJ could not be characterized by a slower rate of repair. We speculated that if a fast form of B-NHEJ was enhanced by ara-A treatment, which was not distinguishable from D-NHEJ in A549 cells, it may be observable in D-NHEJ deficient cells.

5.5.4 Ara-A enhances B-NHEJ in D-NHEJ deficient HCT116 cells

We used a panel of human HCT116 colon carcinoma cells including two knockout mutants for core components of D-NHEJ. We performed experiments with exponentially growing and serum deprived cells. We found that for the D-NHEJ deficient HCT116 LIG4$^{-/-}$ and HCT116 DNA-PKcs$^{-/-}$ cells DSB repair was enhanced by treatment with ara-A in the exponential phase of growth as well as after serum deprivation. On the other hand, in agreement with results previously obtained for A549 cells, the DSB repair kinetics of HCT116 WT cells were not altered by ara-A treatment. Previous work from our group has demonstrated that B-NHEJ is suppressed in the plateau phase of growth respectively under conditions of serum deprivation (Singh, 2011). Our results obtained with serum deprived D-NHEJ deficient HCT116 cells had also shown this inhibition and concomitantly an even greater repair enhancement after treatment with ara-A.

5.5.5 Relieve of B-NHEJ suppression in plateau phase MEF Lig4$^{-/-}$ cells by ara-A

This indicated that ara-A treatment could not only promote B-NHEJ, but also relieve the suppression of DSB repair observed in the plateau phase of growth (Singh, 2012). In MEF Lig4$^{-/-}$ cells, repair is essentially absent in the plateau phase of growth (Figure 26 B). Therefore we chose this cell system to conduct further experiments. Indeed we found

that DSB repair was promoted when those cells were treated with ara-A. Treatment with ara-A did not only restore B-NHEJ to nearly normal efficiency (25 µM-50 µM), but could also improve it beyond that point (125 µM- 250 µM). In fact, after 4h treatment of serum deprived Lig4$^{-/-}$ MEFs with 125 µM or 250 µM ara-A, the repair of DSBs observed was closer to the repair usually observed in wild type cells than to the repair in exponentially growing Lig4$^{/-}$ MEFs.

These impressive results clearly demonstrated that backup pathways of NHEJ can be promoted by treatment with ara-A. This strongly suggests that ara-A treatment creates conditions that are generally favorable or even required for B-NHEJ, but which are usually prevented in G1/G0 cells. A candidate process could be 5´- 3´ resection of DSB ends. End resection is highly cell cycle regulated. While end resection mechanisms are active in the S and G2 phases of the cycle, in G1/G0 only very limited nucleolytic processing takes place (Jazayeri, 2006). B-NHEJ on the other hand, has been shown to be associated with and benefit from end-resection (Bennardo, 2008; Rass, 2009; Xie, 2009; Bothmer, 2010; Lee-Theilen, 2011; Symington and Gautier, 2011; Grabarz, 2013). In accordance with this, B-NHEJ has been found to be enhanced in the G2 phase of the cell cycle (Wu, 2008a; Wu, 2008b), where end resection is active. Thus, end-resection may be enhanced under ara-A treatment, thereby facilitating repair by B-NHEJ in plateau phase Lig4$^{-/-}$ MEFs.

5.5.6 Promotion of B-NHEJ is not productive for survival

The improved DSB repair capacity induced in plateau phase Lig4$^{-/-}$ MEFs by ara-A treatment, could have been possible to be associated with an increase of survival of these cells after irradiation. To verify this we performed preliminary survival experiments with serum deprived MEF Lig4-/- cells with or without ara-A treatment. We found no increase in the survival of ara-A treated cells. On the contrary we observed radiosensitization of treated cells, demonstrating that enhanced B-NHEJ function is not associated with improved chances for cell survival (Figure 40).

Cells that show DSB repair defects are usually more radiosensitive than their repair proficient counter parts. However, some very radiosensitive cell lines also show only a mild or no DSB repair defect at all, indicating that removal of breaks as measured by

physical methods alone is not predictive of survival (Iliakis, 2009). It follows that not only the capacity for and rate of DSB repair are important for cell survival, but also the type and outcome of the repair. Thus over-activation of erroneous repair pathways may even negatively affect survival.

B-NHEJ has been implicated in the formation of translocations and other chromosomal aberrations (Bunting and Nussenzweig, 2013). Formation of chromosomal aberrations is adverse to survival and thus increased repair by B-NHEJ may not support survival, but even contribute to sensitization of cells to IR.

5.5.7 Detection of IRIF in plateau phase MEF cells

We sought to confirm and extend the observations we had made in the MEF Lig4$^{-/-}$ cells with a complementary method. We decided to use immunofluorescence microscopy to investigate formation and decay of radiation induced foci of γH2AX, 53BP1 and phosphorylated ATM. From this combination we hoped not only to gain information about the rate of DSB repair, but to gather some mechanistic information on DSB processing and signaling as well.

The phosphorylation of H2AX on Serine 139 (S139), also known as γH2AX, is one of the first events in the response to DSB and has been frequently used as a surrogate marker for DSB (Rogakou, 1998; Nakamura, 2010). Formation and decay of 53BP1 foci also has been used to quantify induction and repair of DSB (Asaithamby and Chen, 2009). 53BP1 is a protein that acts early in the response to DSB and forms foci that colocalize with γH2AX (Schultz, 2000; Polo and Jackson, 2011). Importantly, 53BP1 is not only a general component of the DDR, but is also known to play an important role in the regulation of DNA end-resection as well. It has been shown that 53BP1 and BRCA1 act antagonistically on end-resection and thereby influence pathway choice (Cao, 2009; Bouwman, 2010; Bunting, 2010; Escribano-Diaz, 2013). ATM is a central kinase in IR induced damage signaling. Phosphorylation of ATM at Serine 1981 (pATM) occurs in response to DSB and is required for its activation (Bakkenist and Kastan, 2003). pATM accumulates at sites of DSB where it can be detected as nuclear protein foci.

Phosphorylations mediated by ATM in response to DSB enable the analysis of key interactions during DSB repair. Thus, the presence or absence of pATM foci may provide important information about activation and maintenance of DDR signaling.

Lig4$^{-/-}$ MEFs had developed a large number (~50/cell) of bright, distinct γH2AX foci after 1h and untreated cells retained the same level of γH2AX foci until 24h (Figure 28). This finding was in full accordance with the almost complete defect in DSB repair observed with PFGE. In contrast, when cells were treated with 250 µM ara-A, they developed a pan-nuclear γH2AX staining, which intensified with time. After 8h of ara-A treatment no cells with scorable foci were left, but the total phosphorylation of H2AX was increased enormously. Pan-nuclear γH2AX staining can also be observed in cells that become apoptotic. However, hyperphosphorylation of γH2AX related to apoptosis has been reported to be preceded by a ring shaped staining of the nuclear periphery and to be closely correlated with apoptotic DNA fragmentation (Talasz, 2002) (Solier and Pommier, 2009). Furthermore, pan-nuclear γH2AX staining is ensued by the development of the characteristic pyknotic nuclear morphology of apoptotic cells.

Among many thousands of cells observed we did not find any of those earlier or later apoptotic signs at any time point. Importantly, if the ara-A induced pan-nuclear γH2AX staining was due to apoptosis induced DNA fragmentation, massive DNA release into the gel should have been detected in PFGE experiments. Strikingly the exact opposite was what we had found: Reduced DNA release indicating improved repair (see above).

In the literature a variety of reports can be found that describe pan-nuclear phosphorylation of H2AX, which is not related to apoptosis and can be caused by different stimuli or stressors. Ewald et al. found that checkpoint abrogation by a CHK1 inhibitor in previously gemcitabine treated cells elicited pan-nuclear phosphorylation of H2AX, which was not related to apoptosis (Ewald, 2007). Similarly, Gagou et al. reported pan-nuclear staining in CHK1 depleted cells in response to prolonged treatment with thymidine and also excluded apoptosis as a cause (Gagou, 2010). Ewald et al., as well as Gagou et al., both performed their experiments in cycling cells and link the effects they observe to replication stress, collapsed replication forks, or the inappropriate firing of replication origins. Interestingly Gagou et al. report that depletion of the helicase

co-factor CDC45 greatly reduced pan-nuclear γH2AX staining. Pan-nuclear staining can also be elicited by transfection of small DNA molecules mimicking DSB, which results in DNA-PK hyperactivation (Quanz, 2009). Pan-nuclear H2AX phosphorylation in response to adeno-associated virus infection is also coordinated by DNA-PK (Schwartz, 2009). Furthermore, pan-nuclear γH2AX staining can be caused by UV-C radiation in G1 cells (Marti, 2006) or hypotonic treatment that induces chromatin changes (Baure, 2009). Finally, induction of pan-nuclear γH2AX has been reported to occur in cells that received clustered DNA damage from traversing heavy ions (Meyer, 2013).

Taken together, our observations and the reports from others strongly suggest that pan-nuclear H2AX phosphorylation does not have to be associated with apoptosis and that other factors and mechanisms are capable of inducing γH2AX in a nuclear wide manner. It is noteworthy, that pan-nuclear γH2AX was not only caused by the combination of irradiation and ara-A treatment. In unirradiated cells not treated with ara-A around 15% of cells exhibited pan-nuclear γH2AX staining (Figure 28 A, C&D). In irradiated cells without ara-A the frequency was similar. Unirradiated cells treated with ara-A for 24h also developed pan-nuclear γH2AX staining in 100% of the cases (Figure 28 C).

We found high numbers of pATM foci (~60/cell), similar to the amount of γH2AX foci, in ara-A treated and untreated cells 1h after irradiation. Slow decay of pATM foci was observed in cells without ara-A treatment, but after 24h still about 50% of initial foci were present (~30/cell). In contrast, in cells treated with 250 µM ara-A, repair appeared to progress much faster and 24h after irradiation no foci were detectable. This observation was again in accordance with the repair defect and reactivation of B-NHEJ observed in PFGE experiments. However, we did also notice that the cells which lost their foci under ara-A treatment exhibited a diffuse, homogenous nuclear staining that appeared to be a little higher than background. Thus, it is possible that decline of pATM-foci number was not only due to completion of DSB repair, but to redistribution of pATM by the genome wide generation of γH2AX. It was apparent that in serum deprived Lig4$^{-/-}$ MEFs without ara-A treatment, DDR signaling remains active up to 24h and probably longer. This was evidenced by the persistence of bright pATM foci and was likely due to the persistence of DSB as also observed in PFGE. So far it is unclear if dissolution of pATM foci under

ara-A treatment is a consequence of ongoing DSB repair or whether loss of pATM foci is part of the mechanistic basis for the observed enhancement of rejoining.

The numbers of initial 53BP1 foci we found 1h after irradiation (~12/cell) were 4-5 fold lower than the numbers of γH2AX or pATM foci. The initial number of foci was almost equal in ara-A treated and untreated cells. However, in untreated cells foci became brighter and appeared to increase in size over time, while in cells treated with 250 µM 53BP1 foci formation was almost completely abolished after 4h and additional foci could not be detected up to 24h. This finding was again in accordance with increased repair in ara-A treated cells, although DSB repair-unrelated processes cannot be excluded at this time.

Furthermore, the rapid disappearance of 53BP1 foci may also offer first insights for a mechanistic explanation as to how B-NHEJ may be reactivated in serum deprived MEF Lig4$^{-/-}$ cells. As mentioned above, 53BP1 is known to play an important role in the regulation of end-resection (Cao, 2009; Bouwman, 2010; Bunting, 2010; Escribano-Diaz, 2013). 53BP1 is antagonized by BRCA1 which forms, together with its interaction partner CtIP, a module that promotes resection of DSB ends (Yun and Hiom, 2009). The balance between those two counteracting forces is shifted towards 53BP1 dependent end-protection in G1 and towards BRCA1-CtIP dependent promotion of end resection in S and G2 by cell cycle regulatory mechanisms. These shifts reflect the potential and requirement of a cell to perform HRR at different stages during the cell cycle. In G1/G0 a sister chromatid is not available and end resection is suppressed in favor of D-NHEJ mediated repair, while in S and G2 DNA ends become frequently resected to allow for repair by HRR. The fact that CtIP has also been shown to be required for the repair by alternative or backup pathways of NHEJ in G1 (Yun and Hiom, 2009) together with other reports strengthen the notion that B-NHEJ is more active in G2 than in G1 because it benefits from resection of DNA ends (Bennardo, 2008; Wu, 2008a; Wu, 2008b; Rass, 2009; Xie, 2009; Yun and Hiom, 2009; Bothmer, 2010; Lee-Theilen, 2011; Symington and Gautier, 2011; Grabarz, 2013).

Decay of 53BP1 foci may therefore indicate that the protection of DSB ends from resection typical in G1/0 cells is reverted by ara-A. B-NHEJ and possibly also SSA are

the only known DSB repair processes expected to benefit from resection in serum deprived Lig4$^{-/-}$ MEFs. Thus, enhancement of DNA end-resection in ara-A treated G1/G0 cells may be an important contributor of the observed B-NHEJ reactivation.

5.6 Radiosensitization by other NAs

5.6.1 Clonogenic survival after exposure to IR

The interesting results obtained for ara-A prompted us to test additional NAs and compare to the effects found for ara-A. First, we performed survival experiments in which we tested the NAs ara-C, gemcitabine and fludarabine for their radiosensitizing potential, and compared the results obtained to those of ara-A. Both, gemcitabine and fludarabine have been reported to act as radiosensitizers (Gregoire, 1994; Shewach, 1994; Lawrence, 1996; Latz, 1998; Pauwels, 2006; Nitsche, 2008). In fact, these observations have lead to the initiation of a number of clinical trials to assess the therapeutic potential of these NAs in combination with radiation therapy (Gregoire, 2002; Aguilar-Ponce, 2004; Nitsche, 2012; Gurka, 2013). Ara-C on the other hand is not regarded as a radiosensitizer in the medical literature, but there are primary reports that show some inhibition of PLD repair by ara-C (Iliakis and Bryant, 1983; Nakatsugawa, 1984; Iliakis, 1989b).

We used a 4h post-irradiation treatment protocol like in previous survival experiments and concentrations that generated similar cytotoxicity as 500 µM ara-A.

For fludarabine, we observed that treatment with 500 µM was able to generate significant radiosensitization in cycling A549 cells. However, the observed sensitization was weaker than after treatment with ara-A at the same concentration. Furthermore, we found that ara-C was able to sensitize A549 cells to a similar extend as fludarabine. This finding was not in agreement with the general tenor of the literature (D'Angio, 2005), but was not entirely surprising considering previous reports about inhibition of PLD repair by ara-C.

We were surprised not to find any radiosensitization by gemcitabine despite the large amount of publications that report radiosensitization by this drug. This is most likely due

to the different treatment schedule we applied. The vast majority of studies reporting radiosensitization by gemcitabine use long pretreatments (usually 24h) at drug concentrations generating low cytotoxicity (Shewach, 1994; Rosier, 1999; Pauwels, 2003). In our study, on the other hand, and as a result of its focus on the analysis of NAs effects on DSB repair processes, treatment was post-irradiation, relatively short (4h), and included only a 40 min pre-treatment allowed mainly for drug entry into cells before DNA damage induction.

In a pilot study by Shewach et al. that assessed the dependence of treatment schedule on radiosensitization by gemcitabine, significant sensitization was only found for pre-irradiation, but not post-irradiation incubation with gemcitabine (Shewach, 1994). The radiation enhancement ratios found in this study increased with the duration of pre-treatment. It should be noted, however, that relatively low drug concentrations (10nM-30nM) were used to produce these results, whereas in our study 100-fold higher concentrations were applied (1µM-10µM).

Our results and the findings by Shewach et al. suggest that the effects of gemcitabine on cells when given before irradiation, seem to be indispensable for radiosensitization. Accumulation of cells in S-phase as well as depletion of intracellular dATP pools for example have been correlated with radiosensitization by gemcitabine (Shewach, 1994; McGinn, 1996)

Collectively, these observations allowed us to conclude that post-irradiation treatment is sufficient to induce radiosensitization in the case of ara-A, fludarabine and ara-C but not in the case of gemcitabine. The great dependence of gemcitabine on a pre-irradiation treatment schedule suggests that other effects than direct inhibition of DSB repair pathways play the major role in radiosensitization by this NA. Therefore we did not include it in further test, but continued to analyze the effects of ara-C and fludarabine.

5.6.2 Effect of other NAs in reporter cell assays

We started investigating the effects of ara-C and fludarabine on HRR, SSA and the joining of distal ends with U2OS reporter cell lines. For fludarabine we found inhibition of

HRR with efficiency similar to ara-A. Ara-C showed some, but comparatively weak inhibition of HRR.

Investigation of the effects of the same NAs on SSA showed that fludarabine induced a biphasic response similar to that seen with ara-A. This is in accordance with the model discussed above, in which SSA benefits from HRR inhibition at higher drug concentrations. The net benefit for SSA appeared to be larger in the case of fludarabine than for ara-A. Ara-C showed moderate suppression of the SSA repair pathway that did not increase further above 5 µM.

We also investigated effects of NAs on the joining of distal ends in U2OS cells carrying the EJ5-GFP construct. Fludarabine, in contrast to ara-A, showed almost no effect on the rejoining of distal ends. However, a very small trend for increase was observed from 500 µM onwards. Ara-C slightly reduced distal-end joining.

Neither nor HU showed a substantial reduction of the repair efficiency of any of the examined DSB repair pathways, confirming that inhibition of S-phase related DNA synthesis does not play a role for the effects observed with the nucleoside analogs.

It is interesting to note that ara-A remained the only drug that caused a substantial increase in the rejoining of distal ends. The EJ5-GFP construct differs from all other reporter constructs used in this study, in that it contains two sites for the induction of a DSB. Only if the distal ends of these DSB interact a signal is generated. Such an event is highly mutagenic, as it is accompanied by a large deletion. Such sequence loss is by itself dangerous and highly undesirable for the cell, but may also pose larger threats to chromatin stability and genome integrity. Selection of distal ends over the very proximal ends may be the result of rare endonucleolytic cleavage of the intervening DNA segment and other chromatin destabilizing activities. Similar processes of misrepair are most likely also responsible for the generation of translocations and other chromosomal aberrations frequently observed in irradiated cells and implicated in cell killing and transformation {Nambiar, 2011 #266}{Bunting, 2013 #524}.

By inhibiting DNA-PKcs we have shown that this reporter provides a measure for the activity of a form of B-NHEJ. As mentioned before, B-NHEJ has been heavily implicated in translocation formation. In addition, work from our Institute shows that a single DSB

introduced by I-SceI in a chromosome has a far lower toxicity than multiple (two or more) DSBs induced in close proximity (Schipler, 2013). The corresponding project was devised based on the assumption that increased complexity resulting from multiple breaks may lead to loss of whole nucleosomes or even larger chromatin units (Figure 4 D). In conclusion: Although the repair event that is detected by the EJ5-GFP reporter cannot easily be assigned to a single, well defined repair pathway, it is tempting to speculate that it is indicative of a type of repair that can have particularly lethal outcomes.

Finally, we investigated the effects of fludarabine and ara-C in EJ-DR cells. Those cells carried the EJ-RFP system for the measurement of the general mutagenicity of DSB repair. We found increased mutagenic repair when cells were treated with fludarabine. However, the increase was substantially smaller than in the case of ara-A. In cells treated with ara-C no increase in mutagenic repair could be observed. On the contrary, overall repair appeared to be even somewhat more accurate.

Taken together fludarabine and ara-C exhibited a very different profile of effects on DSB repair pathways, when assayed with I-SceI inducible reporter systems. Fludarabine performed similar to ara-A with respect to the homology directed repair pathways HRR and SSA, but showed lower potency for increasing mutagenic repair related to NHEJ. Ara-C on the other hand did neither show strong inhibitory effects nor a promotional effect on any of the modes of repair analyzed. Nevertheless, both drugs showed similar radiosensitizing potential in clonogenic survival assays. In the case of ara-C this strongly suggests that other mechanisms than inhibition of DSB repair pathways play an important role for radiosensitization, as it also appears to be the case for gemcitabine, although ara-C was effective as a post-irradiation treatment. On the other hand, it appears likely that radiosensitization by fludarabine for a good part is related to its inhibitory effect on HRR.

Ara-A distinguished itself from fludarabine and ara-C mostly by its superior capability to enhance mutagenic end-joining and was the only drug that caused a significant increase in the usage of distal ends. Together with the PFGE data from D-NHEJ deficient cells and the results of immunofluorescence detection of IRIF in plateau phase MEFs, we

could conclusively show that ara-A effectively promotes the activity of B-NHEJ. Furthermore, lack of additional radiosensitization after silencing of Rad51 and suppression of Rad51 foci formation by ara-A convincingly confirmed inhibition of HRR observed with the DR-GFP construct. We conclude that ara-A exerts its superior radiosensitizing effects through a shift in the balance from DSB repair that helps to maintain genomic stability and promotes survival, represented by HRR and D-NHEJ, to error-prone mechanisms that threaten genomic integrity and are adverse to survival, represented by B-NHEJ and SSA.

It will be important to investigate the effects of ara-C and fludarabine with complementary methods as well. Future work will also focus on the This, together with the results obtained for distal end-joining may indicate that fludarabine has a lesser propensity to promote mutagenic NHEJ than ara-A.

6 Summary and Conclusions

Achieving improvements in cancer therapy is one of the major challenges of contemporary medicine. Combining drug treatment and radiotherapy to achieve synergistic killing of cancer cells is one of the most promising current approaches towards this goal. Aim of this thesis was to elucidate mechanisms of radiosensitization by nucleoside analogs (NAs), a highly promising class of chemotherapeutics, using 9-β-D-arabinofuranosyladenosine (ara-A) as a model compound.

Towards this goal, we investigated in detail the effect of ara-A on the repair of DSB. We established that ara-A inhibits homologous recombination repair (HRR) and showed that this inhibition plays an important role in the radiosensitization of exponentially growing human tumor cells.

We also examined the effect of ara-A on pathways of non-homologous end-joining (NHEJ). We found an increase in the frequency of erroneous DSB repair events in two cellular reporter assays. However, we could not detect a decrease by ara-A in the overall DSB repair efficiency in repair proficient cancer cells exposed to high doses of IR, when tested in the G1 or G2 phase of the cell cycle by pulsed-field gel

electrophoresis (PFGE). This result implied a switch between DSB repair pathways, rather than an overall inhibition of DSB repair.

Through examination of DSB repair by PFGE in repair deficient cells we could show for the first time promotion of error prone backup pathways of non-homologous end-joining (B-NHEJ) by a NA. Ara-A enhanced the repair of DSB by B-NHEJ in human tumor cells. Furthermore, ara-A treatment completely abrogated the plateau-phase-dependent inhibition of B-NHEJ in mouse cells, causing a dramatic restoration of DSB repair.

Investigation of IR induced damage foci by immunofluorescence microscopy confirmed the above observations and implicated end-resection and deregulation of DSB signaling as underlying mechanisms. We conclude that in cycling cells treatment with ara-A causes direct inhibition of HRR resulting in radiosensitization. At the same time the balance of NHEJ is shifted towards the more error prone B-NHEJ. Over-activation of mutagenic B-NHEJ is likely to make an important contribution to radiosensitization by ara-A, especially in G1 and plateau phase cells, but also in G2 and S-phase cells.

Our findings reveal a novel mechanism of radiosensitization by nucleoside analogs. That opens new avenues in the investigation of interactions of these drugs with IR and may have important implications for the clinical application of NAs as radiosensitizers.

7 Bibliography

Adimoolam, S., M. Sirisawad, J. Chen, P. Thiemann, J. M. Ford and J. J. Buggy (2007). "HDAC inhibitor PCI-24781 decreases RAD51 expression and inhibits homologous recombination." Proceedings of the National Academy of Sciences of the United States of America **104**(49): 19482-19487.

Aguilar-Ponce, J., M. Granados-Garcia, V. Villavicencio, A. Poitevin-Chacon, D. Green, A. Duenas-Gonzalez, A. Herrera-Gomez, K. Luna-Ortiz, A. Alvarado, H. Martinez-Said, C. Castillo-Henkel, B. Segura-Pacheco and J. De la Garza (2004). "Phase II trial of gemcitabine concurrent with radiation for locally advanced squamous cell carcinoma of the head and neck." Ann Oncol **15**(2): 301-306.

Ahmad, S. S., S. Duke, R. Jena, M. V. Williams and N. G. Burnet (2012). "Advances in radiotherapy." BMJ **345**: e7765.

Al-Minawi, A. Z., N. Saleh-Gohari and T. Helleday (2008). "The ERCC1/XPF endonuclease is required for efficient single-strand annealing and gene conversion in mammalian cells." Nucleic acids research **36**(1): 1-9.

Alberts, B., J. H. Wilson and T. Hunt (2008). Molecular biology of the cell. New York, Garland Science.

Aly, A. and S. Ganesan (2011). "BRCA1, PARP, and 53BP1: conditional synthetic lethality and synthetic viability." Journal of molecular cell biology **3**(1): 66-74.

Arner, E. S. J. and S. Eriksson (1995). "Mammalian Deoxyribonucleoside Kinases." Pharmacology & Therapeutics **67**(2): 155-186.

Asaad, N. A., Z. C. Zeng, J. Guan, J. Thacker and G. Iliakis (2000). "Homologous recombination as a potential target for caffeine radiosensitization in mammalian cells: reduced caffeine radiosensitization in XRCC2 and XRCC3 mutants." Oncogene **19**(50): 5788-5800.

Asaithamby, A. and D. J. Chen (2009). "Cellular responses to DNA double-strand breaks after low-dose gamma-irradiation." Nucleic Acids Research **37**(12): 3912-3923.

Badie, C., G. Iliakis, N. Foray, G. Alsbeih, B. Cedervall, N. Chavaudra, G. Pantelias, C. Arlett and E. P. Malaise (1995). "Induction and rejoining of DNA double-strand breaks and interphase chromosome breaks after exposure to X rays in one normal and two hypersensitive human fibroblast cell lines." Radiation Research **144**: 26-35.

Bakkenist, C. J. and M. B. Kastan (2003). "DNA damage activates ATM through intermolecular autophosphorylation and dimer dissociation." Nature **421**(6922): 499-506.

Balcer-Kubiczek, E. K. (2012). "Apoptosis in radiation therapy: a double-edged sword." Exp Oncol **34**(3): 277-285.

Bartelink, H., F. Roelofsen, F. Eschwege, P. Rougier, J. F. Bosset, D. G. Gonzalez, D. Peiffert, M. vanGlabbeke and M. Pierart (1997). "Concomitant radiotherapy and chemotherapy is superior to radiotherapy alone in the treatment of locally advanced anal cancer: Results of a phase III randomized trial of the European organization for research and treatment of cancer radiotherapy and gastrointestinal cooperative groups." Journal of Clinical Oncology **15**(5): 2040-2049.

Baure, J., A. Izadi, V. Suarez, E. Giedzinski, J. E. Cleaver, J. R. Fike and C. L. Limoli (2009). "Histone H2AX phosphorylation in response to changes in chromatin structure induced by altered osmolarity." Mutagenesis **24**(2): 161-167.

Beetham, K. L. and L. J. Tolmach (1984). "The Action of Caffeine on X-Irradiated Hela-Cells .7. Evidence That Caffeine Enhances Expression of Potentially Lethal Radiation-Damage." Radiation Research **100**(3): 585-593.

Begonie, J. T., L. (1906). "L´interpretation de quelques resultats de la radiotherapie et essai de fixation d´une technique rationelle." C.R. Seances. Acad. Sci. **143**: 983-985.

Bekker-Jensen, S. and N. Mailand (2010). "Assembly and function of DNA double-strand break repair foci in mammalian cells." DNA Repair (Amst) **9**(12): 1219-1228.

Bender, M. A., H. G. Griggs and J. S. Bedford (1974). "Mechanisms of Chromosomal Aberration Production .3. Chemicals and Ionizing-Radiation." Mutation Research **23**(2): 197-212.

Bennardo, N., A. Cheng, N. Huang and J. M. Stark (2008). "Alternative-NHEJ is a mechanistically distinct pathway of mammalian chromosome break repair." PLoS genetics **4**(6): e1000110.

Bennardo, N., A. Gunn, A. Cheng, P. Hasty and J. M. Stark (2009). "Limiting the persistence of a chromosome break diminishes its mutagenic potential." PLoS genetics **5**(10): e1000683.

Bertout, J. A., S. A. Patel and M. C. Simon (2008). "The impact of O2 availability on human cancer." Nature reviews. Cancer **8**(12): 967-975.

Bindra, R. S., A. G. Goglia, M. Jasin and S. N. Powell (2013). "Development of an assay to measure mutagenic non-homologous end-joining repair activity in mammalian cells." Nucleic acids research **41**(11): e115.

Boboila, C., M. Jankovic, C. T. Yan, J. H. Wang, D. R. Wesemann, T. Zhang, A. Fazeli, L. Feldman, A. Nussenzweig, M. Nussenzweig and F. W. Alt (2010). "Alternative end-joining catalyzes robust IgH locus deletions and translocations in the combined absence

of ligase 4 and Ku70." Proceedings of the National Academy of Sciences of the United States of America **107**(7): 3034-3039.

Boboila, C., V. Oksenych, M. Gostissa, J. H. Wang, S. Zha, Y. Zhang, H. Chai, C. S. Lee, M. Jankovic, L. M. Saez, M. C. Nussenzweig, P. J. McKinnon, F. W. Alt and B. Schwer (2012). "Robust chromosomal DNA repair via alternative end-joining in the absence of X-ray repair cross-complementing protein 1 (XRCC1)." Proceedings of the National Academy of Sciences of the United States of America **109**(7): 2473-2478.

Bogue, M. A., C. Wang, C. Zhu and D. B. Roth (1997). "V(D)J recombination in Ku86-deficient mice: distinct effects on coding, signal, and hybrid joint formation." Immunity **7**(1): 37-47.

Bohgaki, T., M. Bohgaki and R. Hakem (2010). "DNA double-strand break signaling and human disorders." Genome Integr **1**(1): 15.

Bohm, L. (2006). "Inhibition of homologous recombination repair with Pentoxifylline targets G2 cells generated by radiotherapy and induces major enhancements of the toxicity of cisplatin and melphalan given after irradiation." Radiation oncology **1**(1): 12.

Bothmer, A., D. F. Robbiani, N. Feldhahn, A. Gazumyan, A. Nussenzweig and M. C. Nussenzweig (2010). "53BP1 regulates DNA resection and the choice between classical and alternative end joining during class switch recombination." The Journal of experimental medicine **207**(4): 855-865.

Bouwman, P., A. Aly, J. M. Escandell, M. Pieterse, J. Bartkova, H. van der Gulden, S. Hiddingh, M. Thanasoula, A. Kulkarni, Q. Yang, B. G. Haffty, J. Tommiska, C. Blomqvist, R. Drapkin, D. J. Adams, H. Nevanlinna, J. Bartek, M. Tarsounas, S. Ganesan and J. Jonkers (2010). "53BP1 loss rescues BRCA1 deficiency and is associated with triple-negative and BRCA-mutated breast cancers." Nature structural & molecular biology **17**(6): 688-695.

Brockman, R. W., F. M. Schabel and J. A. Montgomery (1977). "Biologic Activity of 9-Beta-D-Arabinofuranosyl-2-Fluoroadenine - Metabolically Stable Analog of 9-Beta-D-Arabinofuranosyladenine." Biochemical Pharmacology **26**(22): 2193-2196.

Bruso, C. E., D. S. Shewach and T. S. Lawrence (1990). "Fluorodeoxyuridine-induced radiosensitization and inhibition of DNA double strand break repair in human colon cancer cells." Int J Radiat Oncol Biol Phys **19**(6): 1411-1417.

Bryant, P. E. (1983). "9-beta-D-arabinofuranosyladenine increases the frequency of X-ray induced chromosome abnormalities in mammalian cells." Int J Radiat Biol Relat Stud Phys Chem Med **43**(4): 459-464.

Bryant, P. E. (1988). "Use of restriction endonucleases to study relationships between DNA double-strand breaks, chromosomal aberrations and other end-points in mammalian cells." International journal of radiation biology **54**(6): 869-890.

Bryant, P. E., L. J. Gray and N. Peresse (2004). "Progress towards understanding the nature of chromatid breakage." Cytogenet Genome Res **104**(1-4): 65-71.

Buchholz, D. J., K. J. Lepek, T. A. Rich and D. Murray (1995). "5-Fluorouracil-radiation interactions in human colon adenocarcinoma cells." Int J Radiat Oncol Biol Phys **32**(4): 1053-1058.

Bunting, S. F., E. Callén, N. Wong, H.-T. Chen, F. Polato, A. Gunn, A. Bothmer, N. Feldhahn, O. Fernandez-Capetillo, L. Cao, X. Xu, C.-X. Deng, T. Finkel, M. Nussenzweig, J. M. Stark and A. Nussenzweig (2010). "53BP1 Inhibits Homologous Recombination in Brca1-Deficient Cells by Blocking Resection of DNA Breaks." Cell **141**: 243-254.

Bunting, S. F. and A. Nussenzweig (2013). "End-joining, translocations and cancer." Nat Rev Cancer **13**(7): 443-454.

Burma, S., B. P. Chen and D. J. Chen (2006). "Role of non-homologous end joining (NHEJ) in maintaining genomic integrity." DNA repair **5**(9-10): 1042-1048.

Canitrot, Y., J. P. Capp, N. Puget, A. Bieth, B. Lopez, J. S. Hoffmann and C. Cazaux (2004). "DNA polymerase beta overexpression stimulates the Rad51-dependent homologous recombination in mammalian cells." Nucleic Acids Research **32**(17): 5104-5112.

Cao, L., X. L. Xu, S. F. Bunting, J. Liu, R. H. Wang, L. Y. L. Cao, J. J. Wu, T. N. Peng, J. J. Chen, A. Nussenzweig, C. X. Deng and T. Finkel (2009). "A Selective Requirement for 53BP1 in the Biological Response to Genomic Instability Induced by Brca1 Deficiency." Molecular Cell **35**(4): 534-541.

Cappella, P., F. Gasparri, M. Pulici and J. Moll (2008). "A novel method based on click chemistry, which overcomes limitations of cell cycle analysis by classical determination of BrdU incorporation, allowing multiplex antibody staining." Cytometry A **73**(7): 626-636.

Carney, J. P., R. S. Maser, H. Olivares, E. M. Davis, M. Le Beau, I. Yates, J.R., L. Hays, W. F. Morgan and J. H. J. Petrini (1998). "The hMre 11/hRad50 protein complex and Nijmegen breakage syndrome: Linkage of double-strand break repair." Cell **93**: 477-486.

Carr, A. M. and S. Lambert (2013). "Replication Stress-Induced Genome Instability: The Dark Side of Replication Maintenance by Homologous Recombination." J Mol Biol.

Carrano, A. V. (1973). "Chromosome Aberrations and Radiation-Induced Cell Death .2. Predicted and Observed Cell Survival." Mutation Research **17**(3): 355-366.

Carrico, C. K. and R. I. Glazer (1979). "Effect of 5-fluorouracil on the synthesis and translation of polyadenylic acid-containing RNA from regenerating rat liver." Cancer Res **39**(9): 3694-3701.

Cass, C. E., M. Selner and J. R. Phillips (1983). "Resistance to 9-Beta-D-Arabinofuranosyladenine in Cultured Leukemia L 1210 Cells." Cancer Research **43**(10): 4791-4798.

Catapano, C. V., F. W. Perrino and D. J. Fernandes (1993). "Primer RNA chain termination induced by 9-beta-D-arabinofuranosyl-2-fluoroadenine 5'-triphosphate. A mechanism of DNA synthesis inhibition." J Biol Chem **268**(10): 7179-7185.

Catton, C., M. Milosevic, P. Warde, A. Bayley, J. Crook, R. Bristow and M. Gospodarowicz (2003). "Recurrent prostate cancer following external beam radiotherapy: follow-up strategies and management." Urol Clin North Am **30**(4): 751-763.

Cavanagh, B. L., T. Walker, A. Norazit and A. C. Meedeniya (2011). "Thymidine analogues for tracking DNA synthesis." Molecules **16**(9): 7980-7993.

Chan, V. L. and P. Juranka (1981). "Isolation and preliminary characterization of 9-beta-d-arabinofuranosyladenine-resistant mutants of baby hamster cells." Somatic Cell Genet **7**(2): 147-160.

Chang, A. E., J. M. Collins, P. A. Speth, R. Smith, J. B. Rowland, L. Walton, M. G. Begley, E. Glatstein and T. J. Kinsella (1989). "A phase I study of intraarterial iododeoxyuridine in patients with colorectal liver metastases." J Clin Oncol **7**(5): 662-668.

Chang, C. H. and Y. C. Cheng (1980). "Effects of deoxyadenosine triphosphate and 9-beta-D-arabinofuranosyl-adenine 5'-triphosphate on human ribonucleotide reductase from Molt-4F cells and the concept of "self-potentiation"." Cancer Res **40**(10): 3555-3558.

Chapman, T. R. and T. J. Kinsella (2011). "Ribonucleotide reductase inhibitors: a new look at an old target for radiosensitization." Front Oncol **1**: 56.

Chavaudra, N., M. Halimi, C. Parmentier, N. Gaillard, S. Grinfeld and E. P. Malaise (1989). "The initial slope of human tumor cell survival curves: its modification by the oxic cell sensitizer beta-arabinofuranosyladenine." Int J Radiat Oncol Biol Phys **16**(5): 1267-1271.

Chehab, N. H., A. Malikzay, M. Appel and T. D. Halazonetis (2000). "Chk2/hCds1 functions as a DNA damage checkpoint in G(1) by stabilizing p53." Genes Dev **14**(3): 278-288.

Chen, L. C., C. J. Nievera, A. Y. L. Lee and X. H. Wu (2008). "Cell cycle-dependent complex formation of BRCA1.CtIP.MRN is important for DNA double-strand break repair." Journal of Biological Chemistry **283**(12): 7713-7720.

Cheong, N., X. M. Wang, Y. Wang and G. Iliakis (1994). "Loss of S-Phase-Dependent Radioresistance in Irs-1 Cells Exposed to X-Rays." Mutation Research **314**(1): 77-85.

Chinnaiyan, P., S. Huang, G. Vallabhaneni, E. Armstrong, S. Varambally, S. A. Tomlins, A. M. Chinnaiyan and P. M. Harari (2005). "Mechanisms of enhanced radiation response following epidermal growth factor receptor signaling inhibition by erlotinib (Tarceva)." Cancer research **65**(8): 3328-3335.

Choudhury, A., H. Zhao, F. Jalali, S. Al Rashid, J. Ran, S. Supiot, A. E. Kiltie and R. G. Bristow (2009). "Targeting homologous recombination using imatinib results in enhanced tumor cell chemosensitivity and radiosensitivity." Molecular Cancer Therapeutics **8**(1): 203-213.

Chuang, R. Y. and L. F. Chuang (1976). "Inhibition of RNA polymerase as a possible anti-leukaemic action of cytosine arabinoside." Nature **260**(5551): 549-550.

Chun, H. G., B. Leyland-Jones and B. D. Cheson (1991). "Fludarabine phosphate: a synthetic purine antimetabolite with significant activity against lymphoid malignancies." J Clin Oncol **9**(1): 175-188.

Connell, P. P. and S. Hellman (2009). "Advances in radiotherapy and implications for the next century: a historical perspective." Cancer research **69**(2): 383-392.

Consoli, U., I. El-Tounsi, A. Sandoval, V. Snell, H. D. Kleine, W. Brown, J. R. Robinson, F. DiRaimondo, W. Plunkett and M. Andreeff (1998). "Differential induction of apoptosis by fludarabine monophosphate in leukemic B and normal T cells in chronic lymphocytic leukemia." Blood **91**(5): 1742-1748.

Corneo, B., R. L. Wendland, L. Deriano, X. Cui, I. A. Klein, S. Y. Wong, S. Arnal, A. J. Holub, G. R. Weller, B. A. Pancake, S. Shah, V. L. Brandt, K. Meek and D. B. Roth (2007). "Rag mutations reveal robust alternative end joining." Nature **449**(7161): 483-486.

Cornforth, M. N. and J. S. Bedford (1987). "A Quantitative Comparison of Potentially Lethal Damage Repair and the Rejoining of Interphase Chromosome Breaks in Low Passage Normal Human-Fibroblasts." Radiation Research **111**(3): 385-405.

Cory, A. H. and J. G. Cory (1994). "Use of Nucleoside Kinase-Deficient Mouse Leukemia-L1210 Cell-Lines to Determine Metabolic Routes of Activation of Antitumor Nucleoside Analogs." Advances in Enzyme Regulation, Vol 34 **34**: 1-12.

Costantino, L., S. K. Sotiriou, J. K. Rantala, S. Magin, E. Mladenov, T. Helleday, J. E. Haber, G. Iliakis, O. Kallioniemi and T. D. Halazonetis (2013). "Break-Induced Replication Repair of Damaged Forks Induces Genomic Duplications in Human Cells." Science.

Costantino, L., S. K. Sotiriou, J. K. Rantala, S. Magin, E. Mladenov, T. Helleday, J. E. Haber, G. Iliakis, O. P. Kallioniemi and T. D. Halazonetis (2014). "Break-Induced Replication Repair of Damaged Forks Induces Genomic Duplications in Human Cells." Science **343**(6166): 88-91.

Cui, X., M. Brenneman, J. Meyne, M. Oshimura, E. H. Goodwin and D. J. Chen (1999). "The *XRCC2* and *XRCC3* repair genes are required for chromosome stability in mammalian cells." Mutation Research **434**: 75-88.

D'Angio, G. J. (2005). "Regarding the alleged radiosensitization of intrathecal cytarabine." Journal of Pediatric Hematology Oncology **27**(7): 349-350.

D'Silva, I., J. D. Pelletier, J. Lagueux, D. D'Amours, M. A. Chaudhry, M. Weinfeld, S. P. Lees-Miller and G. G. Poirier (1999). "Relative affinities of poly(ADP-ribose) polymerase and DNA-dependent protein kinase for DNA strand interruptions." Biochim Biophys Acta **1430**(1): 119-126.

Daboussi, F., S. Courbet, S. Benhamou, P. Kannouche, M. Z. Zdzienicka, M. Debatisse and B. S. Lopez (2008). "A homologous recombination defect affects replication-fork progression in mammalian cells." J Cell Sci **121**(Pt 2): 162-166.

Davis, A. P. and L. S. Symington (2004). "RAD51-dependent break-induced replication in yeast." Mol Cell Biol **24**(6): 2344-2351.

Davis, M. A., H. Y. Tang, J. Maybaum and T. S. Lawrence (1995). "Dependence of fluorodeoxyuridine-mediated radiosensitization on S phase progression." Int J Radiat Biol **67**(5): 509-517.

de Vries, J. F., J. H. Falkenburg, R. Willemze and R. M. Barge (2006). "The mechanisms of Ara-C-induced apoptosis of resting B-chronic lymphocytic leukemia cells." Haematologica **91**(7): 912-919.

Deacon, J., M. J. Peckham and G. G. Steel (1984). "The radioresponsiveness of human tumours and the initial slope of the cell survival curve." Radiotherapy and oncology : journal of the European Society for Therapeutic Radiology and Oncology **2**(4): 317-323.

Delaney, G., S. Jacob, C. Featherstone and M. Barton (2005). "The role of radiotherapy in cancer treatment: estimating optimal utilization from a review of evidence-based clinical guidelines." Cancer **104**(6): 1129-1137.

Dewey, W. C. and R. M. Humphrey (1965). "Increase in radiosensitivity to ionizing radiation related to replacement of thymidine in mammalian cells with 5-bromodeoxyuridine." Radiat Res **26**(4): 538-553.

Dewey, W. C., R. S. L. Wong and N. Albright (1997). "Pulsed-field gel electrophoretic migration of DNA broken by X irradiation during DNA synthesis: Experimental results compared with Monte Carlo calculations." Radiation Research **148**(5): 413-420.

Dibiase, S. J., Z. C. Zeng, R. Chen, T. Hyslop, W. J. Curran and G. Iliakis (2000). "DNA-dependent protein kinase stimulates an independently active, nonhomologous, end-joining apparatus." Cancer Research **60**(5): 1245-1253.

Dicioccio, R. A. and B. I. Srivastava (1977). "Kinetics of inhibition of deoxynucleotide-polymerizing enzyme activities from normal and leukemic human cells by 9-beta-D-arabinofuranosyladenine 5'-triphosphate and 1-beta-D-arabinofuranosylcytosine 5'-triphosphate." Eur J Biochem **79**(2): 411-418.

Djordjevic, B. and W. Szybalski (1960). "Genetics of human cell lines. III. Incorporation of 5-bromo- and 5-iododeoxyuridine into the deoxyribonucleic acid of human cells and its effect on radiation sensitivity." J Exp Med **112**: 509-531.

Donnianni, R. A. and L. S. Symington (2013). "Break-induced replication occurs by conservative DNA synthesis." Proc Natl Acad Sci U S A **110**(33): 13475-13480.

Dow, L. W., D. E. Bell, L. Poulakos and A. Fridland (1980). "Differences in Metabolism and Cyto-Toxicity between 9-Beta-D Arabinofuranosyladenine and 9-Beta-D-Arabinofuranosyl-2-Fluoroadenine in Human-Leukemic Lymphoblasts." Cancer Research **40**(5): 1405-1410.

Dueva, R. and G. Iliakis (2013). "Alternative pathways of non-homologous end joining (NHEJ) in genomic instability and cancer." 2013 **2**(3).

Early, A. P., H. D. Preisler, H. Slocum and Y. M. Rustum (1982). "A pilot study of high-dose 1-beta-D-arabinofuranosylcytosine for acute leukemia and refractory lymphoma: clinical response and pharmacology." Cancer Res **42**(4): 1587-1594.

Edwards, S. L., R. Brough, C. J. Lord, R. Natrajan, R. Vatcheva, D. A. Levine, J. Boyd, J. S. Reis-Filho and A. Ashworth (2008). "Resistance to therapy caused by intragenic deletion in BRCA2." Nature **451**(7182): 1111-1115.

Eggler, A. L., R. B. Inman and M. M. Cox (2002). "The Rad51-dependent pairing of long DNA substrates is stabilized by replication protein A." Journal of Biological Chemistry **277**(42): 39280-39288.

Eisbruch, A., D. S. Shewach, C. R. Bradford, J. F. Littles, T. N. Teknos, D. B. Chepeha, L. J. Marentette, J. E. Terrell, N. D. Hogikyan, L. A. Dawson, S. Urba, G. T. Wolf and T. S. Lawrence (2001). "Radiation concurrent with gemcitabine for locally advanced head and neck cancer: a phase I trial and intracellular drug incorporation study." J Clin Oncol **19**(3): 792-799.

Elliott, B., C. Richardson and M. Jasin (2005). "Chromosomal translocation mechanisms at intronic alu elements in mammalian cells." Molecular cell **17**(6): 885-894.

Eriksson, D., P. O. Lofroth, L. Johansson, K. A. Riklund and T. Stigbrand (2007). "Cell cycle disturbances and mitotic catastrophes in HeLa Hep2 cells following 2.5 to 10 Gy of ionizing radiation." Clinical cancer research : an official journal of the American Association for Cancer Research **13**(18 Pt 2): 5501s-5508s.

Escribano-Diaz, C., A. Orthwein, A. Fradet-Turcotte, M. Xing, J. T. Young, J. Tkac, M. A. Cook, A. P. Rosebrock, M. Munro, M. D. Canny, D. Xu and D. Durocher (2013). "A Cell Cycle-Dependent Regulatory Circuit Composed of 53BP1-RIF1 and BRCA1-CtIP Controls DNA Repair Pathway Choice." Molecular cell.

Evans, D. B., G. R. Varadhachary, C. H. Crane, C. C. Sun, J. E. Lee, P. W. Pisters, J. N. Vauthey, H. Wang, K. R. Cleary, G. A. Staerkel, C. Charnsangavej, E. A. Lano, L. Ho, R. Lenzi, J. L. Abbruzzese and R. A. Wolff (2008). "Preoperative gemcitabine-based chemoradiation for patients with resectable adenocarcinoma of the pancreatic head." J Clin Oncol **26**(21): 3496-3502.

Ewald, B., D. Sampath and W. Plunkett (2007). "H2AX phosphorylation marks gemcitabine-induced stalled replication forks and their collapse upon S-phase checkpoint abrogation." Molecular Cancer Therapeutics **6**(4): 1239-1248.

Ewald, B., D. Sampath and W. Plunkett (2008). "Nucleoside analogs: molecular mechanisms signaling cell death." Oncogene **27**(50): 6522-6537.

Ewing, D. (1998). "The oxygen fixation hypothesis: a reevaluation." American journal of clinical oncology **21**(4): 355-361.

Fattah, F., E. H. Lee, N. Weisensel, Y. Wang, N. Lichter and E. A. Hendrickson (2010). "Ku regulates the non-homologous end joining pathway choice of DNA double-strand break repair in human somatic cells." PLoS genetics **6**(2): e1000855.

Feng, Z., S. P. Scott, W. Bussen, G. G. Sharma, G. Guo, T. K. Pandita and S. N. Powell (2011). "Rad52 inactivation is synthetically lethal with BRCA2 deficiency." Proceedings of the National Academy of Sciences of the United States of America **108**(2): 686-691.

Ferguson, D. O. and F. W. Alt (2001). "DNA double strand break repair and chromosomal translocation: lessons from animal models." Oncogene **20**(40): 5572-5579.

Ferlay, J., P. Autier, M. Boniol, M. Heanue, M. Colombet and P. Boyle (2007). "Estimates of the cancer incidence and mortality in Europe in 2006." Ann Oncol **18**(3): 581-592.

Fertil, B. and E. P. Malaise (1981). "Inherent cellular radiosensitivity as a basic concept for human tumor radiotherapy." International journal of radiation oncology, biology, physics **7**(5): 621-629.

Fietkau, R. (2012). "[Concurrent radiochemotherapy for the treatment of solid tumors]." Strahlentherapie und Onkologie : Organ der Deutschen Rontgengesellschaft ... [et al] **188 Suppl 3**: 263-271.

Fishman-Lobell, J., N. Rudin and J. E. Haber (1992). "Two alternative pathways of double-strand break repair that are kinetically separable and independently modulated." Molecular and cellular biology **12**(3): 1292-1303.

Foray, N., C. F. Arlett and E. P. Malaise (1997a). "Radiation-induced DNA double-strand breaks and the radiosensitivity of human cells: a closer look." Biochimie **79**(9-10): 567-575.

Foray, N., C. Colin and M. Bourguignon (2012). "100 Years of Individual Radiosensitivity: How We Have Forgotten the Evidence." Radiology **264**(3): 627-631.

Foray, N., A. Priestley, G. Alsbeih, C. Badie, E. P. Capulas, C. F. Arlett and E. P. Malaise (1997b). "Hypersensitivity of ataxia telangiectasia fibroblasts to ionizing radiation is associated with a repair deficiency of DNA double-strand breaks." International Journal of Radiation Biology **72**(3): 271-283.

Foray, N., V. Randrianarison, D. Marot, M. Perricaudet, G. Lenoir and J. Feunteun (1999). "Gamma-rays-induced death of human cells carrying mutations of BRCA1 or BRCA2." Oncogene **18**(51): 7334-7342.

Frank, K. M., N. E. Sharpless, Y. Gao, J. M. Sekiguchi, D. O. Ferguson, C. Zhu, J. P. Manis, J. Horner, R. A. DePinho and F. W. Alt (2000). "DNA ligase IV deficiency in mice leads to defective neurogenesis and embryonic lethality via the p53 pathway." Mol Cell **5**(6): 993-1002.

Frankenberg-Schwager, M., A. Gebauer, C. Koppe, H. Wolf, E. Pralle and D. Frankenberg (2009). "Single-strand annealing, conservative homologous recombination, nonhomologous DNA end joining, and the cell cycle-dependent repair of DNA double-strand breaks induced by sparsely or densely ionizing radiation." Radiation research **171**(3): 265-273.

Frankenberg, D., M. Frankenberg-Schwager, D. Blocher and R. Harbich (1981). "Evidence for DNA double-strand breaks as the critical lesions in yeast cells irradiated with sparsely or densely ionizing radiation under oxic or anoxic conditions." Radiat Res **88**(3): 524-532.

Friedland, W., P. Kundrat and P. Jacob (2012). "Stochastic modelling of DSB repair after photon and ion irradiation." International journal of radiation biology **88**(1-2): 129-136.

Gagou, M. E., P. Zuazua-Villar and M. Meuth (2010). "Enhanced H2AX Phosphorylation, DNA Replication Fork Arrest, and Cell Death in the Absence of Chk1." Molecular Biology of the Cell **21**(5): 739-752.

Galluzzi, L., I. Vitale, J. M. Abrams, E. S. Alnemri, E. H. Baehrecke, M. V. Blagosklonny, T. M. Dawson, V. L. Dawson, W. S. El-Deiry, S. Fulda, E. Gottlieb, D. R. Green, M. O. Hengartner, O. Kepp, R. A. Knight, S. Kumar, S. A. Lipton, X. Lu, F. Madeo, W. Malorni, P. Mehlen, G. Nunez, M. E. Peter, M. Piacentini, D. C. Rubinsztein, Y. Shi, H. U. Simon, P. Vandenabeele, E. White, J. Yuan, B. Zhivotovsky, G. Melino and G. Kroemer (2012). "Molecular definitions of cell death subroutines: recommendations of the Nomenclature Committee on Cell Death 2012." Cell Death Differ **19**(1): 107-120.

Galmarini, C. M., J. R. Mackey and C. Dumontet (2002). "Nucleoside analogues and nucleobases in cancer treatment." Lancet Oncol **3**(7): 415-424.

Gardiner, K. (1991). "Pulsed field gel electrophoresis." Analytical chemistry **63**(7): 658-665.

Gerweck, L. E., S. Vijayappa, A. Kurimasa, K. Ogawa and D. J. Chen (2006). "Tumor cell radiosensitivity is a major determinant of tumor response to radiation." Cancer research **66**(17): 8352-8355.

Goffman, T., Z. Tochner and E. Glatstein (1991). "Primary treatment of large and massive adult sarcomas with iododeoxyuridine and aggressive hyperfractionated irradiation." Cancer **67**(3): 572-576.

Goodhead, D. T. (1994). "Initial events in the cellular effects of ionizing radiations: clustered damage in DNA." International journal of radiation biology **65**(1): 7-17.

Grabarz, A., A. Barascu, J. Guirouilh-Barbat and B. S. Lopez (2012). "Initiation of DNA double strand break repair: signaling and single-stranded resection dictate the choice between homologous recombination, non-homologous end-joining and alternative end-joining." American Journal of Cancer Reserarch **2**(3): 249-268.

Grabarz, A., J. Guirouilh-Barbat, A. Barascu, G. Pennarun, D. Genet, E. Rass, S. M. Germann, P. Bertrand, I. D. Hickson and B. S. Lopez (2013). "A Role for BLM in Double-Strand Break Repair Pathway Choice: Prevention of CtIP/Mre11-Mediated Alternative Nonhomologous End-Joining." Cell Reports **5**(1): 21-28.

Graham, F. L. and G. F. Whitmore (1970). "Studies in mouse L-cells on the incorporation of 1-beta-D-arabinofuranosylcytosine into DNA and on inhibition of DNA polymerase by 1-beta-D-arabinofuranosylcytosine 5'-triphosphate." Cancer Res **30**(11): 2636-2644.

Greaves, M. F. and J. Wiemels (2003). "Origins of chromosome translocations in childhood leukaemia." Nature reviews. Cancer **3**(9): 639-649.

Gregoire, V., K. K. Ang, J. F. Rosier, M. Beauduin, A. S. Garden, M. Hamoir, W. N. Hittelman, Y. Humblet, F. R. Khuri, L. Milas, C. Mitine and P. Scalliet (2002). "A phase I study of fludarabine combined with radiotherapy in patients with intermediate to locally advanced head and neck squamous cell carcinoma." Radiother Oncol **63**(2): 187-193.

Gregoire, V., M. Beauduin, M. Bruniaux, B. De Coster, M. O. Prignot and P. Scalliet (1998). "Radiosensitization of mouse sarcoma cells by fludarabine (F-ara-A) or gemcitabine (dFdC), two nucleoside analogues, is not mediated by an increased induction or a repair inhibition of DNA double-strand breaks as measured by pulsed-field gel electrophoresis." International Journal of Radiation Biology **73**(5): 511-520.

Gregoire, V., N. Hunter, W. A. Brock, L. Milas, W. Plunkett and W. N. Hittelman (1994). "Fludarabine Improves the Therapeutic Ratio of Radiotherapy in Mouse-Tumors after Single-Dose Irradiation." International Journal of Radiation Oncology Biology Physics **30**(2): 363-371.

Group, G. T. S. (1985). "Radiation therapy combined with Adriamycin or 5-fluorouracil for the treatment of locally unresectable pancreatic carcinoma." Cancer **56**(11): 2563-2568.

Gunn, A., N. Bennardo, A. Cheng and J. M. Stark (2011). "Correct end use during end joining of multiple chromosomal double strand breaks is influenced by repair protein RAD50, DNA-dependent protein kinase DNA-PKcs, and transcription context." The Journal of biological chemistry **286**(49): 42470-42482.

Gunn, A. and J. M. Stark (2012). "I-SceI-based assays to examine distinct repair outcomes of mammalian chromosomal double strand breaks." Methods in molecular biology **920**: 379-391.

Gurka, M. K., S. P. Collins, R. Slack, G. Tse, A. Charabaty, L. Ley, L. Berzcel, S. Lei, S. Suy, N. Haddad, R. Jha, C. D. Johnson, P. Jackson, J. L. Marshall and M. J. Pishvaian (2013). "Stereotactic body radiation therapy with concurrent full-dose gemcitabine for locally advanced pancreatic cancer: a pilot trial demonstrating safety." Radiat Oncol **8**: 44.

Gurrieri, S., S. B. Smith and C. Bustamante (1999). "Trapping of megabase-sized DNA molecules during agarose gel electrophoresis." Proceedings of the National Academy of Sciences of the United States of America **96**(2): 453-458.

Haince, J. F., D. McDonald, A. Rodrigue, U. Dery, J. Y. Masson, M. J. Hendzel and G. G. Poirier (2008). "PARP1-dependent kinetics of recruitment of MRE11 and NBS1 proteins to multiple DNA damage sites." J Biol Chem **283**(2): 1197-1208.

Hajdo, L., A. B. Szulc, B. Klajnert and M. Bryszewska (2010). "Metabolic Limitations of the Use of Nucleoside Analogs in Cancer Therapy May Be Overcome by Application of Nanoparticles as Drug Carriers: A Review." Drug Development Research **71**(7): 383-394.

Hall, E. J. and A. J. Giaccia (2006). Radiobiology for the radiologist. Philadelphia, Lippincott Williams & Wilkins.

Harrigan, J. A., R. Belotserkovskaya, J. Coates, D. S. Dimitrova, S. E. Polo, C. R. Bradshaw, P. Fraser and S. P. Jackson (2011). "Replication stress induces 53BP1-containing OPT domains in G1 cells." J Cell Biol **193**(1): 97-108.

Heidelberger, C., L. Griesbach, B. J. Montag, D. Mooren, O. Cruz, R. J. Schnitzer and E. Grunberg (1958). "Studies on fluorinated pyrimidines. II. Effects on transplanted tumors." Cancer Res **18**(3): 305-317.

Heinemann, V., Y. Z. Xu, S. Chubb, A. Sen, L. W. Hertel, G. B. Grindey and W. Plunkett (1990). "Inhibition of ribonucleotide reduction in CCRF-CEM cells by 2',2'-difluorodeoxycytidine." Molecular pharmacology **38**(4): 567-572.

Heinemann, V., Y. Z. Xu, S. Chubb, A. Sen, L. W. Hertel, G. B. Grindey and W. Plunkett (1992). "Cellular Elimination of 2',2'-Difluorodeoxycytidine 5'-Triphosphate - a Mechanism of Self-Potentiation." Cancer Research **52**(3): 533-539.

Held, K. D. (1997). "Radiation-induced apoptosis and its relationship to loss of clonogenic survival." Apoptosis **2**(3): 265-282.

Hendrickson, E. A., X.-Q. Qin, E. A. Bump, D. G. Schatz, M. Oettinger and D. T. Weaver (1991). "A link between double-strand break-related repair and V(D)J recombination: The *scid* mutation." Proceedings of the National Academy of Sciences of the United States of America **88**: 4061-4065.

Hershfield, M. S., J. E. Fetter, W. C. Small, A. S. Bagnara, S. R. Williams, B. Ullman, D. W. Martin, D. B. Wasson and D. A. Carson (1982). "Effects of Mutational Loss of Adenosine Kinase and Deoxycytidine Kinase on Deoxy-Atp Accumulation and Deoxyadenosine Toxicity in Cultured Cem Human T-Lymphoblastoid Cells." Journal of Biological Chemistry **257**(11): 6380-6386.

Hertel, L. W., G. B. Boder, J. S. Kroin, S. M. Rinzel, G. A. Poore, G. C. Todd and G. B. Grindey (1990). "Evaluation of the Antitumor-Activity of Gemcitabine (2',2'-Difluoro-2'-Deoxycytidine)." Cancer Research **50**(14): 4417-4422.

Hertel, L. W., J. S. Kroin, J. W. Misner and J. M. Tustin (1988). "Synthesis of 2-Deoxy-2,2-Difluoro-D-Ribose and 2-Deoxy-2,2-Difluoro-D-Ribofuranosyl Nucleosides." Journal of Organic Chemistry **53**(11): 2406-2409.

Heyer, W. D., K. T. Ehmsen and J. Liu (2010). "Regulation of homologous recombination in eukaryotes." Annu Rev Genet **44**: 113-139.

Huang, P., S. Chubb, L. W. Hertel, G. B. Grindey and W. Plunkett (1991). "Action of 2',2'-Difluorodeoxycytidine on DNA-Synthesis." Cancer Research **51**(22): 6110-6117.

Huang, P., S. Chubb and W. Plunkett (1990). "Termination of DNA-Synthesis by 9-Beta-D-Arabinofuranosyl-2-Fluoroadenine - a Mechanism for Cytotoxicity." Journal of Biological Chemistry **265**(27): 16617-16625.

Huang, P. and W. Plunkett (1991). "Action of 9-beta-D-arabinofuranosyl-2-fluoroadenine on RNA metabolism." Mol Pharmacol **39**(4): 449-455.

Hubeek I, K. G., Ossenkoppele GJ, Peters GJ (2006). Cytosine arabinoside Deoxynucleoside Analogs in Cancer Therapy. . P. GJ. Totowa, NJ, Humana Press**:** pp 289-329

Huertas, P. (2010). "DNA resection in eukaryotes: deciding how to fix the break." Nature structural & molecular biology **17**(1): 11-16.

Huertas, P. and S. P. Jackson (2009). "Human CtIP Mediates Cell Cycle Control of DNA End Resection and Double Strand Break Repair." Journal of Biological Chemistry **284**(14): 9558-9565.

Ikegami, S., T. Taguchi and M. Ohashi (1978). "Aphidicolin Prevents Mitotic Cell-Division by Interfering with Activity of DNA Polymerase-Alpha." Nature **275**(5679): 458-460.

Iliakis, G. (1980). "Effects of beta-arabinofuranosyladenine on the growth and repair of potentially lethal damage in Ehrilch ascites tumor cells." Radiat Res **83**(3): 537-552.

Iliakis, G. (1988a). "Radiation-induced potentially lethal damage: DNA lesions susceptible to fixation." Int J Radiat Biol Relat Stud Phys Chem Med **53**(4): 541-584.

Iliakis, G. (1991). "The role of DNA double strand breaks in ionizing radiation-induced killing of eukaryotic cells." Bioessays **13**(12): 641-648.

Iliakis, G. (2009). "Backup pathways of NHEJ in cells of higher eukaryotes: cell cycle dependence." Radiother Oncol **92**(3): 310-315.

Iliakis, G. and P. E. Bryant (1983). "Effects of the nucleoside analogues alpha-ara A, beta-ara A and beta-ara C on cell growth and repair of both potentially lethal damage and DNA double strand breaks in mammalian cells in culture." Anticancer Res **3**(2): 143-149.

Iliakis, G., S. Kurtzman, G. Pantelias and R. Okayasu (1989a). "Mechanism of radiosensitization by halogenated pyrimidines: effect of BrdU on radiation induction of DNA and chromosome damage and its correlation with cell killing." Radiat Res **119**(2): 286-304.

Iliakis, G. and F. Q. Ngo (1985). "Effects of adenosine deaminase inhibitor 2'-deoxycoformycin on the repair and expression of potentially lethal damage sensitive to beta-araA." Radiat Environ Biophys **24**(2): 81-88.

Iliakis, G. and M. Nusse (1983a). "Effects of caffeine on X-irradiated synchronous, asynchronous and plateau phase mouse ascites cells: the importance of progression

through the cell cycle for caffeine enhancement of killing." Int J Radiat Biol Relat Stud Phys Chem Med **43**(6): 649-663.

Iliakis, G. and M. Nusse (1983b). "Evidence that repair and expression of potentially lethal damage cause the variations in cell survival after X irradiation observed through the cell cycle in Ehrlich ascites tumor cells." Radiat Res **95**(1): 87-107.

Iliakis, G., G. Pantelias, R. Okayasu and R. Seaner (1989b). "Comparative studies on repair inhibition by araA, araC and aphidicolin of radiation induced DNA and chromosome damage in rodent cells: comparison with fixation of PLD." Int J Radiat Oncol Biol Phys **16**(5): 1261-1265.

Iliakis, G., G. E. Pantelias and R. Seaner (1988b). "Effect of arabinofuranosyladenine on radiation-induced chromosome damage in plateau-phase CHO cells measured by premature chromosome condensation: implications for repair and fixation of alpha-PLD." Radiation research **114**(2): 361-378.

Iliakis, G., H. Wang, A. R. Perrault, W. Boecker, B. Rosidi, F. Windhofer, W. Wu, J. Guan, G. Terzoudi and G. Pantelias (2004). "Mechanisms of DNA double strand break repair and chromosome aberration formation." Cytogenetic and genome research **104**(1-4): 14-20.

Iliakis, G. E. and R. Okayasu (1990). "Radiosensitivity Throughout the Cell-Cycle and Repair of Potentially Lethal Damage and DNA Double-Strand Breaks in an X-Ray-Sensitive Cho Mutant." International Journal of Radiation Biology **57**(6): 1195-1211.

IMPACT (1995). "Efficacy of adjuvant fluorouracil and folinic acid in colon cancer. International Multicentre Pooled Analysis of Colon Cancer Trials (IMPACT) investigators." Lancet **345**(8955): 939-944.

Ingraham, H. A., L. Dickey and M. Goulian (1986). "DNA fragmentation and cytotoxicity from increased cellular deoxyuridylate." Biochemistry **25**(11): 3225-3230.

Invitrogen (2011). Click-iT® EdU Imaging Kits Application Manual. **MP 10338**.

Ira, G., A. Pellicioli, A. Balijja, X. Wang, S. Fiorani, W. Carotenuto, G. Liberi, D. Bressan, L. H. Wan, N. M. Hollingsworth, J. E. Haber and M. Foiani (2004). "DNA end resection, homologous recombination and DNA damage checkpoint activation require CDK1." Nature **431**(7011): 1011-1017.

Ivanov, E. L., N. Sugawara, J. Fishman-Lobell and J. E. Haber (1996). "Genetic requirements for the single-strand annealing pathway of double-strand break repair in Saccharomyces cerevisiae." Genetics **142**(3): 693-704.

Jazayeri, A., J. Falck, C. Lukas, J. Bartek, G. C. M. Smith, J. Lukas and S. P. Jackson (2006). "ATM- and cell cycle-dependent regulation of ATR in response to DNA double-strand breaks." Nature Cell Biology **8**(1): 37-U13.

Jeggo, P. and M. F. Lavin (2009a). "Cellular radiosensitivity: How much better do we understand it?" International Journal of Radiation Biology **85**(12): 1061-1081.

Jeggo, P. and M. F. Lavin (2009b). "Cellular radiosensitivity: how much better do we understand it?" International journal of radiation biology **85**(12): 1061-1081.

Jeggo, P. A. and L. M. Kemp (1983). "X-Ray-Sensitive Mutants of Chinese-Hamster Ovary Cell-Line - Isolation and Cross-Sensitivity to Other DNA-Damaging Agents." Mutation Research **112**(6): 313-327.

Jemal, A., F. Bray, M. M. Center, J. Ferlay, E. Ward and D. Forman (2011). "Global cancer statistics." CA Cancer J Clin **61**(2): 69-90.

Jensen, R. B., A. Ozes, T. Kim, A. Estep and S. C. Kowalczykowski (2013). "BRCA2 is epistatic to the RAD51 paralogs in response to DNA damage." DNA Repair **12**(4): 306-311.

Jordheim, L. P., D. Durantel, F. Zoulim and C. Dumontet (2013). "Advances in the development of nucleoside and nucleotide analogues for cancer and viral diseases." Nat Rev Drug Discov **12**(6): 447-464.

Joubert, A., K. M. Zimmerman, Z. Bencokova, J. Gastaldo, N. Chavaudra, V. Favaudon, C. F. Arlett and N. Foray (2008). "DNA double-strand break repair defects in syndromes associated with acute radiation response: at least two different assays to predict intrinsic radiosensitivity?" International journal of radiation biology **84**(2): 107-125.

Juranka, P. and V. L. Chan (1980). "Relative cytotoxicity of 9-beta-D-arabinofuranosyladenine and 9-beta-D-arabinofuranosyladenine 5'-monophosphate." Cancer Res **40**(11): 4123-4126.

Kabotyanski, E. B., L. Gomelsky, J. O. Han, T. D. Stamato and D. B. Roth (1998). "Double-strand break repair in Ku86- and XRCC4-deficient cells." Nucleic acids research **26**(23): 5333-5342.

Kanamaru, R., H. Kakuta, T. Sato, C. Ishioka and A. Wakui (1986). "The inhibitory effects of 5-fluorouracil on the metabolism of preribosomal and ribosomal RNA in L-1210 cells in vitro." Cancer Chemother Pharmacol **17**(1): 43-46.

Kane, D. P., M. Shusterman, Y. Rong and M. McVey (2012). "Competition between replicative and translesion polymerases during homologous recombination repair in Drosophila." PLoS Genet **8**(4): e1002659.

Kinner, A., W. Wu, C. Staudt and G. Iliakis (2008). "Gamma-H2AX in recognition and signaling of DNA double-strand breaks in the context of chromatin." Nucleic Acids Res **36**(17): 5678-5694.

Kuchta, R. D. and L. Willhelm (1991). "Inhibition of DNA primase by 9-beta-D-arabinofuranosyladenosine triphosphate." Biochemistry **30**(3): 797-803.

Kufe, D. W., P. P. Major, E. M. Egan and G. P. Beardsley (1980). "Correlation of cytotoxicity with incorporation of ara-C into DNA." J Biol Chem **255**(19): 8997-8900.

Kufe, D. W., P. P. Major, D. Munroe, M. Egan and D. Herrick (1983). "Relationship between Incorporation of 9-Beta-D-Arabinofuranosyladenine in L1210 DNA and Cyto-Toxicity." Cancer Research **43**(5): 2000-2004.

Kun, E., E. Kirsten and C. P. Ordahl (2002). "Coenzymatic activity of randomly broken or intact double-stranded DNAs in auto and histone H1 trans-poly(ADP-ribosylation), catalyzed by poly(ADP-ribose) polymerase (PARP I)." J Biol Chem **277**(42): 39066-39069.

Kuo, M. L. and T. J. Kinsella (1998). "Expression of ribonucleotide reductase after ionizing radiation in human cervical carcinoma cells." Cancer Res **58**(10): 2245-2252.

Latz, D., W. C. Dewey, M. Flentje, F. Lohr, F. Wenz and K. J. Weber (1996). "Migration patterns in pulsed-field electrophoresis of DNA restriction fragments from log-phase mammalian cells after irradiation and incubation for repair." International Journal of Radiation Biology **70**(6): 637-646.

Latz, D., K. Fleckenstein, M. Eble, J. Blatter, M. Wannenmacher and K. J. Weber (1998). "Radiosensitizing potential of gemcitabine (2 ',2 '-difluoro-2 '-deoxycytidine) within the cell cycle in vitro." International Journal of Radiation Oncology Biology Physics **41**(4): 875-882.

Laurent, D., O. Pradier, H. Schmidberger, M. Rave-Frank, D. Frankenberg and C. F. Hess (1998). "Radiation rendered more cytotoxic by fludarabine monophosphate in a human oropharynx carcinoma cell line than in fetal lung fibroblasts." Journal of Cancer Research and Clinical Oncology **124**(9): 485-492.

Lavin, M. F. (2007). "ATM and the Mre11 complex combine to recognize and signal DNA double-strand breaks." Oncogene **26**(56): 7749-7758.

Lawrence, T. S., E. Y. Chang, T. M. Hahn, L. W. Hertel and D. S. Shewach (1996). "Radiosensitization of pancreatic cancer cells by 2',2'-difluoro-2'-deoxycytidine." Int J Radiat Oncol Biol Phys **34**(4): 867-872.

Lawrence, T. S., M. A. Davis, J. Maybaum, P. L. Stetson and W. D. Ensminger (1990). "The effect of single versus double-strand substitution on halogenated pyrimidine-induced radiosensitization and DNA strand breakage in human tumor cells." Radiat Res **123**(2): 192-198.

Lawrence, T. S., M. A. Davis and D. P. Normolle (1995). "Effect of bromodeoxyuridine on radiation-induced DNA damage and repair based on DNA fragment size using pulsed-field gel electrophoresis." Radiat Res **144**(3): 282-287.

Lee-Theilen, M., A. J. Matthews, D. Kelly, S. Zheng and J. Chaudhuri (2011). "CtIP promotes microhomology-mediated alternative end joining during class-switch recombination." Nature structural & molecular biology **18**(1): 75-79.

Lee, M. W., W. B. Parker and B. Xu (2013). "New insights into the synergism of nucleoside analogs with radiotherapy." Radiation Oncology **8**.

Lepage, G. A., S. R. Naik, S. B. Katakkar and A. Khaliq (1975). "9-Beta-D-Arabinofuranosyladenine 5'-Phosphate Metabolism and Excretion in Humans." Cancer Research **35**(11): 3036-3040.

Levin, V. A., M. R. Prados, W. M. Wara, R. L. Davis, P. H. Gutin, T. L. Phillips, K. Lamborn and C. B. Wilson (1995). "Radiation therapy and bromodeoxyuridine chemotherapy followed by procarbazine, lomustine, and vincristine for the treatment of anaplastic gliomas." Int J Radiat Oncol Biol Phys **32**(1): 75-83.

Li, L., H. Wang, E. S. Yang, C. L. Arteaga and F. Xia (2008). "Erlotinib attenuates homologous recombinational repair of chromosomal breaks in human breast cancer cells." Cancer research **68**(22): 9141-9146.

Li, X. and W. D. Heyer (2008). "Homologous recombination in DNA repair and DNA damage tolerance." Cell Res **18**(1): 99-113.

Liang, F., M. G. Han, P. J. Romanienko and M. Jasin (1998). "Homology-directed repair is a major double-strand break repair pathway in mammalian cells." Proceedings of the National Academy of Sciences of the United States of America **95**(9): 5172-5177.

Lieber, M. R. (2010). "The mechanism of double-strand DNA break repair by the nonhomologous DNA end-joining pathway." Annual review of biochemistry **79**: 181-211.

Liliemark, J. O., W. Plunkett and D. O. Dixon (1985). "Relationship of 1-beta-D-arabinofuranosylcytosine in plasma to 1-beta-D-arabinofuranosylcytosine 5'-triphosphate levels in leukemic cells during treatment with high-dose 1-beta-D-arabinofuranosylcytosine." Cancer Res **45**(11 Pt 2): 5952-5957.

Little, J. B. (1969). "Repair of sub-lethal and potentially lethal radiation damage in plateau phase cultures of human cells." Nature **224**(5221): 804-806.

Little, J. B., A. M. Ueno and W. K. Dahlberg (1989). "Differential response of human and rodent cell lines to chemical inhibition of the repair of potentially lethal damage." Radiat Environ Biophys **28**(3): 193-202.

Liu, P. F., C. M. B. Carvalho, P. J. Hastings and J. R. Lupski (2012a). "Mechanisms for recurrent and complex human genomic rearrangements." Current Opinion in Genetics & Development **22**(3): 211-220.

Liu, Q., H. Jiang, Z. Liu, Y. Wang, M. Zhao, C. Hao, S. Feng, H. Guo, B. Xu, Q. Yang, Y. Gong and C. Shao (2011). "Berberine radiosensitizes human esophageal cancer cells by downregulating homologous recombination repair protein RAD51." PLoS One **6**(8): e23427.

Liu, X. J., H. Kantarjian and W. Plunkett (2012b). "Sapacitabine for cancer." Expert Opinion on Investigational Drugs **21**(4): 541-555.

Longley, D. B., D. P. Harkin and P. G. Johnston (2003). "5-fluorouracil: mechanisms of action and clinical strategies." Nat Rev Cancer **3**(5): 330-338.

Lydeard, J. R., S. Jain, M. Yamaguchi and J. E. Haber (2007). "Break-induced replication and telomerase-independent telomere maintenance require Pol32." Nature **448**(7155): 820-823.

Lydeard, J. R., Z. Lipkin-Moore, Y. J. Sheu, B. Stillman, P. M. Burgers and J. E. Haber (2010). "Break-induced replication requires all essential DNA replication factors except those specific for pre-RC assembly." Genes Dev **24**(11): 1133-1144.

MacLeod, R. A. and P. E. Bryant (1992). "Effects of adenine arabinoside and coformycin on the kinetics of G2 chromatid aberrations in X-irradiated human lymphocytes." Mutagenesis **7**(4): 285-290.

Magin, S., J. Saha, M. Wang, V. Mladenova, N. Coym and G. Iliakis (2013). "Lipofection and nucleofection of substrate plasmid can generate widely different readings of DNA end-joining efficiency in different cell lines." DNA repair **12**(2): 148-160.

Malkova, A., M. L. Naylor, M. Yamauchi, G. Ira and J. E. Haber (2005). "RAD51-dependent break-induced replication differs in kinetics and checkpoint responses from RAD51-mediated gene conversion." Molecular and Cellular Biology **25**(3): 933-944.

Malkova, A., L. Signon, C. B. Schaefer, M. L. Naylor, J. F. Theis, C. S. Newlon and J. E. Haber (2001). "RAD51-independent break-induced replication to repair a broken chromosome depends on a distant enhancer site." Genes Dev **15**(9): 1055-1060.

Maloisel, L., F. Fabre and S. Gangloff (2008). "DNA polymerase delta is preferentially recruited during homologous recombination to promote heteroduplex DNA extension." Molecular and Cellular Biology **28**(4): 1373-1382.

Mansour, W. Y., T. Rhein and J. Dahm-Daphi (2010). "The alternative end-joining pathway for repair of DNA double-strand breaks requires PARP1 but is not dependent upon microhomologies." Nucleic acids research **38**(18): 6065-6077.

Mansour, W. Y., S. Schumacher, R. Rosskopf, T. Rhein, F. Schmidt-Petersen, F. Gatzemeier, F. Haag, K. Borgmann, H. Willers and J. Dahm-Daphi (2008). "Hierarchy of nonhomologous end-joining, single-strand annealing and gene conversion at site-directed DNA double-strand breaks." Nucleic Acids Research **36**(12): 4088-4098.

Manthey, G. M. and A. M. Bailis (2010). "Rad51 inhibits translocation formation by non-conservative homologous recombination in Saccharomyces cerevisiae." PloS one **5**(7): e11889.

Mao, Z., M. Bozzella, A. Seluanov and V. Gorbunova (2008). "Comparison of nonhomologous end joining and homologous recombination in human cells." DNA repair **7**(10): 1765-1771.

Markova, E., N. Schultz and I. Y. Belyaev (2007). "Kinetics and dose-response of residual 53BP1/gamma-H2AX foci: co-localization, relationship with DSB repair and clonogenic survival." Int J Radiat Biol **83**(5): 319-329.

Marti, T. M., E. Hefner, L. Feeney, V. Natale and J. E. Cleaver (2006). "H2AX phosphorylation within the G(1) phase after UV irradiation depends on nucleotide excision repair and not DNA double-strand breaks." Proceedings of the National Academy of Sciences of the United States of America **103**(26): 9891-9896.

Matsukage, A., T. Takahashi, C. Nakayama and M. Saneyoshi (1978). "Inhibition of Mouse Myeloma DNA Polymerase-Alpha by 5'-Triphosphates of 1-Beta-D-Arabinofuranosylthymine and 1-Beta-D-Arabinofuranosylcytosine." Journal of Biochemistry **83**(5): 1511-1515.

Matsumoto, Y., T. Miyamoto, H. Sakamoto, H. Izumi, Y. Nakazawa, T. Ogi, H. Tahara, S. Oku, A. Hiramoto, T. Shiiki, Y. Fujisawa, H. Ohashi, Y. Sakemi and S. Matsuura (2011). "Two unrelated patients with MRE11A mutations and Nijmegen breakage syndrome-like severe microcephaly." DNA repair **10**(3): 314-321.

McGinn, C. J. and T. S. Lawrence (2001). "Recent advances in the use of radiosensitizing nucleosides." Semin Radiat Oncol **11**(4): 270-280.

McGinn, C. J., D. S. Shewach and T. S. Lawrence (1996). "Radiosensitizing nucleosides." J Natl Cancer Inst **88**(17): 1193-1203.

McVey, M. and S. E. Lee (2008). "MMEJ repair of double-strand breaks (director's cut): deleted sequences and alternative endings." Trends in genetics : TIG **24**(11): 529-538.

Meike, S., T. Yamamori, H. Yasui, M. Eitaki, A. Matsuda, M. Morimatsu, M. Fukushima, Y. Yamasaki and O. Inanami (2011). "A nucleoside anticancer drug, 1-(3-C-ethynyl-beta-D-ribo-pentofuranosyl)cytosine (TAS106), sensitizes cells to radiation by suppressing BRCA2 expression." Molecular cancer **10**: 92.

Merlano, M., M. Benasso, R. Corvo, R. Rosso, V. Vitale, F. Blengio, G. Numico, G. Margarino, L. Bonelli and L. Santi (1996). "Five-year update of a randomized trial of alternating radiotherapy and chemotherapy compared with radiotherapy alone in treatment of unresectable squamous cell carcinoma of the head and neck." J Natl Cancer Inst **88**(9): 583-589.

Meyer, B., K. O. Voss, F. Tobias, B. Jakob, M. Durante and G. Taucher-Scholz (2013). "Clustered DNA damage induces pan-nuclear H2AX phosphorylation mediated by ATM and DNA-PK." Nucleic Acids Research **41**(12): 6109-6118.

Miller, M. R. and D. N. Chinault (1982). "Evidence that DNA polymerases alpha and beta participate differentially in DNA repair synthesis induced by different agents." J Biol Chem **257**(1): 46-49.

Miser, J. S., J. Roloff, J. Blatt, G. H. Reaman, M. D. Krailo and G. D. Hammond (1992). "Lack of significant activity of 2'-deoxycoformycin alone or in combination with adenine arabinoside in relapsed childhood acute lymphoblastic leukemia. A randomized phase II trial from the Childrens Cancer Study Group." Am J Clin Oncol **15**(6): 490-493.

Mizuno, K., I. Miyabe, S. A. Schalbetter, A. M. Carr and J. M. Murray (2013). "Recombination-restarted replication makes inverted chromosome fusions at inverted repeats." Nature **493**(7431): 246-249.

Mladenov, E. and G. Iliakis (2011). "Induction and repair of DNA double strand breaks: The increasing spectrum of non-homologous end joining pathways." Mutat Res.

Mladenov, E., S. Magin, A. Soni and G. Iliakis (2013). "DNA double-strand break repair as determinant of cellular radiosensitivity to killing and target in radiation therapy." Frontiers in oncology **3**: 113.

Montgomery, J. A. and K. Hewson (1969). "Nucleosides of 2-Fluoroadenine." Journal of Medicinal Chemistry **12**(3): 498-&.

Moore, E. C. and S. S. Cohen (1967). "Effects of arabinonucleotides on ribonucleotide reduction by an enzyme system from rat tumor." The Journal of biological chemistry **242**(9): 2116-2118.

Moore, N. and S. Lyle (2011). "Quiescent, slow-cycling stem cell populations in cancer: a review of the evidence and discussion of significance." J Oncol **2011**.

Morgan, M. A., L. A. Parsels, L. Zhao, J. D. Parsels, M. A. Davis, M. C. Hassan, S. Arumugarajah, L. Hylander-Gans, D. Morosini, D. M. Simeone, C. E. Canman, D. P. Normolle, S. D. Zabludoff, J. Maybaum and T. S. Lawrence (2010). "Mechanism of Radiosensitization by the Chk1/2 Inhibitor AZD7762 Involves Abrogation of the G2 Checkpoint and Inhibition of Homologous Recombinational DNA Repair." Cancer research **70**(12): 4972-4981.

Moshous, D., I. Callebaut, R. de Chasseval, B. Corneo, M. Cavazzana-Calvo, F. Le Deist, I. Tezcan, O. Sanal, Y. Bertrand, N. Philippe, A. Fischer and J. de Villartay (2001). "Artemis, a novel dna double-strand break repair/v(d)j recombination protein, is mutated in human severe combined immune deficiency." Cell **105**: 177-186.

Mozdarani, H. and P. E. Bryant (1987). "The effect of 9-beta-D-arabinofuranosyladenine on the formation of X-ray induced chromatid aberrations in X-irradiated G2 human cells." Mutagenesis **2**(5): 371-374.

Muller, W. E., H. J. Rohde, R. Beyer, A. Maidhof, M. Lachmann, H. Taschner and R. K. Kahn (1975). "Mode of action of 9-beta-D-arabinofuranosyladenine on the synthesis of DNA, RNA, and protein in vivo and in vitro." Cancer Res **35**(8): 2160-2168.

Murakawa, Y., E. Sonoda, L. J. Barber, W. Zeng, K. Yokomori, H. Kimura, A. Niimi, A. Lehmann, G. Y. Zhao, H. Hochegger, S. J. Boulton and S. Takeda (2007). "Inhibitors of the Proteasome Suppress Homologous DNA Recombination in Mammalian Cells." Cancer research **67**(18): 8536-8543.

Mustafi, R., D. Heaton, W. Brinkman and J. L. Schwartz (1994). "Enhancement of X-ray toxicity in squamous cell carcinoma cell lines by DNA polymerase inhibitors." Int J Radiat Biol **65**(6): 675-681.

Nakamura, A. J., V. A. Rao, Y. Pommier and W. M. Bonner (2010). "The complexity of phosphorylated H2AX foci formation and DNA repair assembly at DNA double-strand breaks." Cell Cycle **9**(2): 389-397.

Nakatsugawa, S., T. Kada, O. Nikaido, Y. Tanaka and T. Sugahara (1984). "PLDR inhibitors: their biological and clinical implications." Br J Cancer Suppl **6**: 43-47.

Nambiar, M. and S. C. Raghavan (2011). "How does DNA break during chromosomal translocations?" Nucleic acids research **39**(14): 5813-5825.

Natarajan, A. T., G. Obe, A. A. Vanzeeland, F. Palitti, M. Meijers and E. A. M. Verdegaalimmerzeel (1980). "Molecular Mechanisms Involved in the Production of Chromosomal-Aberrations .2. Utilization of Neurospora Endonuclease for the Study of Aberration Production by X-Rays in G1 and G2 Stages of the Cell-Cycle." Mutation Research **69**(2): 293-305.

Nevaldine, B., J. A. Longo and P. J. Hahn (1997). "The scid defect results in much slower repair of DNA double-strand breaks but not high levels of residual breaks." Radiation research **147**(5): 535-540.

Nikjoo, H., P. O'Neill, M. Terrissol and D. T. Goodhead (1999). "Quantitative modelling of DNA damage using Monte Carlo track structure method." Radiation and environmental biophysics **38**(1): 31-38.

Nitsche, M., H. Christiansen, R. M. Hermann, E. M. Lucke, K. Peters, M. Rave-Frank, H. Schmidberger and O. Pradier (2008). "The combined effect of fludarabine monophosphate and radiation as well as gemcitabine and radiation on squamous carcinoma tumor cell lines in vitro." International Journal of Radiation Biology **84**(8): 643-657.

Nitsche, M., H. Christiansen, K. Lederer, F. Griesinger, H. Schmidberger and O. Pradier (2012). "Fludarabine combined with radiotherapy in patients with locally advanced NSCLC lung carcinoma: a phase I study." Journal of Cancer Research and Clinical Oncology **138**(7): 1113-1120.

Noguchi, M., D. Yu, R. Hirayama, Y. Ninomiya, E. Sekine, N. Kubota, K. Ando and R. Okayasu (2006). "Inhibition of homologous recombination repair in irradiated tumor cells pretreated with Hsp90 inhibitor 17-allylamino-17-demethoxygeldanamycin." Biochemical and Biophysical Research Communications **351**(3): 658-663.

Obe, G., C. Johannes and D. Schulte-Frohlinde (1992). "DNA double-strand breaks induced by sparsely ionizing radiation and endonucleases as critical lesions for cell death, chromosomal aberrations, mutations and oncogenic transformation." Mutagenesis **7**(1): 3-12.

Ohashi, M., T. Taguchi and S. Ikegami (1978). "Aphidicolin - Specific Inhibitor of DNA-Polymerases in Cytosol of Rat-Liver." Biochemical and Biophysical Research Communications **82**(4): 1084-1090.

Ohno, Y., D. Spriggs, A. Matsukage, T. Ohno and D. Kufe (1988). "Effects of 1-beta-D-arabinofuranosylcytosine incorporation on elongation of specific DNA sequences by DNA polymerase beta." Cancer Res **48**(6): 1494-1498.

Ohno, Y., D. Spriggs, A. Matsukage, T. Ohno and D. Kufe (1989). "Sequence-specific inhibition of DNA strand elongation by incorporation of 9-beta-D-arabinofuranosyladenine." Cancer Res **49**(8): 2077-2081.

Okayasu, R. and G. Iliakis (1993). "Ionizing radiation induces two forms of interphase chromosome breaks in Chinese hamster ovary cells that rejoin with different kinetics and show different sensitivity to treatment in hypertonic medium or beta-araA." Radiat Res **136**(2): 262-270.

Pardee, T. S., E. Gomes, J. Jennings-Gee, D. Caudell and W. H. Gmeiner (2012). "Unique dual targeting of thymidylate synthase and topoisomerase1 by FdUMP[10] results in high efficacy against AML and low toxicity." Blood **119**(15): 3561-3570.

Parker, W. B. (2009). "Enzymology of purine and pyrimidine antimetabolites used in the treatment of cancer." Chemical reviews **109**(7): 2880-2893.

Pauwels, B., A. E. Korst, G. G. Pattyn, H. A. Lambrechts, D. R. Van Bockstaele, K. Vermeulen, M. Lenjou, C. M. de Pooter, J. B. Vermorken and F. Lardon (2003). "Cell

cycle effect of gemcitabine and its role in the radiosensitizing mechanism in vitro." Int J Radiat Oncol Biol Phys **57**(4): 1075-1083.

Pauwels, B., A. E. C. Korst, G. G. O. Pattyn, H. A. J. Lambrechts, J. A. E. Kamphuis, C. M. J. De Pooter, G. J. Peters, F. Lardon and J. B. Vermorken (2006). "The relation between deoxycytidine kinase activity and the radiosensitising effect of gemcitabine in eight different human tumour cell lines." Bmc Cancer **6**.

Payen, C., R. Koszul, B. Dujon and G. Fischer (2008). "Segmental Duplications Arise from Pol32-Dependent Repair of Broken Forks through Two Alternative Replication-Based Mechanisms." Plos Genetics **4**(9).

Perrault, R., H. Wang, M. Wang, B. Rosidi and G. Iliakis (2004). "Backup pathways of NHEJ are suppressed by DNA-PK." J Cell Biochem **92**(4): 781-794.

Petermann, E., M. L. Orta, N. Issaeva, N. Schultz and T. Helleday (2010). "Hydroxyurea-Stalled Replication Forks Become Progressively Inactivated and Require Two Different RAD51-Mediated Pathways for Restart and Repair." Molecular Cell **37**(4): 492-502.

Phillips, R. A. and L. J. Tolmach (1966). "Repair of potentially lethal damage in x-irradiated HeLa cells." Radiat Res **29**(3): 413-432.

Pierce, A. J., R. D. Johnson, L. H. Thompson and M. Jasin (1999). "XRCC3 promotes homology-directed repair of DNA damage in mammalian cells." Genes Dev **13**(20): 2633-2638.

Plowman, P. N., B. A. Bridges, C. F. Arlett, A. Hinney and J. E. Kingston (1990). "An instance of clinical radiation morbidity and cellular radiosensitivity, not associated with ataxia-telagiectasia." British Journal of Radiology **63**: 624-628.

Plunkett, W., P. Huang and V. Gandhi (1995). "Preclinical characteristics of gemcitabine." Anti-Cancer Drugs **6**: 7-13.

Plunkett, W., L. Lapi, P. J. Ortiz and S. S. Cohen (1974). "Penetration of mouse fibroblasts by the 5'-phosphate of 9-beta-D-arabinofuranosyladenine and incorporation of the nucleotide into DNA." Proc Natl Acad Sci U S A **71**(1): 73-77.

Polo, S. E. and S. P. Jackson (2011). "Dynamics of DNA damage response proteins at DNA breaks: a focus on protein modifications." Genes Dev **25**(5): 409-433.

Prados, M. D., C. Scott, H. Sandler, J. C. Buckner, T. Phillips, C. Schultz, R. Urtasun, R. Davis, P. Gutin, T. L. Cascino, H. S. Greenberg and W. J. Curran (1999). "A phase 3 randomized study of radiotherapy plus procarbazine, CCNU, and vincristine (PCV) with or without BUdR for the treatment of anaplastic astrocytoma: A preliminary report of RTOG 9404." International Journal of Radiation Oncology Biology Physics **45**(5): 1109-1115.

Prevo, R., E. Fokas, P. M. Reaper, P. A. Charlton, J. R. Pollard, W. G. McKenna, R. J. Muschel and T. B. Brunner (2012). "The novel ATR inhibitor VE-821 increases sensitivity of pancreatic cancer cells to radiation and chemotherapy." Cancer Biology & Therapy **13**(11): 1072-1081.

Puck, T. T. and P. I. Marcus (1956). "Action of x-rays on mammalian cells." The Journal of experimental medicine **103**(5): 653-666.

Quanz, M., D. Chassoux, N. Berthault, C. Agrario, J. S. Sun and M. Dutreix (2009). "Hyperactivation of DNA-PK by Double-Strand Break Mimicking Molecules Disorganizes DNA Damage Response." Plos One **4**(7).

Raderschall, E., E. I. Golub and T. Haaf (1999). "Nuclear foci of mammalian recombination proteins are located at single-stranded DNA regions formed after DNA damage." Proceedings of the National Academy of Sciences of the United States of America **96**(5): 1921-1926.

Radford, I. R. (1985). "The Level of Induced DNA Double-Strand Breakage Correlates with Cell Killing after X-Irradiation." International Journal of Radiation Biology **48**(1): 45-54.

Rass, E., A. Grabarz, I. Plo, J. Gautier, P. Bertrand and B. S. Lopez (2009). "Role of Mre11 in chromosomal nonhomologous end joining in mammalian cells." Nature Structural & Molecular Biology **16**(8): 819-U838.

Reinhardt, H. C. and M. B. Yaffe (2009). "Kinases that control the cell cycle in response to DNA damage: Chk1, Chk2, and MK2." Curr Opin Cell Biol **21**(2): 245-255.

Robert, I., F. Dantzer and B. Reina-San-Martin (2009). "Parp1 facilitates alternative NHEJ, whereas Parp2 suppresses IgH/c-myc translocations during immunoglobulin class switch recombination." The Journal of experimental medicine **206**(5): 1047-1056.

Roberts, S. A., A. R. Spreadborough, B. Bulman, J. B. Barber, D. G. Evans and D. Scott (1999). "Heritability of cellular radiosensitivity: a marker of low-penetrance predisposition genes in breast cancer?" American journal of human genetics **65**(3): 784-794.

Rogakou, E. P., D. R. Pilch, A. H. Orr, V. S. Ivanova and W. M. Bonner (1998). "DNA double-stranded breaks induce histone H2AX phosphorylation on serine 139." J Biol Chem **273**(10): 5858-5868.

Rosidi, B., M. Wang, W. Wu, A. Sharma, H. Wang and G. Iliakis (2008). "Histone H1 functions as a stimulatory factor in backup pathways of NHEJ." Nucleic acids research **36**(5): 1610-1623.

Rosier, J. F., M. Beauduin, M. Bruniaux, M. De Bast, B. De Coster, M. Octave-Prignot, P. Scalliet and V. Gregoire (1999). "The effect of 2 '-2 ' difluorodeoxycytidine (dFdC, gemcitabine) on radiation-induced cell lethality in two human head and neck squamous

carcinoma cell lines differing in intrinsic radiosensitivity." International Journal of Radiation Biology **75**(2): 245-251.

Ross, G. M. (1999). "Induction of cell death by radiotherapy." Endocr Relat Cancer **6**(1): 41-44.

Roth, D. B. and J. H. Wilson (1986). "Nonhomologous recombination in mammalian cells: role for short sequence homologies in the joining reaction." Molecular and cellular biology **6**(12): 4295-4304.

Rothkamm, K., I. Kruger, L. H. Thompson and M. Lobrich (2003). "Pathways of DNA double-strand break repair during the mammalian cell cycle." Molecular and cellular biology **23**(16): 5706-5715.

Ruis, B. L., K. R. Fattah and E. A. Hendrickson (2008). "The catalytic subunit of DNA-dependent protein kinase regulates proliferation, telomere length, and genomic stability in human somatic cells." Molecular and cellular biology **28**(20): 6182-6195.

Ruiz, J. F., B. Gomez-Gonzalez and A. Aguilera (2009). "Chromosomal Translocations Caused by Either Pol32-Dependent or Pol32-Independent Triparental Break-Induced Replication." Molecular and Cellular Biology **29**(20): 5441-5454.

Saini, N., S. Ramakrishnan, R. Elango, S. Ayyar, Y. Zhang, A. Deem, G. Ira, J. E. Haber, K. S. Lobachev and A. Malkova (2013). "Migrating bubble during break-induced replication drives conservative DNA synthesis." Nature **502**(7471): 389-+.

Salic, A. and T. J. Mitchison (2008). "A chemical method for fast and sensitive detection of DNA synthesis in vivo." Proceedings of the National Academy of Sciences of the United States of America **105**(7): 2415-2420.

San Filippo, J., P. Sung and H. Klein (2008). "Mechanism of eukaryotic homologous recombination." Annu Rev Biochem **77**: 229-257.

Santi, D. V. and L. W. Hardy (1987). "Catalytic mechanism and inhibition of tRNA (uracil-5-)methyltransferase: evidence for covalent catalysis." Biochemistry **26**(26): 8599-8606.

Sasaki, M. S., A. Tachibana and S. Takeda (2013). "Cancer risk at low doses of ionizing radiation: artificial neural networks inference from atomic bomb survivors." J Radiat Res.

Schipler, A. (2013). "Homing endonuclease-based model systems for the study of DNA double strand break induced cell signaling and repair." Inaugural-Dissertation zur Erlangung des Doktorgrades Dr. rer. nat.: Fakultät für Biologie an der Universität Duisburg-Essen.

Schipler, A. and G. Iliakis (2013). "DNA double-strand-break complexity levels and their possible contributions to the probability for error-prone processing and repair pathway choice." Nucleic acids research.

Schultz, L. B., N. H. Chehab, A. Malikzay and T. D. Halazonetis (2000). "p53 Binding protein 1 (53BP1) is an early participant in the cellular response to DNA double-strand breaks." Journal of Cell Biology **151**(7): 1381-1390.

Schwartz, R. A., C. T. Carson, C. Schuberth and M. D. Weitzman (2009). "Adeno-Associated Virus Replication Induces a DNA Damage Response Coordinated by DNA-Dependent Protein Kinase." Journal of Virology **83**(12): 6269-6278.

Seiwert, T. Y., J. K. Salama and E. E. Vokes (2007). "The concurrent chemoradiation paradigm--general principles." Nature clinical practice. Oncology **4**(2): 86-100.

Shaheen, F. S., P. Znojek, A. Fisher, M. Webster, R. Plummer, L. Gaughan, G. C. Smith, H. Y. Leung, N. J. Curtin and C. N. Robson (2011). "Targeting the DNA double strand break repair machinery in prostate cancer." PLoS One **6**(5): e20311.

Sharma, S., J. K. Hicks, C. L. Chute, J. R. Brennan, J. Y. Ahn, T. W. Glover and C. E. Canman (2012). "REV1 and polymerase zeta facilitate homologous recombination repair." Nucleic Acids Res **40**(2): 682-691.

Shewach, D. S., T. M. Hahn, E. Chang, L. W. Hertel and T. S. Lawrence (1994). "Metabolism of 2',2'-difluoro-2'-deoxycytidine and radiation sensitization of human colon carcinoma cells." Cancer Res **54**(12): 3218-3223.

Shewach DS, L. T. (2006). Nucleoside radiosensitizers
Deoxynucleoside Analogs in Cancer Therapy. . P. GJ. Totowa, NJ, Humana Press**:** pp 289-329

Shewach, D. S. and W. Plunkett (1979). "Effect of 2'-Deoxycoformycin on the Biologic Half-Life of 9-Beta-D-Arabinofuranosyladenine 5'-Triphosphate in Cho Cells." Biochemical Pharmacology **28**(15): 2401-2404.

Short, S. C., S. Giampieri, M. Worku, M. Alcaide-German, G. Sioftanos, S. Bourne, K. I. Lio, M. Shaked-Rabi and C. Martindale (2011). "Rad51 inhibition is an effective means of targeting DNA repair in glioma models and CD133+tumor-derived cells." Neuro-Oncology **13**(5): 487-499.

Shrivastav, M., L. P. De Haro and J. A. Nickoloff (2008). "Regulation of DNA double-strand break repair pathway choice." Cell Research **18**(1): 134-147.

Siegel, R., C. DeSantis, K. Virgo, K. Stein, A. Mariotto, T. Smith, D. Cooper, T. Gansler, C. Lerro, S. Fedewa, C. Lin, C. Leach, R. S. Cannady, H. Cho, S. Scoppa, M. Hachey, R. Kirch, A. Jemal and E. Ward (2012). "Cancer treatment and survivorship statistics, 2012." CA: a cancer journal for clinicians **62**(4): 220-241.

Siglin, J., C. E. Champ, Y. Vakhnenko, P. R. Anne and N. L. Simone (2012). "Radiation therapy for locally recurrent breast cancer." Int J Breast Cancer **2012**: 571946.

Simsek, D., E. Brunet, S. Y. Wong, S. Katyal, Y. Gao, P. J. McKinnon, J. Lou, L. Zhang, J. Li, E. J. Rebar, P. D. Gregory, M. C. Holmes and M. Jasin (2011). "DNA ligase III promotes alternative nonhomologous end-joining during chromosomal translocation formation." PLoS genetics **7**(6): e1002080.

Simsek, D. and M. Jasin (2010). "Alternative end-joining is suppressed by the canonical NHEJ component Xrcc4-ligase IV during chromosomal translocation formation." Nature structural & molecular biology **17**(4): 410-416.

Singh, S. K., T. Bednar, L. H. Zhang, W. Q. Wu, E. Mladenov and G. Iliakis (2012). "Inhibition of B-NHEJ in Plateau-Phase Cells Is Not a Direct Consequence of Suppressed Growth Factor Signaling." International Journal of Radiation Oncology Biology Physics **84**(2): E237-E243.

Singh, S. K., A. Bencsik-Theilen, E. Mladenov, B. Jakob, G. Taucher-Scholz and G. Iliakis (2013). "Reduced contribution of thermally labile sugar lesions to DNA double strand break formation after exposure to heavy ions." Radiat Oncol **8**: 77.

Singh, S. K., W. Wu, L. Zhang, H. Klammer, M. Wang and G. Iliakis (2011). "Widespread dependence of backup NHEJ on growth state: ramifications for the use of DNA-PK inhibitors." International journal of radiation oncology, biology, physics **79**(2): 540-548.

Singh, S. K., W. Z. Wu, W. Q. Wu, M. L. Wang and G. Iliakis (2009). "Extensive Repair of DNA Double-Strand Breaks in Cells Deficient in the DNA-PK-Dependent Pathway of NHEJ after Exclusion of Heat-Labile Sites." Radiation Research **172**(2): 152-164.

Smith, C. E., B. Llorente and L. S. Symington (2007). "Template switching during break-induced replication." Nature **447**(7140): 102-105.

Solier, S. and Y. Pommier (2009). "The apoptotic ring A novel entity with phosphorylated histones H2AX and H2B and activated DNA damage response kinases." Cell Cycle **8**(12): 1853-1859.

Sonoda, E., H. Hochegger, A. Saberi, Y. Taniguchi and S. Takeda (2006). "Differential usage of non-homologous end-joining and homologous recombination in double strand break repair." DNA Repair **5**(9-10): 1021-1029.

Sonoda, E., M. S. Sasaki, J. M. Buerstedde, O. Bezzubova, A. Shinohara, H. Ogawa, M. Takata, Y. Yamaguchi-Iwai and S. Takeda (1998). "Rad51-deficient vertebrate cells accumulate chromosomal breaks prior to cell death." Embo Journal **17**(2): 598-608.

Soulas-Sprauel, P., G. Le Guyader, P. Rivera-Munoz, V. Abramowski, C. Olivier-Martin, C. Goujet-Zalc, P. Charneau and J. P. de Villartay (2007). "Role for DNA repair factor XRCC4 in immunoglobulin class switch recombination." The Journal of experimental medicine **204**(7): 1717-1727.

Spycher, C., E. S. Miller, K. Townsend, L. Pavic, N. A. Morrice, P. Janscak, G. S. Stewart and M. Stucki (2008). "Constitutive phosphorylation of MDC1 physically links the MRE11-RAD50-NBS1 complex to damaged chromatin." J Cell Biol **181**(2): 227-240.

Stamato, T. D., A. Dipatri and A. Giaccia (1988). "Cell-cycle-dependent repair of potentially lethal damage in the XR-1 gamma-ray-sensitive Chinese hamster ovary cell." Radiat Res **115**(2): 325-333.

Stark, J. M., P. Hu, A. J. Pierce, M. E. Moynahan, N. Ellis and M. Jasin (2002). "ATP hydrolysis by mammalian RAD51 has a key role during homology-directed DNA repair." Journal of Biological Chemistry **277**(23): 20185-20194.

Stark, J. M., A. J. Pierce, J. Oh, A. Pastink and M. Jasin (2004). "Genetic steps of mammalian homologous repair with distinct mutagenic consequences." Molecular and cellular biology **24**(21): 9305-9316.

Steel, G. G., T. J. McMillan and J. H. Peacock (1989). "The 5Rs of radiobiology." International journal of radiation biology **56**(6): 1045-1048.

Stewart, G. S., S. Panier, K. Townsend, A. K. Al-Hakim, N. K. Kolas, E. S. Miller, S. Nakada, J. Ylanko, S. Olivarius, M. Mendez, C. Oldreive, J. Wildenhain, A. Tagliaferro, L. Pelletier, N. Taubenheim, A. Durandy, P. J. Byrd, T. Stankovic, A. M. Taylor and D. Durocher (2009). "The RIDDLE syndrome protein mediates a ubiquitin-dependent signaling cascade at sites of DNA damage." Cell **136**(3): 420-434.

Stewart, G. S., T. Stankovic, P. J. Byrd, T. Wechsler, E. S. Miller, A. Huissoon, M. T. Drayson, S. C. West, S. J. Elledge and A. M. Taylor (2007). "RIDDLE immunodeficiency syndrome is linked to defects in 53BP1-mediated DNA damage signaling." Proc Natl Acad Sci U S A **104**(43): 16910-16915.

Stiff, T., M. O'Driscoll, N. Rief, K. Iwabuchi, M. Lobrich and P. A. Jeggo (2004). "ATM and DNA-PK function redundantly to phosphorylate H2AX after exposure to ionizing radiation." Cancer Res **64**(7): 2390-2396.

Stucki, M., J. A. Clapperton, D. Mohammad, M. B. Yaffe, S. J. Smerdon and S. P. Jackson (2005). "MDC1 directly binds phosphorylated histone H2AX to regulate cellular responses to DNA double-strand breaks." Cell **123**(7): 1213-1226.

Sugawara, N. and J. E. Haber (1992). "Characterization of double-strand break-induced recombination: homology requirements and single-stranded DNA formation." Molecular and cellular biology **12**(2): 563-575.

Symington, L. S. (2002). "Role of RAD52 epistasis group genes in homologous recombination and double-strand break repair." Microbiology and molecular biology reviews : MMBR **66**(4): 630-670, table of contents.

Symington, L. S. and J. Gautier (2011). "Double-strand break end resection and repair pathway choice." Annual review of genetics **45**: 247-271.

Szafraniec, S. I., K. J. Stachnik and J. S. Skierski (2004). "New nucleoside analogs in the treatment of solid tumors." Acta Pol Pharm **61**(4): 297-305.

Takagi, M., K.-i. Sakata, M. Someya, H. Tauchi, K. Iijima, Y. Matsumoto, T. Torigoe, A. Takahashi, M. Hareyama and M. Fukushima (2010). "Gimeracil sensitizes cells to radiation via inhibition of homologous recombination." Radiotherapy and Oncology **96**(2): 259-266.

Talasz, H., W. Helliger, B. Sarg, P. L. Debbage, B. Puschendorf and H. Lindner (2002). "Hyperphosphorylation of histone H2A.X and dephosphorylation of histone H1 subtypes in the course of apoptosis." Cell Death and Differentiation **9**(1): 27-39.

Tamulevicius, P., M. Wang and G. Iliakis (2007). "Homology-directed repair is required for the development of radioresistance during S phase: interplay between double-strand break repair and checkpoint response." Radiat Res **167**(1): 1-11.

Tanaka, H., H. Arakawa, T. Yamaguchi, K. Shiraishi, S. Fukuda, K. Matsui, Y. Takei and Y. Nakamura (2000). "A ribonucleotide reductase gene involved in a p53-dependent cell-cycle checkpoint for DNA damage." Nature **404**(6773): 42-49.

Tanaka, Y., K. Akagi, K. Sokawa and T. Sugahara (1984). "Pld Repair Inhibitors as Radiosensitizer and Clinical-Trials." International Journal of Radiation Oncology Biology Physics **10**(9): 1803-1803.

Thariat, J., J. M. Hannoun-Levi, A. Sun Myint, T. Vuong and J. P. Gerard (2013). "Past, present, and future of radiotherapy for the benefit of patients." Nat Rev Clin Oncol **10**(1): 52-60.

Tomimatsu, N., B. Mukherjee and S. Burma (2009). "Distinct roles of ATR and DNA-PKcs in triggering DNA damage responses in ATM-deficient cells." EMBO Rep **10**(6): 629-635.

Trovesi, C., M. Falcettoni, G. Lucchini, M. Clerici and M. P. Longhese (2011). "Distinct Cdk1 requirements during single-strand annealing, noncrossover, and crossover recombination." PLoS genetics **7**(8): e1002263.

Tu, W. Z., B. Li, B. Huang, Y. Wang, X. D. Liu, H. Guan, S. M. Zhang, Y. Tang, W. Q. Rang and P. K. Zhou (2013). "gammaH2AX foci formation in the absence of DNA damage: mitotic H2AX phosphorylation is mediated by the DNA-PKcs/CHK2 pathway." FEBS Lett **587**(21): 3437-3443.

Tucker, S. L. and H. D. Thames, Jr. (1989). "The effect of patient-to-patient variability on the accuracy of predictive assays of tumor response to radiotherapy: a theoretical evaluation." International journal of radiation oncology, biology, physics **17**(1): 145-157.

Tutt, A., D. Bertwistle, J. Valentine, A. Gabriel, S. Swift, G. Ross, C. Griffin, J. Thacker and A. Ashworth (2001). "Mutation in Brca2 stimulates error-prone homology-directed repair of DNA double-strand breaks occurring between repeated sequences." The EMBO journal **20**(17): 4704-4716.

Tzung, T.-Y. and T. M. Rünger (1998). "Reduced joining of DNA double strand breaks with an abnormal mutation spectrum in rodent mutants of DNA-PKcs and Ku80." International Journal of Radiation Biology **73**: 469-474.

Uziel, T., Y. Lerenthal, L. Moyal, Y. Andegeko, L. Mittelman and Y. Shiloh (2003). "Requirement of the MRN complex for ATM activation by DNA damage." EMBO J **22**(20): 5612-5621.

Vallerga, A. K., D. A. Zarling and T. J. Kinsella (2004). "New radiosensitizing regimens, drugs, prodrugs, and candidates." Clin Adv Hematol Oncol **2**(12): 793-805.

Vanhaperen, V. W. T. R., G. Veerman, J. B. Vermorken and G. J. Peters (1993). "2',2'-Difluoro-Deoxycytidine (Gemcitabine) Incorporation into Rna and DNA of Tumor-Cell Lines." Biochemical Pharmacology **46**(4): 762-766.

Verkaik, N. S., R. E. Esveldt-van Lange, D. van Heemst, H. T. Bruggenwirth, J. H. Hoeijmakers, M. Z. Zdzienicka and D. C. van Gent (2002). "Different types of V(D)J recombination and end-joining defects in DNA double-strand break repair mutant mammalian cells." European journal of immunology **32**(3): 701-709.

Virsik, R. P. and D. Harder (1980). "Numerical Relationship between Cells with Radiation-Induced Chromosome-Aberrations and Cells Lethally Injured by Radiation." Radiation and Environmental Biophysics **18**(1): 73-77.

Waltes, R., R. Kalb, M. Gatei, A. W. Kijas, M. Stumm, A. Sobeck, B. Wieland, R. Varon, Y. Lerenthal, M. F. Lavin, D. Schindler and T. Dork (2009). "Human RAD50 deficiency in a Nijmegen breakage syndrome-like disorder." American journal of human genetics **84**(5): 605-616.

Wang, C. R., A. Hu and Q. B. Lu (2006a). "Direct observation of the transition state of ultrafast electron transfer reaction of a radiosensitizing drug bromodeoxyuridine." J Chem Phys **124**(24): 241102.

Wang, H., W. Boecker, H. Wang, X. Wang, J. Guan, L. H. Thompson, J. A. Nickoloff and G. Iliakis (2004a). "Caffeine inhibits homology-directed repair of I-SceI-induced DNA double-strand breaks." Oncogene **23**(3): 824-834.

Wang, H., B. Hu, R. Liu and Y. Wang (2005a). "CHK1 affecting cell radiosensitivity is independent of non-homologous end joining." Cell cycle **4**(2): 300-303.

Wang, H., A. R. Perrault, Y. Takeda, W. Qin and G. Iliakis (2003a). "Biochemical evidence for Ku-independent backup pathways of NHEJ." Nucleic acids research **31**(18): 5377-5388.

Wang, H., S. N. Powell, G. Iliakis and Y. Wang (2004b). "ATR affecting cell radiosensitivity is dependent on homologous recombination repair but independent of nonhomologous end joining." Cancer research **64**(19): 7139-7143.

Wang, H., B. Rosidi, R. Perrault, M. Wang, L. Zhang, F. Windhofer and G. Iliakis (2005b). "DNA ligase III as a candidate component of backup pathways of nonhomologous end joining." Cancer research **65**(10): 4020-4030.

Wang, H., X. Wang, G. Iliakis and Y. Wang (2003b). "Caffeine could not efficiently sensitize homologous recombination repair-deficient cells to ionizing radiation-induced killing." Radiat Res **159**(3): 420-425.

Wang, H., Z. C. Zeng, T. A. Bui, E. Sonoda, M. Takata, S. Takeda and G. Iliakis (2001a). "Efficient rejoining of radiation-induced DNA double-strand breaks in vertebrate cells deficient in genes of the RAD52 epistasis group." Oncogene **20**(18): 2212-2224.

Wang, H., Z. C. Zeng, A. R. Perrault, X. Cheng, W. Qin and G. Iliakis (2001b). "Genetic evidence for the involvement of DNA ligase IV in the DNA-PK-dependent pathway of non-homologous end joining in mammalian cells." Nucleic acids research **29**(8): 1653-1660.

Wang, H. Y., M. L. Wang, H. C. Wang, W. Bocker and G. Iliakis (2005c). "Complex H2AX phosphorylation patterns by multiple kinases including ATM and DNA-PK in human cells exposed to ionizing radiation and treated with kinase inhibitors." Journal of Cellular Physiology **202**(2): 492-502.

Wang, M., W. Wu, B. Rosidi, L. Zhang, H. Wang and G. Iliakis (2006b). "PARP-1 and Ku compete for repair of DNA double strand breaks by distinct NHEJ pathways." Nucleic acids research **34**(21): 6170-6182.

Wang, X., G. Ira, J. A. Tercero, A. M. Holmes, J. F. X. Diffley and J. E. Haber (2004c). "Role of DNA replication proteins in double-strand break-induced recombination in Saccharomyces cerevisiae." Molecular and Cellular Biology **24**(16): 6891-6899.

Ward, I. M., K. Minn and J. J. Chen (2004). "UV-induced ataxia-telangiectasia-mutated and Rad3-related (ATR) activation requires replication stress." Journal of Biological Chemistry **279**(11): 9677-9680.

Weinstock, D. M., B. Elliott and M. Jasin (2006). "A model of oncogenic rearrangements: differences between chromosomal translocation mechanisms and simple double-strand break repair." Blood **107**(2): 777-780.

West, C. M. and G. C. Barnett (2011). "Genetics and genomics of radiotherapy toxicity: towards prediction." Genome medicine **3**(8): 52.

Weterings, E. and D. J. Chen (2008). "The endless tale of non-homologous end-joining." Cell Research **18**(1): 114-124.

White, E. L., S. C. Shaddix, R. W. Brockman and L. L. Bennett, Jr. (1982). "Comparison of the actions of 9-beta-D-arabinofuranosyl-2-fluoroadenine and 9-beta-D-arabinofuranosyladenine on target enzymes from mouse tumor cells." Cancer research **42**(6): 2260-2264.

Williams, R. S., G. Moncalian, J. S. Williams, Y. Yamada, O. Limbo, D. S. Shin, L. M. Groocock, D. Cahill, C. Hitomi, G. Guenther, D. Moiani, J. P. Carney, P. Russell and J. A. Tainer (2008). "Mre11 dimers coordinate DNA end bridging and nuclease processing in double-strand-break repair." Cell **135**(1): 97-109.

Windhofer, F., W. Wu, M. Wang, S. K. Singh, J. Saha, B. Rosidi and G. Iliakis (2007). "Marked dependence on growth state of backup pathways of NHEJ." International journal of radiation oncology, biology, physics **68**(5): 1462-1470.

Withers, H., editor (1975). Advances in radiation biology. The four R´s of radiotherapy. New York, Academic Press.

Wray, J., E. A. Williamson, S. B. Singh, Y. Wu, C. R. Cogle, D. M. Weinstock, Y. Zhang, S. H. Lee, D. Zhou, L. Shao, M. Hauer-Jensen, R. Pathak, V. Klimek, J. A. Nickoloff and R. Hromas (2013). "PARP1 is required for chromosomal translocations." Blood **121**(21): 4359-4365.

Wu, W., M. Wang, T. Mussfeldt and G. Iliakis (2008a). "Enhanced use of backup pathways of NHEJ in G2 in Chinese hamster mutant cells with defects in the classical pathway of NHEJ." Radiation research **170**(4): 512-520.

Wu, W., M. Wang, S. K. Singh, T. Mussfeldt and G. Iliakis (2008b). "Repair of radiation induced DNA double strand breaks by backup NHEJ is enhanced in G2." DNA repair **7**(2): 329-338.

Xie, A., A. Kwok and R. Scully (2009). "Role of mammalian Mre11 in classical and alternative nonhomologous end joining." Nature structural & molecular biology **16**(8): 814-818.

Yan, C. T., C. Boboila, E. K. Souza, S. Franco, T. R. Hickernell, M. Murphy, S. Gumaste, M. Geyer, A. A. Zarrin, J. P. Manis, K. Rajewsky and F. W. Alt (2007). "IgH class switching and translocations use a robust non-classical end-joining pathway." Nature **449**(7161): 478-482.

Yang, H. J., Q. B. Li, J. Fan, W. K. Holloman and N. P. Pavletich (2005). "The BRCA2 homologue Brh2 nucleates RAD51 filament formation at a dsDNA-ssDNA junction." Nature **433**(7026): 653-657.

Yang, S. W., P. Huang, W. Plunkett, F. F. Becker and J. Y. Chan (1992). "Dual mode of inhibition of purified DNA ligase I from human cells by 9-beta-D-arabinofuranosyl-2-fluoroadenine triphosphate." J Biol Chem **267**(4): 2345-2349.

Yoshihisa Matsumoto, S. I., Mikoto Fukuchi, Sicheng Liu,, S. K. Wanotayan Rujira, Kazuki Yoshida, Yasuhiro Mae and a. M. K. Sharma (2013). Radiosensitization Strategies Through Modification of DNA Double-Strand Break Repair.

Yu, X. and J. Chen (2004). "DNA Damage-Induced Cell Cycle Checkpoint Control Requires CtIP, a Phosphorylation-Dependent Binding Partner of BRCA1 C-Terminal Domains." Molecular and cellular biology **24**(21): 9478-9486.

Yun, M. H. and K. Hiom (2009). "CtIP-BRCA1 modulates the choice of DNA double-strand-break repair pathway throughout the cell cycle." Nature **459**(7245): 460-U184.

Zhang, Y. and M. Jasin (2011). "An essential role for CtIP in chromosomal translocation formation through an alternative end-joining pathway." Nature structural & molecular biology **18**(1): 80-84.

Zimbrick, J. D., J. F. Ward and L. S. Myers, Jr. (1969). "Studies on the chemical basis of cellular radiosensitization by 5-bromouracil substitution in DNA. II. Pulse- and steadystate radiolysis of bromouracil-substituted and unsubstituted DNA." Int J Radiat Biol Relat Stud Phys Chem Med **16**(6): 525-534.

8 Appendix

8.1 Part A: Supplementary data

8.1.1 Effect of earlier start of ara-A treatment in DRaa40 cells

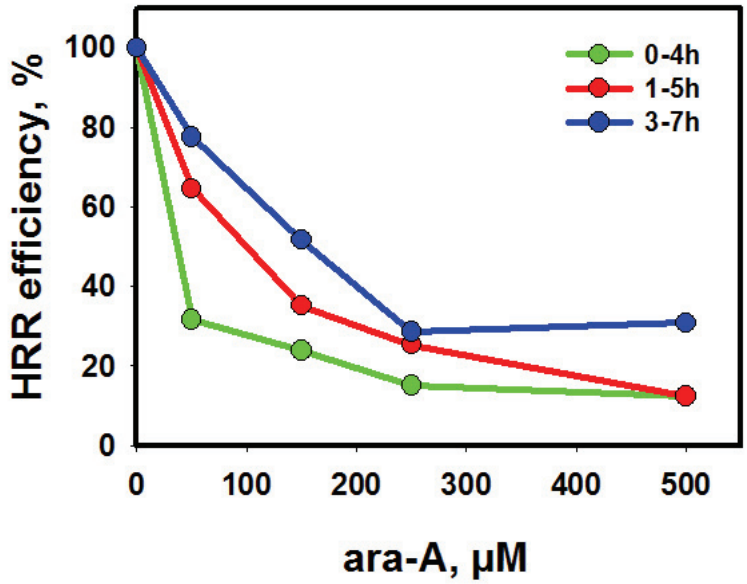

Figure 35 Effect of earlier start of ara-A treatment in DRaa40 cells Effect of a shift of the 4h treatment window to earlier times. Cells were treated with different concentrations of ara-A for 4h. Green circles and line represent treatment for 4h beginning immediately after transfection. Red circles and line represent treatment starting 1h after transfection and blue circles and line represent treatment starting 3h after transfection. Graph shows data from one experiment.The strong correlation between HRR suppression and the onset of ara-A treatment shown in Figure 18 prompted us to inquire whether an earlier ara-A treatment start would influence the outcome of the experiments. We found that treatment of cells with ara-A immediately after transfection, including a medium change after 4h, resulted in 70% inhibition already at 50 µM (Figure 35). This effect was equivalent to the maximum effect that was obtained at 500 µM when ara-A was given 3-7h after transfection (Figure 18 and Figure 35). Using the immediate treatment protocol, 88% inhibition was observed at 500 µM ara-A (Figure 35). When ara-A treatment was initiated 1h after transfection, inhibition was also stronger than in 3-7h hour treatments, but allowed for a larger effect-range of approximately 53% (Figure 35). The results obtained with delayed treatment start as opposed to the immediate

treatment start, clearly indicated a strong concentration dependence of the effect, which we wanted to follow-up. Furthermore, results from another line of investigation showed that ara-A reduced the transfection efficiency when added immediately after transfection. Also we could not rule out direct toxicity of immediate drug treatment after electroporation stress. These complications and the interpretation difficulties they generated made us decide to use the delayed treatment schedules in further experiments, but initiate treatment 1.5h after transfection.

8.1.2 Inherent problems with the interpretation of data obtained at later times in I-SceI inducible reporter systems

8.1.2.1 Analysis of GFP signal after 24h or 48h in U2OS 282C cells (DR-GFP) treated with ara-A

As laid out in the discussion (5.3.3) it is a characteristic of I-SceI reporter assays, that DSB are induced over a long time span that may last several days (Schipler, 2013). With regard to short term drug treatment this can create complications when it is attempted to collect data at later times, e.g. 48h or 72h after transfection of the I-SceI plasmid. At this time most drugs will have been fully metabolized. Ara-A which is rapidly inactivated by deamination through ADA has an intracellular half-life of 1.5h-2h (Shewach and Plunkett, 1979; Cass, 1983), meaning that 18h after the end of treatment the cell has been qualitatively cleared of ara-A. Repair of DSB that are induced by cutting at this time will not any longer underlie any potential inhibitory or beneficial effects of the drug, which will likely have waned already earlier due to declining concentrations. The situation is further complicated by the fact that 18h after the end of ara-A treatment, a dramatic redistribution in the cell cycle can be observed with about 70-80% of cells accumulating in the S-phase (Figure 36). That means a massive concentration of cells in a phase of the cell cycle where HRR may occur as opposed to the normal situation in an exponentially growing culture, where 40% of cells or more are in the G1 phase and cannot perform HRR. This creates conditions in which the likelihood for HRR is

increased, but inhibition by the drug is no longer present. At the same time, DSB continue to be induced by I-SceI (Schipler, 2013). As the appearance of fluorescence after a signal generating event requires several hours to develop, this leads to an increase of the portion of GFP positive cells in ara-A treated cells that can be detected when cells are measured 48h or later after transfection of the I-SceI plasmid (i.e. ~42h after the end of ara-A treatment). This translates into an ostensible recovery of HRR efficiency that can be calculated at 48h. However, this increase does not represent a characteristic of the interaction of ara-A with HRR, but is a consequence of the continuous induction of DSB by I-SceI, rapid deactivation of ara-A and reassortment of cells in the cycle.

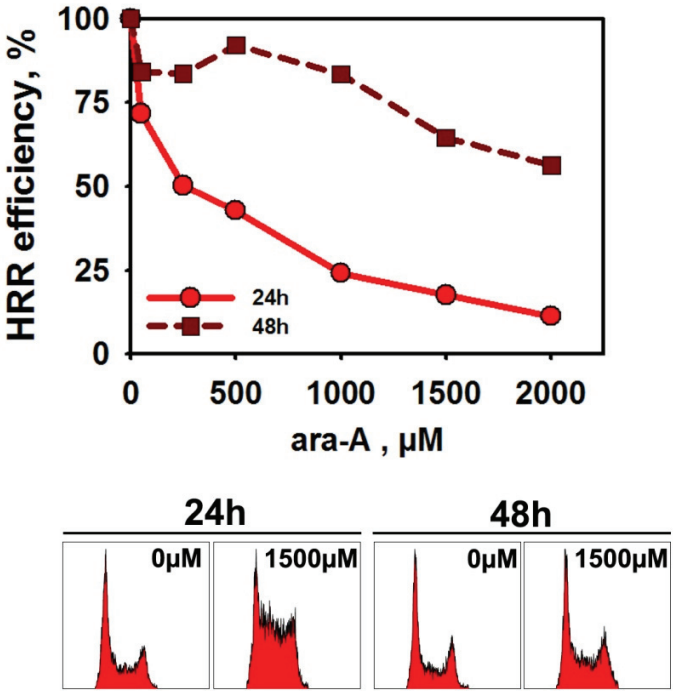

Figure 36 Continuous damage induction and shifts in cell cycle distribution lead to deceptive signal generation in late measurements in I-SceI reporter assays. Upper panel: Calculated HRR efficiency. A pool of cells was transfected and distributed in several dishes that were treated accordingly. One dish from each concentration was analyzed at the indicated time point. Light red circles and solid line, 24h after transfection. Dark red squares and dashed line, 48h after transfection. Data from one experiment is shown. Lower panel: PI Histograms for U2OS 282C cells 24h and 48h after transfection of the I-SceI plasmid. Ara-A treated cells are highly enriched in S-phase cells at 24h. At 48h Cell cycle distribution of treated cells is almost back to normal.

8.1.2.2 Development of fluorescence signals over time in EJ-DR cells (EJ-RFP & DR-GFP)

The EJ-DR cell line was generated by introduction of the EJ-RFP into a U2OS cell line that also already harbored a DR-GFP insertion. The DsRed signal originating from the EJ-RFP system started to appear only 3 days after transfection and still showed strong increase up to 96h (Figure 37 A&B). Due to the kinetics of signal development of the EJ-RFP system, the information provided by which was our primary interest in this series of experiments, measurements had to be taken 4 days after transfection. For the signal originating from the DR-GFP construct this meant that it was subjected to the same problematic described for U2OS 282C cells above (8.1.2.1). Consequently, measurements taken 96h after I-SceI transfection (i.e. ~90h after the end of ara-A treatment) showed only little effect of ara-A on the proportion of GFP positive cells in the EJ-DR system. To confirm that inhibition of HRR takes place in EJ-DR cells, we performed a time course experiment. We transfected EJ-DR cells with I-SceI and treated them for 4h with 1000 µM ara-A. Cells were split on 4 different dishes and analyzed at 24h, 48h, 72h and 96h after transfection to measure the proportion of cells positive for GFP. We observed strong suppression in the development of a GFP signal up to 48h after transfection (Figure 37 C). This confirmed that ara-A had an inhibitory effect on the HRR mediated repair in the DR-GFP construct in the EJ-DR cells as well. As expected and in agreement with the findings for U2OS 282C cells, at later times GFP positive cells started to appear in the population, as a consequence of continuous induction of DSB by I-SceI and metabolic inactivation of ara-A.

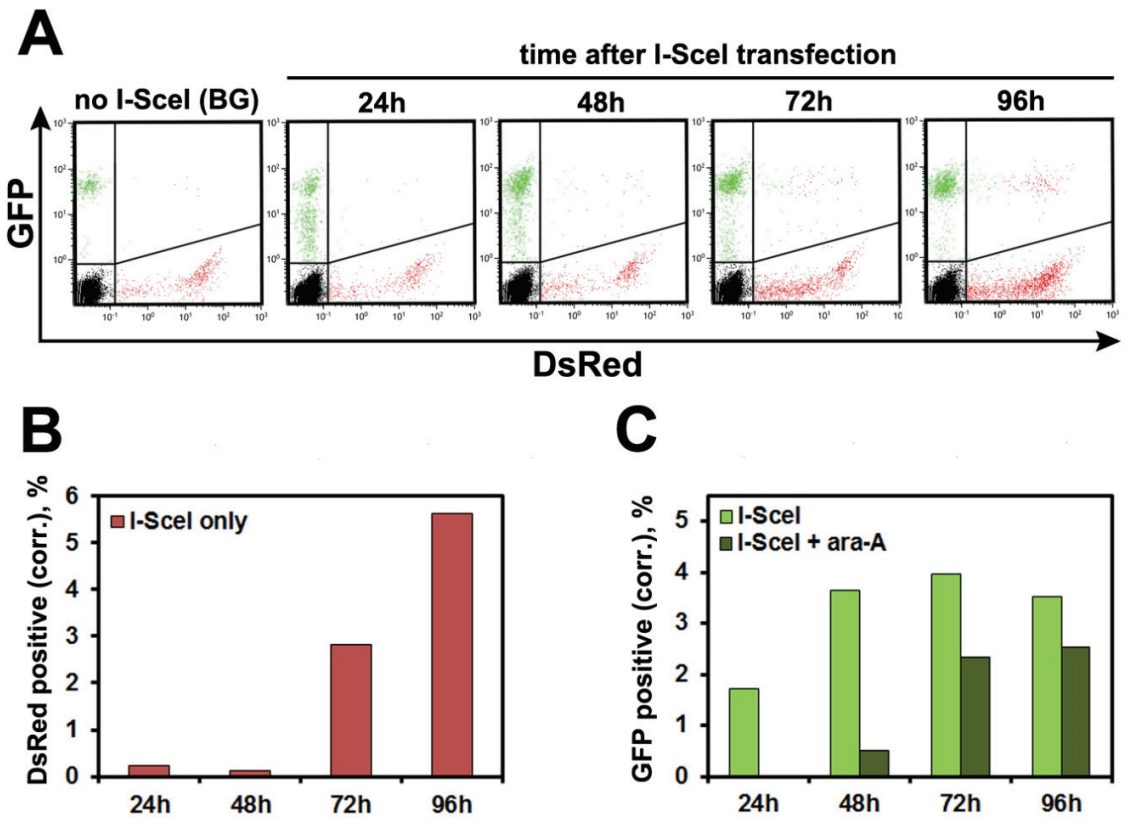

Figure 37 Kinetics of reporter gene expression in EJ-DR cells. A) Development of the signals from the DR-GFP construct (GFP) and the EJ-RFP system (DsRed) over time within a population of EJ-DR cells transfected with I-SceI (no ara-A treatment). Significant increase of DsRed positive cells above the background occurs only 72h after transfection. The GFP signal begins to develop already 24h after transfection and has almost reached maximum after 48h already. **B)** Graphical depiction of the DsRed Data shown in (A). Measured values were corrected by the background (BG) of untransfected cells. **C)** Graphical depiction of the GFP Data shown in (A) (light green bars) together with data for the development of GFP expression in cells treated with 1000µM ara-A (dark green bars) collected in the same experiment. Measured values were corrected by the background (BG) of untransfected cells. Cells that were treated with 1000 µM ara-A for 4h show almost complete inhibition of HRR at 24h and 48h, but a robust signal starts to appear after 72h.

8.1.3 Effects of Nu7441 on DSB repair

8.1.3.1 Effect of Nu7441 on kinetics of DSB repair in A549 cells measured by PFGE

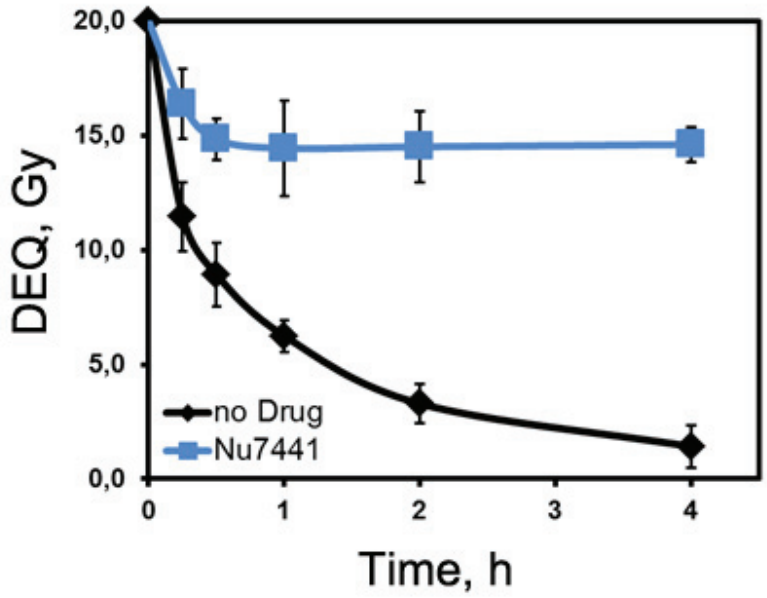

Figure 38 A549 exponentially growing with or without 5 µM Nu7441. PFGE data from an experiment performed with exponentially growing A549 cells irradiated with 20Gy X-rays. Incubation with 5µM of the DNA-PKcs inhibitor Nu7441 induces a strong DSB repair defect in D-NHEJ proficient cells.

8.1.3.2 Effects of different treatment durations with Nu7441 on distal end-joining

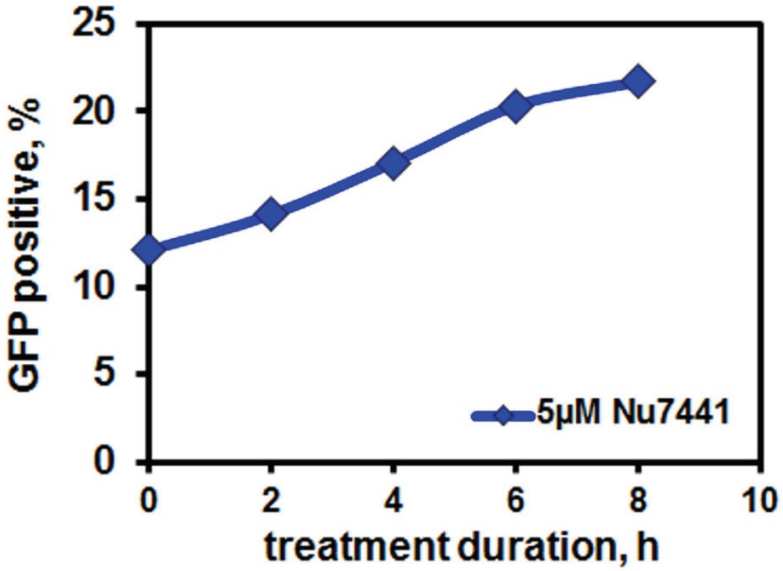

Figure 39 Treatment of U2OS 280A (EJ5-GFP) with 5µM Nu7441 for different length of time. U2OS 280A cells were transfected with an I-SceI expression plasmid and treated with 5µM Nu7441 for different length of time before the drug was washed away. The portion of GFP positive cells increases with time indicating increased usage of distal ends for re-joining. After 6h a plateau is reached.

8.1.4 Enhancement of B-NHEJ by ara-A does not confer radioresistance

It was reasonable to assume that the improvement of DSB rejoining upon treatment with ara-A we observed in serum deprived Lig4$^{-/-}$ MEFs may allow cells to repair PLD, which would result in increased cell survival after irradiation. Therefore we inquired whether the enhancement of B-NHEJ was accompanied by an increase in radioresistance. To address this question we performed delayed plating survival experiments with serum deprived MEF Lig4$^{-/-}$ cells. We followed the serum deprivation protocol as described before. Since these cells are extremely radiosensitive, especially in G1/G0, we only applied up to 2 Gy in steps of 0.5 Gy. Different concentrations of ara-A or solvent were added 15 min before irradiation. Cells were irradiated in the plateau-phase like state and incubated under these conditions in the presence or absence of ara-A for 2h after

irradiation. After 2h, cells were collected and plated as single cell suspensions at appropriate dilutions. Colonies were fixed and stained after 7 days.

We observed no improvement of survival in ara-A treated cells (Figure 40). On the contrary, ara-A treatment further sensitized cells. Plating efficiency values indicated that ara-A treatment had no strong cytotoxic effect on non-cycling MEFs. In fact we noticed, that the PE of cells treated with 25 µM (PE= 55%) was substantially higher than that of untreated cells (PE= 39%). When the ara-A concentration was further increased the PE declined again to 51% at 50 µM and 43% at 125 µM, which was still slightly higher than that for untreated cells.

We concluded that the enhancement of B-NHEJ we had observed in serum deprived MEF Lig4$^{-/-}$ cells after treatment with ara-A had no positive effect on the repair of PLD and thus could not confer radioresistance. On the contrary, it appears to enhance PLD fixation, probably due to misrepair of DSB.

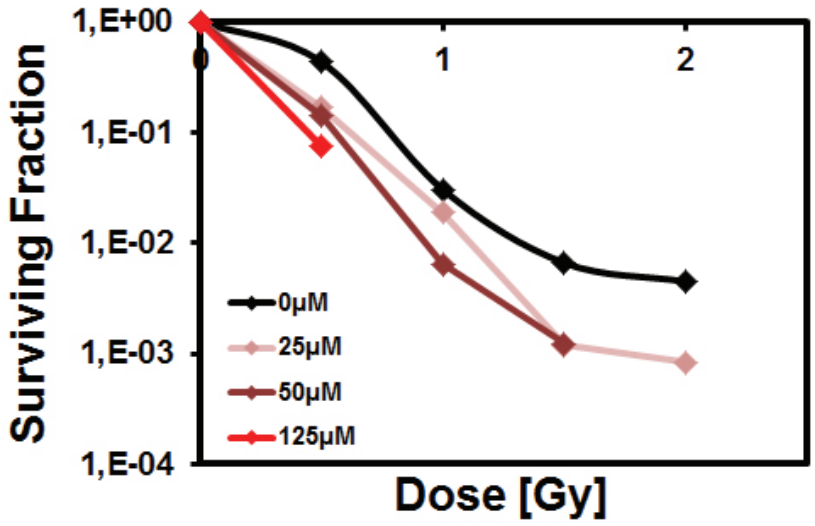

Figure 40 Ara-A does not improve survival in serum deprived MEF Lig4$^{-/-}$ cells Serum deprived Lig4$^{-/-}$ cells were irradiated in the plateau phase and incubated for 2h after irradiation in the presence or absence of ara-A before plating. The means of double determinations from one experiment are shown. Black symbols and curve, no ara-A treatment (PE=0.39). Pink symbols and curve, 25µM ara-A (PE=0.55). Dark red symbols and curve, 50µM ara-A (PE=0.51). Light red symbols and curve, 125 µM ara-A (PE=0.43).

8.1.5 53BP1 bodies in serum deprived MEF Lig4$^{-/-}$

In addition to the observations described under 4.4.6 we noticed that a large portion of MEF Lig4$^{-/-}$ cells contained one large, very bright focus of 53BP1 after 24h of serum deprivation in the absence of any further treatment (Figure 41). These foci always colocalized with γH2AX and were too big and distributed too regularly as it would be expected from background foci. Literature research revealed that such a phenomenon has already been described to arise in G0/G1 cells and has been linked to replication stress and common fragile sites (Harrigan, 2011). Common fragile sites are chromosome areas that show a higher incidence of spontaneous chromosome breakage than the average of genomic sequences. These 53BP1 bodies or domains were hypothesized to form after replication problems in these areas in the subsequent G1 phase to protect common fragile sites against erosion.

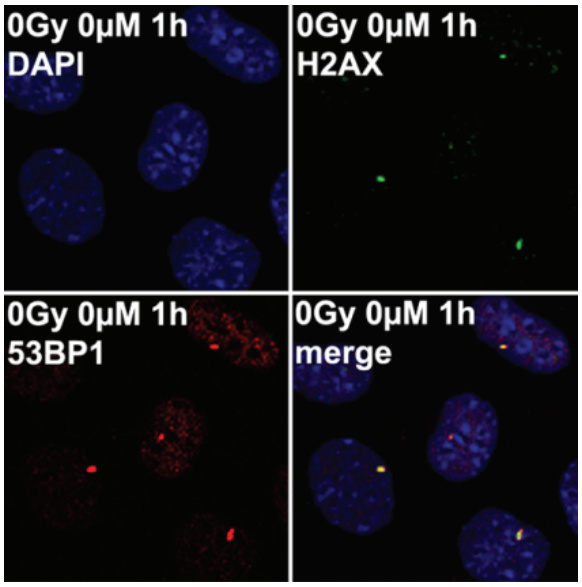

Figure 41 53BP1 bodies in serum deprived MEF Lig4$^{-/-}$ Depiction of 53BP1 nuclear bodies in unirradiated, serum deprived MEF Lig4$^{-/-}$ cells. Blue = DNA; red=53BP1; green=γH2AX; yellow= Colocalization of 53BP1 and γH2AX.

8.1.6 Inhibition of DNA replication by ara-C and gemcitabine

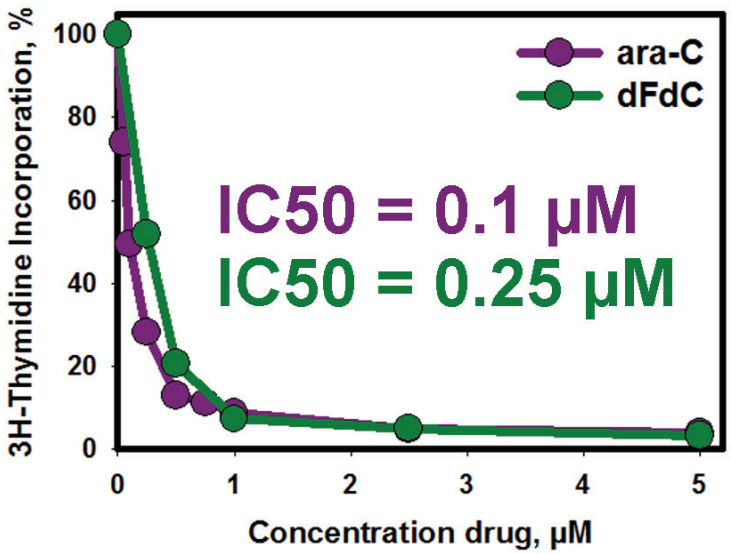

Figure 42 Inhibition of replication by ara-C and gemcitabine. Effects of ara-C (ara-C; violet curve) or gemcitabine (dFdC; green curve) treatment on DNA replication. Data points show the results of one experiment (Data generated by Dr. Maria Papaioannou).

We performed preliminary experiments with ara-C and gemcitabine (dFdC) to evaluate their effectiveness as replication inhibitors. Replication was assayed by incorporation of tritium labeled thymidine (3H-thymidine). Inhibitors were added prior to a 20 min pulse treatment with 3H-thymidine. Subsequently cells were lysed and incorporation of 3H-thymidine was measured in a liquid scintillation counter.

Figure 42 shows the results obtained with the replication inhibitors normalized to controls incubated without drug. The concentration at which 50% of the maximum inhibition of replication was achieved ($IC50_{repl}$) was determined. Gemcitabine and ara-C both inhibited replication very effectively with $IC50_{repl}$ values of 0.25 µM and 0.1 µM, respectively.

8.2 Part B: Supplementary information on NAs

In this section the intracellular metabolism and mechanisms of cytotoxicity and radiosensitization of some NAs that are considered to be of clinical and/or historical importance are described. This overview is intended as a complementary reference for the interested reader.

8.2.1 BrdU and IdU

The first results showing radiosensitization by NAs were reported in the late 1950s, only a few years after it became clear that DNA is the hereditary material and its structure was resolved. They were obtained with the halogenated deoxythymidine analogs 5-bromo-2´-deoxyuridine (BrdU) and 5-iodo-2´-deoxyuridine (IdU) (Djordjevic and Szybalski, 1960). The van-der-Waals-radius of Bromine and Iodine is comparable to the size of a methyl-group, thus BrdU and IdU act mainly as competitors of thymidine in the cell. BrdU and IdU were shown to synergistically enhance radiation induced cell killing when administered before irradiation and radiosensitization correlated with the degree of incorporation into the DNA (Dewey and Humphrey, 1965; Iliakis, 1989a; Lawrence, 1990).

In contrast to most NAs used in chemotherapy, these C-5 halogenated thymidine analogs don´t markedly interfere with replication. Many types of cells can be cultured in the presence of BrdU at micro molar concentrations for prolonged times without significant cytotoxic effects. In this way high rates of substitution for thymidine by BrdU can be achieved in both strands of the DNA. A specific radiochemical mechanism was described as an important factor for the radiosensitization elicited by these halogenated thymidine analogs. It has been shown that the presence of the halogenated pyrimidine bases in DNA during irradiation leads to the generation of uracilyl radicals by radiolysis that can extract hydrogen atoms from the sugar residues of nucleotides (Wang, 2006a). This results in the formation of strand breaks and also increases the yield of DSB per Gy IR (Zimbrick, 1969; Lawrence, 1995; Shewach DS, 2006).

Despite very promising results *in vitro* and some clinical phase I-II studies (Chang, 1989; Goffman, 1991; Levin, 1995) neither BrdU nor IdU ever achieved approval for medical use as radiosensitizers, because the results of phase III clinical trials did not yield satisfactory results (Prados, 1999). The special properties of BrdU and IdU are exploited in diverse labeling strategies for research purposes, e.g. for the detection of S-Phase cells, progression of replication forks, sister chromatid exchanges or DNA resection (Cavanagh, 2011).

8.2.2 5-FU

In contrast, the fluorinated base analog 5-fluorouracil (5-FU) developed into a great clinical success. 5-FU is utilized in the treatment of breast, lung, head and neck cancers and has proven to be particularly effective in colorectal cancers (IMPACT, 1995). Several prodrugs of 5-FU exist to date (e.g. Capecitabine, Floxuridine) that have different pharmacokinetics but share similar or identical mechanisms of action. Upon entry into the cell 5-FU is converted to three major metabolites: fluorodeoxyuridine monophosphate (FdUMP), fluorodeoxyuridine triphosphate (FdUTP) and fluorouridine triphosphate (FUTP) (Longley, 2003). The majority of the cytotoxic effect of 5-FU is usually ascribed to the inhibition of thymidilate synthase (TS) it exerts through FdUMP. Inhibition of TS results in depletion of dTTP pools and consequently leads to disruption of DNA synthesis.

Due to the smaller van-der-Waals radius of the fluorine atom as compared to bromine or iodine, the nucleotides derived from 5-FU have more similarity with uridine than thymidine (Shewach DS, 2006). Consequently FUTP can be incorporated into RNA. This can lead to toxicity through disturbance on several levels, including mRNA polyadenylation, rRNA maturation and posttranscriptional modification of tRNAs (Carrico and Glazer, 1979; Kanamaru, 1986; Santi and Hardy, 1987). Another metabolite of 5-FU, FdUTP, is also misincorporated into DNA, where it can lead to DNA strand break formation (Ingraham, 1986). The enzyme uracil-DNA-glycosylase excises the faulty base, which in the presence of high concentrations of FdUTP leads to futile cycles of

excision and re-incorporation (Longley, 2003). Radiosensitizing effects of 5-FU on transplanted tumors were recognized as early as 1958 (Heidelberger, 1958).

Radiosensitization by 5-FU has been demonstrated *in vitro* for administration before and after irradiation (Bruso, 1990; Buchholz, 1995). For pre-incubation with 5-FU re-distribution in the cell cycle apparently plays a significant role (Davis, 1995). An inhibition of DSB repair has been described as well, that may contribute to the radiosensitization achieved when 5-FU is administered after irradiation (Bruso, 1990). A number of clinical trials have shown a clear benefit in a number or tumors when radiotherapy was combined with 5-FU (Group, 1985; Merlano, 1996; Bartelink, 1997). Consequently concurrent chemoradiotherapy with 5-FU has become the standard of care for several solid tumor entities (Vallerga, 2004).

9 Acknowledgements

I thank the BMBF for funding (Grant: 03NUK005C) as part of the Projektverbund: “Biodosimetrie: Ein systembiologischer Ansatz für die Strahlenbiodosimetrie und der Analyse der individuellen Strahlensensitivität: ATM/ATR Signaltransduktionswege und Strahlenempfindlichkeit in Normal- und Tumor-Zellen”. Many thanks also to the initiative for the preservation of radiation biology expertise in Germany (KVSF) for their commitment to the interests of the german radiobiological community.

I would like to thank my supervisor Prof. Dr. George Iliakis for his trust, support and the many enjoyable and lively scientific discussions. Your ceaseless energy is a great motivation. Thanks also for the introduction to the fascinating realm of radiobiology and for providing such an excellent working environment.

Jenny und Rafi für die Geduld mit der ihr meine fortwährende Abwesenheit ertragen habt und dafür, dass mich das zu Euch nach Hause Kommen immer sofort in gute Laune versetzen kann. Auch wenn die zeitliche Aufteilung es vielleicht nicht immer hat erkennen lassen, Ihr seid für mich das wichtigste auf der Welt.

Thanks to all colleagues in the lab, present and past, who were always very helpful.

Special thanks go to Tamara Mußfeldt for her help in cell sorting and the long days spent together at the Altra.

Many thanks to Emil Mladenov for his expertise in everything, and here in particular for Western Blotting. I hope we will participate together in many more excellent colaborations and I´m looking forward to many more jam sessions outside the lab as well!

Thanks to Veronika Mladenova, for her contributions to the plasmid work and joining in with her voice to our house music.

Thanks to Nadine Coym, for the good teamwork and helping to speed things up a bit.

Thanks also to Malihe Mesbah for her fundamental contributions in keeping the lab running.

Thanks to Fr. Lander, the good spirit of the basement.

Thanks a lot to Marcel Thissen for shuttle navigation on the last meters. Live long and prosper!

Thanks to all those who accompanied me on parts or all along my scientific education.

Vielen Dank Andre für die moralische Unterstützung und gelegentliche Ablenkung. Bald können wir mal wieder ein paar triumphale Bälle schlagen.

Simon Gengler für die gegenseitige Bestätigung unserer Ansichten.

Steffen, Uli und Simon für viele schöne Erinnerungen an die Uni-Zeit. Hoffentlich können wir bald die letzte Promotion zusammen feiern.

Bernd Giebel für den soliden Drill der Grundausbildung.

Allen anderen Essener rund um die Transfusionsmedizin.

Und natürlich meinen Eltern und Geschwistern, für alle Unterstützung und schönen Zeiten über die Jahre.

Vielen Dank auch an den ganzen Rest meiner Familie, ob angeheiratet oder angeboren. Vielen Dank vor allem auch an Tante Anni, Oma Ulla und Opa Udo für das gelegentliche Entlasten wenn sonst gar nichts gegangen wäre.

10 Curriculum vitae

Der Lebenslauf ist in der Online-Version aus Gründen des Datenschutzes nicht enthalten.

Der Lebenslauf ist in der Online-Version aus Gründen des Datenschutzes nicht enthalten.

Der Lebenslauf ist in der Online-Version aus Gründen des Datenschutzes nicht enthalten.

11 Publications

Research papers

Magin, S., J. Saha, M. Wang, V. Mladenova, N. Coym and G. Iliakis. "Lipofection and Nucleofection of Substrate Plasmid Can Generate Widely Different Readings of DNA End-Joining Efficiency in Different Cell Lines." ***DNA repair*** 12, no. 2 (2013): 148-60.

Costantino, L., S. K. Sotiriou, J. K. Rantala, S. Magin, E. Mladenov, T. Helleday, J. E. Haber, G. Iliakis, O. P. Kallioniemi and T. D. Halazonetis. "Break-Induced Replication Repair of Damaged Forks Induces Genomic Duplications in Human Cells." ***Science*** 343, no. 6166 (2014): 88-91.

Review articles

Mladenov, E., S. Magin, A. Soni and G. Iliakis. "DNA Double-Strand Break Repair as Determinant of Cellular Radiosensitivity to Killing and Target in Radiation Therapy." ***Frontiers in oncology*** 3, (2013): 113.

12 Declaration

Erklärung:

Hiermit erkläre ich, gem. § 6 Abs. 2, g der Promotionsordnung der Fakultät für Biologie zur Erlangung der Dr. rer. nat., dass ich das Arbeitsgebiet, dem das Thema „A balance shift between error-free and error-prone DNA double-strand break repair pathways as a novel mechanism of radiosensitization by nucleoside analogs.“ zuzuordnen ist, in Forschung und Lehre vertrete und den Antrag von Herrn Simon Magin befürworte.

Essen, _____ _____ _____

Name d. wissenschaftl. Betreuers/ Mitglieds der Universität Duisburg-Essen	Unterschrift d. wissenschaftl. Betreuers/ Mitglieds der Universität Duisburg-Essen

Erklärung:

Hiermit erkläre ich, gem. § 7 Abs. 2, d und f der Promotionsordnung Fakultät für Biologie zur Erlangung des Dr. rer. nat., dass ich die vorliegende Dissertation selbständig verfasst und mich keiner anderen als der angegebenen Hilfsmittel bedient habe und alle wörtlich oder inhaltlich übernommenen Stellen als solche gekennzeichnet habe.

Essen, _____ _____

Unterschrift des Doktoranden

Erklärung:

Hiermit erkläre ich, gem. § 7 Abs. 2, e und g der Promotionsordnung der Fakultät für Biologie zur Erlangung des Dr. rer. nat., dass ich keine anderen Promotionen bzw. Promotionsversuche in der Vergangenheit durchgeführt habe, dass diese Arbeit von keiner anderen Fakultät abgelehnt worden ist, und dass ich die Dissertation nur in diesem Verfahren einreiche.

Essen, _____ _____

Unterschrift des Doktoranden